

**ISTANBUL TECHNICAL UNIVERSITY ★ GRADUATE SCHOOL OF SCIENCE**  
**ENGINEERING AND TECHNOLOGY**

**VERTICAL VIBRATION OF SUSPENSION BRIDGES DUE TO TRAFFIC AND  
VERTICAL GROUND ACCELERATION**



**M.Sc. THESIS**

**Ali AHANI**

**Department of Civil Engineering**  
**Structural Engineering Programme**

**October 2018**



**ISTANBUL TECHNICAL UNIVERSITY ★ GRADUATE SCHOOL OF SCIENCE**  
**ENGINEERING AND TECHNOLOGY**

**VERTICAL VIBRATION OF SUSPENSION BRIDGES DUE TO TRAFFIC AND  
VERTICAL GROUND ACCELERATION**



**M.Sc. THESIS**

**Ali AHANI  
(501151062)**

**Department of Civil Engineering**

**Structural Engineering Programme**

**Thesis Advisor: Assoc. Prof. Dr. A. Necmettin GÜNDÜZ**

**October 2018**



**İSTANBUL TEKNİK ÜNİVERSİTESİ ★ FEN BİLİMLERİ ENSTİTÜSÜ**

**ASMA KÖPRÜLERİN TRAFİK VE DÜŞEY DEPREM YER HAREKETİ  
ALTINDA TİTREŞİMİ**

**YÜKSEK LİSANS TEZİ**

**Ali AHANI  
(501151062)**

**İnşaat Mühendisliği Anabilim Dalı**

**Yapı Mühendisliği Programı**

**Tez Danışmanı: Doç. Dr. A. Necmettin GÜNDÜZ**

**Ekim 2018**



Ali Ahani, a M.Sc. student of İTÜ Graduate School of Science Engineering and Technology student ID 501151062, successfully defended the thesis entitled “VERTICAL VIBRATION OF SUSPENSION BRIDGES DUE TO TRAFFIC AND VERTICAL GROUND EXCIATATIONS”, which he prepared after fulfilling the requirements specified in the associated legislations, before the jury whose signatures are below.

**Thesis Advisor :**     **Assoc. Prof. Dr. A. Necmettin GÜNDÜZ** .....  
ISTANBUL Technical University

**Jury Members :**     **Assoc. Prof. Dr. Ali SARI** .....  
ISTANBUL Technical University

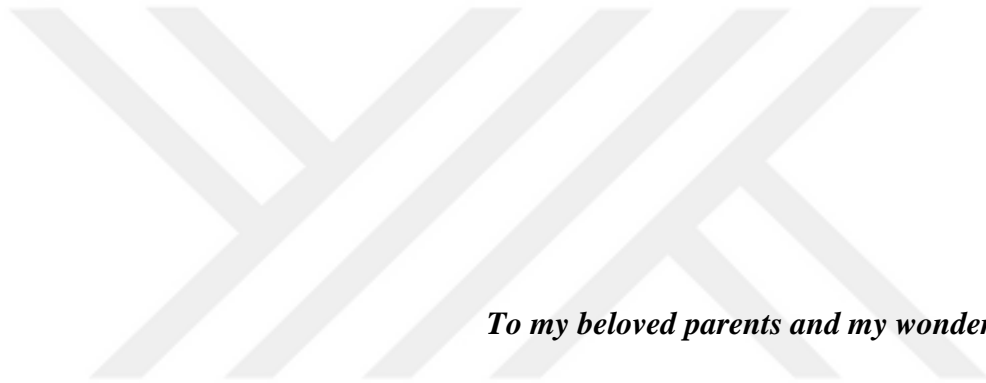
**Asst. Prof. Dr. Meltem ŞAHİN** .....  
Mimar Sinan Fine Arts University

**Date of Submission : 7 September 2018**

**Date of Defense : 5 October 2018**







*To my beloved parents and my wonderful brother*



## **FOREWORD**

Purpose of this research was to expand our knowledge from suspension bridges during an earthquake and vibrations and to achieve this goal computational, analytical and software modeling utilized to increase accuracy of our result.

I would like to thank my parents who supported me with love and understanding, my elder brother who advised and guided me throughout my educational era and my dear advisor Assoc. Prof. Dr. A. Necmettin GÜNDÜZ for his priceless advices and advises throughout the courses that taken during master programme and wonderful knowledge, navigation and guideness with extreme patience during thesis.

September 2018

Ali AHANI



## TABLE OF CONTENTS

	<u>Page</u>
<b>FOREWORD</b> .....	<b>ix</b>
<b>TABLE OF CONTENTS</b> .....	<b>xi</b>
<b>ABBREVIATIONS</b> .....	<b>xiii</b>
<b>SYMBOLS</b> .....	<b>xv</b>
<b>LIST OF TABLES</b> .....	<b>xvii</b>
<b>LIST OF FIGURES</b> .....	<b>xix</b>
<b>SUMMARY</b> .....	<b>xxiii</b>
<b>ÖZET</b> .....	<b>xxvii</b>
<b>1. INTRODUCTION</b> .....	<b>1</b>
1.1 Classification of Bridges .....	2
1.1.1 Classification based on superstructure.....	3
1.1.1.1 Beam Bridge.....	3
1.1.1.2 Arch Bridge.....	5
1.1.1.3 Cantilever Bridge .....	6
1.1.1.4 Truss Bridge .....	8
1.1.1.5 Cable-stayed Bridge.....	9
1.1.1.6 Suspension Bridge.....	11
1.2 Cable Bridges Structural System.....	13
1.2.1 Cable-stayed bridge structural system .....	13
1.2.2 Suspension bridge structural system .....	14
1.2.3 Famous suspension bridges.....	15
1.2.4 Advantages and disadvantages of suspension bridges .....	18
1.3 Structural Components of Suspension Bridge .....	20
1.3.1 Tower .....	21
1.3.1.1 Towers classification in longitudinal and transverse direction .....	21
1.3.2 Deck .....	22
1.3.3 Hangers .....	24
1.3.4 Suspension cable .....	25
1.3.5 Anchorages.....	25
1.3.5.1 Types of cable anchoring .....	25
1.4 Literature Review .....	26
<b>2. DETERMINING EQUATION OF MOTION OF SUSPENSION BRIDGES</b> .....	<b>33</b>
2.1 Suspension Bridge Free Body diagram .....	35
2.2 Cable Tension and Increment of Tension Mathematical Formulation.....	36
2.3 Decomposition of the Displacements.....	40
2.3.1 Static equations for beam and cable.....	40
2.3.2 Boundary conditions for cable and beam.....	41
2.3.3 Solution method for static .....	41
2.3.4 Inertial equation of the cable and beam .....	42
2.4 Equation of Motion for Suspension Bridge Deck .....	43
2.5 Equation of Motion for Suspension Bridge Cable .....	45
2.6 Solution Method For Equation Of Motion .....	47

2.7 Earthquake Effects on Equation of Motion .....	48
2.8 Determining Natural Frequencies.....	49
<b>3. ANALYTICAL STUDIES.....</b>	<b>51</b>
3.1 Verification.....	51
3.2 Numerical Modeling.....	55
3.2.1 Static.....	57
3.2.2 Moving load .....	64
3.2.2.1 Case I result .....	65
3.2.2.2 Case II result.....	69
3.2.2.3 Case III result .....	74
3.2.2.4 Hangers elongation.....	78
3.2.3 Result for inextensible hangers .....	85
3.2.3.1 Case I result .....	85
3.2.3.2 Case II result.....	87
3.2.3.3 Case III result .....	88
3.2.4 Result comparison .....	90
3.2.5 Total deflection of the suspension bridge .....	91
3.2.6 Natural frequencies .....	92
3.2.7 Maximum acceleration response .....	96
3.3 FEM Result.....	97
3.4 Ground Motion .....	102
3.4.1 Coyote Lake .....	103
3.4.2 Kobe .....	106
3.4.3 El Mayor.....	110
3.5 Ground Motion and Moving Load Simultaneously.....	113
3.5.1 Coyote Lake .....	114
3.5.2 Kobe .....	117
3.5.3 El Mayor.....	120
<b>4. CONCLUSION.....</b>	<b>123</b>
<b>REFERENCES .....</b>	<b>127</b>
<b>APPENDICES .....</b>	<b>131</b>
APPENDIX A: Finite Difference Method .....	131
APPENDIX B: Mathematics.....	132
APPENDIX C: Cable Parabolic Equation.....	133
APPENDIX D: Deriving Equilibrium Equation .....	134
APPENDIX E: Deriving Equation For Increment In Horizontal Component Of Cable Tension.....	135
APPENDIX F: Integrating First Term In Equation 2.17 .....	136
APPENDIX G: MATLAB Scripts .....	137
G.1 Length Of The Cable .....	137
G.2 Computing Cable Tension & Deflection Of The Bridge .....	137
G.3 Fitting Equation For static Displacement.....	145
G.4 Extensible Hangers.....	145
G.5 Inextensible Hangers .....	153
G.6 Maximum Acceleration.....	158
<b>CURRICULUM VITAE.....</b>	<b>163</b>

## **ABBREVIATIONS**

<b>App</b>	: Appendix
<b>BVP</b>	: Boundary Value Problem
<b>FDM</b>	: Finite Difference Method
<b>FEM</b>	: Finite Element Method
<b>IDE</b>	: Integro Differential Equation
<b>IVP</b>	: Initial Value Problem
<b>ODE</b>	: Ordinary Differential Equation
<b>PDE</b>	: Partial Differential Equation





## SYMBOLS

$A_c$	: Area of cable
$ds$	: Finite length of the cable
$ds'$	: Finite length of the elongated cable
$du$	: Horizontal differential deflection of the cable due to the moving load
$dw$	: Vertical differential deflection of the cable due to the moving load
$dy$	: Vertical differential deflection of the cable due to the static load
$dz$	: Vertical differential deflection of the beam due to the moving load
$E_b$	: Modulus of elasticity of beam
$E_c$	: Modulus of elasticity of cable
$f_n$	: Natural frequency for n'th mode
$g$	: Gravitational acceleration
$H$	: Horizontal component of cable tension
$I_b$	: Moment of inertia of beam
$I_c$	: Moment of inertia of cable
$K$	: Distributed stiffness of the hangers
$L$	: Span length of suspension bridge
$L_C$	: Cable length of suspension bridge
$M$	: Vehicle mass
$m_b$	: Beam mass per length
$m_c$	: Cable mass per length
$n$	: Mode number
$T$	: Cable tension
$T_n$	: Period for n'th mode
$t$	: Time
$u_0, u_L$	: Horizontal displacements at tower
$v$	: Vehicle velocity
$W$	: Cable displacement
$w_d$	: Dynamic component of the cable displacement
$w_0, w_L$	: Vertical displacements at tower
$Z$	: Beam displacement

$z_d$	: Dynamic component of the beam displacement
$\Delta H$	: Increment in horizontal component of cable tension
$\phi_n$	: Shape function for n'th mode
$\rho$	: Density
$\omega_n$	: Angular velocity for n'th mode
$\tau$	: Increment in cable tension
$\mathbb{Z}$	: Set of integers
$\forall$	: For all
$\wedge$	: Logical and



## LIST OF TABLES

	<u>Page</u>
<b>Table 1.1</b> : Longest suspension bridges .....	15
<b>Table 3.1</b> : Material and geometric properties of the deck.....	52
<b>Table 3.2</b> : Material and geometric properties of the suspension cable .....	52
<b>Table 3.3</b> : Material and geometric properties of the hanger .....	52
<b>Table 3.4</b> : Material and geometric properties of the tower .....	52
<b>Table 3.5</b> : Geometric values of verified suspension bridge .....	52
<b>Table 3.6</b> : Details of load acting on verified bridge.....	53
<b>Table 3.7</b> : Comparing maximum deflection from MATLAB and Choi’s article ....	55
<b>Table 3.8</b> : Material and geometric properties of the deck.....	55
<b>Table 3.9</b> : Material and geometric properties of the suspension cable .....	56
<b>Table 3.10</b> : Material and geometric properties of the hanger .....	56
<b>Table 3.11</b> : Material and geometric properties of the tower .....	56
<b>Table 3.12</b> : Geometric values of suspension bridge .....	56
<b>Table 3.13</b> : Details of load acting on numerical bridge .....	57
<b>Table 3.14</b> : Cable tension and increment in cable tension horizontal component...	57
<b>Table 3.15</b> : Numeric Values Of Deflection Of The Cable And The Deck In Main Span.....	58
<b>Table 3.16</b> : Numeric Values Of The Cable and The Deck Deflection In Side Span	61
<b>Table 3.17</b> : Elongation, stress and axial force in main span hangers.....	61
<b>Table 3.18</b> : Elongation, stress and axial force in side span hangers .....	64
<b>Table 3.19</b> : Details of moving load.....	65
<b>Table 3.20</b> : Elongation, stress and axial force in hangers for case I.....	78
<b>Table 3.21</b> : Elongation, stress and axial force in hangers for case II.....	81
<b>Table 3.22</b> : Elongation, stress and axial force in hangers for case III .....	83
<b>Table 3.23</b> : Comparison of Middle Point Deflection at the time moving load reaches middle of the span .....	90
<b>Table 3.24</b> : Comparison of Middle Point Max Deflection.....	91
<b>Table 3.25</b> : Natural frequencies .....	93
<b>Table 3.26</b> : Angular speed .....	93
<b>Table 3.27</b> : Comparison of Mid Point Deflection Computed by MATLAB and ABAQUS .....	98
<b>Table 3.28</b> : Comparison result of MATLAB and ABAQUS for cable mid point deflection.....	102
<b>Table 3.29</b> : Comparison result of MATLAB and ABAQUS for deck mid point deflection.....	102
<b>Table 4.1</b> : Comparison of Middle Point Deflection at the time moving load reaches middle of the span .....	123
<b>Table 4.2</b> : Comparison of Middle Point Max Deflection .....	123
<b>Table 4.3</b> : Natural frequencies .....	124
<b>Table 4.4</b> : Comparison result of MATLAB and ABAQUS for cable mid point deflection.....	124

**Table 4.5 :** Comparison result of MATLAB and ABAQUS for deck mid point deflection..... **124**



## LIST OF FIGURES

	<u>Page</u>
<b>Figure 1.1</b> : Beam Bridge schematic view. ....	5
<b>Figure 1.2</b> : Arch Bridge schematic view. ....	6
<b>Figure 1.3</b> : Cantilever Bridge schematic view. ....	7
<b>Figure 1.4</b> : Truss Bridge schematic view. ....	9
<b>Figure 1.5</b> : Cable-stayed Bridge schematic view. ....	11
<b>Figure 1.6</b> : Suspension Bridge schematic view. ....	12
<b>Figure 1.7</b> : Cable stayed bridge cable arrangement. ....	14
<b>Figure 1.8</b> : Akashi Kaikyō Bridge .....	16
<b>Figure 1.9</b> : Xihoumen Bridge .....	16
<b>Figure 1.10</b> : Great Belt Bridge.....	17
<b>Figure 1.11</b> : Osman Gazi Bridge .....	17
<b>Figure 1.12</b> : Yavuz Sultan Selim Bridge .....	18
<b>Figure 1.13</b> : Structural components of the suspension bridge.....	21
<b>Figure 1.14</b> : Towers classification in Longitudinal Direction .....	22
<b>Figure 1.15</b> : Towers classification in Transverse Direction .....	22
<b>Figure 1.16</b> : Girder types (a) Truss girder (b) Box girder and (c) I-girder.....	23
<b>Figure 1.17</b> : Stiffening girder (a) Hinged stiffening girder and (b) Continuous stiffening girder.....	23
<b>Figure 1.18</b> : Hangers type (a) Vertical hangers, (b) Diagonal hangers and (c) Combined suspension and cable-stayed system.....	24
<b>Figure 1.19</b> : Anchorage type (a) Self anchored type and (b) Externally anchored type.....	25
<b>Figure 2.1</b> : Elastic theory and deflection theory .....	34
<b>Figure 2.2</b> : Free body diagram of the deck .....	35
<b>Figure 2.3</b> : Free body diagram of the cable .....	36
<b>Figure 2.4</b> : Equilibrium of the finite length of the cable .....	36
<b>Figure 2.5</b> : Force equilibrium of the deck.....	48
<b>Figure 3.1</b> : Verified bridge details .....	53
<b>Figure 3.2</b> : Suspension bridge deflection plot for interval length of 100 meters (In meters).....	53
<b>Figure 3.3</b> : Suspension bridge deflection plot for interval length of 50 meters (In meters).....	54
<b>Figure 3.4</b> : Suspension bridge deflection plot for interval length of 25 meters (In meters).....	54
<b>Figure 3.5</b> : Suspension bridge deflection plot for interval length of 10 meters (In meters).....	54
<b>Figure 3.6</b> : Schematic view of assumed bridge .....	56
<b>Figure 3.7</b> : Static Analysis of the Suspension Bridge.....	58
<b>Figure 3.8</b> : The middle point deflection of the cable and the deck for Case I (In meters).....	65

<b>Figure 3.9 :</b>	The middle point velocity of the cable and the deck for Case I .....	<b>66</b>
<b>Figure 3.10 :</b>	The middle point acceleration of the cable and the deck for Case I....	<b>66</b>
<b>Figure 3.11 :</b>	3D Plot of span deflection for Case I (In meters).....	<b>67</b>
<b>Figure 3.12 :</b>	The Case I middle point deflection of the cable and the deck at the time the moving load reach the span center (In meters) .....	<b>67</b>
<b>Figure 3.13 :</b>	Deflection of center span in case I for first 50 modes .....	<b>68</b>
<b>Figure 3.14 :</b>	Velocity of center span in case I for first 50 modes .....	<b>68</b>
<b>Figure 3.15 :</b>	Acceleration of center span in case I for first 50 modes .....	<b>69</b>
<b>Figure 3.16 :</b>	The middle point deflection of the cable and the deck for Case II (In meters).....	<b>70</b>
<b>Figure 3.17 :</b>	The middle point velocity of the cable and the deck for Case II.....	<b>70</b>
<b>Figure 3.18 :</b>	The middle point acceleration of the cable and the deck for Case II ..	<b>71</b>
<b>Figure 3.19 :</b>	3D Plot of span deflection for Case II (In meters) .....	<b>71</b>
<b>Figure 3.20 :</b>	The Case II middle point deflection of the cable and the deck at the time the moving load reach the span center (In meters) .....	<b>72</b>
<b>Figure 3.21 :</b>	Deflection of center span in case II for first 50 modes.....	<b>72</b>
<b>Figure 3.22 :</b>	Velocity of center span in case II for first 50 modes.....	<b>73</b>
<b>Figure 3.23 :</b>	Acceleration of center span in case II for first 50 modes .....	<b>74</b>
<b>Figure 3.24 :</b>	The middle point deflection of the cable and the deck for Case III (In meters).....	<b>74</b>
<b>Figure 3.25 :</b>	The middle point velocity of the cable and the deck for Case III .....	<b>75</b>
<b>Figure 3.26 :</b>	The middle point acceleration of the cable and the deck for Case III.	<b>75</b>
<b>Figure 3.27 :</b>	3D Plot of span deflection for Case III (In meters) .....	<b>76</b>
<b>Figure 3.28 :</b>	The Case III middle point deflection of the cable and the deck at the time the moving load reach the span center (In meters) .....	<b>76</b>
<b>Figure 3.29 :</b>	Deflection of center span in case III for first 50 modes .....	<b>77</b>
<b>Figure 3.30 :</b>	Velocity of center span in case III for first 50 modes .....	<b>77</b>
<b>Figure 3.31 :</b>	Acceleration of center span in case III for first 50 modes.....	<b>78</b>
<b>Figure 3.32 :</b>	Deck middle point deflection in case hangers are inextensible for Case I (In meters).....	<b>86</b>
<b>Figure 3.33 :</b>	3D Plot of span deflection in case hangers are inextensible for Case I (In meters) .....	<b>86</b>
<b>Figure 3.34 :</b>	The Case I middle point deflection of the deck at the time the moving load reach the span center (In meters).....	<b>87</b>
<b>Figure 3.35 :</b>	Deck middle point deflection in case hangers are inextensible for Case II (In meters).....	<b>87</b>
<b>Figure 3.36 :</b>	3D Plot of span deflection in case hangers are inextensible for Case II (In meters) .....	<b>88</b>
<b>Figure 3.37 :</b>	The Case II middle point deflection of the deck at the time the moving load reach the span center (In meters).....	<b>88</b>
<b>Figure 3.38 :</b>	Deck middle point deflection in case hangers are inextensible for Case III (In meters) .....	<b>89</b>
<b>Figure 3.39 :</b>	3D Plot of span deflection in case hangers are inextensible for Case III (In meters) .....	<b>89</b>
<b>Figure 3.40 :</b>	The Case III middle point deflection of the deck at the time the moving load reach the span center (In meters).....	<b>90</b>
<b>Figure 3.41 :</b>	3D Plot of Total Deflection of The Suspension bridge for Case I (In meters).....	<b>91</b>
<b>Figure 3.42 :</b>	3D Plot of Total Deflection of The Suspension bridge for Case II (In meters).....	<b>92</b>

<b>Figure 3.43</b> : 3D Plot of Total Deflection of The Suspension bridge for Case III (In meters).....	<b>92</b>
<b>Figure 3.44</b> : 1 <sup>st</sup> Mode Shape .....	<b>94</b>
<b>Figure 3.45</b> : 2 <sup>nd</sup> Mode Shape .....	<b>94</b>
<b>Figure 3.46</b> : 3 <sup>rd</sup> Mode Shape.....	<b>95</b>
<b>Figure 3.47</b> : 4 <sup>th</sup> Mode Shape.....	<b>95</b>
<b>Figure 3.48</b> : 5 <sup>th</sup> Mode Shape.....	<b>95</b>
<b>Figure 3.49</b> : 6 <sup>th</sup> Mode Shape.....	<b>96</b>
<b>Figure 3.50</b> : Max acceleration response of the suspension bridge .....	<b>96</b>
<b>Figure 3.51</b> : ABAQUS model for static analysis.....	<b>97</b>
<b>Figure 3.52</b> : Plot of static deformation (In meters).....	<b>97</b>
<b>Figure 3.53</b> : 3D plot of static deformation (In meters).....	<b>98</b>
<b>Figure 3.54</b> : ABAQUS model for dynamic analysis .....	<b>98</b>
<b>Figure 3.55</b> : Middle Point Deflection For Case I (In meters).....	<b>99</b>
<b>Figure 3.56</b> : Middle Point Deflection For Case II (In meters).....	<b>99</b>
<b>Figure 3.57</b> : Middle Point Deflection For Case III (In meters) .....	<b>99</b>
<b>Figure 3.58</b> : U2 Vector Deflection for Case I (In meters).....	<b>100</b>
<b>Figure 3.59</b> : U2 Vector Deflection for Case II (In meters).....	<b>100</b>
<b>Figure 3.60</b> : U2 Vector Deflection for Case III (In meters) .....	<b>100</b>
<b>Figure 3.61</b> : 3D Plot of Suspension Bridge Deflection for Case I (In meters).....	<b>101</b>
<b>Figure 3.62</b> : 3D Plot of Suspension Bridge Deflection for Case II (In meters).....	<b>101</b>
<b>Figure 3.63</b> : 3D Plot of Suspension Bridge Deflection for Case III (In meters) ...	<b>101</b>
<b>Figure 3.64</b> : Vertical Ground Acceleration Record for Coyote Lake Ground Motion .....	<b>103</b>
<b>Figure 3.65</b> : 3D Plot of Span Deflection Due to the Coyote Lake Earthquake Motion for Case I (In Meters) .....	<b>103</b>
<b>Figure 3.66</b> : 3D Plot of Span Deflection Due to the Coyote Lake Earthquake Motion for Case II (In Meters).....	<b>104</b>
<b>Figure 3.67</b> : 3D Plot of Span Deflection Due to the Coyote Lake Earthquake Motion for Case III (In Meters) .....	<b>104</b>
<b>Figure 3.68</b> : Suspension Bridge Middle Point Deflection Due to the Coyote Lake Earthquake for Case I (In Meters).....	<b>105</b>
<b>Figure 3.69</b> : Suspension Bridge Middle Point Deflection Due to the Coyote Lake Earthquake for Case II (In Meters) .....	<b>105</b>
<b>Figure 3.70</b> : Suspension Bridge Middle Point Deflection Due to the Coyote Lake Earthquake for Case III (In Meters).....	<b>106</b>
<b>Figure 3.71</b> : Vertical Ground Acceleration Record for Kobe Ground Motion.....	<b>106</b>
<b>Figure 3.72</b> : 3D Plot of Span Deflection Due to the Kobe Earthquake Motion for Case I (In Meters).....	<b>107</b>
<b>Figure 3.73</b> : 3D Plot of Span Deflection Due to the Kobe Earthquake Motion for Case II (In Meters) .....	<b>107</b>
<b>Figure 3.74</b> : 3D Plot of Span Deflection Due to the Kobe Earthquake Motion for Case III (In Meters).....	<b>108</b>
<b>Figure 3.75</b> : Suspension Bridge Middle Point Deflection Due to the Kobe Earthquake for Case I (In Meters).....	<b>108</b>
<b>Figure 3.76</b> : Suspension Bridge Middle Point Deflection Due to the Kobe Earthquake for Case II (In Meters) .....	<b>109</b>
<b>Figure 3.77</b> : Suspension Bridge Middle Point Deflection Due to the Kobe Earthquake for Case III (In Meters).....	<b>109</b>
<b>Figure 3.78</b> : Vertical Ground Acceleration Record for El Mayor Ground Motion	<b>110</b>

<b>Figure 3.79</b> : 3D Plot of Span Deflection Due to the El Mayor Earthquake Motion for Case I (In Meters) .....	<b>110</b>
<b>Figure 3.80</b> : 3D Plot of Span Deflection Due to the El Mayor Earthquake Motion for Case II (In Meters).....	<b>111</b>
<b>Figure 3.81</b> : 3D Plot of Span Deflection Due to the El Mayor Earthquake Motion for Case III (In Meters) .....	<b>111</b>
<b>Figure 3.82</b> : Suspension Bridge Middle Point Deflection Due to the El Mayor Earthquake for Case I (In Meters).....	<b>112</b>
<b>Figure 3.83</b> : Suspension Bridge Middle Point Deflection Due to the El Mayor Earthquake for Case II (In Meters) .....	<b>112</b>
<b>Figure 3.84</b> : Suspension Bridge Middle Point Deflection Due to the El Mayor Earthquake for Case III (In Meters) .....	<b>113</b>
<b>Figure 3.85</b> : 3D Plot of Span Deflection Due to the Coyote Lake Earthquake Motion and Moving Load for Case I.....	<b>114</b>
<b>Figure 3.86</b> : 3D Plot of Span Deflection Due to the Coyote Lake Earthquake Motion and Moving Load for Case II .....	<b>114</b>
<b>Figure 3.87</b> : 3D Plot of Span Deflection Due to the Coyote Lake Earthquake Motion and Moving Load for Case III .....	<b>115</b>
<b>Figure 3.88</b> : Suspension Bridge Middle Point Deflection Due to the Coyote Lake Earthquake Motion and Moving Load for Case I .....	<b>115</b>
<b>Figure 3.89</b> : Suspension Bridge Middle Point Deflection Due to the Coyote Lake Earthquake Motion and Moving Load for Case II .....	<b>116</b>
<b>Figure 3.90</b> : Suspension Bridge Middle Point Deflection Due to the Coyote Lake Earthquake Motion and Moving Load for Case III.....	<b>116</b>
<b>Figure 3.91</b> : 3D Plot of Span Deflection Due to the Kobe Earthquake Motion and Moving Load for Case I .....	<b>117</b>
<b>Figure 3.92</b> : 3D Plot of Span Deflection Due to the Kobe Earthquake Motion and Moving Load for Case II.....	<b>117</b>
<b>Figure 3.93</b> : 3D Plot of Span Deflection Due to the Kobe Earthquake Motion and Moving Load for Case III.....	<b>118</b>
<b>Figure 3.94</b> : Suspension Bridge Middle Point Deflection Due to the Kobe Earthquake Motion and Moving Load for Case I .....	<b>118</b>
<b>Figure 3.95</b> : Suspension Bridge Middle Point Deflection Due to the Kobe Earthquake Motion and Moving Load for Case II .....	<b>119</b>
<b>Figure 3.96</b> : Suspension Bridge Middle Point Deflection Due to the Kobe Earthquake Motion and Moving Load for Case III.....	<b>119</b>
<b>Figure 3.97</b> : 3D Plot of Span Deflection Due to the El Mayor Earthquake Motion and Moving Load for Case I .....	<b>120</b>
<b>Figure 3.98</b> : 3D Plot of Span Deflection Due to the El Mayor Earthquake Motion and Moving Load for Case II .....	<b>120</b>
<b>Figure 3.99</b> : 3D Plot of Span Deflection Due to the El Mayor Earthquake Motion and Moving Load for Case III.....	<b>121</b>
<b>Figure 3.100</b> : Suspension Bridge Middle Point Deflection Due to the El Mayor Earthquake Motion and Moving Load for Case I .....	<b>121</b>
<b>Figure 3.101</b> : Suspension Bridge Middle Point Deflection Due to the El Mayor Earthquake Motion and Moving Load for Case II .....	<b>122</b>
<b>Figure 3.102</b> : Suspension Bridge Middle Point Deflection Due to the El Mayor Earthquake Motion and Moving Load for Case III.....	<b>122</b>



## **VERTICAL VIBRATION OF SUSPENSION BRIDGES DUE TO TRAFFIC AND VERTICAL GROUND EXCIATATIONS**

### **SUMMARY**

Bridges are among the important civil infrastructures and are normally designed to have long life spans. Suspension bridges has a larger span in comparison to any other form of bridges. As it get larger span it become more flexible structure. As a structure get flexible its behaviour under dynamic load become more complicated. Suspension bridges are infrastructures in which the load-bearing portion is hung under the suspension cables upon the vertical hangers. Due to their aesthetic, architectural beauty and capability of utilization in long spans suspension bridges, have gained much popularity in recent decades. Throughout the history of suspension bridges, their tendency to vibrate under different dynamic loadings such as wind, earthquake, and traffic loads has been a matter of concern for engineers and researchers. Along with the rapid development of modern transportation networks, suspension bridges are often adopted to wide span rivers or deep valleys. Increasing the construction of suspension bridges and the challenge of modelling their behaviour has attracted the interest of researchers. Many difficulties related to design arises due to its long central span. There are many suspension bridges around the world and dynamic behaviour has been found to be the primary concern for those bridges. Several investigations have been taken place in recent years to determine the behaviour of suspension bridges and dynamical characteristics of it when they are vibrating. However, the complexity of the structure of a suspension bridge makes difficulties on determining dynamical behaviour and dynamical features of suspension bridge.

Various studies on dynamic response of moving loads have been conducted on ordinary bridges. However because of complex structures of suspension bridge which consist of various components with different properties, they cannot be directly applied to cable supported bridges. Consequently, more research is required on cable supported bridges to consider the complex structural response and realistically predict their response under moving loads. Various methods of analysis have been applied to the study of the behavior of suspension bridges. One of analytical methods for determining behavior of a suspension bridge is deflection theory. A historical review of the approximate methods that lead to the deflection theory can be found elsewhere. The well-established deflection theory tries to solve the differential equilibrium equation and allows the use of analytical expressions for the solutions. However, explicit analytical solutions are not always possible, and numerical techniques must be used. With the advent of high-speed computer and through the use of numerical methods, major advances in studying the dynamic characteristics of suspension bridges have been achieved. Many efforts have been given to develop a simplified model that can predict the consistency of the responses with detailed model. In recent years, several commercially available finite element software packages have been used by practicing engineers as well as researchers to evaluate the response of suspension

bridges for operational traffic, wind and earthquake loads by considering both property and geometry non-linear behavior.

Vibration of the suspension bridges are important topic in design of them and it must taken into account in areas where seismic activity is high or in places where a typhoon and a strong wind blowing occurs. For this purpose, displacement response of the suspension bridge when it was subjected to the moving load and ground motions simultaneously investigated in this study. In previous studies static deflection of the suspension bridge, cable tension and also increment in cable tension are investigated. Some of researchers focused on the vibration of the suspension bridge due to the moving load and oscillator, but in most of the studies, the hangers extensibility have neglected. In this research in addition to computing cable tension due to live loads, deflection, velocity and acceleration response of the suspension bridge computed.

In this order, at first equation of motion for the deck and the suspension cable of the suspension bridge is derived. Since extensibility of the hangers is considered in this study, a coupled PDE equation must be solved to determine deflection, velocity and acceleration response of the suspension bridge. After derivation of the equation of motion for the cable and the deck, separating variables performed in order to simplify PDE equation to two separate ODE equations which are dependent on time and ordinate of the suspension bridge. To determine deflection of the suspension bridge, behavior of the suspension bridge divided into two parts, first part was static analysis and second part was dynamic analysis. Numerical method has been used to solve static part since it has integral term in equation. Finite difference method as numerical method implemented for static analysis while in dynamic part exact solutions achieved.

To verify the written code in MATLAB, obtained result in static analysis from MATLAB compared with achieved result by Choi's article which was published in 2013. Difference of the results were in acceptable range and it indicates that decreasing intervals in FDM method reduces the difference.

To this purpose, a suspension bridge which is subjected to moving load and ground motions simultaneously assumed. Three different load cases considered for analyzing. All of load cases were identical in all aspects and the only difference between them was velocity of the moving load. For this purpose written code prepared in MATLAB to determine deflection, velocity and acceleration response of the suspension bridge with use of improved deflection theory. Outcomes indicate that increasing velocity of the moving load would results in increasing deflection of the suspension bridge. Number of modes that considered in determining deflection, velocity and acceleration of the suspension bridge was 50 modes. Obtained result from improved deflection theory compared with results that achieved by deflection theory. Comparison of these results shows that deflection theory is reliable method for determining deflection of the suspension bridge. Hence, in order to determine elongation, axial forces and stresses in hangers, use of improved deflection theory advised.

Natural frequency of a suspension bridge mainly dependent on the span and other structural dimensions related to the stiffness. According to the outcomes, the first two vibration modes of the suspension bridge are symmetric and the first anti symmetric mode of the suspension bridge was appeared on third mode.

Three different vertical ground motion records were considered in this study in order to determine behavior of the suspension bridge when it was subjected to the moving load and ground motion simultaneously. To prove the validity of the result, FEM

commercial software, ABAQUS were used to simulate behavior of the suspension bridge. and when it is subjected to the moving load and after that obtained result from MATLAB was compared with the result that obtained from ABAQUS software. Results shows that achieved outcomes from both of the softwares are in good agreement which proves the reliability of the written code in MATLAB.





## ASMA KÖPRÜLERİN TRAFİK VE DÜŞEY DEPREM YER HAREKETİ ALTINDA TİTREŞİMİ

### ÖZET

Köprüler önemli sivil altyapılar arasındadır ve normal olarak uzun ömürlü olacak şekilde tasarlanırlar. Asma köprüler diğer köprülerle karşılaştırıldığında daha uzun bir açıklığa sahiptir. Daha uzun açıklığa sahip olduğu için de daha esnek bir yapı haline gelir. Bir yapı esnekleştikçe dinamik yük altındaki davranışları daha karmaşık hale gelir.

Asma köprüler, yük taşıyıcı kısmı olan tabliyesi düşey veya eğik askılar ile yine taşıyıcı olan kabloya asılmış yapılardır. Estetik, mimari güzellikleri ve uzun erimli asma köprülerdeki kullanım yetenekleri nedeniyle son yıllarda büyük bir ilgi görmüştür. Asma köprüler, ekonomik ömürleri süresince rüzgâr, deprem ve trafik yükleri gibi farklı dinamik yükler altında titreşme eğilimleri nedeniyle mühendisler ve araştırmacılar için endişe kaynağı olmuştur. Modern ulaşım ağlarının hızlı gelişimi ile birlikte, asma köprüler genellikle geniş açıklıklı nehirleri ve derin vadileri geçmek için inşa edilirler. Asma köprülerin sayısının artması ve davranışlarını modelleme zorluğu araştırmacıların ilgisini çekmiştir. Tasarımla ilgili birçok zorluk, uzun merkezi açıklığı nedeniyle ortaya çıkar. Dünyada birçok asma köprü vardır ve bu köprüler için dinamik davranışın birincil sorun olduğu anlaşılmıştır. Son yıllarda, asma köprülerinin davranışlarını ve titreştikleri zaman dinamik özelliklerini belirlemek için çeşitli araştırmalar yapılmıştır. Bununla birlikte, bir asma köprünün yapısının karmaşıklığı, asma köprünün dinamik davranışını anlamada ve dinamik özelliklerini belirlemede önemli zorluklar çıkarır.

Sıradan köprülerde hareketli yüklerin dinamik etkisi üzerine çeşitli çalışmalar yapılmıştır. Ancak, farklı özelliklere sahip çeşitli bileşenlerden oluşan karmaşık asma köprü yapıları nedeniyle, kablo destekli köprülere doğrudan uygulanamazlar. Sonuç olarak, karmaşık yapısal yanıtı dikkate almak ve hareketli yükler altında tepkilerini gerçekçi bir şekilde tahmin etmek için kablo destekli köprüler üzerinde daha fazla araştırma yapılması gerekmektedir. Asma köprülerinin davranışının incelenmesi için çeşitli çözüm yöntemleri uygulanmıştır. Bir asma köprünün davranışını belirlemek için kullanılan analitik yöntemlerden biri Yerdeğiştirme (Deflection) Teorisi' ne dayanır. Yerdeğiştirme Teorisi' ne giden yaklaşık yöntemlerin tarihsel bir incelemesi başka bir yerde bulunabilir. İyi ortaya konulmuş yerdeğiştirme teorisi, diferansiyel denge denklemini çözmeye çalışır ve çözümler için analitik ifadelerin kullanılmasına izin verir. Bununla birlikte kapalı açık analitik çözümler her zaman mümkün değildir ve bir çok durumda sayısal hesap yöntemleri kullanılmalıdır. Yüksek hızlı bilgisayarların ortaya çıkması ve sayısal yöntemlerin kullanılmasıyla asma köprülerin dinamik özelliklerinin incelenmesinde büyük ilerlemeler sağlanmıştır. Ayrıntılı modellerle elde edilen yaklaşık çözümlerin tutarlılığını tahmin edebilecek basitleştirilmiş modeller geliştirmek için birçok çaba gösterilmiştir. Son yıllarda, hem

malzeme ve hem de geometri deęişimi bakımından doęrusal olmayan köprü davranışını göz önünde bulundurarak işletme trafięi, rüzgar ve deprem yükleri etkisi altındaki asma köprülerin tepkisini deęerlendirmek için arařtırmacıların yanı sıra arařtırmacıların da uyguladıęı birçok ticari sonlu eleman yazılım paketi geliřtirilmiřtir.

Asma köprülerinin titreřimi tasarımıda göz önünde tutulması gerekli önemli bir konudur ve depremsel aktivitenin yüksek olduęu yerlerde ve tayfunun ve kuvvetli rüzgarların meydana geldięi yerlerde dikkate alınmalıdır. Bu amaçla bu çalıřmada, asma köprünün yer deęiřtirme yanıtı hareketli yük ile düşey depremin köprüye aynı anda etki etmesi durumunda incelenmiřtir. Önceki çalıřmalarda, asma köprünün düşey yerdeęiřtirmeleri, kablo gerilmesi ve ayrıca kablo gerilmesindeki deęiřim incelenmiřtir. Bazı arařtırmacılar hareketli yük nedeniyle asma köprülerin titreřimine odaklanmıřtı, ancak çalıřmaların çoęunda askıların uzayabilirlięi ihmal edilmiřtir. Bu çalıřmada hareketli yüklere baęlı olarak kablo kuvvetinin hesaplanmasına ek olarak, asma köprünün yerdeęiřtirme hız ve ivme yanıtı hesaplanmıřtır.

Bu sırada, ilk olarak asma köprünün tabliyesi ile kablosunun hareket denklemi türetilmiřtir. Hareket denklemleri türetirken, bu çalıřmanın metninde kapsamlı bir řekilde ele alınan bazı varsayımlar yapılmıřtır. Bu çalıřmada askıların uzayabilirlięi göz önüne alındıęından, asma köprünün düşey yerdeęiřtirme, hız ve ivme yanıtını belirlemek için hareket denklemi olan bir kısmi türevli diferansiyel denklem sistemi çözülmektedir. Kablo ve tabliye için hareket denkleminin türetilmesinden sonra, kısmi türevli diferansiyel denklem sistemi, deęiřkenlerin ayrılması yöntemi uygulanarak sadece zamana ve sadece uzay koordinatlarına baęlı olan iki ayrı adi türevli diferansiyel denkleme dönüřtürülmüřtür. Asma köprünün düşey yerdeęiřtirmelerini belirlemek için, asma köprünün davranıřı iki kısma ayrılmıřtır, ilk kısım statik analiz ve ikinci kısım dinamik analizdir. Psüdo-statik parçanın çözümleri için, denklemde integral bir terim olduęundan sonlu farklar yöntemi kullanılmıřtır. Dinamik parçanın çözümleri ise herhangi bir sayısal çözüm yöntemine bařvurulmadan kapalı olarak elde edilmiřtir.

Sayısal çözümleri gerçekleřtirmek için bir MATLAB programı hazırlanmıř, bu programın doęruluęunu belirlemek için de 2013 yılında yayınlanmıř olan Choi makalesinde çözümleri uygulama kullanılmıřtır. Sonuçlar arasındaki fark kabul edilebilir mertebededir ve sonlu fark yönteminde kullanılan aralık uzunluęu küçültüldükçe çözüm yakınsamaktadır.

Bu amaçla, asma köprü eř zamanlı olarak hareketli trafik yüküne ve düşey yer hareketlerine maruz bırakılmıřtır. Analiz için üç farklı yük durumu dikkate alınmıřtır. Tüm trafik yükü durumları trafik yükünün köprü üzerinde ilerleme hızı dışında aynı biçimdedir. Bu amaçla, MATLAB' da, iyileřtirilmiř yerdeęiřtirme yöntemi kullanılarak asma köprünün düşey yerdeęiřtirme, hız ve ivme yanıtları belirlenmiřtir. Sonuç olarak, hareketli yükün köprü üzerinde ilerleme hızının artmasının, asma köprünün düşey yerdeęiřtirmesinin de artmasına neden olacaęını göstermektedir. Asma köprünün düşey yerdeęiřtirme, hız ve ivmelerinin belirlenmesinde 50 mod dikkate alınmıřtır. İyileřtirilmiř yerdeęiřtirme teorisi ile elde edilen sonuçlar yerdeęiřtirme teorisi ile elde edilen sonuçlarla karřılařtırılmıř, yerdeęiřtirme teorisi ile elde edilen asma köprü düşey yerdeęiřtirme sonuçlarının güvenilir olduęu görülmüřtür. Askı kablolarında uzama, aksenal kuvvetler ve gerilmeleri belirlemek için, iyileřtirilmiř yerdeęiřtirme teorisinin kullanılması önerilmektedir.

Asma köprülerin doęal frekansları, köprünün eęilme rijitlięinin etki eden açıklık uzunluęu ile dięer yapısal boyutlara baęlıdır. Sonuçlara göre, asma köprünün ilk iki

titreşim modu simetriktir ve üçüncü modu ise asma köprünün ilk antimetrik modu olarak ortaya çıkmıştır.

Asma köprünün trafik yükü ile eşzamanlı olarak etki eden düşey deprem yer hareketine vereceği yanıtı belirlemek için üç farklı düşey deprem yer hareketi kaydı dikkate alınmıştır. Yazılan MATLAB programının doğruluğunu saptamak için de sonlu elemanlar yöntemi kullanılarak ABAQUS ortamında hazırlanan bir bilgisayar modeli kuruldu. Her iki program çalıştırılarak elde edilen sonuçlar karşılaştırıldığında sonuçların oldukça yakın olduğu ve uyum içinde olduğu görüldü.







## 1. INTRODUCTION

One of the most important civil infrastructures are bridges and they are normally designed to have long life spans. In suspension bridges which are flexible infrastructures the load-bearing portion is hung below suspension cables on vertical suspenders. Because of their aesthetic, architectural beauty and capability of utilization in long spans suspension bridges and cable-stayed, have gained much popularity and attention in recent decades. Vibration of the suspension bridges due to different dynamic loadings such as earthquake, wind, and moving loads has been a matter of concern throughout the history. Multiple support motions is a dynamic problem for structural engineers when they are trying to analyze long-span structures. Along with the rapid development of modern transportation networks, suspension bridges are mostly used to span deep valleys or wide rivers. Lot of studies have been performed in recent years to find out the vibrational properties of suspension bridges. Despite these researches and studies, the complexity of a suspension bridge structure makes difficult to determine vibrational characteristics.

Various studies have been performed for dynamic response of ordinary bridges when they are subjected to moving loads. However, for cable supported bridges, they cannot be directly applied since cable supported bridges are more complicate structures consisting of various components with different properties. Consequently, more research is required on cable supported bridges to consider the complex structural response and realistically predict their response due to moving vehicles. To determine and study the behavior of suspension bridges various methods of analysis have been applied. A historical review of the approximate methods that lead to the deflection theory can be found elsewhere. The well-established deflection theory tries to solve the differential equilibrium equation and allows the use of analytical expressions for the solutions. However, explicit analytical solutions are not always possible, and numerical techniques must be used. With the advancement in computer technology and emergence of high-speed computers, major progresses in studying the dynamic characteristics of suspension bridges have been achieved through the use of numerical

methods. In addition, effort has also been given for developing simplified models that can predict response consistent with detailed model. In recent years, several commercially available finite element software packages have been used by engineers and researchers in order to predict and analyze the response of a suspension bridge from operational traffic, wind and earthquake loads taking into account both material and geometric non-linear behavior.

## **1.1 Classification of Bridges**

Bridges are structures constructed to connect places to overcome physical obstacles as well as provide passage for the road, railway, pedestrians, a canal or a pipeline. The obstacles to be spanned could be either developed by natural or man made causes and may belong to a river, a road, railway or a valley. Purpose and function of the bridge are important parameters in designing of bridges, the type of the terrain where the bridge is constructed and anchored, the required material for developing it, and the existing funds to construct it. There are several methods to categorize and classify bridge, the four usual and typical ways to classify bridges are:

### 1. Classification based on superstructure

- Beam bridges
- Truss bridges
- Arch bridges
- Cantilever bridges
- Cable-stayed bridges
- Suspension bridges

### 2. Classification based on material used

- Timber bridge
- R.C.C bridge (Reinforced Cement Concrete)
- Concrete bridge
- P.C.C bridge (Plain Cement Concrete)
- Aluminum bridge

- Composite bridge
  - Stone bridge
  - Steel bridge
3. Classification based on purpose
- Double-decked bridges
  - Car Traffic
  - Pedestrian bridges
  - Viaducts
  - Train bridges
  - Commercial bridges
  - Pipelines
4. Classification based on inter span relation
- Simple bridge
  - Continuous bridge
  - Cantilever bridge

### **1.1.1 Classification based on superstructure**

We are going to comprehensively describe classification based on superstructure in this section.

#### **1.1.1.1 Beam Bridge**

The most simple and oldest bridge type is Beam bridge or girder bridge. It generally made of one or more spans which are rested on pier or an abutment at each end.

First beam bridges that built by humans was an imitation of nature – seeing tree that had fallen across a stream inspired prehistoric humans to use the same technique where presence of bridge is necessary and crucial and also building of it was convenient for them. Herodotus, Greek historian, was the first person to leave the written document about the bridge in 484 BC. Bridge he wrote and mentioned about had been constructed across the Euphrates River in 8<sup>th</sup> century BC and was made from stone and

wood. Ancient Romans are famous for their arch bridges made of concrete and stone but they began to build bridges with simpler bridge types. The oldest known ancient Roman beam bridge was constructed across the Tiber River in 7<sup>th</sup> century BC which was in Rome and also known as “Pons Sublicius” which literally means “bridge made of wooden beams.” Romans were also the first to use cofferdams to build columns. They would drive a circular construction, made of wood and lined with clay, into the riverbed and pumped out water. That would leave the place to pour the concrete in and would also serve as a mold. When French engineer Hubert Gautier wrote the first book about building bridges in 18<sup>th</sup> century, bridge building became more of an exact science. Next book, “A Work on Bridge Building” written by American Squire Whipple improved this further by being the first text on analytical methods for calculating the stresses and strains in a bridge.

For building a simple bridge over a creek all you need is a wood plank or a stone slab. To carry road traffic and railroad modern beam bridges are built of steel or reinforced concrete which can also be post-tensioned or prestressed.

Placing of cofferdams which are constructed around each column location in the riverbed is first and crucial step in constructing of a beam bridge. Water is pumped from inside of them and shafts are drilled into the riverbed until they reach bedrock (which can be more than twenty five meters in depth.) To construct a foundation cylindrical cage of reinforcing steel is lowered into the shaft and then concrete is poured. Columns can be cast onto the foundation or precast and then placed there. The bridge end will rest on abutments and abutments are built on the riverbank where bridge ends by pouring concrete between the top of the bank and the riverbed. It will hold the deck of the bridge and prevent dirt from getting into the river. Prestressed concrete or steel girders are placed with crane onto columns and then bolted to the column caps. To complete bridge superstructure, precast concrete slabs or steel plates are placed across the girders which forms a solid platform. After last step, hot-applied polymer-modified asphalt is placed on the platform. Purpose of it is to be a moisture barrier. Above of the asphalt is placed a grid of reinforcing steel bars and then encased in a concrete slab. This grid contains two layers. As a final layer of the deck a concrete pavement is poured in a layer between twenty and thirty centimeters. Concrete can be poured into stay-in-place forms if they are used. If not, concrete pours a paving machine that spreads, consolidates, and smooth the concrete – all at once. Before

concrete stiffens, a skid-resistant texture is placed on it by manually or mechanically scoring the surface. Concrete also gets joints to prevent cracking every five meters before it is poured or after. These joints are the sealed with flexible sealant.

When a bridge is consist of beams spanning between only two supports, it is called a simply supported beam bridge. If more than two beams are connected rigidly together above the supports, bridge is called a continuous bridge. Schematic view of the beam bridge is displayed in **Figure 1.1**.

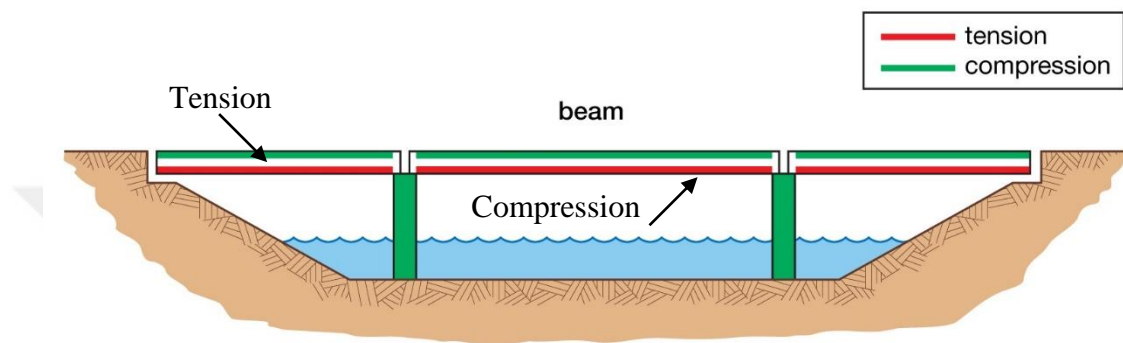


**Figure 1.1** : Beam Bridge schematic view.

### 1.1.1.2 Arch Bridge

One of the most popular types of bridges is arch bridge, which has been used for three millenniums and it was in height of popularity till industrial revolution when there were invention of advanced materials which can bear more stress allowed architect to create other modern bridge designs. However, even today arch bridges are still in use, and with the advent of modern materials which could bear more force and load, longer and larger arches can be build.

The basic principle of arch bridge is its curved design, instead of transferring load forces straight down they are conveyed along the curve of the arch to the supports on each end. These supports which called abutments withstand the load of entire bridge and are responsible for holding the arch in the precise position. Conveying of forces across the arch is done via central keystone on the top of the arch. Weight of the arch bridge pushes the surrounding rocks down and outward which results in very rigid and strong structure.

Because of this design, stone and wood arch bridges become very popular during the Roman Empire, whose architects managed to construct over one thousand stone arch bridges in Europe, North Africa and Asia. Even though many years passed a lot of

those bridges remain standing today, giving us the chance to personally see the wonders of the ancient architecture. There were usually semicircular arches in Roman designs, although several segmented arch bridges were made during their reign. These segmental arch bridges had one crucial design advantage which separated them from ordinary semicircular bridges – they allowed bridge builders to build arch of the bridge much higher and reduce the mass of the entire structure. These changes extended life span of bridges and also protected them from stresses of floods and strong rivers. During the life of Roman Empire, they built many wondrous and amazing bridges, lengthy aqueducts with multiple arches, bridges with flood openings on the piers, and many others.

As centuries passed on, medieval architects improved the designs of Romans, creating arch bridges with thinner arch barrels, narrower piers, pointed arches, lower span-rise ratios, and increased spans of arches (increasing to over 70 meters, most famously on the bridge at Trezzo sull'Adda who was in use from 17<sup>th</sup> to the end of 18<sup>th</sup> century). In Renaissance era architects attracted into arch bridges which not only sound engineering, but also fashion of their time, creating some of the most beautiful and famous bridges of the modern human civilization (such as Rialto Bridge in Venice). In the last 150 years, concrete, iron and steel helped engineers to create much more ambitious arch bridges which can now be seen in every country in the world. Arch bridge Schematic view is illustrated in **Figure 1.2**.

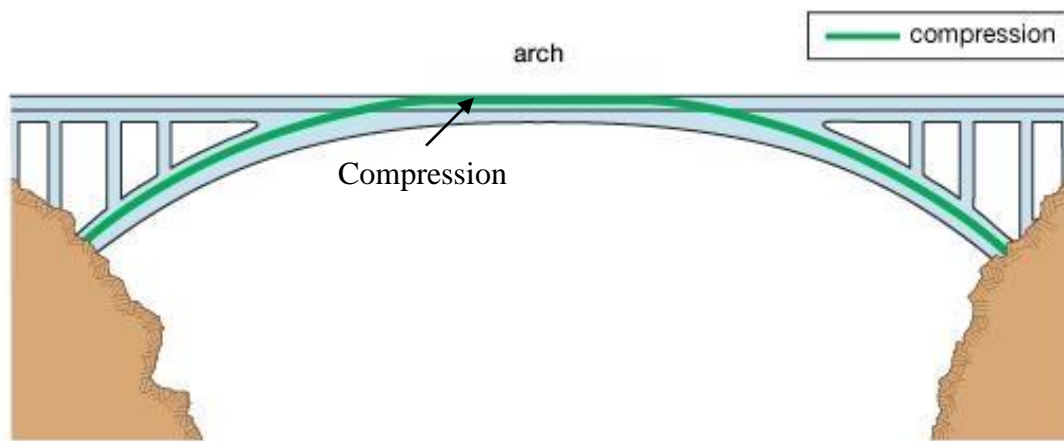


**Figure 1.2 :** Arch Bridge schematic view.

### 1.1.1.3 Cantilever Bridge

Main elements in cantilever bridge are cantilevers (cantilevers are horizontal beams, which are supported at only one end). Beams can be used in these bridges for smaller

(pedestrian) bridges or trusses which is made of box girders of prestressed concrete, or structural steel for larger bridges that bear road or rail traffic.

First cantilever bridges emerged in 19<sup>th</sup> century when a need for longer bridges showed itself. To overcome the problem of length, engineers of that time found out that presence of many supports would distribute the loads among them and help to achieve longer length. Predecessors of cantilever bridges were bridges which had hinge points at their mid-span. Heinrich Gerber was the one to be the first to invent and patent a cantilever bridge which did it in 1866. The first cantilever bridge that he designed was the Hassfurt Bridge over the Main River in Germany. It wasn't too impressive by today's standards - it had 38 meters in length but is considered the first modern cantilever bridge. Other early cantilever bridges were the High Bridge of Kentucky, designed by C. Shaler Smith in 1877, the Niagara Cantilever Bridge designed by Charles Conrad Schneider in 1883, and the Poughkeepsie Bridge designed by John Francis O'Rourke and Pomeroy P. Dickinson in 1889. The Forth Bridge, which is located in the east of Scotland was built over the Firth of Forth and it is one of the most famous early cantilever bridges. Full length of this railway bridge is 2,528.7 meters while its longest span has length of 520 m and construction of the bridge began in 1882 and it was completed on 1890. It remained the bridge with the longest span in the world until Quebec Bridge wasn't built in 1919 with its span of 549 meters.

In simple cantilever bridge we can see two cantilever arms extending from opposite sides of an obstacle that has to be spanned and they meet at the center. One of great advantages of cantilever bridges is that they can be built without false-works below nor temporary supporting towers and cables above. These tyoe of bridges are very stiff and they can carry large amount of loads without being threat to construction. Schematic view of the Cantilever bridge is indicated in **Figure 1.3**.

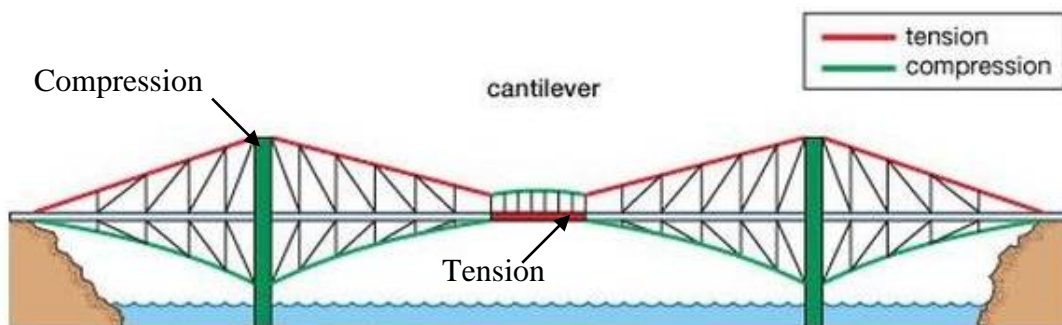


**Figure 1.3 :** Cantilever Bridge schematic view.

#### **1.1.1.4 Truss Bridge**

In Truss bridge main element is a truss which also is the main feature for these type of bridges. Truss is a system, which for being stable needs to be triangulated and usually made up straight interconnected structural elements. Since truss is a very rigid structure and it conveys the load from a single point to a much larger area it is used as bridge. Appearance of truss bridges return to very early time in the history of modern bridges and since they use materials efficiently are economic to construct.

Until industrial revolution in 19<sup>th</sup> century, nearly all bridges in use were made of stone. But iron and wood can withstand compression and tension force better comparing to stone and United States was rich in wood so they made many wooden bridges in those times and structure system for most of them were truss bridges. Town's lattice truss, a very simple variant of truss, was patented in 1820. In first half of 19<sup>th</sup> century very few truss bridges which made of iron were built although the first patent for an iron truss bridge was issued to Squire Whipple in 1841. But metal eventually started to replace wood, and wrought iron bridges started appearing in the United States in the 1870s only to be replaced by steel in 1880s and 1890s. In time in some states (like Pennsylvania) continued building of truss bridges for long spans continued till 1930s, while other (like Michigan) started building standard plan concrete girder and beam bridges.

Since the built of the first truss bridge, engineers made different shapes of truss bridge to overcome their particular problem and find better shape. This is the reason for appearance various forms of truss bridges. In truss bridge deck (roadbed) can be placed on top (deck truss), in the middle (through truss), or at the bottom of the truss. In case that the sides of the truss extend above the roadbed but are not connected, it is called a half-through truss or pony truss. Schematic view of the Truss Bridge displayed in **Figure 1.4**.



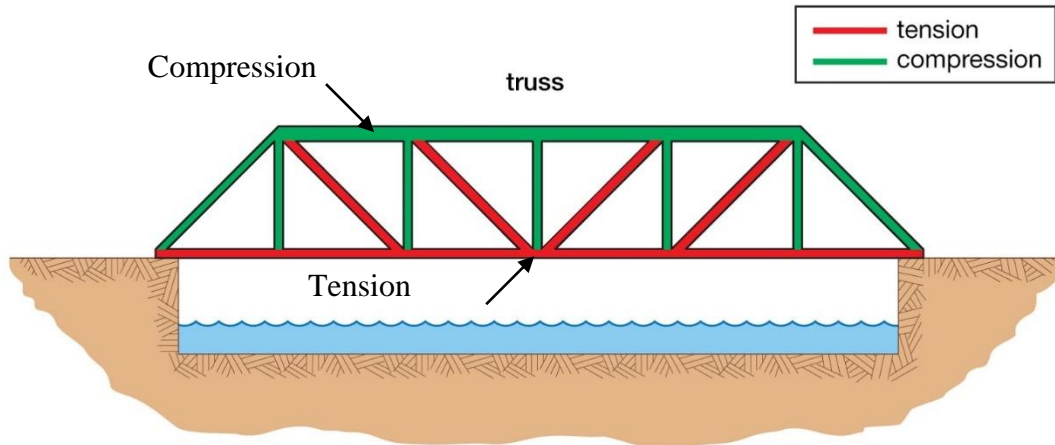


**Figure 1.4 :** Truss Bridge schematic view.

### 1.1.1.5 Cable-stayed Bridge

Cable-stayed bridge like suspended bridge has towers and cables which hold the deck, but instead of holding by suspender cables, deck is held by connecting cables directly to the towers. These type of bridges are usually designed to carry pedestrians, bicycles, automobiles, trucks and light rail. Usage of this kind of bridge is usually at places where cantilever bridges are short to cover the spanned length. First person who designed cable stayed bridges was Venetian inventor Fausto Veranzio (It is worth to note that he was the first person who designed modern suspended bridge). He published his works in 1595 in his book “Machinae Novae”. Appearance of first built cable-stayed bridges was around the 19<sup>th</sup> century and many early versions of suspension bridges were cable-stayed like footbridge Dryburgh Abbey Bridge (built in 1818), James Dredge's Victoria Bridge, in Bath, England (Built in 1836), Albert Bridge (built in 1872) and Brooklyn Bridge (1883). Other early cable-stayed bridges in the United States were Barton Creek Bridge between Huckabay, Texas and Gordon, Texas (built in 1889), bridge over Bluff Dale, Texas, (built in 1890a and it still largely stands). suspension bridge is not practical there economically.

Until the 20<sup>th</sup> century construction of this type of bridge continued when where built “Cassagnes bridge” (designed by A. Gisclard and built in 1909), le Coq's bridge at Lézardrieux in Brittany, France (designed by G. Leinekugel and built in 1924), and aqueduct at Tempul in 1926. Concrete-decked cable-stayed bridge over the Donzère-Mondragon canal at Pierrelatte was designed by Albert Caquot in 1952 and was one of the first the modern cable-stayed bridges but no other that came after, looked up to

it. Strömsund Bridge designed by Franz Dischinger completed in 1955 had more influence on the design of the later bridges and is more often mentioned as the first modern. Riccardo Morandi, Fabrizio de Miranda and Fritz Leonhardt are the design pioneers of the modern cable-stayed bridge and their designs had very few stay cables which was modern but resulted in higher erection costs. Later designs consists of much more cables which is more economic in the terms of building.

There are different variations for building a cable-stayed bridge:

“A side-spar cable-stayed bridge” consist of one tower and it has only one support which is at the one side of the bridge. One bridge constructed based on this principle is bridge in Winnipeg, Manitoba, Canada and is made to only bear the loads that caused by pedestrians.

“Cantilever-spar cable-stayed bridge” has a single cantilever spar on one side of the span. The purpose of the spar is to withstand the bending caused by the cables because cable forces of this bridge are not balanced by opposing cables and bridge applies large overturning force on its foundation. Some example of this bridge type are Puente de la Mujer (2001), Sundial Bridge (2004) and Chords Bridge (2008), which all of them are located in Spain.

When number of spans in a cable-stayed bridge exceeds three, bridge is called “Multiple-span cable-stayed bridge”. This kind of bridge is more complex since the loads from the main spans are not anchored back near the end abutments. In this case structure become less stiff so additional design solutions (like “cross-bracing” stays and stiff multi-legged frame towers) have to be applied.

In “Extradosed bridge” cables are connected to the deck further from the towers which are also lower than those of standard cable-stayed bridges, while it has stiffer and stronger deck.

In “Cable-stayed cradle-system Bridge” which is one of the latest forms, It has “cradle system” which carries the strands within the stays from bridge deck to bridge deck. These cables are continuous which means that there are not anchorages in the towers and its cables can be inspected, removed and replaced individually. Schematic view of the Cable-Stay bridge is illustrated in **Figure 1.5**.

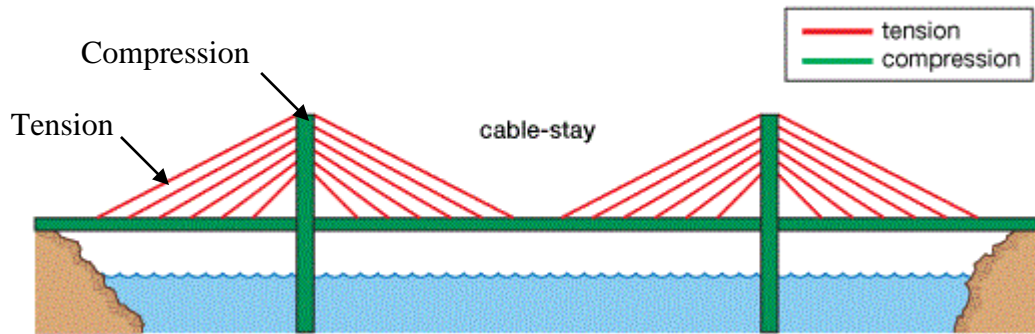


**Figure 1.5 :** Cable-stayed Bridge schematic view.

### 1.1.1.6 Suspension Bridge

Suspension cable in suspension bridge is an important feature of suspension bridge. Suspension cable is between pylons and the deck are hanged from them vertical hangers. Almost all of the load is carried by Suspension cables which are anchored at each end of the bridge.

Current Suspension bridges and examples of them which were built in the early 1800s, actually evolved from the simple suspension bridges. These bridges are one of the oldest versions of bridge which made by man. They have cables for load-bearing but don't have towers. Thangtong Gyalpo King of the Empty Plain, Tibetan saint and bridge-builder from the 15<sup>th</sup> century was the one who built Earliest versions of suspension bridges. He built over 58 iron chain suspension bridges around Tibet and Bhutan and it is worth to note that one of his bridges survived until 2004 when it was destroyed by a flood. Majority of his bridges had chains which acts as suspension cables while in earlier bridges that designed by him, he used ropes from twisted willows or yak skins.

The first design of a suspension bridge that is similar to today's modern designs appeared in book "Machinae Novae" from 1599 which was written by Venetian polymath Fausto Veranzio. He also has designs in his book for a timber and rope suspension bridge, and a cable-stayed bridge and hybrid suspension using iron chains.

Suspension bridge at Jacob's Creek in Westmoreland County, Pennsylvania is the first iron chain suspension bridge built in United States. This bridge was the first to have all the necessary components of a modern suspension bridge and was designed by James Finley who patented a system for suspending a rigid deck from a bridge's cables in 1808. This years is considered as a Beginning of an era of the modern suspension

bridges. After that, two bridges were built in England: Dryburgh Abbey Bridge which is built in 1817 and Union Bridge which is built in 1820. The first large bridge that implemented the technique invented by Finley was bridge over the Menai Straits in Wales built by Thomas Telford and finished in 1826. For the first time Cables consisting of many strands of wire for suspension were used instead of chains in 1930 by French engineers. Instead of transporting cables prefabricated John Roebling, American inventor, found a way to spin them at the place of building. He also comes up with rigid deck platform idea which is stiffened by trusses.

From that time suspension bridges gain more attention because they allowed to span spaces that could not be spanned with conventional methods. Its advantages are that it could have longer spans comparing to other types; Since it uses less material it is cheaper bridge type (even with longer spans); during construction it does not require access from below so bridge elevation would not affect construction procedure; it can resist earthquake more than other types; and it can be changed and modified easily to accommodate wider vehicles or to add additional lanes. Like everything it also has its disadvantages: In order to avoid vibration it must be made very stiff or aerodynamic so winds with high speed would not cause any vibrations; due to relatively lower stiffness of a board it is very difficult to carry heavy rail traffic compared to other bridge types. Length of the suspension bridges main span (longest span in bridge) are often used for comparing suspension bridges. Akashi Kaikyō Bridge is the suspension bridge which is built in 1998. Main span length is 1,991 meters and it connects Awaji Island and Kobe in Japan. Xihoumen Bridge on the Zhoushan Archipelago is another example of long suspension bridge, which located in the largest offshore island group in China with length of 1,650 meters. Schematic view of the Suspension Bridge is displayed in **Figure 1.6**.

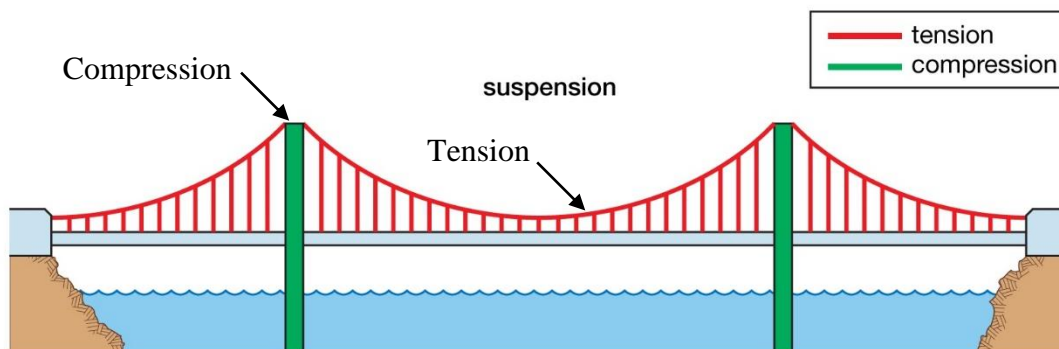


**Figure 1.6** : Suspension Bridge schematic view.

## 1.2 Cable Bridges Structural System

In cable bridges, cables play an important role in integrity and stability of the bridge. For instance in cable stayed bridge deck is connected directly to towers which existence of the cables are necessary for stability of the bridge and this is same for suspension bridge in which hangers hold the deck at position which are connected to the suspender cable or main cable. In the following subsection structural system of both bridges are discussed.

### 1.2.1 Cable-stayed bridge structural system

Cable-stayed systems are categorized based on the different longitudinal and transverse cable arrangements. Cable layout is fundamental issue that concerns cable-stayed bridges. It not only affects the structural performance of the bridge, but also the method of erection and the economics.

The arrangement of the cables involves a number of considerations. It depends on the bridge requirements, site conditions and aesthetics appearance. The longitudinal arrangements are classified as follows:

Harp or parallel system:

In harp or parallel system cables are parallel to each other and they are connected to the tower at different heights. Beauty of this configuration is very pleasant. However, the compression in the girder is higher than the others patterns, and the tower is subjected to bending moments.

Fan System:

Fan system is result of modification of the harp system; the cables are connected at the same distance from the top of the tower. The fan system is attractive for a bridge where the longitudinal layout is a single-plane, because the cable slope is steeper, it needs and consequently the axial force in the girder is smaller.

Radial System:

With the radial configuration, all the cables connect to the top of the tower. This is a convenient cable configuration because all the cables have their maximum inclination; therefore the amount of material required in the girder is reduced. However, this configuration may cause congestion problems and the detailing may be complex.

In **Figure 1.7** cable arrangement of the cable-stay bridge is displayed.

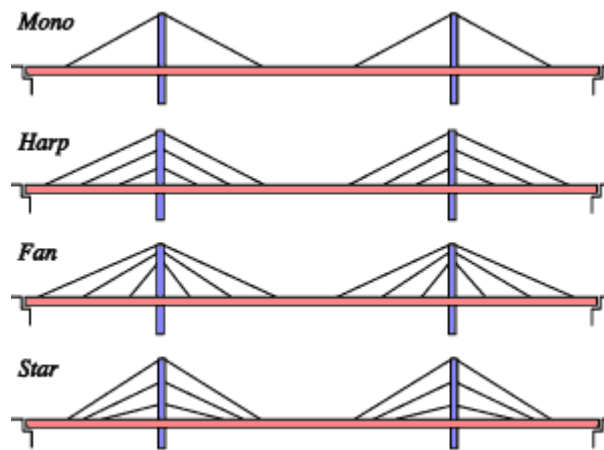


**Figure 1.7 :** Cable stayed bridge cable arrangement.

### **1.2.2 Suspension bridge structural system**

Even though that a modern suspension bridge looks like a cable-stayed bridge, but truth is that they are actually different in construction, concept and principle. The suspension bridge has vertically suspended cables from a main cable to support the deck. The main cable is fastened at both ends of the bridge and runs between towers. The latter, on the other hand, has one or more towers from which taut cables connected directly to tower to support the deck, and these normally creating a series of parallel lines with a fan-like pattern.

For medium distances cable-stayed bridges are best option (since the length is longer than a cantilever bridge and shorter than a suspension bridge). From the 16<sup>th</sup> century cable-stayed bridges have been used and in the 19<sup>th</sup> century they became popular, and early designs combined features from both the suspension bridges and cable-stayed bridges. Famous Brooklyn Bridge is a great example of this. But in the 20<sup>th</sup> century, cable-stayed designs lost their popularity because larger distances used suspension bridges, while shorter gaps could be cover using reinforced concrete. At the end of the 20<sup>th</sup> century, cable-stayed became more popular again because there were larger construction machinery, a combination of new materials, and an increase in the need to replace renewing older bridges. Most of cable-styled bridges are located in the China and the United States.

### 1.2.3 Famous suspension bridges

In this section the most famous suspension bridges are presented. Furthermore the history of the longest bridges around the world and the prominent bridges that are located in Turkey are briefly discussed.

The most longest suspension bridges and their location is presented in **Table 1.1**.

**Table 1.1** : Longest suspension bridges

Name	Year opened	Main span (m)	Location
Akashi Kaikyō Bridge	1998	1991	Japan
Xihoumen Bridge	2009	1650	China
Great Belt Bridge	1998	1624	Denmark
Osman Gazi Bridge	2016	1550	Turkey
Yi Sun-sin Bridge	2012	1545	South Korea
Runyang Bridge	2005	1490	China
Dongting Lake Bridge Hangrui	2018	1480	China
Nanjing Fourth Yangtze Bridge	2012	1418	China
Humber Bridge	1981	1410	United Kingdom
Yavuz Sultan Selim Bridge	2016	1408	Turkey

- Akashi Kaikyō Bridge

Akashi Kaikyō Bridge is longest suspension bridge in world which construction of it ended at 1998. The main span of this bridge is 1991 meters long while side spans length are 960 meters and total length of this bridge is 3911 meters. It is worth to note that at the beginning of the construction main span was 1990 meters which due to the major earthquake which occurred in January of 1995 added extra 1 meter to the space between towers. Height of towers are 282.8 meters and diameter of cable are 112 centimeters. Akashi Kaikyō Bridge is shown in **Figure 1.8**.



**Figure 1.8** : Akashi Kaikyō Bridge

- Xihoumen Bridge

Xihoumen Bridge is opened to traffic at 2009. Main span of this bridge is 1650 meters while total length of the bridge is 2588 meters. Pylons height are 211.286 meters. The side view of the Xihoumen Bridge is depicted in **Figure 1.9**.



**Figure 1.9** : Xihoumen Bridge



- Great Belt Bridge

This bridge is located at Denmark and it opened to rail traffic in 1997 and road traffic in 1998. It has total length of 6790 meters and the main span of it is 1624 meters long. Width of the bridge is 25 meters and height of the towers is 254 meters. The captured photograph of the Great Belt Bridge is displayed in **Figure 1.10**.



**Figure 1.10** : Great Belt Bridge

- Osman Gazi Bridge

Construction of this bridge is started at 2013 and it opened to traffic in 2016. Total length of the suspension bridge is 2682 meters and main span is 1550 meters long. Girder depth is 4.75 meters and is made from steel. Pylons are also made from steel while their height is 236.4 meters. The view of the Osman Gazi bridge is depicted in **Figure 1.11**.



**Figure 1.11** : Osman Gazi Bridge

- Yavuz Sultan Selim Bridge

Construction of this bridge is started at 2013 and construction ended at 2016. Total length of this bridge is 1875 meters and main span is 1408 meters. The width of the bridge is 59 meters, girder depth is 5.5 meters and Pylons are 330 meters tall. Deck of bridge is made from steel and pylons are made from reinforced concrete. The captured photograph of the Yavuz Sultan Selim bridge is presented in **Figure 1.12**.



**Figure 1.12** : Yavuz Sultan Selim Bridge

#### **1.2.4 Advantages and disadvantages of suspension bridges**

The Advantages of Suspension Bridges

##### 1. Low Construction Costs

Since suspension bridges requires less materials for construction they cost less comparing to other type of the bridge. With three basic necessities such as anchorages, roadways and cables, suspension bridges are possible to construct. Having said, this, suspension bridges are great solutions to provide communities with functioning and useful bridges without much need for funding. These are beneficial in areas that lack infrastructure funds. And in the case of allotting budget for projects, the inexpensive costs in building these types of bridges can allow for other projects to be financed.

##### 2. Long Span

Possibility to construct them at different lengths, from 600 to 4000 meters is another advantage of suspension bridges and they are longer comparing to other types of the bridges. This feature allows engineers to build suspension bridges to connect and join very long distance locations. Depending on the demand and possibility given, these

bridges can be underspanned like the Pont des Bergues and the Micklewood Bridge. On the other hand, three long suspension bridges are in Denmark, Japan and China.

### 3. Ease of Maintenance

Apart from inexpensive construction costs, suspension bridges are known for their minimal maintenance requirements. Once construction is completed, there are no immediate needs for additional materials like cables. What is called for is simply regular maintenance. Moreover, it is known for durability and longevity, making major repairs not needed as often. Consequently, maintenance costs are also not that high.

### 4. Versatility

Suspension bridges do not only cost less to build, they can also be built practically anywhere so long as there are places for building support towers and anchorages. This is also because of the design which is suspended in the air, no inflow restrictors are needed to be placed underneath. They can also bear the beatings of earthquakes.

### 5. Attractive

Tourists, local and foreign in America love to cross the Brooklyn Bridge and visit the Golden Gate Bridge in San Francisco. Suspension bridges are more aesthetic and pleasing compared to truss and beam bridges because of the different shapes of these bridges. The linear and curved features of these bridges make them structurally beautiful. This is on top of the cables giving support to these bridges, making them versatile bridges.

The disadvantages of Suspension Bridges

#### 1. Loss of Income

Despite the low costs of constructing suspension bridges and the job opportunities they offer, the length of time needed to finish building these bridges are long. What happens is that the businesses that are within the vicinity will be affected since business operations will be hampered. Consequently, there will be loss of sales and profit. This can have a negative impact on the economy of the city or town. Also, bridges built to connect locations between bodies of water can affect the course of ships carrying supplies since they need to divert their routes. This can also result to loss of money since deliveries of goods can take longer.

#### 2. Weak in Winds

Despite flexibility and strength to withstand earthquakes, these bridges are not too strong when it comes to powerful winds caused by hurricanes. Too much strong winds can result to damages to suspension bridges. Collapse of the Tacoma Narrows Bridge

on November 7, 1940 in winds of at only 40 miles per hour is classic example for weakness of suspension bridges when they are subjected to strong wind loads. Although the disaster was blamed on design and construction, what happened that time presented risks associated with suspension bridges.

### 3. Load Limitations

Another disadvantage of suspension bridges is the material used which are the cables. These cables have limitations when it comes to bearing the weight of loads. Although it can allow a minimal weight with regard to vehicles passing through, too much weight can lead to the breaking of cables.

### 4. Limited Applications

Suspension bridges, despite their cost-effectiveness in construction and flexibility when it comes to site location, have limitations when it comes to its use. This is because they are vulnerable to be damaged and destroyed by strong winds and not durable enough to hold limitless weight, careful consideration should be taken before construction. That said, they can only be used by general traffic.

Suspension bridges have retained popularity around the world and this is evident with the number of these bridges that built all around the world. However, along with advantages also come the disadvantages. This is why engineers building these bridges should study the design and ensure requirements in building these bridges are met with accuracy and compliance.

## **1.3 Structural Components of Suspension Bridge**

Like most of the structures suspension bridges are made of substructure and superstructure. Substructure part is related to foundation, anchorage and piers. Meanwhile superstructure is referred to tower, deck, suspension cable and hangers. In brief, in the following section important parts of the suspension bridge will be discussed. Structural components of the suspension bridge are depicted in **Figure 1.13**.

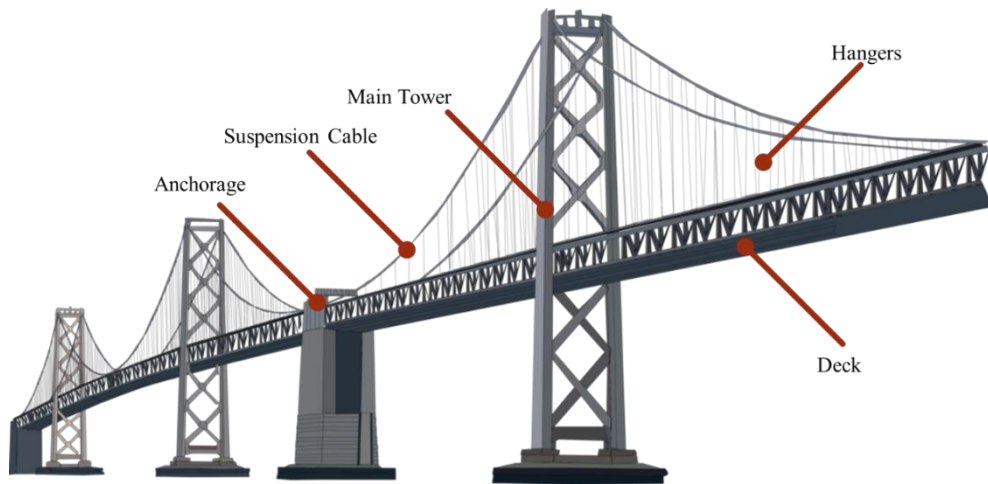


**Figure 1.13 :** Structural components of the suspension bridge

### 1.3.1 Tower

Purpose of tower or pylon is to hold the suspended cable. End points of the cable is attached to the tower to provide cable sag at a sufficient height. Other function of the tower is to carry the stiffening girder and side span. Vertical loads due to suspended cables are static loads applied to the tower, and loads due to wind and traffic are dynamic loads applied to the tower. For building towers usually three materials are used which are reinforced concrete, steel and timber. For building towers of long span cable-stayed and suspension bridge, reinforced concrete and steel can be used whereas the timber is only used for building towers of pedestrian bridge.

#### 1.3.1.1 Towers classification in longitudinal and transverse direction

Towers are classified into rigid, flexible, or locking types which are illustrated in **Figure 1.14**. Flexible towers are commonly used in long-span suspension bridges, rigid towers of multi-span suspension bridges to provide enough stiffness to the bridge, and locking towers occasionally for relatively short-span suspension bridges.

In **Figure 1.15** Towers classification in transverse direction are displayed. Towers in transverse direction are classified into portal or diagonally-braced types. Moreover, the tower shafts can either be vertical or inclined. Typically, the center axis of inclined shafts coincide with the center line of the cable at the top of the tower. Careful examination of the tower configuration is significant, in that towers dominate the bridge aesthetics [1].

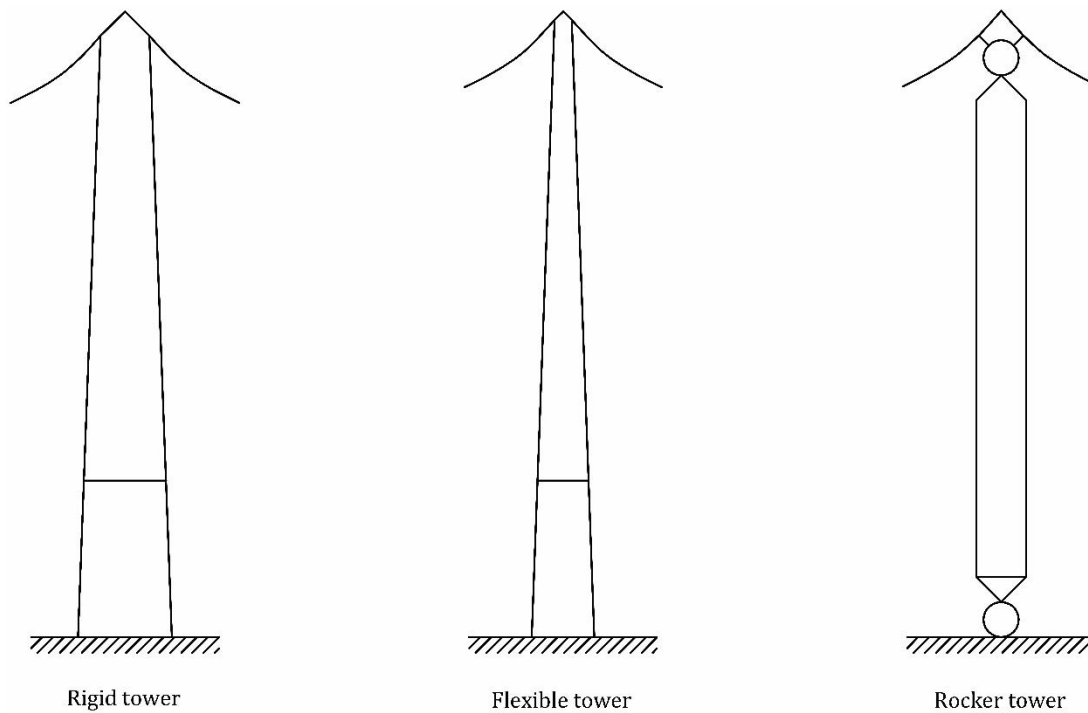


**Figure 1.14 :** Towers classification in Longitudinal Direction

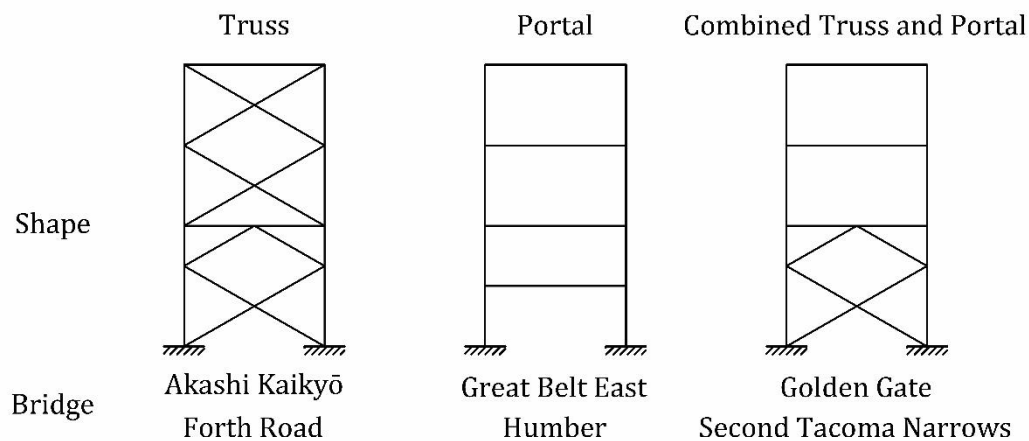


**Figure 1.15 :** Towers classification in Transverse Direction

### 1.3.2 Deck

The duty of the deck is to withstand the load caused by the train and the vehicles. The deck is connected to the main cable by the vertical hangers. The self weight of the deck should be as low as possible, and this is due to the fact that the deck is kept by the hangers. Existence of stiffening girders in suspension bridges is necessary since they withstand wind loads and important example of their crucial role in stability of suspension bridge is Tacoma Narrows Bridge which absence of stiffening girder reduced structure stiffness which bridge colla

d due to moderate wind load. stiffening girder could be in shape of I-girder, truss and box girder. In **Figure 1.16** different types of the girders displayed.

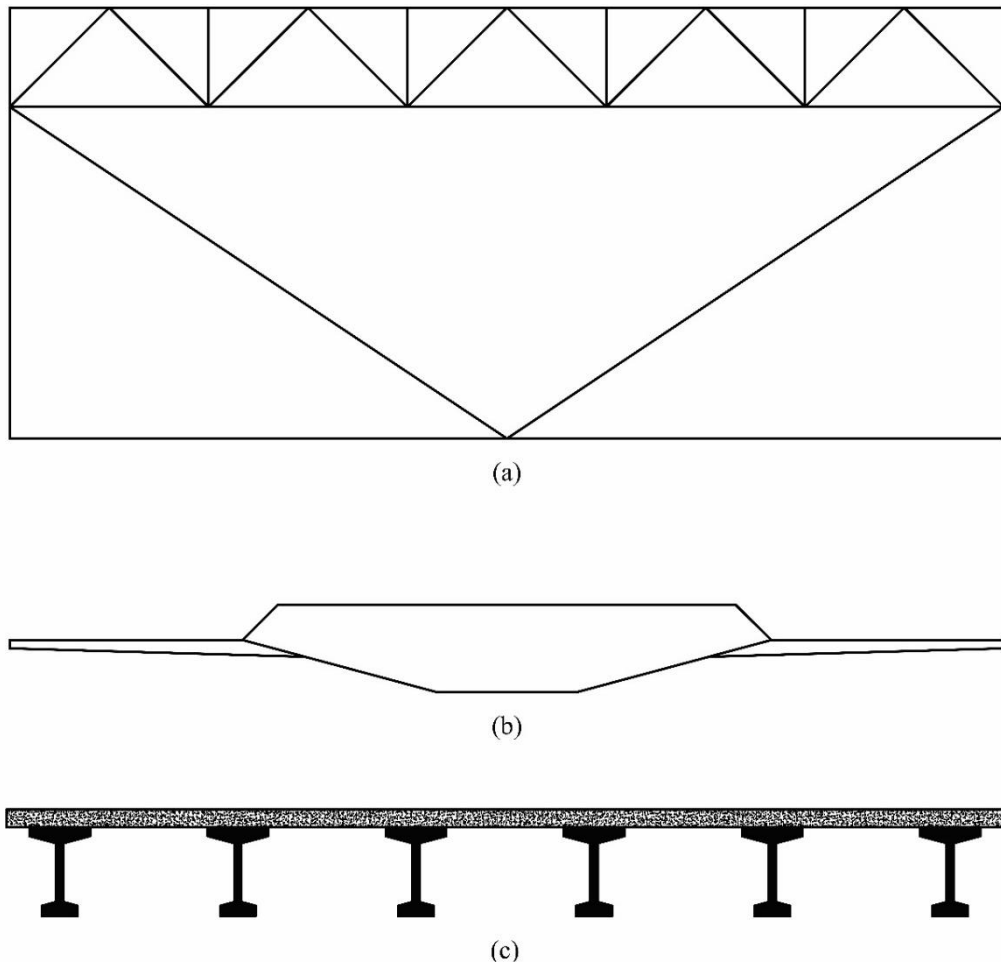


**Figure 1.16 :** Girder types (a) Truss girder (b) Box girder and (c) I-girder

Stiffening girder could be hinged or continuous in former there is not any moments at the tower and deck intersection while in later moment exist at the intersection.

**Figure 1.17** depicts both types of stiffening girder.

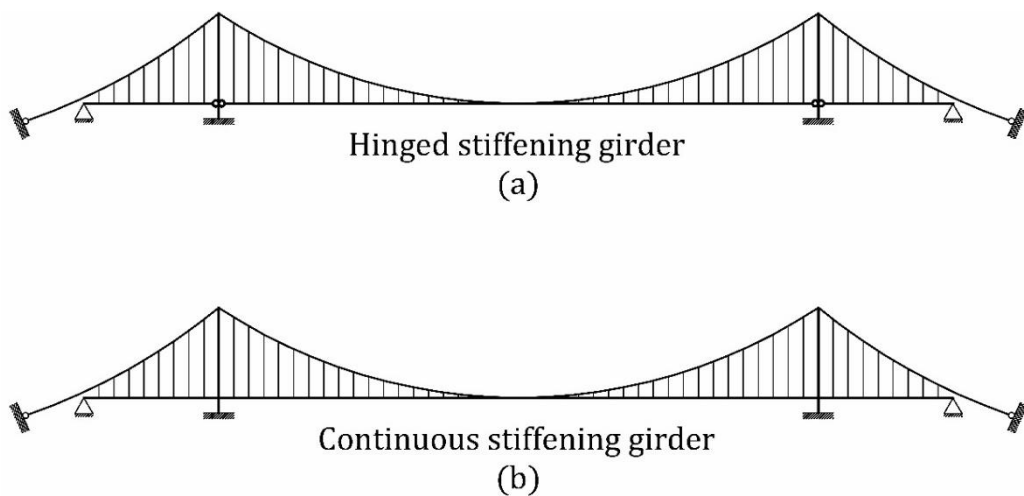


**Figure 1.17 :** Stiffening girder (a) Hinged stiffening girder and (b) Continuous stiffening girder

### 1.3.3 Hangers

The purpose of the hangers is to connect the deck and stiffening girders to the main cable and also to transfer the loads from vehicles and trains to the main cable. Hangers are spaced with equal distances along the span and they could be vertical or diagonal. In **Figure 1.18** different types of hanger and their arrangement illustrated.

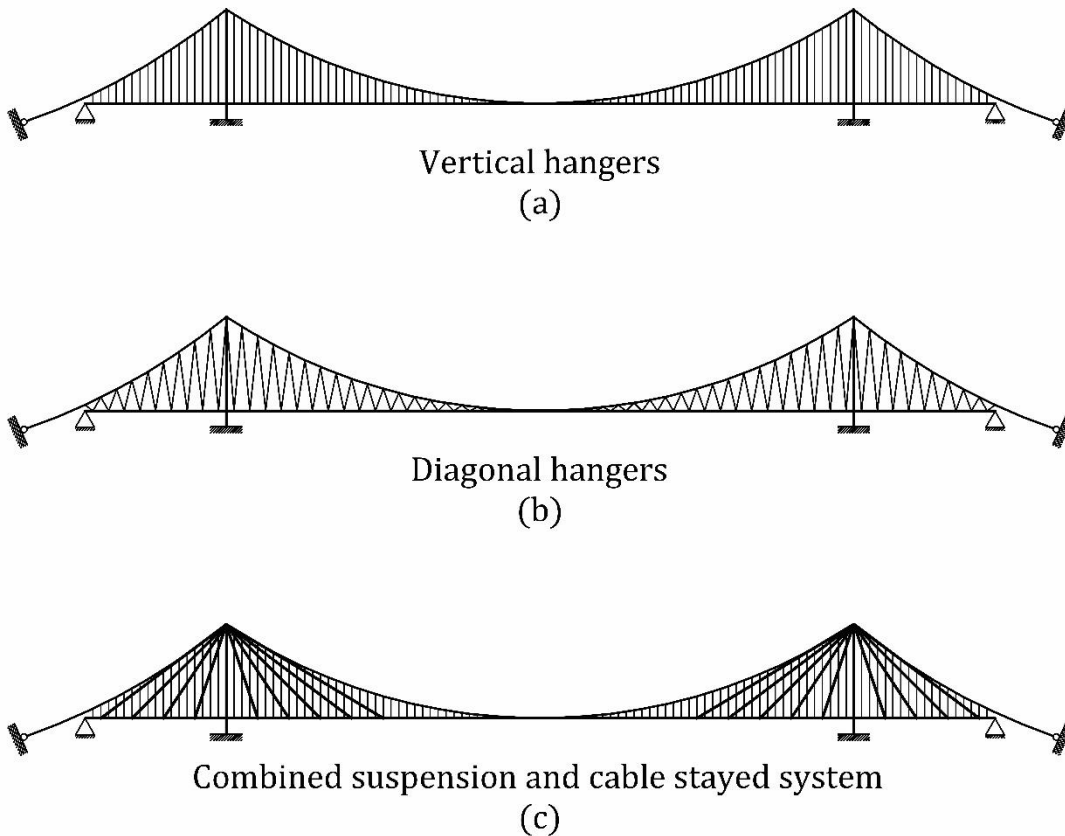


**Figure 1.18 :** Hangers type (a) Vertical hangers, (b) Diagonal hangers and (c) Combined suspension and cable-stayed system

Tsing Ma bridge and Akashi Kaikyō Bridge which are located in China and Japan are famous examples of suspension with vertical hangers. Bosphorus bridge in Turkey and humber bridge in England are examples of the suspension bridge with diagonal hangers. The one of the most famous types of combined suspension and cable-stayed system is Yavuz Sultan Selim Bridge which is the third bridge constructed over the bosphorous and opened to the traffic recently.



### 1.3.4 Suspension cable

Suspension cables hold the deck which carries the traffic loading and also they transfer these load to the towers. Suspension cables usually are designed for tension forces and most of the time they can not withstand any compressive forces. Suspension cables are longer than span of the bridge since at their end points they are connected to top of the towers while there is sag at middle point of them which means that these cables are not taut. In most of the suspension bridges sag to span ratio is between 1:8 and 1:12.

### 1.3.5 Anchorages

The main function of anchorage is to support the ends of the main cable and to prevents any movements in the main cable by transferring the force from the main cable to the ground. Since the anchorage has to resist a large force the design of anchorages is very tough unless the ground on which the anchorage is to be positioned is good and also if sound rock is available in the ground.

#### 1.3.5.1 Types of cable anchoring

Suspension bridge could be either self anchored or externally anchored. External anchorage is most common while in some of bridges self anchored system implemented. In externally anchored, suspension bridges transmit their tensile forces from the main suspension cables to an external anchorage and the possibility of an external anchorage depends on the soil conditions. In Self-anchored main cables are secured to the stiffening girders instead of the anchorage and the axial compression is carried into the girders. The Konohana Bridge in Japan and The Chelsea Bridge in England are examples of the self anchored bridge. Both of these anchorage types are illustrated in **Figure 1.19**.

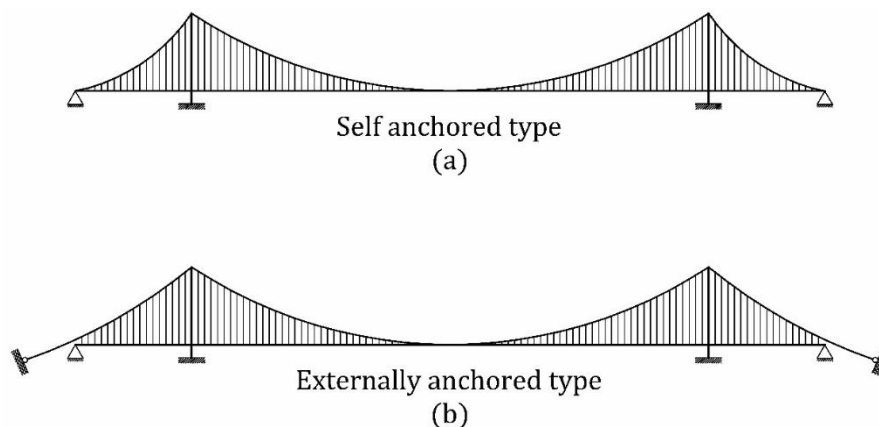


**Figure 1.19** : Anchorage type (a) Self anchored type and (b) Externally anchored type

## 1.4 Literature Review

Lots of studies have been carried out on suspension bridges, in which some of them focused on extensible hangers. In most of these studies researchers considered hangers as inextensible elements during vibration which do not show any axial deformation.

Steinmen in 1959 computed natural frequencies of suspension bridge. In his study he assumed sine-curve for span and also parabolic shape for the cable. By using energy method he found stiffness equation and proposed two equations for each symmetric and anti-symmetric modes. In anti-symmetric equation only  $I$  (moment of inertia) and  $H$  (Horizontal cable tension) is effective while in symmetric equation he introduces new parameter called  $\Delta H$  (increment in Horizontal cable tension) This equation is applicable to symmetric modes while for ease and to increase the speed of calculation former suggested for symmetric modes [2].

Xu et al in 1997 done research about vibration of the Tsing Ma suspension bridge. This bridge connects new infrastructures such as airport and ports located on Lantau island to Hong Kong. In this study they computed dynamic characteristics of the bridge which is built in a typhoon region. They measured dynamic characteristics for lateral, vertical and torsional vibration with finite element method and compared it with the results obtained from numerical method. The first vertical mode of the bridge they compute was almost anti-symmetric while the second and third modes they computed were almost symmetric. The interesting thing in this study was appearance of the first anti-symmetric mode before the symmetric mode [3]. This fact has also been observed in the study of Abdel-Ghaffar and Scanlan in 1985 [4].

Wollmann in his study in 2001 derived fundamental equations of suspension bridge analysis based on the deflection theory and computed cable tension due to the live loads that act on the bridge. This method covers tower flexural rigidity which is different from Steinman's research and Timoshenko and Young research. Since differential equilibrium equation consists of one variable and one unknowns they needed an extra equation to find unknown parameter. Thus, they used compatibility equation in which there is connection between increment in horizontal tension of the cable, tower displacement and cable elongation. After solving this equation which must be solved in iterative manner until the error is considerably small, they introduce increment in tension to the differential equation. It is worth to note they use a numerical example which shows how to find deflection function of the suspension bridge [5].

Compatibility equation and the derivation of it is completely described in second chapter.

Cobo del Arco and Aparicio in 2001 done research for static analysis of the suspension bridge to determine vertical displacement of the bridge. In their research they try to investigate famous suspension bridges in the world. In their study they defined dimensionless parameters which helped them for comparing various suspension bridges. They define dimensionless parameters  $\lambda$  and  $\alpha$  which are dependent on geometric properties and live load which acts on the bridge. They showed that deflection theory is still efficient to determine displacement and deflection even in presence of the computer softwares which implement FEM method to solve problems. Another result that they obtained indicated that the stiffening girder has small influence in the control of the deflections and also  $\lambda^2$  has negligible effect in the determination of bending moments [6]

Yau in 2009 done research in regard of the suspension bridge dynamic response due to the moving oscillator and ground excitation. In this study some assumptions has been made such as stiffening girder is elastic and behaves linear, bridge towers are rigid and they do not show any deflection and the cable sag is adjustable between the suspension cable and bridge deck. He defined equation of motion for the suspension bridge while he assumed that vertical hangers are inextensible. Since equation of motion is partial integro-differential equation they decompose the equation to pseudo static and dynamic part which leads he to solve ODE and IDE. To solve IDE he considered that increment in horizontal component of cable tension is negligible and it is equal to horizontal component of cable tension. To solve time dependent ODE he uses Newmark method. At last part he tries numerical example in which he investigates multiple support motion with uniform support motion and also speed of moving load in which resonant of the bridge occurs [7].

Liu et al. in 2011 in their research they proposed differential equations for both cable and deck. Likewise to yau's research they decomposed differential equation to pseudo-static and dynamic part. In their research they assumed that deck and cable deflection are same during vibration, thus assumption causes that stiffness term related in differential equation to drop. They used newmark method to solve their differential equation which is an iterative method to solve differential equation. At last step they investigated numerical example and for this purpose they investigated Messina Bridge [8].

A research study performed by Choi et al. in 2013 computed multi span suspension bridge deflection with deflection theory method for different load cases and then compared the results with FEM method. In this research the effect of towers displacement on deflection of the bridge considered [9].

Choi and Gwon performed a research in 2015 to compute vertical deflection of the suspension bridge and compared the result for deflection theory, improved deflection theory and FEM method. In their research they investigated different parameters such as continuity of the deck, span length and magnitude of the load. Result indicated that there are not much difference in vertical deflection of the suspension bridge between these three methods but for finding moment in span improved deflection theory and FEM methods are in good agreement while result differ considerably with deflection theory [10].

Gwon and Choi in 2017 investigated free vibration of the suspension bridge. In their research, an improved continuum model for free vibration analysis of three-span suspension bridges with either a hinged girder or a continuous girder was assessed to investigate the effects of hanger extensibility on free vertical vibrations. Their research indicated that hanger extensibility affects higher modes more if the relative girder stiffness is not large [11].

In another research which is performed by Gwon and Choi in 2018 they investigated three dimensional suspension bridge which consists three span. In their study they evaluated response of the bridge for different live loads when a moving load crosses the bridge. They also compute velocity and acceleration response of the bridge. Finally they compared their result with FEM method which proved efficacy of the method they used in their study [12].

Hayashikawa and Watanabe performed a research in 1982 to determine dynamic behavior of the suspension bridge under moving loads. After proposing dynamic equation for the suspension bridge, they investigated three different types of the bridge. Their results indicated that the effect of the cable support at the top of the tower on natural frequencies is negligible while effect of the girder supports at the end of spans are considerable. Values of natural frequencies in continuous suspension bridge are larger than hinged suspension bridge [13].

Materazzi and Ubertini in 2015 investigated behavior of the suspension bridge when the suspension cable which connects the two towers has been damaged at quarter span. Their investigation showed that in static response of the bridge, damaged suspension

cable cause sag augmentation and tension loss which are negligible since the mentioned changes are below the few percent. In dynamic response behavior of the bridge is a bit complicated, in antisymmetric modes damage would not affect mode shapes and with increase in modal order the sensitivity of natural frequencies of the bridge decrease. For symmetric modes, the second mode shows largest sensitivity to damage and likewise to antisymmetric modes, modal order increase cause less sensitivity to damage in symmetric modes. It is worth to note that natural frequency variations are more useful for detecting damage in suspension cable than mode shape variations [14].

Antony and Varma in 2015 modeled suspension bridge which consists of three spans and each span were simply supported at ends. Due to complexity of the problem they made some simplifications in their calculations. Results indicated that hanger flexibility has no effect on dynamic characteristics of the suspension bridge while increasing tower height and pre-stressing main cables increases natural frequencies. In lower modes non-linear calculation would not differ considerably from linear calculation while in higher modes these calculations deviate from each other significantly [15].

Sarker and Manzur in 2013 studied effect of different structural elements on the natural period of suspension bridge along its span. For simplicity they made some assumptions to ease analyze and calculations, such as that the behavior of all materials used are linearly elastic, and nonstructural components won't participate in bridge behavior. In their models deck width was 30m while number of spans varies. Results indicate that natural period of a suspension bridge affects with the tower height. As the ratio of tower height to span decrease, the natural period for vertical vibration decreases with the increment of the central span length. For lateral vibration, decreasing tower height to span ratio is favorable to obtain minimum natural period. Deck depth has significant effect on the natural period for both vertical and lateral vibration. In vertical vibration, with increase of deck depth to span ratio value of natural period decrease. On the other hand, to obtain minimum natural period for lateral vibration reducing ratio of deck depth to span found to be effective [16].

Enrique Luco and Turmo in their study in 2010 indicated that free vibration of suspension bridges are controlled by dimensionless parameters  $\lambda^2$  and  $\mu^2$ .  $\lambda^2$  is indicative of the cable axial stiffness and  $\mu^2$  represents bending stiffness of the girder. Their findings shows that the effects of  $\mu^2$  on the fundamental frequencies appear to

increase with the value of the cable stiffness parameter  $\lambda^2$ . Their study also indicate that effect of  $\mu^2$  on natural frequencies is much more for higher modes while  $\lambda^2$  has a considerable effect on the natural frequencies of the first two symmetric modes, but these effects reduce significantly for third and higher modes which can be neglected [17].

Chatterjee et al., in 1994 investigated the effect of the moving load on dynamic response of the suspension bridge. Likewise to other articles for simplicity they made some assumptions. For modeling the vehicle load, the vehicle is idealized as a 3D, 2D, or single sprung mass system. Results indicate that natural periods of vertical vibration of suspension bridges with rollertype cable connection are generally greater than those with hinged cable connection. Natural periods of torsional vibration with roller-type cable connection are found to decrease with the increase of the parameters  $\delta_1$  and  $\delta_2$  the variation of the natural periods is less sensitive to the variation of  $\delta_2$  compared to the variation of  $\delta_1$ . Natural periods for both vertical and torsional vibration of the bridge with hinged cable connection are found to decrease with the increase of flexural stiffness of the towers. For suspension bridges with hinged-type cable connection, natural periods of torsional vibration are significantly reduced with the increase of torsional resistance of the towers [18].

Goremikins et al., in 2013 prepared physical model of prestressed suspension bridge. The prestressing is organized in the stabilization cables. Experiment shows that increasing prestressing level increase natural-vibration frequency and this would help to improve dynamic characteristics of the suspension bridge [19].

Turmo and Luco in 2010 in their study shows that free vibrations of a suspended span with unloaded backstays and elastic hangers is controlled by five dimensionless parameters while the response of a symmetric three-span suspension bridge is dependent on six dimensionless parameters. Results indicate that flexibility of the hangers only affects natural frequencies for symmetric and antisymmetric modes higher than third mode and relative girder stiffness parameter  $\mu^2$  is greater than  $10 \times 10^{-3}$ . First three symmetric and antisymmetric mode shapes are not influenced considerably by flexibility of the hangers while for higher modes influence is appreciable. Flexibility of the hangers have been found that have negligible effect on the dynamic deck displacement and additional main cable tension when the bridge is subjected to localized impulsive loads acting at midspan or at the quarter points of the deck [20].

In another research which is performed by Fryba and Yau in 2009 focused on the vibration of suspended bridges subjected to the simultaneous action of moving loads and support motions in vertical direction because of earthquake. Their study shows that response of the suspension bridge increases if they consider earthquake effect. But the maximum acceleration along the main beam did not change a lot even though various time lags of the earthquake exciting the suspended beam have been taken into account. It is concluded that the suspension bridge will behave almost insensitive to the occurrence time of earthquakes when the train-type moving loads are passing the bridge. The dynamic effects are growing with the increasing speed of trains, as regularly on bridges. This phenomenon was observed and confirmed many times with other researchers [21].







## 2. DETERMINING EQUATION OF MOTION OF SUSPENSION BRIDGES

In order to compute deflection, velocity and acceleration response of suspension bridge when it is subjected to the moving load and ground motion simultaneously, equation of motion for suspension bridge derived. In this chapter mathematical approach for deriving equation of motion of suspension bridge for extensible and inextensible hangers assumption, explained in detail.

In the analysis of suspension bridges two theories have dominated over the last century, the elastic theory and the deflection theory. It began somewhere around 1823 with Navier's theory of the unstiffened suspension bridge and revealed the concept of cable stiffness. Around 1850 Rankine revealed a theory about the stiffened suspension bridge. In the late 19<sup>th</sup> century, the elastic theory is improved based on the Rankine theory by considering the elastic flexibility of the deck and cable. The deflection theory used during the early 20<sup>th</sup> century was the first theory of the stiffened suspension bridge to consider the change in shape of the cable and gave theoretical backing to propose very slender stiffening trusses.

Elastic theory assumes that the cable is parabolic under both the dead load and total loads. In elastic theory moment in the girder is computed by equation (2.1).

$$M = M' - y\Delta H \quad (2.1)$$

In above equation

$M'$  is live-load component moment of unsuspended girder.

$\Delta H$  is increment in horizontal component of cable tension.

$y$  is ordinate of main span cable at location of desired moment.

The live load moment acting in the girder is reduced by the effect of the increment in horizontal component of the cable tension.

The deflection theory accounts for an additional relieving moment provided by the horizontal component of the total cable tension when the bridge deflects  $w$ , under live load. This is called cable stiffness and reduces the moment in the girder by an

additional amount of  $(H + \Delta H)w$ . The deflection theory is therefore an extension of the elastic theory and is given in equation (2.2).

$$M = M' - y\Delta H - (H + \Delta H)w \quad (2.2)$$

In which  $(H + \Delta H)$  is horizontal component of tension in the cable is produced by dead and live load. Deflection theory is more accurate and economic comparing than elastic theory but in this theory effect of the cable extensibility neglected. In **Figure 2.1** schematic view of deflection theory has been displayed.

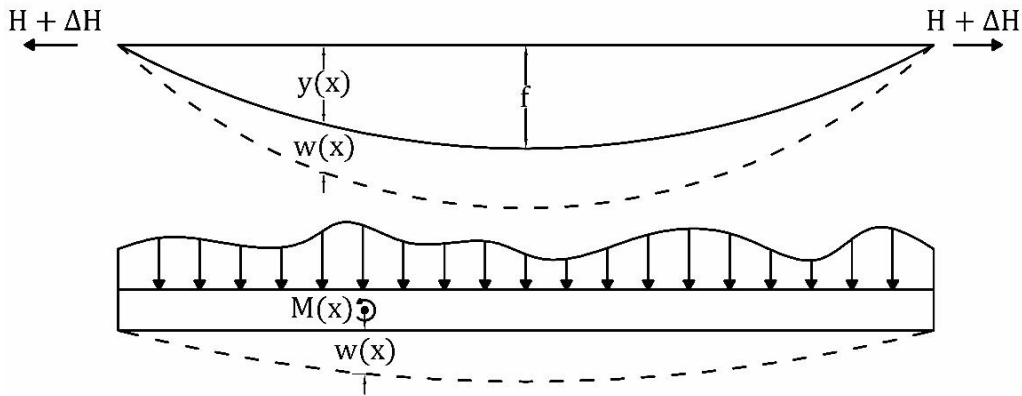


**Figure 2.1** : Elastic theory and deflection theory

However, in order to determine axial forces in the hangers and computing stress in hangers extensibility of the hangers must take into the account. In this study effect of the cable extensibility considered and deflection of the deck and cable of the suspension bridge computed.

During the vibration of the suspension bridges, loads that caused by vibration starts to act on deck and suspended cable of the bridge. The suspension bridge's deck is disconnected at pylons where bending moment (multiplication of  $E$ ,  $I$  and second derivative of the deck deflection) is equal to zero. In order to initiate the research some assumptions made which are:

- 1) The stiffening girder is modeled as a linear elastic Bernoulli-Euler beam with uniform cross section.
- 2) Dead load is uniform and deflected shape of the suspension bridge due to the dead load and own weight of the suspension bridge, considered as reference point for determining deflection of the suspension bridge.
- 3) The cable sag is adjustable between the suspension cable and bridge deck and under dead load cable shape is parabolic.

- 4) All of the dead and live loads are carried by suspension cable.
- 5) Speed of moving load is constant and would not change during vibration and crossing the bridge.
- 6) Hangers are massless, extensible and continuously distributed along the deck.
- 7) Hangers are vertical initially and remains vertical during vibration and no lateral displacement in in-plane and out-of-plane direction occurs.

## 2.1 Suspension Bridge Free Body diagram

Considering that suspension bridge is vibrating free body diagram of the suspended bridge deck is shown in **Figure 2.2**.

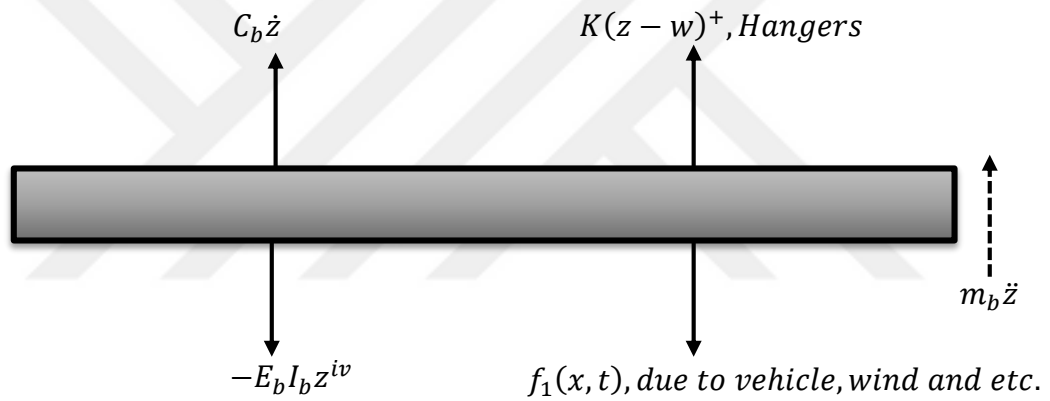


**Figure 2.2 :** Free body diagram of the deck

In above figure  $z$  represents movement of the deck while  $w$  represents movement of the cable,  $m_b$  is beam mass per unit length,  $E_b$  is modulus of elasticity of the deck,  $I_b$  is moment of inertia for deck  $C_b$  is deck damping coefficient,  $K$  is stiffness of the hangers and  $f_1(x, t)$  is external load which caused by traffic, wind and etc.

By considering the free body diagram equation of motion for suspension bridge deck indicated in equation (2.3).

$$m_b \ddot{z} + C_b \dot{z} + K(z - w)^+ - (-E_b I_b z^{iv}) - f_1(x, t) = 0 \quad (2.3)$$

Free body diagram for the cable is indicated in **Figure 2.3**.

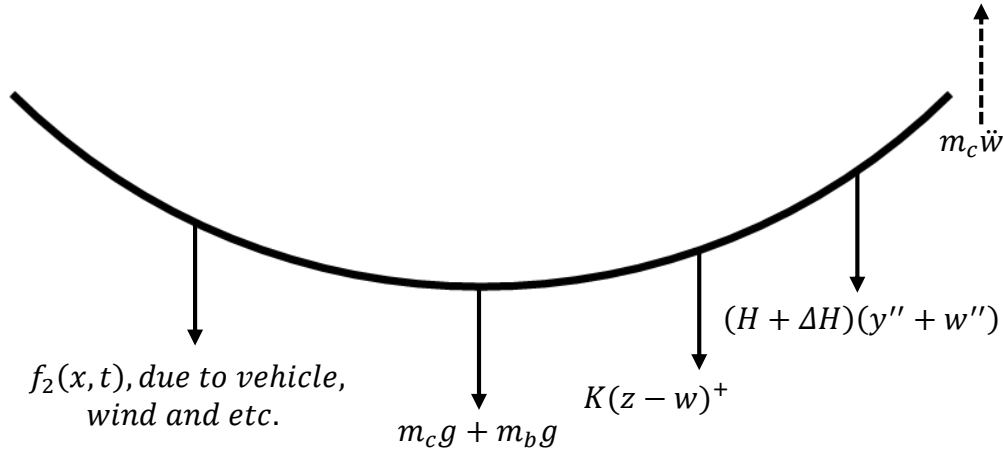


**Figure 2.3 :** Free body diagram of the cable

$H$  is the horizontal component of the cable tension,  $\Delta H$  is the increment in cable tension due to vibration,  $g$  is gravitational acceleration,  $m_c$  is cable mass per unit length and  $f_2(x, t)$  is external load which caused by traffic, wind and etc.

Equation of motion for suspended cable represented in equation (2.4).

$$m_c \ddot{w} - K(z - w)^+ - (H + \Delta H)(y'' + w'') - (m_c g + m_b g) - f_2(x, t) = 0 \quad (2.4)$$

## 2.2 Cable Tension and Increment of Tension Mathematical Formulation

Considering finite length of the cable with the length of  $\Delta s$  and cable Tension of  $T$  equilibrium for the cable has been derived in next steps. In **Figure 2.4** equilibrium of the finite length of the cable has been depicted.

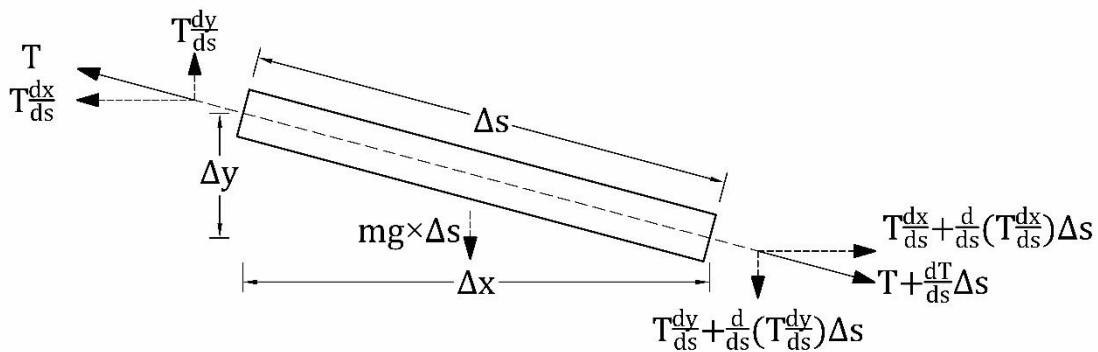


**Figure 2.4 :** Equilibrium of the finite length of the cable

Horizontal component of the cable is manifested in equation (2.5).

$$T \frac{dx}{ds} = H \quad (2.5)$$

$T$  in above equation is representing the cable tension and  $ds$  is finite length of the cable and  $dx$  is horizontal projection of the  $ds$ .

From equation 2.5, the relation between horizontal component of the cable tension and total weight of the cable and deck is obtained and illustrated in equation (2.6).

$$H \frac{d^2y}{dx^2} = -(m_c + m_b)g \frac{ds}{dx} \quad (2.6)$$

Length of the finite length of cable is given in equation (2.7).

$$ds = \sqrt{dx^2 + dy^2} \quad (2.7)$$

Dividing both sides of equation 2.7 by  $dx^2$  results in equation (2.8) which brought hereunder.

$$\left(\frac{ds}{dx}\right)^2 = 1 + \left(\frac{dy}{dx}\right)^2 \quad (2.8)$$

By inserting equation 2.8 to equation 2.6 the relation between total weight of the cable and the deck and cable tension derives which is manifested in equation (2.9).

$$H \frac{d^2y}{dx^2} = -(m_c + m_b)g \left\{1 + \left(\frac{dy}{dx}\right)^2\right\}^{1/2} \quad (2.9)$$

By considering that variation of the  $y$  with respect to  $x$  is negligible and is equal to 0, equation 2.9 would be simplified into equation (2.10).

$$H = -\frac{(m_c + m_b)g}{y''} \quad (2.10)$$

The increase in length of the cable due to vehicle vibration and external loads is presented in equation (2.11).

$$\frac{ds' - ds}{ds} = \frac{du}{ds} \frac{dx}{ds} + \frac{dy}{ds} \frac{dw}{ds} + \frac{1}{2} \left(\frac{dw}{ds}\right)^2 \quad (2.11)$$

Relation between increment in cable tension and increment in horizontal component of cable tension is presented in equation (2.12).

$$\tau = \Delta H \frac{ds}{dx} \quad (2.12)$$

In equation 2.12,  $\tau$  is representing increment in cable tension and  $\Delta H$  represents increment in horizontal component of cable tension.

Multiplying both sides of the equation 2.11 by  $\left(\frac{ds}{dx}\right)^2$  will lead to equation (2.13).

$$\left\{ \frac{1}{E_c A_c} \Delta H \frac{ds}{dx} \right\} \left(\frac{ds}{dx}\right)^2 = \left\{ \frac{du}{ds} \frac{dx}{ds} + \frac{dy}{ds} \frac{dw}{ds} + \frac{1}{2} \left(\frac{dw}{ds}\right)^2 \right\} \left(\frac{ds}{dx}\right)^2 \quad (2.13)$$

Integrating equation 2.13 with respect to x would results in equation (2.14).

$$\int_{x=0}^{x=L} \left\{ \frac{1}{E_c A_c} \right\} \Delta H \left(\frac{ds}{dx}\right)^3 . dx = \int_{x=0}^{x=L} \left\{ \frac{du}{dx} + \frac{dy}{dx} \frac{dw}{dx} + \frac{1}{2} \left(\frac{dw}{dx}\right)^2 \right\} . dx \quad (2.14)$$

Effective length of the cable is manifested in equation (2.15).

$$L_C = \int_{x=0}^{x=L} \left(\frac{ds}{dx}\right)^3 . dx \quad (2.15)$$

Inserting equation 2.13 into equation 2.12 results in equation (2.16).

$$\frac{\Delta H L_C}{E_c A_c} = \int_{x=0}^{x=L} \left\{ \frac{du}{dx} + \frac{dy}{dx} \frac{dw}{dx} + \frac{1}{2} \left(\frac{dw}{dx}\right)^2 \right\} . dx \quad (2.16)$$

Since  $u$  is the horizontal displacement of the top of the pylons which affect the increment in cable tension, equation 2.16 would be simplified into equation (2.17).

$$\frac{\Delta H L_C}{E_c A_c} = (u_L - u_0) + \int_{x=0}^{x=L} \left\{ \frac{dy}{dx} \frac{dw}{dx} + \frac{1}{2} \left(\frac{dw}{dx}\right)^2 \right\} . dx \quad (2.17)$$

Parabolic shape of the cable is manifested in equation (2.18).

$$y = \frac{1}{2} x \left(1 - \frac{x}{L}\right) \quad (2.18)$$

By integrating second term and third term in equation 2.16 and simplifying it, equation (2.19) achieved.

$$\begin{aligned} \frac{\Delta H L_C}{E_c A_c} = & (u_L - u_0) - \left( \frac{1}{2} w_L + \frac{1}{2} w_0 \right) + \frac{(m_c + m_b)g}{H} \int_{x=0}^{x=L} w. dx \\ & + \frac{1}{2} \left( \frac{dw}{dx} w \Big|_0^L - \frac{d^2 w}{dx^2} \int_{x=0}^{x=L} w. dx \right) \end{aligned} \quad (2.19)$$

After rearranging equation 2.19 equation (2.20) obtained.

$$\begin{aligned} \Delta H = & \frac{E_c A_c \left[ (u_L - u_0) - \frac{1}{2} (w_L + w_0) + \frac{(m_c + m_b)g}{H} \int_{x=0}^{x=L} w. dx \right]}{L_C} \\ & + \frac{E_c A_c \left[ \frac{1}{2} \left( \frac{dw}{dx} w \Big|_0^L - \frac{d^2 w}{dx^2} \int_{x=0}^{x=L} w. dx \right) \right]}{L_C} \end{aligned} \quad (2.20)$$

Neglecting  $\frac{dw}{dx}$  and  $\frac{d^2 w}{dx^2}$  in equation 2.20 would result in equation (2.21).

$$\Delta H = \frac{E_c A_c \left[ (u_L - u_0) - \frac{1}{2} (w_L + w_0) + \frac{(m_c + m_b)g}{H} \int_{x=0}^{x=L} w. dx \right]}{L_C} \quad (2.21)$$

Simplified form of third term in equation 2.4 which is multiplication of sum of tension and increment of it with sum of second derivative of the cable shape and second derivative of cable deflection due external loads, is illustrated in equation (2.22).

$$\begin{aligned} (H + \Delta H)(y'' + w'') &= (H + \Delta H)y'' + (H + \Delta H)w'' \\ &= -\frac{1}{L}(H + \Delta H) + (H + \Delta H)w'' \end{aligned} \quad (2.22)$$

Inserting above equation into equation 2.2 would lead to equation (2.23).

$$m_c \ddot{w} - K(z - w)^+ - (H + \Delta H)w'' = y''H + y''\Delta H + (m_c + m_b)g \quad (2.23)$$

After rearranging terms and simplifying the equation 2.21 with considering that

$-\frac{1}{L^2} \frac{E_c A_c}{L_C} = \alpha$  simplified equation of equation 2.23 is shown in equation (2.24).

$$\begin{aligned}
& m_c \ddot{w} - K(z - w)^+ - (H + \Delta H)w'' \\
& = \alpha L \left[ (u_L - u_0) - \frac{1}{2}(w_L + w_0) \right. \\
& \quad \left. + \frac{(m_c + m_b)g}{H} \int_{x=0}^{x=L} w \cdot dx \right]
\end{aligned} \tag{2.24}$$

### 2.3 Decomposition of the Displacements

Since displacement of the suspension bridge compose of static and dynamic parts, decomposing displacement of the beam helps in analyzing of the beam displacement. In equation (2.25) components of the displacements for the deck is presented.

$$z(x, t) = Z(x, t) + z_d(x, t) \tag{2.25}$$

Decomposition of the cable displacement is displayed in equation (2.26).

$$w(x, t) = W(x, t) + w_d(x, t) \tag{2.26}$$

$Z(x, t)$  and  $W(x, t)$  are static parts which are induce by support movements and live loads, while  $z_d(x, t)$  and  $w_d(x, t)$  caused by the moving loads and dynamic effects of moving load.

#### 2.3.1 Static equations for beam and cable

Static displacement for the cable is shown in equation (2.27).

$$\begin{aligned}
W'' = & -\frac{\alpha L(U_L - U_0)}{H(H + \Delta H)} + \frac{\alpha L(W_L + W_0)}{2(H + \Delta H)} - \frac{\alpha L(m_c + m_b)g}{H(H + \Delta H)} \int_{x=0}^{x=L} W \cdot dx \\
& - \frac{K(Z - W)^+}{(H + \Delta H)}
\end{aligned} \tag{2.27}$$

Since the equation 2.27 is an IDE, it must be solve with numerical methods. In equation 2.27 there are two unknowns which is higher than number of equations. To resolve this problem, compatibility equation introduced, which helps in finding  $\Delta H$ . In compatibility equation, sum of cable deflection, tower horizontal and vertical



deflection and total length of the cable must be equal to zero. The compatibility equation with mentioned conditions is displayed in equation (2.28).

$$\frac{\Delta H}{E_c A_c} \int_{x=0}^{x=L} \left\{ 1 + \left( \frac{dy}{dx} \right)^2 \right\}^{\frac{3}{2}} + (U_L - U_0) - \frac{(W_L + W_0)}{2} + y'' \int_{x=0}^{x=L} W \cdot dx = 0 \quad (2.28)$$

In each iteration,  $\Delta H$  value satisfies with less error above equation, iteration continues until the error is equal or less than the desirable error. Static displacement of the deck differential equation presented in equation (2.29).

$$Z^{iv} = -\frac{K}{E_b I_b} (Z - W)^+ \quad (2.29)$$

### 2.3.2 Boundary conditions for cable and beam

To solve the equations with use of FDM method, there is need for an extra equations, since number of equations are less than unknowns. To this purpose, extra equations must be introduced. Using the boundary conditions provides extra equations for getting trivial solution.

Displacement and moment at the both ends of the deck are zero thus, for the deck of the suspension bridge boundary conditions are shown in equation (2.30).

$$\begin{cases} Z_{(0)} = 0 \\ Z_{(L)} = 0 \\ -E_b I_b Z''_{(0)} = 0 \\ -E_b I_b Z''_{(L)} = 0 \end{cases} \quad (2.30)$$

Displacements at the top of tower are zero which in equation (2.31) boundary conditions for cable is displayed.

$$\begin{cases} W_{(0)} = 0 \\ W_{(L)} = 0 \end{cases} \quad (2.31)$$

### 2.3.3 Solution method for static

Since equations 2.27 and 2.29 are coupled, they must be solved simultaneously. Solving equations with numerical methods is required since equations are IDE. To

solve the equations, finite difference<sup>1</sup> method is chosen, which is applicable to both BVP and IVP problems.

### 2.3.4 Inertial equation of the cable and beam

After deriving static equation for the suspension bridge, inertial equation for the deck of the suspension bridge derived. For defining inertial equation, mass of the deck and external dynamic loads which is caused by moving load introduced. Inertial equation of the cable is displayed in equation (2.32).

$$m_b \ddot{z}_d + K(z_d - w_d)^+ + E_b I_b z_d^{iv} = f_1(x, t) \quad (2.32)$$

There is no external dynamic load which acts on the cable so inertial equation for cable after introducing mass of the cable presented in equation (2.33).

$$\begin{aligned} m_c \ddot{w}_d - K(z_d - w_d)^+ - (H + \Delta H) w_d'' \\ = \alpha L \left[ (u_L - u_0) - \frac{1}{2} (w_L + w_0) \right. \\ \left. + \frac{(m_c + m_b)g}{H} \int_{x=0}^{x=L} w_d \cdot dx \right] \end{aligned} \quad (2.33)$$

Dynamic force that caused by moving load is function of the Dirac's delta function which is illustrated in equation (2.34).

$$f(x, t) = Mg\delta(x - vt) \quad (2.34)$$

Assuming that deck of suspension bridge deflection is in shape that can be decomposed to time and location variables, decomposing of these variables helps in converting PDE equations to IDE and ODE equations. Separation of variables for the deck of the suspension bridge is depicted in equation (2.35).

$$z_d(x, t) = \sum_{n=1} \phi_n(x) q_{zn}(t) \quad (2.35)$$

---

<sup>1</sup> APPENDIX A

The above concept is also applicable to cable. Separation of the variables for the cable is illustrated in equation (2.36).

$$w_d(x, t) = \sum_{n=1} \phi_n(x) q_{w_n}(t) \quad (2.36)$$

Shape function for both the deck and the cable considered to be in shape of sine equation. It must be noted that modes superimposition utilized in this study. So shape function in above equations for n'th mode of vibration is manifested in equation (2.37).

$$\phi_n(x) = \sin\left(\frac{n\pi x}{L}\right) \quad (2.37)$$

## 2.4 Equation of Motion for Suspension Bridge Deck

After implementing separation variable technique, equation of motion with time dependent variable derived which is presented in equation (2.38).

$$m_b \sum_{n=1} \phi_n(x) \ddot{q}_{z_n}(t) + K \left( \sum_{n=1} \phi_n(x) q_{z_n}(t) - \sum_{n=1} \phi_n(x) q_{w_n}(t) \right) + E_b I_b \sum_{n=1} \phi_n^{iv}(x) q_{z_n}(t) = f_1(x, t) \quad (2.38)$$

Multiplying equation 2.38 it by  $\phi_{n(x)}$  and integrating above equation between 0 and L interval equation (2.39) obtained which is depicted below.

$$\begin{aligned}
m_b \int_{x=0}^{x=L} \sum_{n=1} \ddot{q}_{z_n}(t) \phi_n^2(x) \cdot dx & \\
+ K \int_{x=0}^{x=L} \left( \sum_{n=1} \phi_n^2(x) q_{z_n}(t) \right. & \\
\left. - \sum_{n=1} \phi_n^2(x) q_{w_n}(t) \right)^+ \cdot dx & \quad (2.39) \\
+ E_b I_b \int_{x=0}^{x=L} \sum_{n=1} \left( \frac{n\pi}{L} \right)^4 q_{z_n}(t) \phi_n^2(x) \cdot dx & \\
= \int_{x=0}^{x=L} f_1(x, t) \phi_n(x) \cdot dx &
\end{aligned}$$

By knowing that  $\int_{x=0}^{x=L} \phi_n(x) \phi_j(x) \cdot dx \Rightarrow \begin{cases} 0, n \neq j \\ \frac{L}{2}, n = j \end{cases}$  equation of motion for n'th mode is depicted in equation (2.40).

$$\begin{aligned}
m_b \frac{L}{2} \ddot{q}_{z_n}(t) + K \int_{x=0}^{x=L} \left( \phi_n^2(x) q_{z_n}(t) - \phi_n^2(x) q_{w_n}(t) \right)^+ \cdot dx & \\
+ \frac{L}{2} \left( \frac{n\pi}{L} \right)^4 E_b I_b q_{z_n}(t) = \int_{x=0}^{x=L} Mg \delta(x - vt) \phi_n(x) \cdot dx & \quad (2.40)
\end{aligned}$$

By inserting Dirac's delta function value into equation 2.40, simplified form of equation 2.40, which is equation (2.41) achieves.

$$\begin{aligned}
m_b \frac{L}{2} \ddot{q}_{z_n}(t) + K \frac{L}{2} q_{z_n}(t) - K \frac{L}{2} q_{w_n}(t) + \frac{L}{2} \left( \frac{n\pi}{L} \right)^4 E_b I_b q_{z_n}(t) & \\
= Mg \sin \left( \frac{n\pi vt}{L} \right) & \quad (2.41)
\end{aligned}$$

Matrix form of the equation of motion of the deck is presented in equation (2.42).

$$\begin{aligned}
m_b \frac{L}{2} \ddot{Q}_z(t) + K \frac{L}{2} Q_z(t) - K \frac{L}{2} Q_w(t) + \frac{L}{2} \left( \frac{n\pi}{L} \right)^4 E_b I_b Q_z(t) & \\
= Mg \sin \left( \frac{n\pi vt}{L} \right) & \quad (2.42)
\end{aligned}$$

---

<sup>2</sup> Appendix B

Simplified form of equation 2.42 is presented in equation (2.43).

$$m_b \ddot{Q}_z(t) + \left[ K + \left( \frac{n\pi}{L} \right)^4 E_b I_b \right] Q_z(t) - K Q_w(t) = \frac{2Mg}{L} \sin \left( \frac{n\pi vt}{L} \right) \quad (2.43)$$

Dividing equation 2.43 by  $m_b$  would give generalized equation of motion of the deck which is illustrated in equation (2.44).

$$\ddot{Q}_z(t) + \frac{\left[ K + \left( \frac{n\pi}{L} \right)^4 E_b I_b \right]}{m_b} Q_z(t) - \frac{K}{m_b} Q_w(t) = \frac{2Mg}{m_b L} \sin \left( \frac{n\pi vt}{L} \right) \quad (2.44)$$

## 2.5 Equation of Motion for Suspension Bridge Cable

Implementing same procedure in previous section for the cable of the suspension bridge would result in equation (2.45).

$$\begin{aligned} m_c \sum_{n=1}^+ \phi_n(x) \ddot{q}_{w_n}(t) - K \left( \sum_{n=1}^+ \phi_n(x) q_{z_n}(t) - \sum_{n=1}^+ \phi_n(x) q_{w_n}(t) \right) \\ - (H + \Delta H) \sum_{n=1}^+ \phi_n''(x) q_{w_n}(t) \\ = \alpha L \left[ (u_L - u_0) - \frac{1}{2} (w_L + w_0) \right. \\ \left. + \frac{(m_c + m_b)g}{H} \int_{x=0}^{x=L} w_d \cdot dx \right] \end{aligned} \quad (2.45)$$

Same as the previous section multiplying the equation 2.45 by  $\phi_n(x)$  and then integrate it between 0 and L would lead to equation (2.46).

$$\begin{aligned}
& \int_{x=0}^{x=L} m_c \sum_{n=1} \phi_n(x) \ddot{q}_{w_n}(t) \phi_n(x) . dx \\
& - \int_{x=0}^{x=L} K \left( \sum_{n=1} \phi_n(x) q_{z_n}(t) \phi_n(x) - \sum_{n=1} \phi_n(x) q_{w_n}(t) \phi_n(x) \right)^+ . dx \\
& + \int_{x=0}^{x=L} (H + \Delta H) \sum_{n=1} \left( \frac{n\pi}{L} \right)^2 \phi_n(x) q_{w_n}(t) \phi_n(x) . dx \tag{2.46} \\
& = \alpha L \int_{x=0}^{x=L} \phi_n(x) \left[ (u_L - u_0) - \frac{1}{2} (w_L + w_0) \right] . dx \\
& + \alpha L \frac{(m_c + m_b)g}{H} \int_{x=0}^{x=L} \phi_n(x) \int_{x=0}^{x=L} \sum_{n=1} \phi_n(x) q_{w_n}(t) \phi_n(x) . dx . dx
\end{aligned}$$

Considering that  $\left[ \cos \left( \frac{n\pi x}{L} \right) \right]_0^L$  is equal to zero when  $n$  is odd and equal to two when  $n$  is even and after doing mathematical actions, equation of motion for the  $n$ 'th mode of the cable would be obtained which is presented in equation (2.47).

$$\begin{aligned}
m_c \frac{L}{2} \ddot{q}_{w_n}(t) - K \frac{L}{2} \left( q_{z_n}(t) - q_{w_n}(t) \right)^+ + (H + \Delta H) \left( \frac{n\pi}{L} \right)^2 \frac{L}{2} q_{w_n}(t) \\
= \alpha \frac{L^2}{n\pi} \left[ (u_L - u_0) - \frac{1}{2} (w_L + w_0) \right] [(-1)^{n+1} + 1] \\
+ \alpha \left( \frac{L}{n\pi} \right)^2 [(-1)^{n+1} + 1]^2 . q_{w_n}(t) \tag{2.47}
\end{aligned}$$

Matrix form of the equation of motion is displayed in equation (2.48).

$$\begin{aligned}
m_c \frac{L}{2} \ddot{Q}_w(t) - K \frac{L}{2} (Q_z(t) - Q_w(t))^+ + (H + \Delta H) \left( \frac{n\pi}{L} \right)^2 \frac{L}{2} Q_w(t) \\
= \alpha \frac{L^2}{n\pi} \left[ (u_L - u_0) - \frac{1}{2} (w_L + w_0) \right] [(-1)^{n+1} + 1] \\
+ \alpha \left( \frac{L}{n\pi} \right)^2 [(-1)^{n+1} + 1]^2 . Q_w(t) \tag{2.48}
\end{aligned}$$

After applying same procedure for equation 2.48 that taken place in previous section equation (2.49) obtained.

$$\begin{aligned}
m_c \ddot{Q}_w(t) - K Q_z(t) &+ \left[ K + (H + \Delta H) \left( \frac{n\pi}{L} \right)^2 \right. \\
&- \left. 2\alpha \frac{L}{(n\pi)^2} [(-1)^{n+1} + 1]^2 \right] Q_w(t) \\
&= 2\alpha \frac{L}{n\pi} \left[ (u_L - u_0) - \frac{1}{2} (w_L + w_0) \right] [(-1)^{n+1} + 1]
\end{aligned} \tag{2.49}$$

Dividing equation 2.49 by  $m_c$  would give generalized equation of motion for n'th vibration mode which is presented in equation (2.50).

$$\begin{aligned}
\ddot{Q}_w(t) - \frac{K}{m_c} Q_z(t) &+ \frac{\left[ K + (H + \Delta H) \left( \frac{n\pi}{L} \right)^2 - 2\alpha \frac{L}{(n\pi)^2} [(-1)^{n+1} + 1]^2 \right]}{m_c} Q_w(t) \\
&= \frac{2\alpha \frac{L}{n\pi} \left[ (u_L - u_0) - \frac{1}{2} (w_L + w_0) \right] [(-1)^{n+1} + 1]}{m_c}
\end{aligned} \tag{2.50}$$

## 2.6 Solution Method For Equation Of Motion

MATLAB software is used to solve equation of motion. Same as static there are initial conditions which helps to determine the constants of the equation.

Since deck of the suspension bridge is resting at the beginning of the vibration the initial conditions displacement and velocity of the deck are equal zero at the time bridge starts to vibrate. Initial conditions for the deck is presented in equation (2.51).

$$\begin{cases} q_{z_n}(t) = 0 \\ \dot{q}_{z_n}(t) = 0 \end{cases} \tag{2.51}$$

For the cable there are similar initial conditions and when bridge starts to vibrate displacement and velocity of the cable is equal to zero so initial conditions for the cable of the suspension bridge is presented in equation (2.52).

$$\begin{cases} q_{w_n}(t) = 0 \\ \dot{q}_{w_n}(t) = 0 \end{cases} \tag{2.52}$$

## 2.7 Earthquake Effects on Equation of Motion

Computing earthquake effects on suspension requires huge amount of computation and solving lot of coupled equations. To reduce amount of time that are going to spent on solving equation, instead of coupled equation or improved deflection theory solving effect of the earthquake excitation by deflection theory would be helpful. Since in deflection theory there is no coupled equation of motion and it depends only on deflection of the cable.

To consider effect of the earthquake on the suspension bridge introduction of  $(m_b + m_c)\ddot{z}_g$  term is sufficient, which is ground acceleration acting on the suspension bridge. Force equilibrium of the deck is shown in **Figure 2.5**. Considering that cable and deck have the same deflection during vibration, equation of motion for the vibration of the deck would be like equation (2.53).

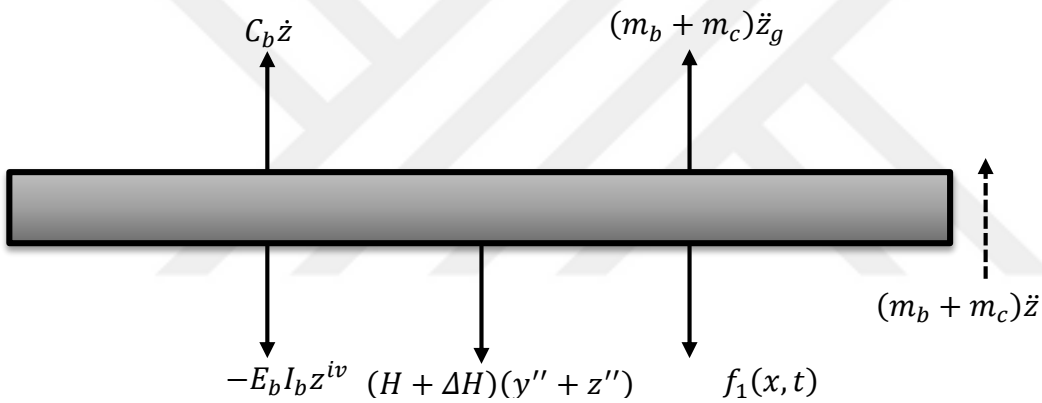


**Figure 2.5** : Force equilibrium of the deck

$$\begin{aligned} (m_b + m_c)\ddot{z} - (H + \Delta H)(y'' + z'') + E_b I_b z^{iv} \\ = (m_b + m_c)g + Mg \sin\left(\frac{n\pi vt}{L}\right) - (m_b + m_c)\ddot{z}_g \end{aligned} \quad (2.53)$$

Equation (2.54) obtained by Substituting equation 2.22 into equation 2.53.

$$\begin{aligned} (m_b + m_c)\ddot{z} - (H + \Delta H)z'' + E_b I_b z^{iv} \\ = (m_b + m_c)g + Mg \sin\left(\frac{n\pi vt}{L}\right) - (m_b + m_c)\ddot{z}_g \\ + y''H + y''\Delta H \end{aligned} \quad (2.54)$$

Simplified form of equation 2.54 is presented in equation (2.55).



$$\begin{aligned}
& (m_b + m_c)\ddot{z} - (H + \Delta H)z'' + E_b I_b z^{iv} \\
& = Mg \sin\left(\frac{n\pi vt}{L}\right) - (m_b + m_c)\ddot{z}_g \\
& + \alpha L \left[ (u_L - u_0) - \frac{1}{2}(w_L + w_0) \right. \\
& \left. + \frac{(m_b + m_c)g}{H} \int_0^L w \cdot dx \right]
\end{aligned} \tag{2.55}$$

Performing separation of variable and the same procedure that have taken place in previous sections on equation 2.55 would result in equation (2.56).

$$\begin{aligned}
& \ddot{Q}_z(t) \\
& + \frac{\left(\frac{n\pi}{L}\right)^2 \left[ H + \Delta H + \left(\frac{n\pi}{L}\right)^2 E_b I_b \right] - 2\alpha \frac{L}{(n\pi)^2} [(-1)^{n+1} + 1]^2}{(m_b + m_c)} Q_z(t) \\
& = \frac{2Mg}{(m_b + m_c)L} \sin\left(\frac{n\pi vt}{L}\right) \\
& + \frac{2\alpha L}{(m_b + m_c)n\pi} \left[ (u_L - u_0) - \frac{1}{2}(w_L + w_0) \right] [(-1)^{n+1} + 1] \\
& - \frac{2}{n\pi} [(-1)^{n+1} + 1] \ddot{z}_g
\end{aligned} \tag{2.56}$$

## 2.8 Determining Natural Frequencies

To determine natural frequency deflection theory is used instead of improved deflection theory. In deflection theory equation of motion for n'th mode would be like

$$\begin{aligned}
& \ddot{Q}_z(t) \\
& + \frac{\left(\frac{n\pi}{L}\right)^2 \left[ H + \Delta H + \left(\frac{n\pi}{L}\right)^2 E_b I_b \right] - 2\alpha \frac{L}{(n\pi)^2} [(-1)^{n+1} + 1]^2}{(m_b + m_c)} Q_z(t) \\
& = \frac{2Mg}{(m_b + m_c)L} \sin\left(\frac{n\pi vt}{L}\right) \\
& + \frac{2\alpha L}{(m_b + m_c)n\pi} \left[ (u_L - u_0) - \frac{1}{2}(w_L + w_0) \right] [(-1)^{n+1} + 1]
\end{aligned} \tag{2.57}$$

Coefficient of the  $Q_z(t)$  is equal to square of angular speed. For determining dynamic features of the suspension bridge equations (2.58 - 2.60) proposed which are respectively used to calculate angular speed, frequency and period of the bridge.

$$\omega_n^2 = \frac{\left(\frac{n\pi}{L}\right)^2 \left[ H + \Delta H + \left(\frac{n\pi}{L}\right)^2 E_b I_b \right] - 2\alpha \frac{L}{(n\pi)^2} [(-1)^{n+1} + 1]^2}{(m_b + m_c)} \quad (2.58)$$

To get the frequency of the suspension bridge

$$f_n = \frac{\omega_n}{2\pi} \quad (2.59)$$

And to get period of the suspension bridge

$$T_n = \frac{1}{f_n} \quad (2.60)$$

### 3. ANALYTICAL STUDIES

Verification and numerical analysis has been performed in this chapter. For verifying suspension bridge that was investigated by Choi in 2013 selected and outcomes of the study which has been carried out by Choi compared with result that obtained by written code in MATLAB. At next step for determining deflection, velocity and acceleration response of the suspension bridge numerical example of the suspension bridge has been assumed. At last results that obtained by MATLAB compared by outcomes of the ABAQUS software.

First of all it is necessary to be assured from validity of the code. This process increase the reliability of the result and also proves the correctness of the computation that has been done by MATLAB. To this purpose, at first, verification of the result that has been obtained from MATLAB compared with article results which is written by Choi and Gwon [10] in 2015. After verification by using equations that introduced in chapter 2, deflection, velocity and acceleration of the suspension bridge when moving load crosses the bridge by using MATLAB computed.

#### 3.1 Verification

To achieve the validity, suspension bridge with span that is 2000 meters long and with the towers that are 200 meters high modeled. After analyzing, obtained results from MATLAB compared with the result that Choi obtained.

Details and material properties of the bridge deck, suspension cable and hanger is depicted in **Tables 3.1-3.3**. Tower stiffness would also affect suspension cable deflection thus details of tower which is analyzed in Choi's article are given in **Table 3.4**. Hangers considered are capable of extension and since they are separated, stiffness of the all cables are computed and then stiffness of them are distributed over the span of suspension bridge.

**Table 3.1** : Material and geometric properties of the deck

Structural part	Modulus of elasticity ( $\frac{kN}{m^2}$ )	Moment of inertia ( $m^4$ )	Weight ( $\frac{kN}{m}$ )
Deck	$2.1 \times 10^8$	3.195	121.47

**Table 3.2** : Material and geometric properties of the suspension cable

Structural part	Modulus of elasticity ( $\frac{kN}{m^2}$ )	Area ( $m^2$ )	Weight ( $\frac{kN}{m}$ )
Suspension cable	$2 \times 10^8$	1.021	81.66

**Table 3.3** : Material and geometric properties of the hanger

Structural part	Modulus of elasticity ( $\frac{kN}{m^2}$ )	Area ( $m^2$ )	Distributed Stiffness ( $\frac{kN}{m}$ )
Hanger	$1.4 \times 10^8$	0.0104	$2.06 \times 10^4$

**Table 3.4** : Material and geometric properties of the tower

Structural part	Modulus of elasticity ( $\frac{kN}{m^2}$ )	Moment of inertia ( $m^4$ )	Length ( $m$ )
Tower	$3 \times 10^7$	340	250

Main span and side span length, sag amount and tower heights of the verified bridge is illustrated in **Figure 3.1** and also numeric values of the verified bridge are presented in **Table 3.5**.

**Table 3.5** : Geometric values of verified suspension bridge

Sag ( $m$ )	Main span length ( $m$ )	Side span length ( $m$ )	Tower height above deck ( $m$ )	Tower height below deck ( $m$ )	Hanger spacing ( $m$ )
199.9	2000	600	200	50	25

Live load considered to be equal to  $40 \frac{kN}{m}$  which only acts on main span. Dead load due to the own weight of the cable and the deck was equal to  $203.13 \frac{kN}{m}$  and uniformly

distributed on main and side span of the bridge. Magnitude of the Dead and the live load are given in **Table 3.6**.

**Table 3.6 :** Details of load acting on verified bridge

Load	Span		
	Left side span	Main span	Right side span
Live load $\frac{kN}{m}$	0	40	0
Dead load $\frac{kN}{m}$	203.13	203.13	203.13

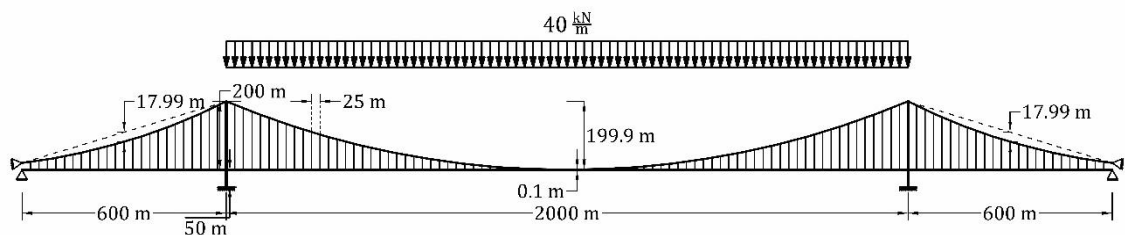


**Figure 3.1 :** Verified bridge details

By using finite difference method deflection of the suspension bridge determined. Four different intervals are assumed for computing deflection of the suspension bridge in order to verify the result. Intervals were equal to 100, 50, 25 and 10 meters. Obtained results for 100, 50, 25 and 10 meters intervals from MATLAB and their schematic graph are illustrated in **Figures 3.2-3.5** respectively.

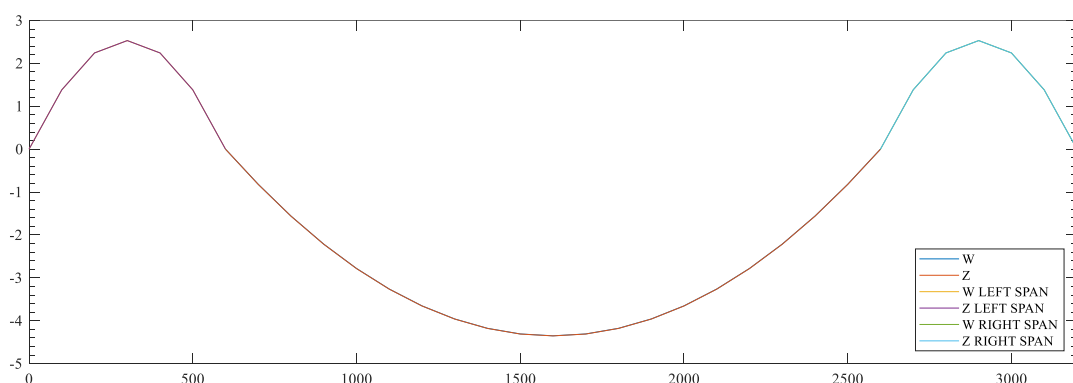


**Figure 3.2 :** Suspension bridge deflection plot for interval length of 100 meters (In meters)

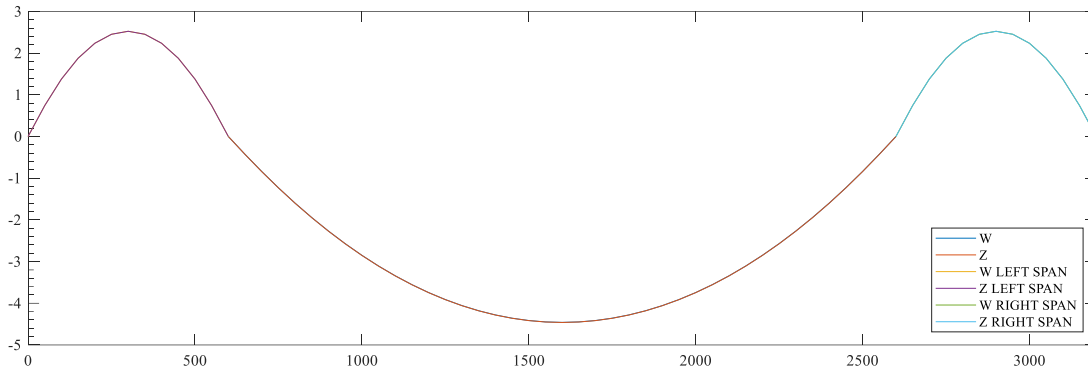


**Figure 3.3 :** Suspension bridge deflection plot for interval length of 50 meters (In meters)

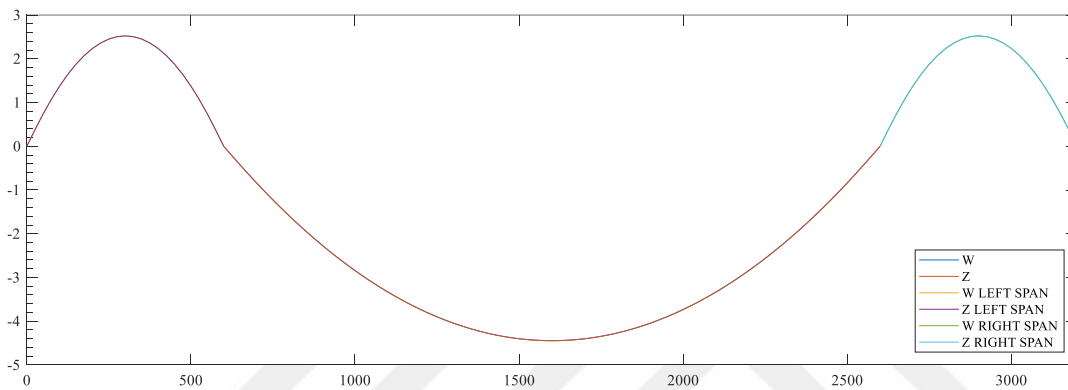


**Figure 3.4 :** Suspension bridge deflection plot for interval length of 25 meters (In meters)

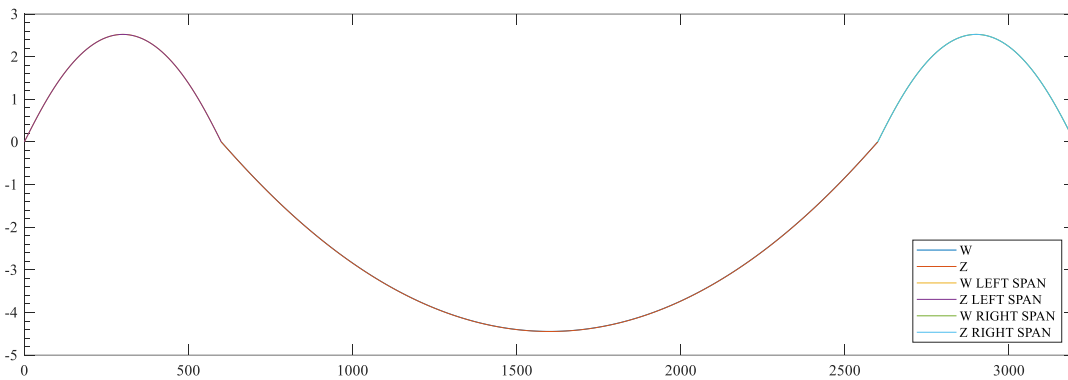


**Figure 3.5 :** Suspension bridge deflection plot for interval length of 10 meters (In meters)

Table 3.7 represents numeric values of the deck maximum deflection with different interval. As it is depicted in **Figure 3.1** live load are acting only on main span and it is equal to  $40 \frac{kN}{m}$ . In **Table 3.7** computed values for deflection of the suspension bridge by use of MATLAB are compared with result that Choi and Gwon obtained are presented [10].

**Table 3.7** : Comparing maximum deflection from MATLAB and Choi's article

Obtained result	Span Interval	Deck Maximum Deflection (m)		Difference		Difference (%)	
		Main Span	Side Span	Main Span	Side Span	Main Span	Side Span
MATLAB	100 m	4.35294	-2.53196	-0.10860	-0.02994	2.434%	1.197%
	50 m	4.38879	-2.52711	-0.07275	-0.02509	1.631%	1.003%
	25 m	4.44617	-2.52284	-0.01537	-0.02082	0.344%	0.832%
	10 m	4.44617	-2.52284	-0.01537	-0.02082	0.344%	0.832%
Choi		4.46154	-2.50202				

As intervals decrease, accuracy of the result increases. It is known fact that in FDM method, decreasing intervals would lead to better approximations and improves accuracy of the result. However, computing small intervals are harder and requires more time to spend because number of unknowns and equations are much more comparing to larger intervals. The most important conclusion that can be extracted from this analysis, is that from some point reducing intervals would not affect result considerably. By analyzing of the outcomes, the 25 meters interval can be described as optimum interval, since computed result for 10 meters interval and 25 meters interval are not much different. This table also shows that written script in MATLAB is effective in computing deflection, because the difference between result obtained in this research from MATLAB and results that published by Choi is 0.344% which is below 1% and it is in acceptable range.

### 3.2 Numerical Modeling

For numerical modeling a suspension bridge assumed, in which main span is 1600 meters long and side spans are 400 meters long assumed. Geometric details of suspension bridge are presented in **Tables 3.8-3.11**.

**Table 3.8** : Material and geometric properties of the deck

Structural part	Modulus of elasticity ( $\frac{kN}{m^2}$ )	Moment of inertia ( $m^4$ )	Area ( $m^2$ )	Mass ( $\frac{kg}{m^3}$ )	Weight ( $\frac{kN}{m}$ )
Deck	$2.1 \times 10^8$	3.5	1.5	7850	115.465

**Table 3.9 :** Material and geometric properties of the suspension cable

Structural part	Modulus of elasticity ( $\frac{kN}{m^2}$ )	Radius (m)	Area ( $m^2$ )	Mass ( $\frac{kg}{m^3}$ )	Weight ( $\frac{kN}{m}$ )
Suspension cable	$2 \times 10^8$	0.5	0.78539	7850	60.457

**Table 3.10 :** Material and geometric properties of the hanger

Structural part	Modulus of elasticity ( $\frac{kN}{m^2}$ )	Radius (m)	Area ( $m^2$ )	Distributed Stiffness ( $\frac{kN}{m^2}$ )
Hanger	$1.4 \times 10^8$	0.1	0.0314159	$8.88 \times 10^3$

**Table 3.11 :** Material and geometric properties of the tower

Structural part	Modulus of elasticity ( $\frac{kN}{m^2}$ )	Moment of inertia ( $m^4$ )	Length (m)
Tower	$3 \times 10^7$	600	230

Schematic view of bridge in which numeric values of sag amount, distance of the hangers, span and side span length, towers height and amount of live load that acts on the bridge is illustrated in **Figure 3.6**.

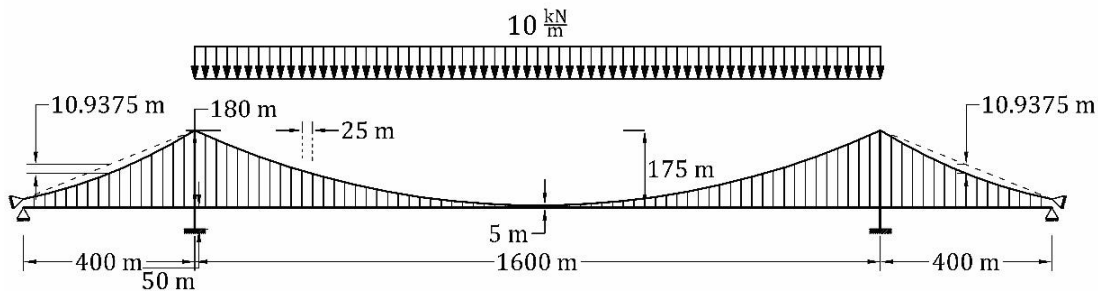


**Figure 3.6 :** Schematic view of assumed bridge

Main span and side span length, sag amount and tower heights of the assumed bridge for numerical analysis are brought in **Table 3.12**.

**Table 3.12 :** Geometric values of suspension bridge

Sag (m)	Main span length (m)	Side span length (m)	Tower height above deck (m)	Tower height below deck (m)	Hanger spacing (m)
175	1600	400	180	50	25



Intensity of Live loads and dead loads which are acting on the suspension bridge are presented in **Table 3.13**.

**Table 3.13** : Details of load acting on numerical bridge

Load	Span		
	Left side span	Main span	Right side span
Live load $\left(\frac{kN}{m}\right)$	0	10	0
Dead load $\left(\frac{kN}{m}\right)$	175.9226	175.9226	175.9226

Horizontal component of cable tension and increment in horizontal component of cable tension due to live load for side spans and main span are presented in **Table 3.14**.

**Table 3.14** : Cable tension and increment in cable tension horizontal component

Load	Span		
	Left side span	Main span	Right side span
Cable tension horizontal component ( $kN$ )	321686.942	321686.942	321686.942
Increment in cable tension horizontal component ( $kN$ )	15703.353	16484.597	15703.353

It is worth to note that increment in horizontal component of cable tension due to live load in comparison to horizontal component of cable tension due to dead load are ignorable and can be neglected. However, in this study effect of the increment in horizontal component of cable tension due to the live load are taken into the account.

### 3.2.1 Static

As it was mentioned earlier, deflected shape of the suspension bridge under the dead load and own weight of the suspension bridge considered as reference point for the deflection. However, under live load which is static load, deflection of the suspension bridge taken into the account. Magnitude of live load is equal to  $10 \frac{kN}{m}$  and only main span was subjected to the live load which was explained before. In **Figure 3.7** deflected shape of suspension bridge under the live load has been illustrated.

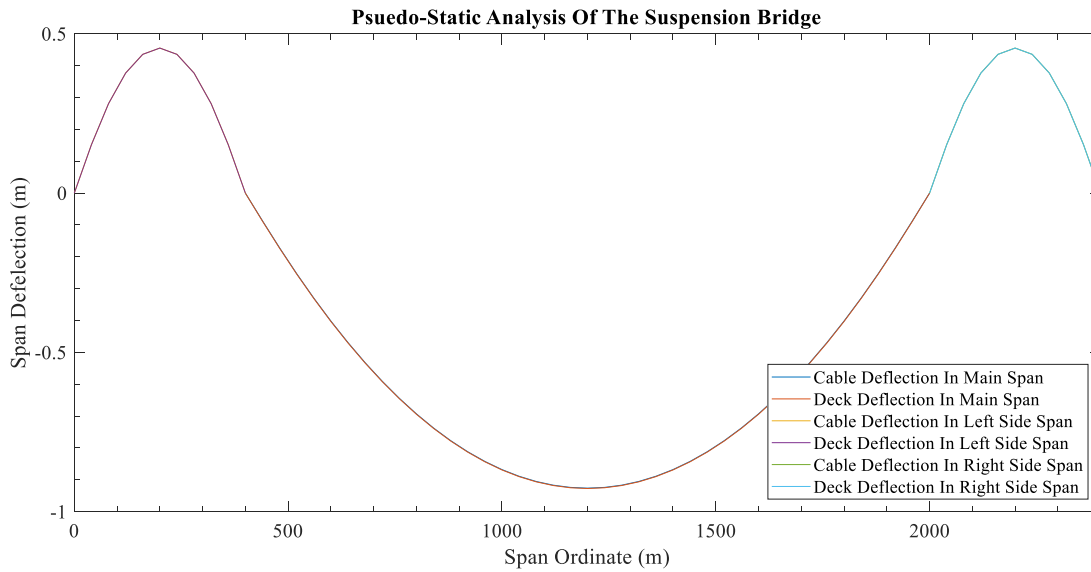


**Figure 3.7 : Static Analysis of the Suspension Bridge**

From figure it can understand that in static analysis of the suspension bridge, deflection of the cable and the deck is very close and almost equal. In **Table 3.15** numeric results for deflection of the cable and the deck in main span is presented.

**Table 3.15 : Numeric Values Of Deflection Of The Cable And The Deck In Main Span**

Span ordinate (m)	Cable deflection in main span (m)	Deck deflection in main span (m)
0	0	0
25	0.05418261	0.055196407
50	0.108387727	0.109478349
75	0.161354488	0.162461492
100	0.21281404	0.213929057
125	0.262634885	0.263754508
150	0.310741425	0.311863741
175	0.357089451	0.358213345
200	0.401653067	0.402777886
225	0.444417105	0.445542466
250	0.485372677	0.486498354
275	0.524514576	0.525640439
300	0.561839751	0.562965723
325	0.597346416	0.598472452

**Table 3.15 (continued):** Numeric Values Of Deflection Of The Cable And The Deck In Main Span

350	0.631033524	0.632159597
375	0.662900462	0.664026557
400	0.692946869	0.694072977
425	0.721172537	0.722298653
450	0.747577341	0.748703461
475	0.772161209	0.773287332
500	0.7949241	0.796050224
525	0.815865987	0.816992112
550	0.834986857	0.836112982
575	0.852286701	0.853412826
600	0.867765513	0.868891639
625	0.881423293	0.882549419
650	0.893260036	0.894386162
675	0.903275743	0.904401869
700	0.911470413	0.912596539
725	0.917844045	0.918970171
750	0.92239664	0.923522766
775	0.925128196	0.926254323
800	0.926038715	0.927164841
825	0.925128196	0.926254323
850	0.92239664	0.923522766
875	0.917844045	0.918970171
900	0.911470413	0.912596539
925	0.903275743	0.904401869
950	0.893260036	0.894386162
975	0.881423293	0.882549419
1000	0.867765513	0.868891639
1025	0.852286701	0.853412826
1050	0.834986857	0.836112982
1075	0.815865987	0.816992112

**Table 3.15 (continued):** Numeric Values Of Deflection Of The Cable And The Deck In Main Span

1100	0.7949241	0.796050224
1125	0.772161209	0.773287332
1150	0.747577341	0.748703461
1175	0.721172537	0.722298653
1200	0.692946869	0.694072977
1225	0.662900462	0.664026557
1250	0.631033524	0.632159597
1275	0.597346416	0.598472452
1300	0.561839751	0.562965723
1325	0.524514576	0.525640439
1350	0.485372677	0.486498354
1375	0.444417105	0.445542466
1400	0.401653067	0.402777886
1425	0.357089451	0.358213345
1450	0.310741425	0.311863741
1475	0.262634885	0.263754508
1500	0.21281404	0.213929057
1525	0.161354488	0.162461492
1550	0.108387727	0.109478349
1575	0.05418261	0.055196407
1600	0	0

Due to the symmetric geometry of the suspension bridge and shape of the live load, deflections of the left and right side span is identical. For this reason, in **Table 3.16** numeric values of the cable and the deck deflection in the left side span has been depicted.

**Table 3.16** : Numeric Values Of The Cable and The Deck Deflection In Side Span

Span ordinate (m)	Cable deflection in side span (m)	Deck deflection in side span (m)
0	0	0
25	-0.096919878	-0.096387276
50	-0.186693044	-0.186351045
75	-0.2661841	-0.265981356
100	-0.333102309	-0.332982285
125	-0.386086944	-0.386014732
150	-0.424351519	-0.424306034
175	-0.447456373	-0.44742433
200	-0.455180381	-0.455152421
225	-0.447456373	-0.44742433
250	-0.424351519	-0.424306034
275	-0.386086944	-0.386014732
300	-0.333102309	-0.332982285
325	-0.2661841	-0.265981356
350	-0.186693044	-0.186351045
375	-0.096919878	-0.096387276
400	0	0

In **Table 3.17** elongation of the vertical hangers due to the live load and stress and axial force in vertical hangers which is caused by elongation of vertical hangers is represented for main span.

**Table 3.17** : Elongation, stress and axial force in main span hangers

Cable length (m)	Elongation (m)	Stress (MPa)	Force (kN)
169.2333984	0.001013796	0.8387	26.34768631
158.8085938	0.001090622	0.9615	30.20496276
148.7255859	0.001107004	1.0421	32.73719287
138.984375	0.001115016	1.1232	35.28525053
129.5849609	0.001119623	1.2096	38.00099889
120.5273438	0.001122316	1.3036	40.95506739

**Table 3.17 (continued) : Elongation, stress and axial force in main span hangers**

111.8115234	0.001123894	1.4072	44.20962132
103.4375	0.001124819	1.5224	47.82801772
95.40527344	0.00112536	1.6514	51.87965125
87.71484375	0.001125677	1.7967	56.44412536
80.36621094	0.001125863	1.9613	61.61551006
73.359375	0.001125972	2.1488	67.50717235
66.69433594	0.001126036	2.3637	74.25764811
60.37109375	0.001126073	2.6114	82.03808452
54.38964844	0.001126095	2.8986	91.06190837
48.75	0.001126108	3.2340	101.5975712
43.45214844	0.001126115	3.6283	113.9854949
38.49609375	0.00112612	4.0954	128.6606905
33.88183594	0.001126122	4.6531	146.1829092
29.609375	0.001126124	5.3246	167.2764789
25.67871094	0.001126125	6.1396	192.881796
22.08984375	0.001126125	7.1371	224.2187958
18.84277344	0.001126126	8.3670	262.8572443
15.9375	0.001126126	9.8922	310.7739786
13.37402344	0.001126126	11.7883	370.341862
11.15234375	0.001126126	14.1367	444.1183953
9.272460938	0.001126126	17.0028	534.1582133
7.734375	0.001126126	20.3840	640.3828698
6.538085938	0.001126126	24.1137	757.5552476
5.68359375	0.001126126	27.7391	871.4488682
5.170898438	0.001126126	30.4894	957.8531498
5	0.001126126	31.5315	990.592272
5.170898438	0.001126126	30.4894	957.8531498
5.68359375	0.001126126	27.7391	871.4488682
6.538085938	0.001126126	24.1137	757.5552476
7.734375	0.001126126	20.3840	640.3828698

**Table 3.17 (continued) :** Elongation, stress and axial force in main span hangers

9.272460938	0.001126126	17.0028	534.1582133
11.15234375	0.001126126	14.1367	444.1183953
13.37402344	0.001126126	11.7883	370.341862
15.9375	0.001126126	9.8922	310.7739786
18.84277344	0.001126126	8.3670	262.8572443
22.08984375	0.001126125	7.1371	224.2187958
25.67871094	0.001126125	6.1396	192.881796
29.609375	0.001126124	5.3246	167.2764789
33.88183594	0.001126122	4.6531	146.1829092
38.49609375	0.00112612	4.0954	128.6606905
43.45214844	0.001126115	3.6283	113.9854949
48.75	0.001126108	3.2340	101.5975712
54.38964844	0.001126095	2.8986	91.06190837
60.37109375	0.001126073	2.6114	82.03808452
66.69433594	0.001126036	2.3637	74.25764811
73.359375	0.001125972	2.1488	67.50717235
80.36621094	0.001125863	1.9613	61.61551006
87.71484375	0.001125677	1.7967	56.44412536
95.40527344	0.00112536	1.6514	51.87965125
103.4375	0.001124819	1.5224	47.82801772
111.8115234	0.001123894	1.4072	44.20962132
120.5273438	0.001122316	1.3036	40.95506739
129.5849609	0.001119623	1.2096	38.00099889
138.984375	0.001115016	1.1232	35.28525053
148.7255859	0.001107004	1.0421	32.73719287
158.8085938	0.001090622	0.9615	30.20496276
169.2333984	0.001013796	0.8387	26.34768631

In **Table 3.18** elongation of the hangers, stress and axial force that appears in hangers due to the live load for side span is represented.

**Table 3.18** : Elongation, stress and axial force in side span hangers

Cable length (m)	Elongation (m)	Stress (MPa)	Force (kN)
8.686523438	0.000532602	8.5839	269.671392
17.71484375	0.000341999	2.7028	84.9112862
27.08496094	0.000202743	1.0480	32.92277246
36.796875	0.000120024	0.4567	14.34610804
46.85058594	7.22126E-05	0.2158	6.77916247
57.24609375	4.54853E-05	0.1112	3.494645794
67.98339844	3.20429E-05	0.0660	2.073038421
79.0625	2.79597E-05	0.0495	1.555391318
90.48339844	3.20429E-05	0.0496	1.557547566
102.2460938	4.54853E-05	0.0623	1.956601112
114.3505859	7.22126E-05	0.0884	2.777491093
126.796875	0.000120024	0.1325	4.163288286
139.5849609	0.000202743	0.2033	6.38831003
152.7148438	0.000341999	0.3135	9.849665761
166.1865234	0.000532602	0.4487	14.09564878

Maximum stress appears in main span and side span hangers are 31.5315 and 8.5839 MPa which are below yielding stress and maximum axial force that appears are 990.5923 and 269.6714 kN respectively .

### 3.2.2 Moving load

For analysis, moving load which is crossing the suspension bridge considered. Moving load considered in this study did not have any inertial effects and it was assumed as a point load. For analysis, three different velocities for moving load considered. Details of moving loads, velocity and location of the load at the beginning of the analysis are manifested in Table 3.19.



**Table 3.19 :** Details of moving load

Case	Mass (ton)	Equivalent Load (kN)	Velocity ( $\frac{m}{s}$ )	Location at $t = 0$
I	20.3956	200	16.6667	0
II	20.3956	200	25	0
III	20.3956	200	33.3333	0

### 3.2.2.1 Case I result

In **Figure 3.8** deflection of the middle point of the deck for period of 96 seconds depicted, which is the time needed for the moving force to cross the bridge. Picture shows that there is not much difference between cable and deck deflection, as a result great amounts of axial tension do not occur in hangers.

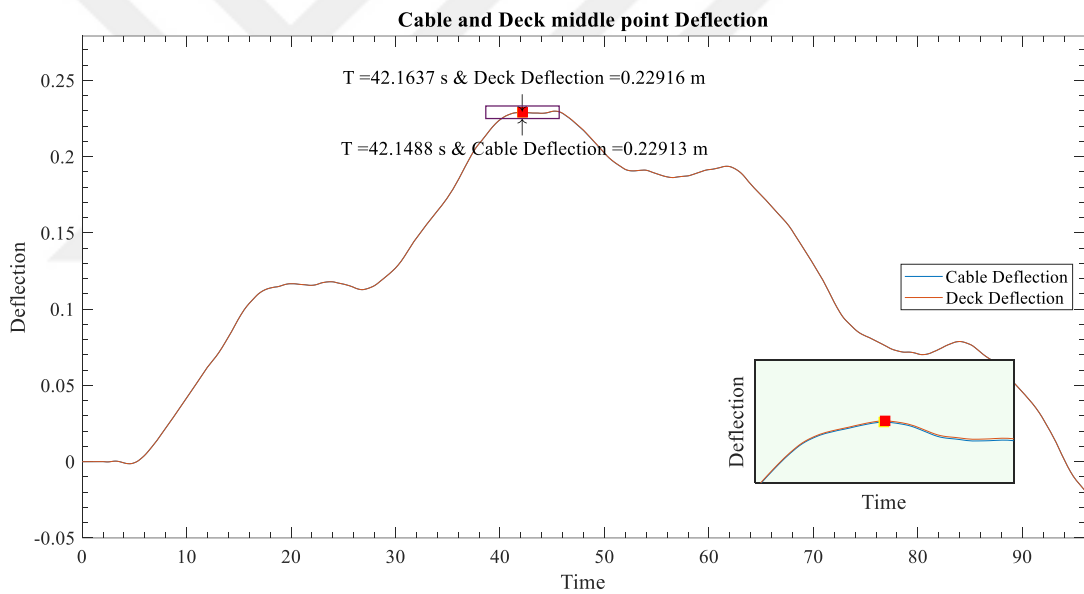


**Figure 3.8 :** The middle point deflection of the cable and the deck for Case I (In meters)

In **Figure 3.9** velocity of the cable and deck has been shown for case I. From figure it can be understood that there are not huge difference between velocity of the cable and deck and the velocities for both of them at different times are almost equal.

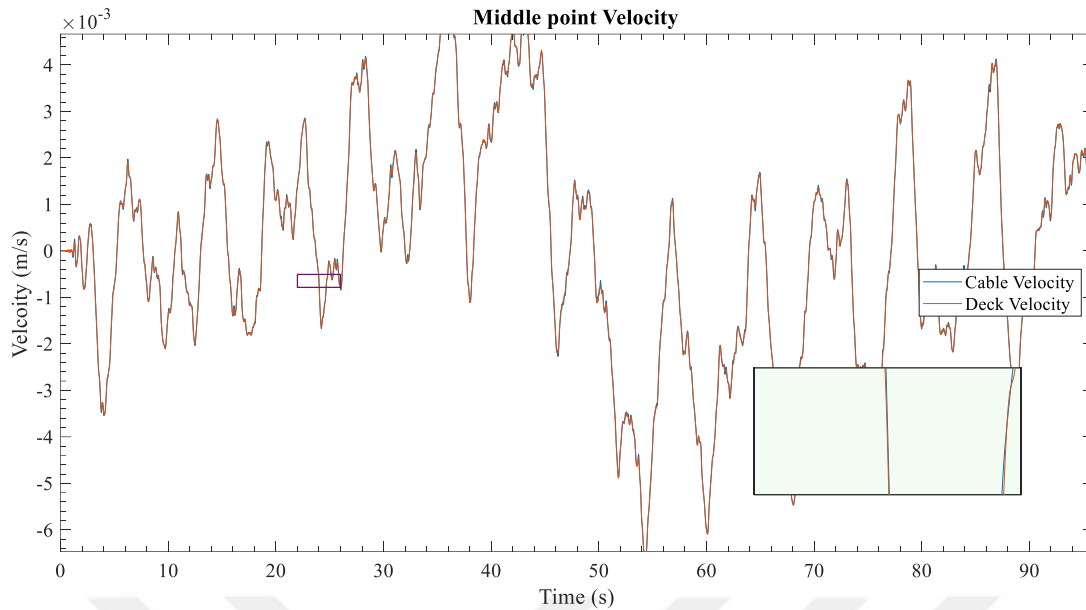


**Figure 3.9 :** The middle point velocity of the cable and the deck for Case I

In **Figure 3.10** acceleration of the cable and deck has been shown for case I. Likewise the velocity, acceleration of the cable and the deck at middle point are not differing significantly.

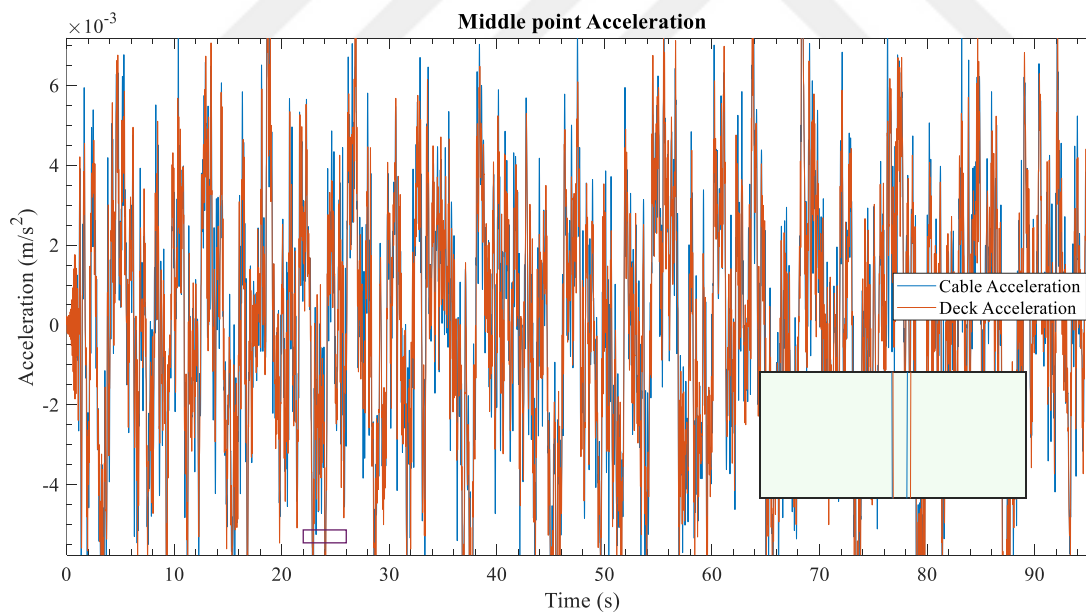


**Figure 3.10 :** The middle point acceleration of the cable and the deck for Case I

3D plot of the suspension bridge deflection due to the moving load is indicated at **Figure 3.11**. Figure shows that the maximum deflection of the suspension bridge occurs at the middle point of the span or around of it at the time moving load is nearby or at the center of the span.

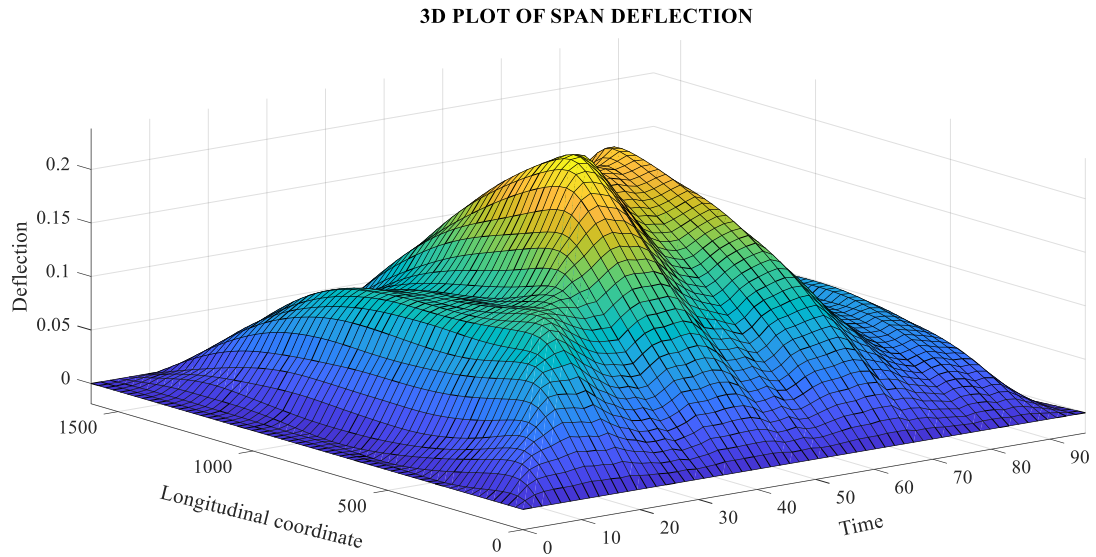


**Figure 3.11 :** 3D Plot of span deflection for Case I (In meters)

**Figure 3.12** shows deflection of the whole bridge at time in which moving load reached middle of the suspension bridge. Magnified region shows that deflection of the suspension bridge is not symmetric and direction of the moving load in which it moves, affects the result.

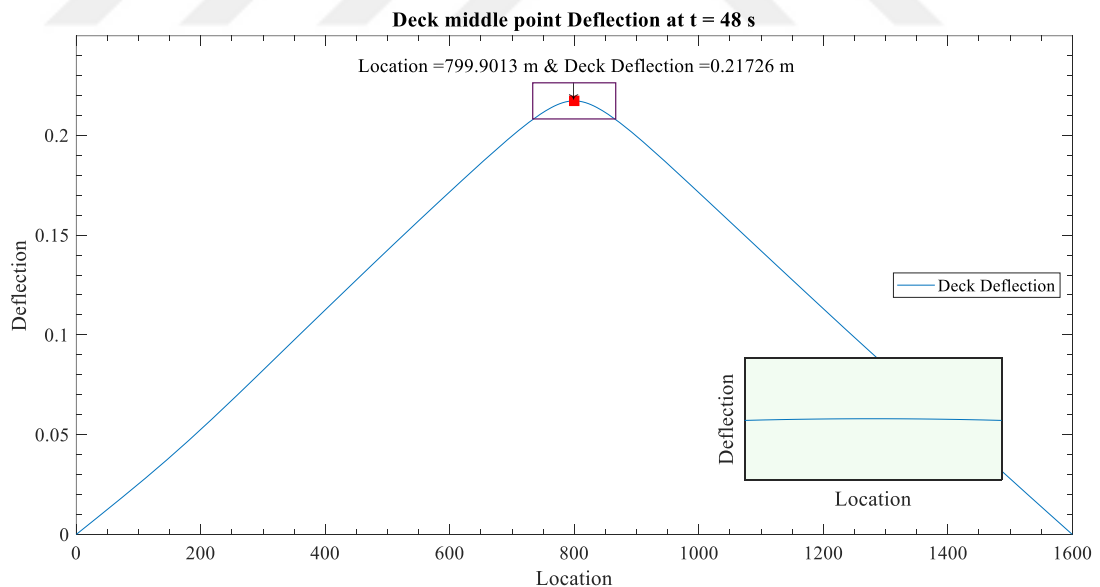


**Figure 3.12 :** The Case I middle point deflection of the cable and the deck at the time the moving load reach the span center (In meters)

In **Figure 3.13**, the deflection response of the cable and the deck is shown when the load reaches the middle of the span. In this figure first fifty modes of the bridge are taken into account. **Figure 3.13** shows that considering only first seven modes is sufficient for determining the deflection of the span.

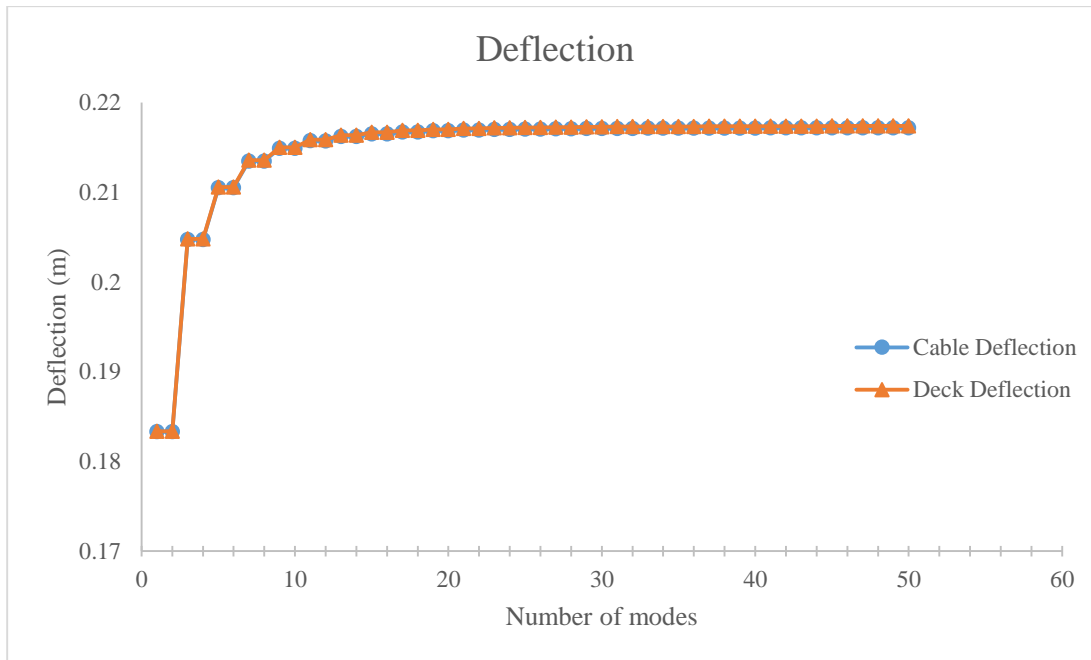


**Figure 3.13 :** Deflection of center span in case I for first 50 modes

**Figure 3.14** illustrates velocity response of the center of the cable and the deck when moving load is at the center of the span. For computing velocity response, first fifty modes of the bridge has been taken into account. For convergence of the velocity first seventeen modes has needed which is higher number comparing to modes that must considered for convergence of the deflection.

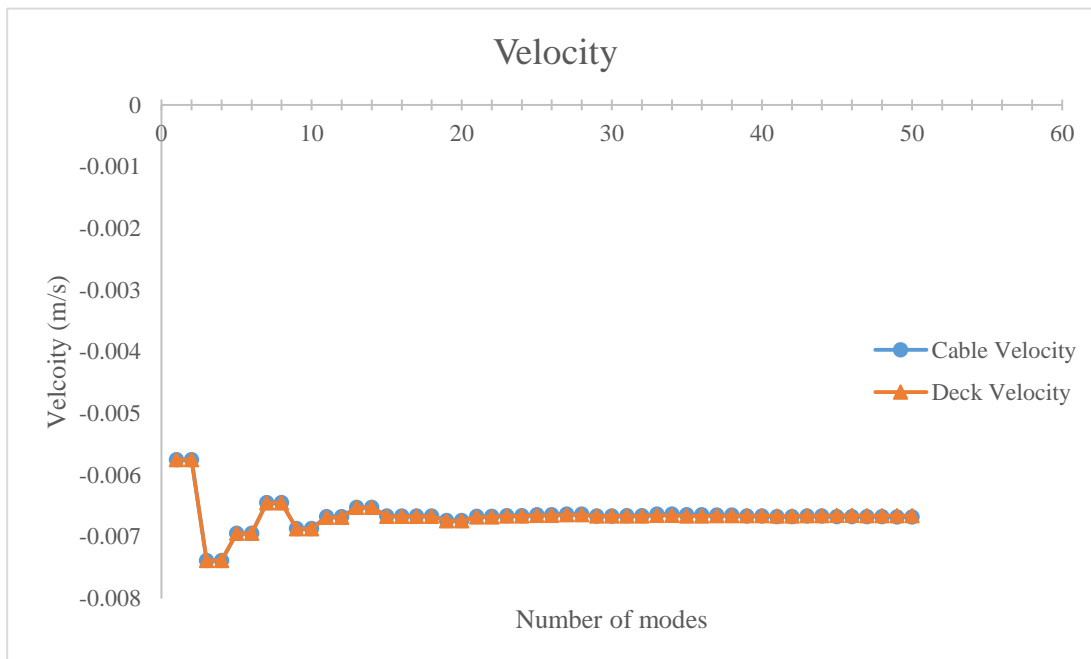


**Figure 3.14 :** Velocity of center span in case I for first 50 modes

**Figure 3.15** depicts acceleration response of the center of the cable and the deck for when moving load reaches the center of the span. Likewise to deflection and velocity response, acceleration response for the first fifty modes has been illustrated. For convergence of acceleration response, higher modes are taken into account since accelerations are fluctuating a lot. For the first twenty seven modes, accelerations are almost the same. However, after mentioned mode acceleration for the cable and the deck starts to differ.

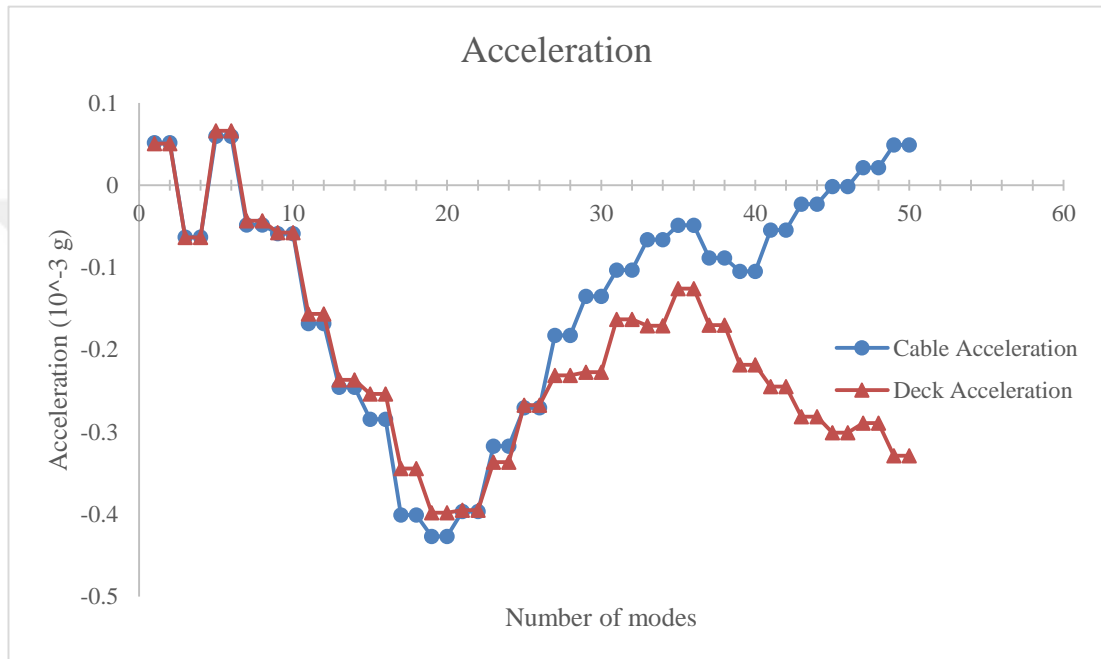


**Figure 3.15 :** Acceleration of center span in case I for first 50 modes

### 3.2.2.2 Case II result

In **Figure 3.16** deflection of the middle point of the cable and the deck with 64 seconds duration depicted. This duration is the time that the moving load needs for crossing the bridge. According to Figure 3.16 difference between cable and deck deflection is little and great amounts of axial tension in hangers do not appear.

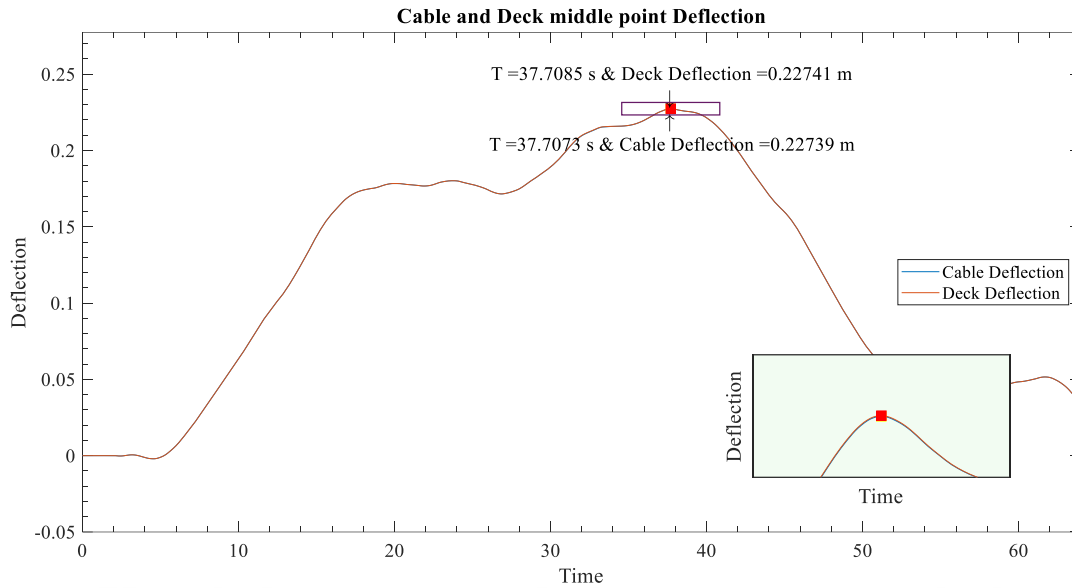


**Figure 3.16 :** The middle point deflection of the cable and the deck for Case II (In meters)

In **Figure 3.17** velocity of the cable and deck has been shown for case II. From figure it can be understood that there are not huge difference between velocity of the cable and deck and the velocities for both of them at different times are almost equal.

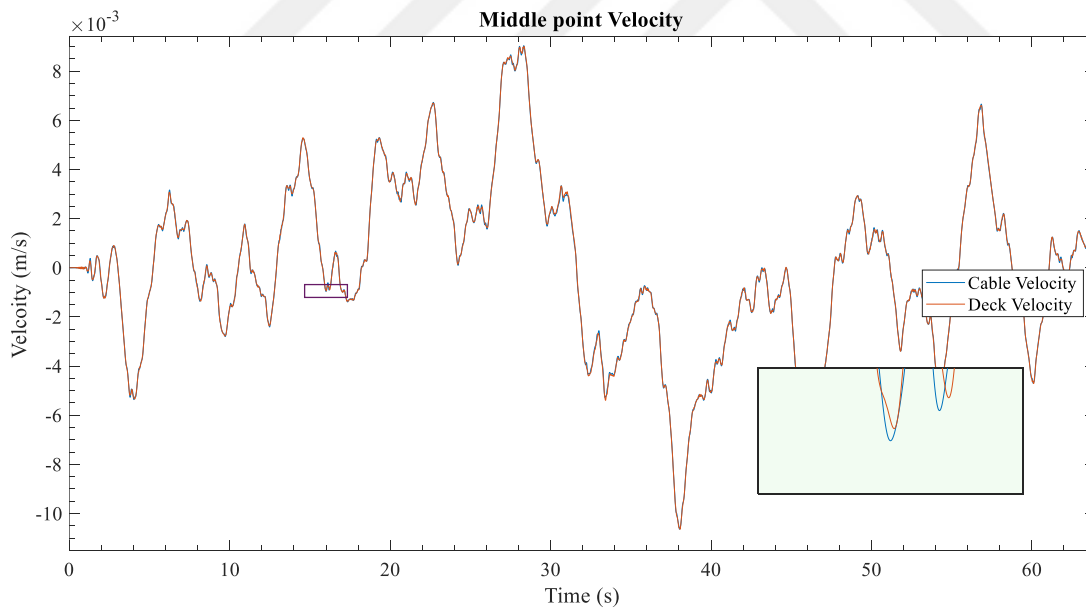


**Figure 3.17 :** The middle point velocity of the cable and the deck for Case II

In **Figure 3.18** acceleration of the cable and deck has been illustrated for case II. Likewise the velocity, acceleration of the cable and the deck at middle point are not differing significantly.

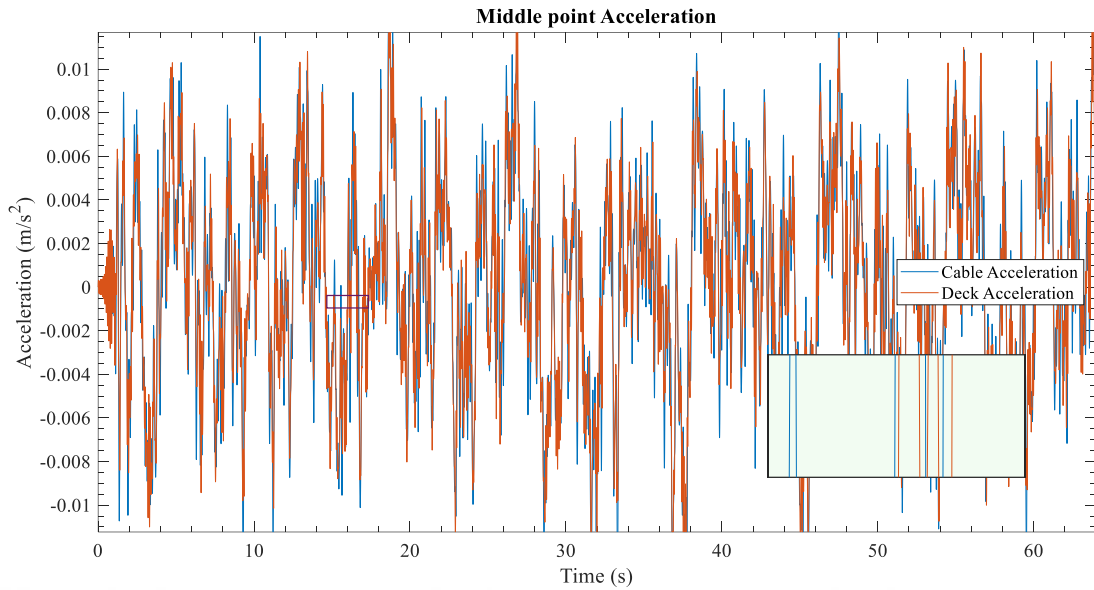


**Figure 3.18 :** The middle point acceleration of the cable and the deck for Case II

3D plot of the suspension bridge deflection due to the moving load is indicated at **Figure 3.19**. Figure shows that the maximum deflection of the suspension bridge occurs at the middle point of the span or around of it at the time moving load is nearby or at the center of the span.

**3D PLOT OF SPAN DEFLECTION**

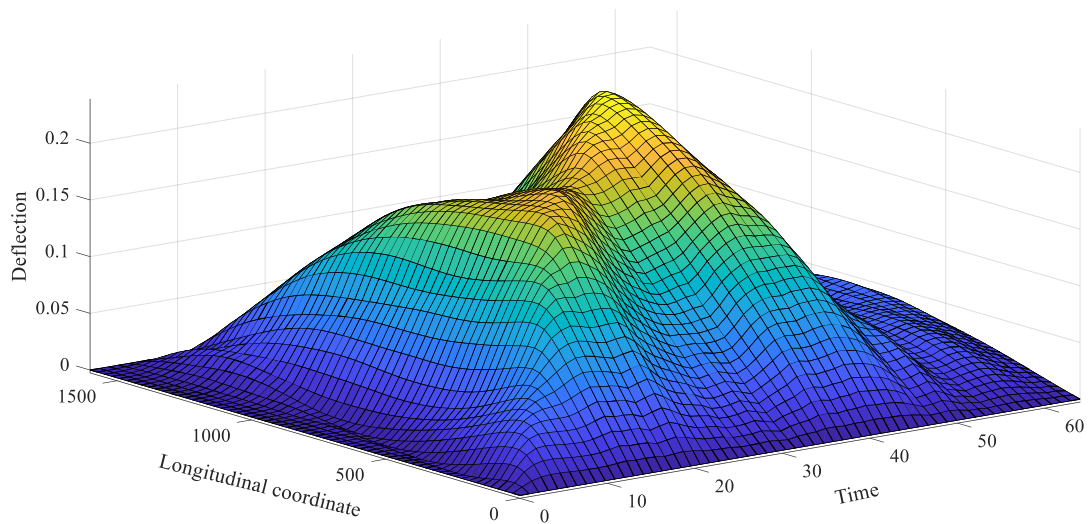


**Figure 3.19 :** 3D Plot of span deflection for Case II (In meters)

**Figure 3.20** shows deflection of the whole bridge at time in which moving load reached middle of the suspension bridge. Magnified region shows that deflection of the suspension bridge is not symmetric and direction of the moving load in which it moves, affects the result.

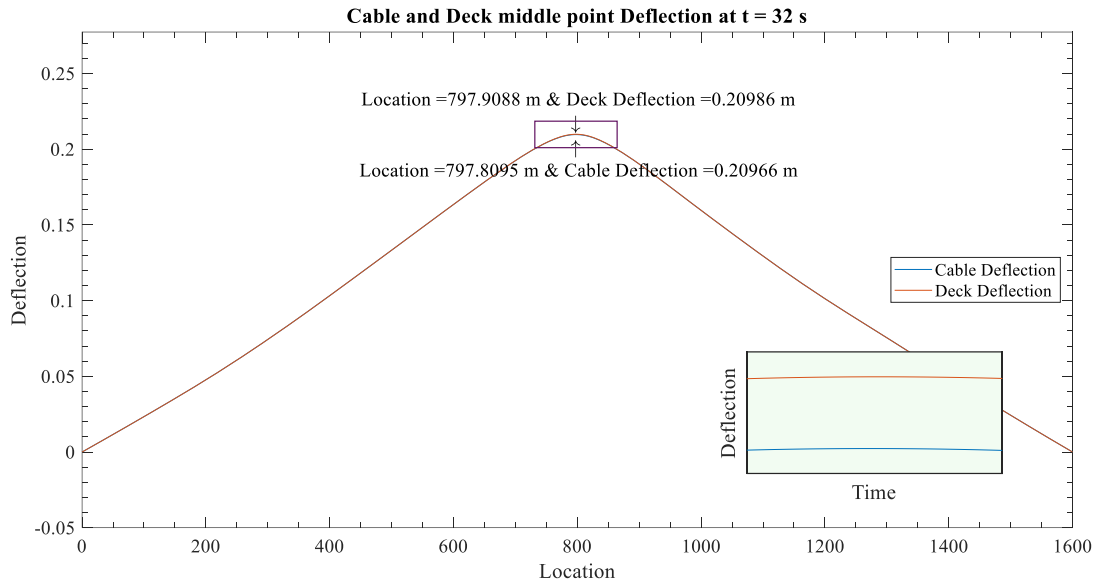


**Figure 3.20 :** The Case II middle point deflection of the cable and the deck at the time the moving load reach the span center (In meters)

In **Figure 3.21**, the deflection response of the cable and the deck as the load reaches the middle of the span is shown. **Figure 3.21** shows the deflection response for the first fifty modes of the bridge. **Figure 3.21** shows that considering only first seven modes same as case I is sufficient for determining the deflection of the span.

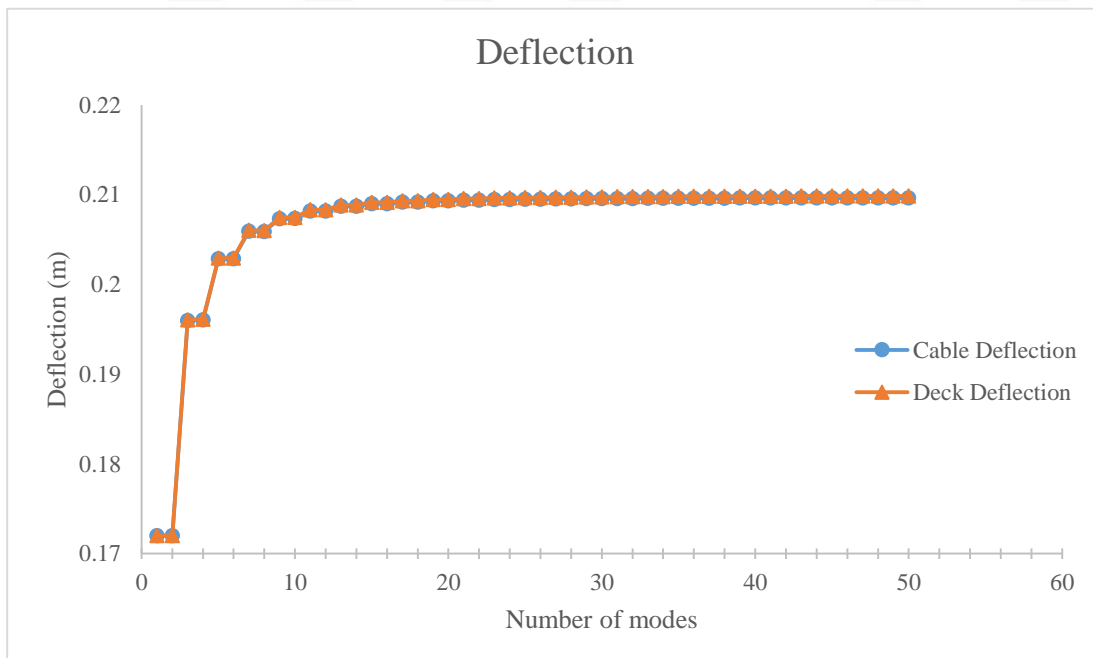


**Figure 3.21 :** Deflection of center span in case II for first 50 modes

In **Figure 3.22** velocity response of the center of the cable and the deck when moving load reaches center of the span has been shown. Likewise to deflection, velocity



response for first fifty modes are taken into account. For convergence of the velocity likewise to case I, consideration of higher modes required. In this case convergence of the velocity response occurs from mode sixteen. However, results for the first fifty modes has been computed.

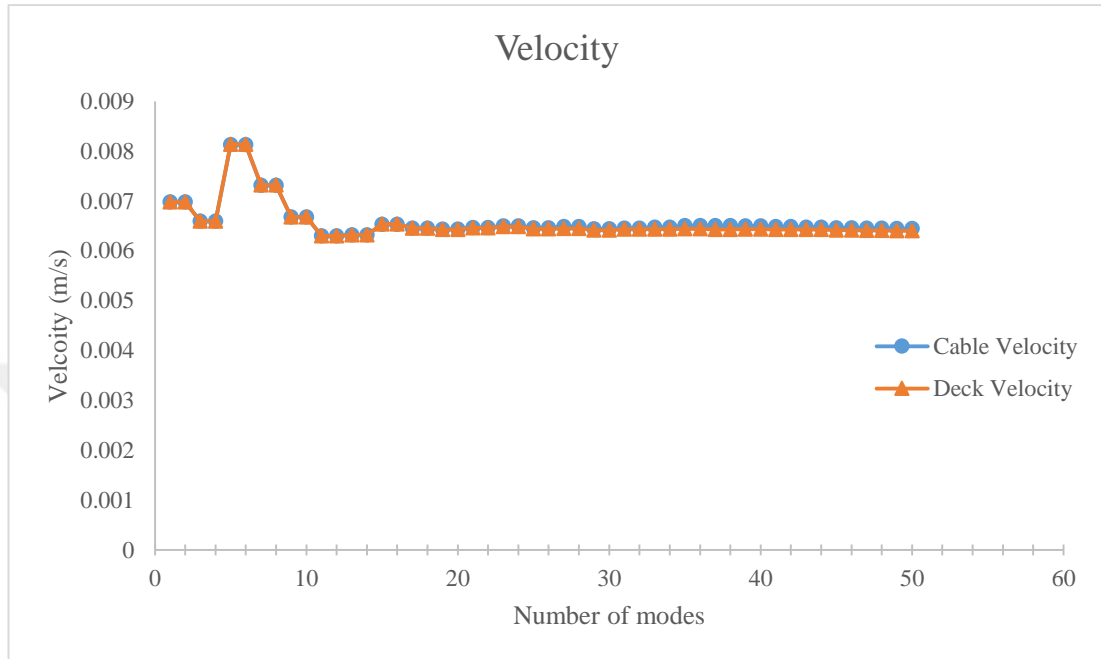


**Figure 3.22 :** Velocity of center span in case II for first 50 modes

In **Figure 3.23** acceleration of the center of the cable and the deck for case II has been displayed. Same as deflection and velocity, **Figure 3.23** shows acceleration response for the first fifty modes of the bridge. Same as case I, in order to reach the convergence in acceleration higher modes must be taken into account. **Figure 3.23** shows that accelerations of the cable and the deck are almost equal for the first forty modes. However, from mode forty one acceleration for the cable and the deck are not same and they differ.

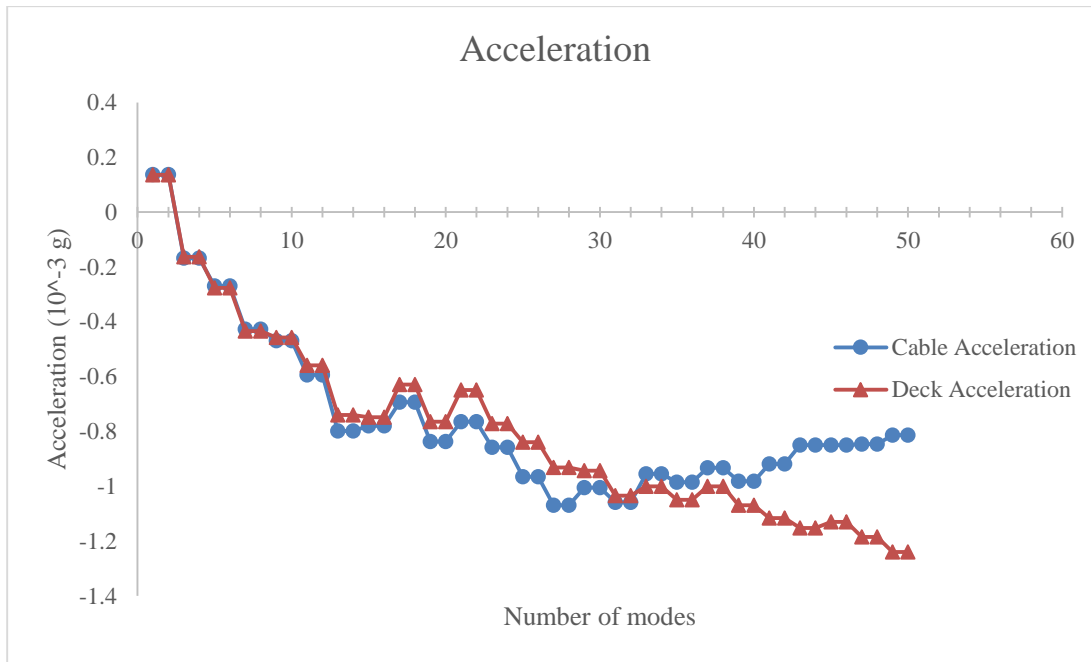


Figure 3.23 : Acceleration of center span in case II for first 50 modes

### 3.2.2.3 Case III result

In Figure 3.24 deflection of the middle point of the deck for period of 48 seconds depicted, which is the time needed for the moving force to cross the bridge. Likewise to case I and II there is not much axial forces in hangers since difference between cable and deck deflection is not that much.

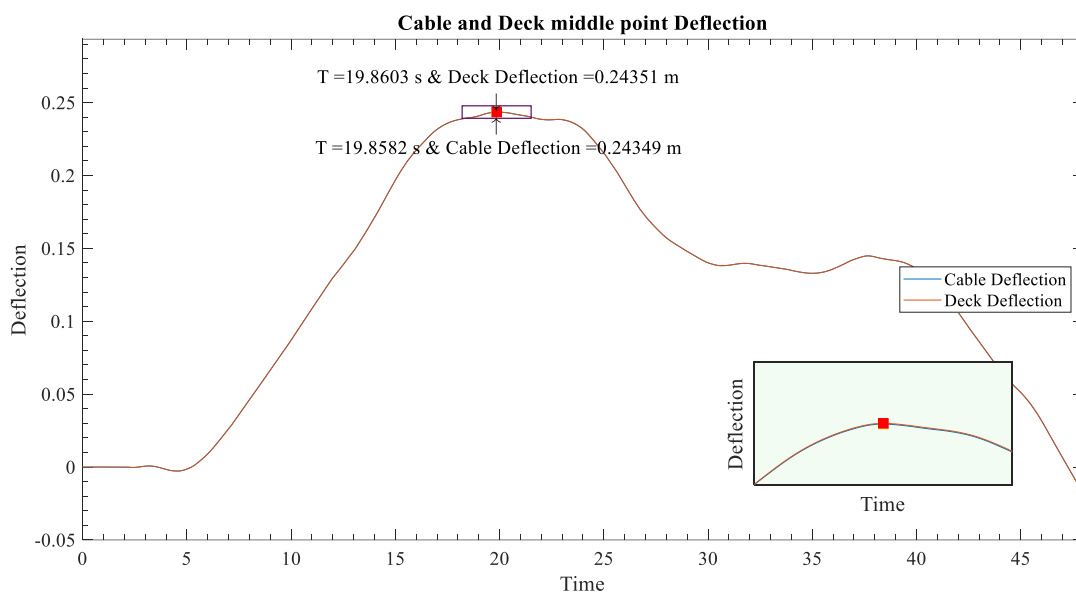
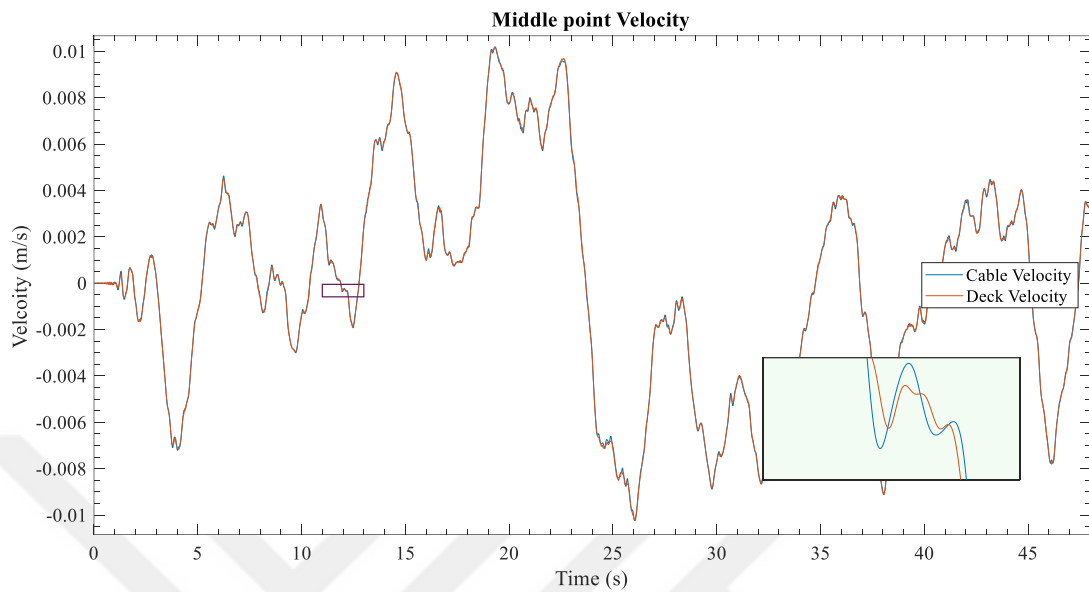


Figure 3.24 : The middle point deflection of the cable and the deck for Case III (In meters)

In **Figure 3.25** velocity of the cable and deck has been shown for case III. From figure it can be understood that there are not huge difference between velocity of the cable and deck and the velocities for both of them at different times are almost equal.



**Figure 3.25** : The middle point velocity of the cable and the deck for Case III

In **Figure 3.26** acceleration of the cable and deck has been displayed for case III. Likewise the velocity, acceleration of the cable and the deck at middle point are not differing significantly.

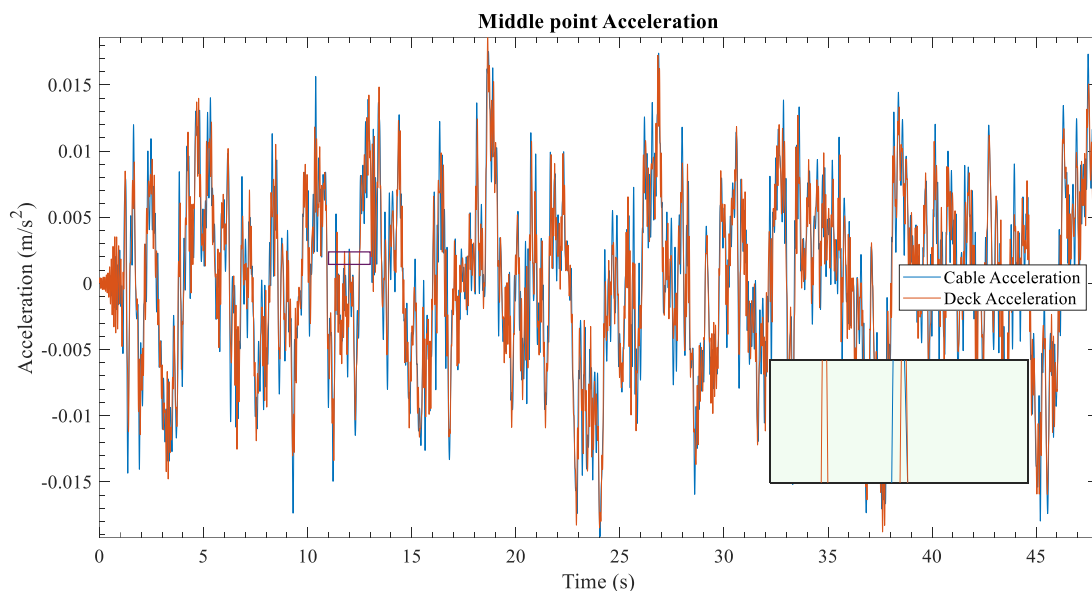


**Figure 3.26** : The middle point acceleration of the cable and the deck for Case III

3D plot of the suspension bridge deflection due to the moving load is indicated at **Figure 3.27**. Figure shows that the maximum deflection of the suspension bridge

occurs at the middle point of the span or around of it at the time moving load is nearby or at the center of the span.

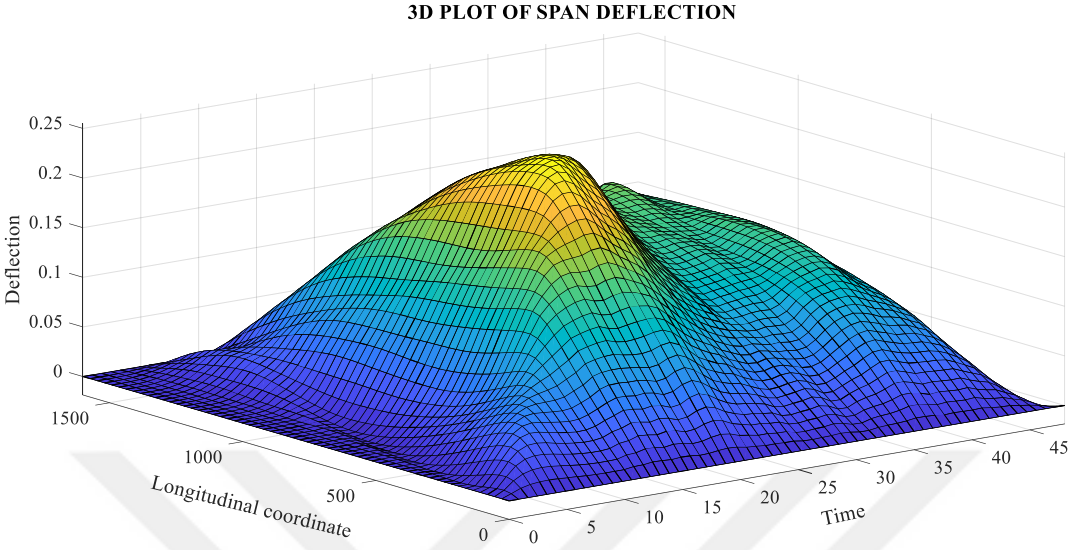


Figure 3.27 : 3D Plot of span deflection for Case III (In meters)

Figure 3.28 shows deflection of the whole bridge when moving load located at the middle of the suspension bridge. Magnified region shows that deflection of the suspension bridge is not symmetric and direction of the moving load in which it moves, affects the result.

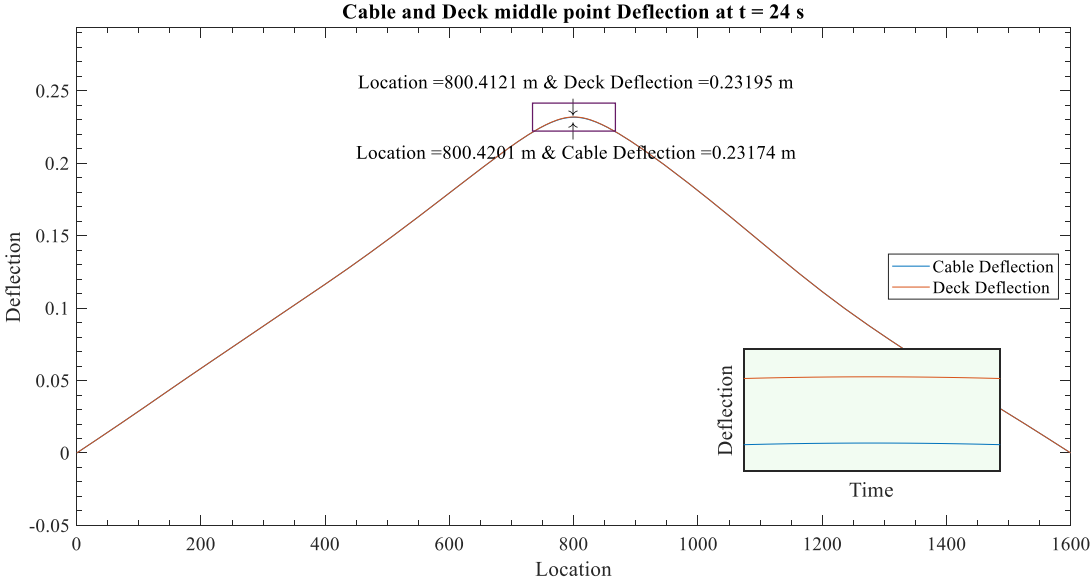
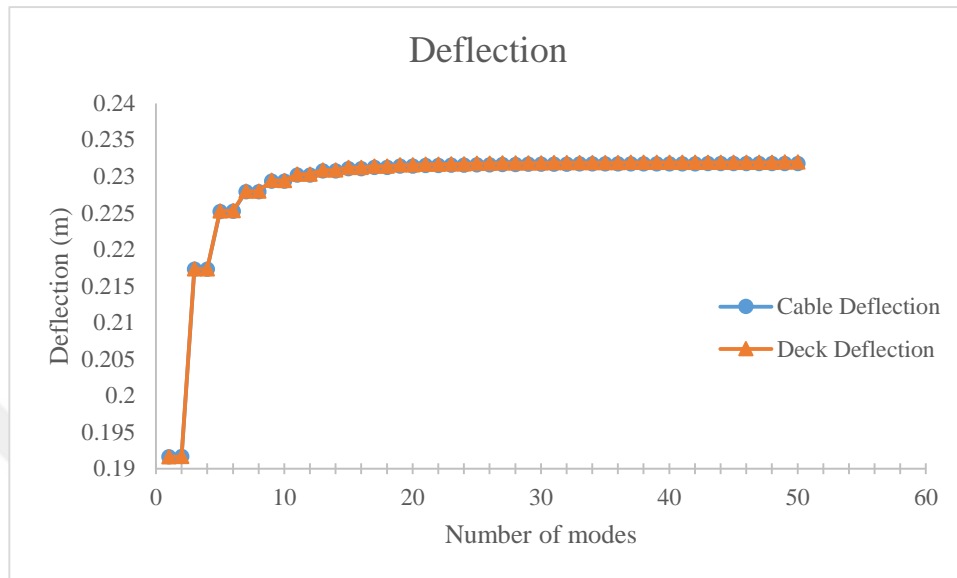


Figure 3.28 : The Case III middle point deflection of the cable and the deck at the time the moving load reach the span center (In meters)

In **Figure 3.29**, the deflection response of the cable and the deck as the moving load reaches the center of the span is illustrated. To compute the deflection first fifty modes of the bridge are taken into account. It can be understood from figure that considering first seven modes is sufficient to determine the deflection of the cable and the deck.



**Figure 3.29** : Deflection of center span in case III for first 50 modes

In **Figure 3.30** velocity response of the center of the cable and the deck when the moving load reaches the center of the span has been displayed. Figure 3.30 shows velocity response for the first fifty modes. To reach convergence in velocity, same as case I and case II, considering higher modes required. Considering first seventeen modes were sufficient to reach convergence for case III.

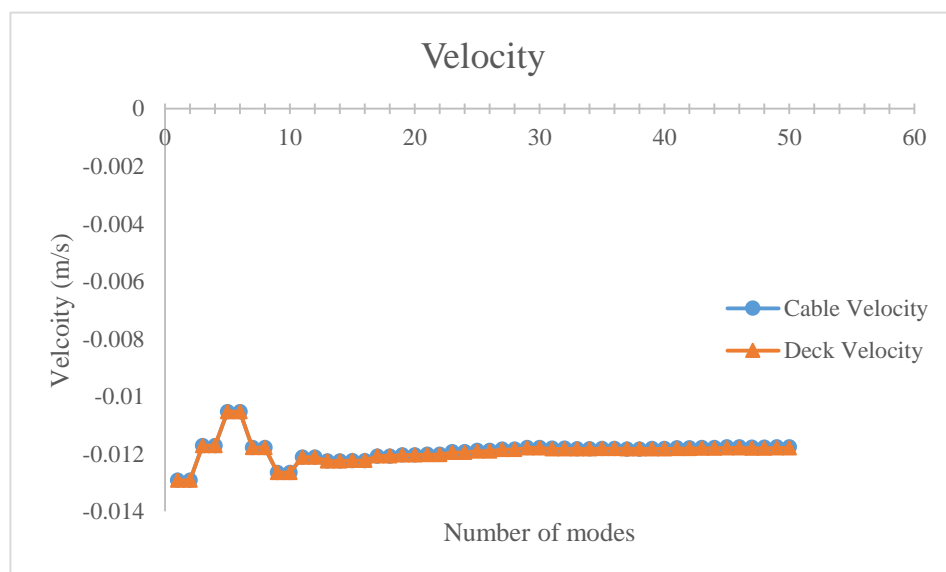


**Figure 3.30** : Velocity of center span in case III for first 50 modes

In **Figure 3.31** acceleration response of the center of the cable and the deck for case III has been illustrated. Likewise to deflection and velocity response, acceleration response is depicted at the time moving load reaches center of the span. Same as case I and case II, in order to reach the convergence in acceleration higher modes must be taken into account. **Figure 3.31** shows that there are not significant difference in accelerations of the cable and the deck for the first thirty eight modes. However, between mode thirty nine and forty five acceleration for the cable and the deck differs.

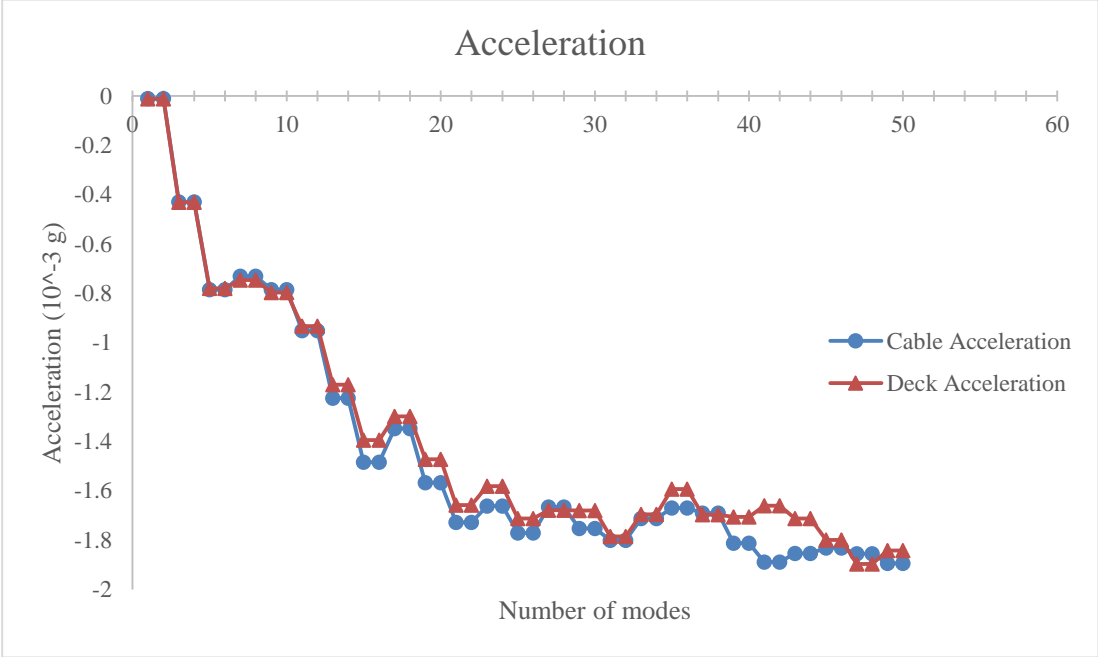


**Figure 3.31** : Acceleration of center span in case III for first 50 modes

**3.2.2.4 Hangers elongation**

Elongation of the hangers are an important topic to discuss since behavior of the hangers during vibration and knowing magnitude of axial forces that appears in hangers are crucial for proper design of the suspension bridge.

In **Tables 3.20 - 3.22** stress and axial forces that appears for case I, II and III are given.

**Table 3.20** : Elongation, stress and axial force in hangers for case I

Cable length	Deflection of the cable t = 48s (m)	Deflection of the Deck t = 48s (m)	Elongation (m)	Stress (MPa)	Axial Force (kN)
169.2333984	0.008462695	0.00846315	4.55478E-07	0.0004	0.011837468
158.8085938	0.016959506	0.016959957	4.50859E-07	0.0004	0.012486618
148.7255859	0.025500836	0.025498874	-1.96285E-06	-0.0018	-0.058046996

**Table 3.20 (continued) :** Elongation, stress and axial force in hangers for case I

138.984375	0.034104184	0.034104258	7.41957E-08	0.0001	0.002347959
129.5849609	0.042751176	0.042752466	1.28993E-06	0.0014	0.043781286
120.5273438	0.051422413	0.05142224	-1.7269E-07	-0.0002	-0.006301715
111.8115234	0.060098866	0.060100051	1.18495E-06	0.0015	0.046611278
103.4375	0.068749082	0.06875121	2.128E-06	0.0029	0.09048392
95.40527344	0.077386253	0.077389194	2.94138E-06	0.0043	0.135598904
87.71484375	0.08601336	0.086014389	1.02882E-06	0.0016	0.051587657
80.36621094	0.094638636	0.094638523	-1.12792E-07	-0.0002	-0.006172823
73.359375	0.103304099	0.103306482	2.38313E-06	0.0045	0.142879325
66.69433594	0.112033734	0.112034693	9.58346E-07	0.0020	0.063199177
60.37109375	0.120852229	0.120854118	1.88924E-06	0.0044	0.137637385
54.38964844	0.12974882	0.129751604	2.78418E-06	0.0072	0.225142915
48.75	0.138696465	0.138696604	1.38531E-07	0.0004	0.012498272
43.45214844	0.147682926	0.147685254	2.32845E-06	0.0075	0.235686104
38.49609375	0.156687724	0.156690776	3.05198E-06	0.0111	0.34869243
33.88183594	0.165743622	0.165748644	5.02194E-06	0.0208	0.651902751
29.609375	0.174854983	0.174862311	7.32851E-06	0.0347	1.088589959
25.67871094	0.183978562	0.183984927	6.36455E-06	0.0347	1.090115364
22.08984375	0.193078618	0.193092006	1.33879E-05	0.0848	2.665610431
18.84277344	0.202049435	0.202067615	1.81798E-05	0.1351	4.243469236
15.9375	0.2107972	0.210826275	2.90747E-05	0.2554	8.023661739
13.37402344	0.219145055	0.219197698	5.26429E-05	0.5511	17.31234694
11.15234375	0.226750789	0.226829251	7.84621E-05	0.9850	30.9436607
9.272460938	0.23311046	0.233255939	0.000145478	2.1965	69.00511948
7.734375	0.23717463	0.237379756	0.000205126	3.7130	116.6470175
6.538085938	0.238095327	0.238257404	0.000162077	3.4706	109.0309735
5.68359375	0.236430948	0.236520068	8.91202E-05	2.1952	68.96533855
5.170898438	0.233256418	0.23331139	5.49717E-05	1.4883	46.75747523
5	0.229131104	0.229161306	3.02019E-05	0.8457	26.56696693
5.170898438	0.224420362	0.224438783	1.84211E-05	0.4987	15.6684989

**Table 3.20 (continued) : Elongation, stress and axial force in hangers for case I**

5.68359375	0.21937632	0.219389812	1.34916E-05	0.3323	10.44046324
6.538085938	0.214104058	0.214109079	5.0216E-06	0.1075	3.37807836
7.734375	0.208689159	0.208692811	3.65204E-06	0.0661	2.076769643
9.272460938	0.203142249	0.203142514	2.64824E-07	0.0040	0.12561452
11.15234375	0.197467004	0.197467255	2.50787E-07	0.0031	0.098904598
13.37402344	0.191680218	0.191683689	3.47072E-06	0.0363	1.141394443
15.9375	0.185768592	0.185767465	-1.12696E-06	-0.0099	-0.311002894
18.84277344	0.179724217	0.17972355	-6.67325E-07	-0.0050	-0.155765126
22.08984375	0.173532136	0.173534197	2.06157E-06	0.0131	0.410472032
25.67871094	0.167196046	0.167195392	-6.54328E-07	-0.0036	-0.112072739
29.609375	0.160720174	0.160719583	-5.90937E-07	-0.0028	-0.08777891
33.88183594	0.15409435	0.154095401	1.0507E-06	0.0043	0.136392115
38.49609375	0.147341662	0.147343063	1.40129E-06	0.0051	0.160098986
43.45214844	0.140472143	0.140472742	5.99378E-07	0.0019	0.060669082
48.75	0.133478828	0.133479689	8.60914E-07	0.0025	0.077671726
54.38964844	0.126357002	0.126359853	2.85113E-06	0.0073	0.230557471
60.37109375	0.119081231	0.119084078	2.84666E-06	0.0066	0.207388714
66.69433594	0.111634081	0.111638013	3.93247E-06	0.0083	0.259330716
73.359375	0.103995969	0.10400148	5.51096E-06	0.0105	0.330407481
80.36621094	0.096146003	0.096150991	4.98867E-06	0.0087	0.273016768
87.71484375	0.0880839	0.088088797	4.89655E-06	0.0078	0.245524732
95.40527344	0.079809481	0.07981364	4.15894E-06	0.0061	0.191729305
103.4375	0.071344069	0.071348291	4.22204E-06	0.0057	0.179523771
111.8115234	0.062723459	0.062727354	3.89448E-06	0.0049	0.153193725
120.5273438	0.053975366	0.053977346	1.98001E-06	0.0023	0.072253768
129.5849609	0.04513597	0.045139101	3.13138E-06	0.0034	0.106281822
138.984375	0.036228114	0.036231017	2.90354E-06	0.0029	0.091884018
148.7255859	0.027255266	0.027255731	4.65044E-07	0.0004	0.013752654
158.8085938	0.018216685	0.018217749	1.06325E-06	0.0009	0.029446743
169.2333984	0.009121336	0.009122676	1.33924E-06	0.0011	0.034805569



**Table 3.21 : Elongation, stress and axial force in hangers for case II**

Cable length	Deflection of the cable t = 48s (m)	Deflection of the Deck t = 48s (m)	Elongation (m)	Stress (MPa)	Axial Force (kN)
169.2333984	0.008790131	0.00879041	2.79613E-07	0.0002	0.007266899
158.8085938	0.017568391	0.017569159	7.67772E-07	0.0007	0.021263581
148.7255859	0.026323635	0.026321398	-2.23686E-06	-0.0021	-0.066150182
138.984375	0.035060161	0.03505718	-2.98118E-06	-0.0030	-0.094340929
129.5849609	0.043777588	0.043776093	-1.49479E-06	-0.0016	-0.050734596
120.5273438	0.052509028	0.052508651	-3.76825E-07	-0.0004	-0.01375094
111.8115234	0.061286529	0.061284977	-1.55121E-06	-0.0019	-0.061018676
103.4375	0.07009061	0.07008724	-3.37026E-06	-0.0046	-0.143305481
95.40527344	0.078894477	0.078894162	-3.15348E-07	-0.0005	-0.014537681
87.71484375	0.087653645	0.087654148	5.0295E-07	0.0008	0.02521912
80.36621094	0.096314701	0.096315422	7.2099E-07	0.0013	0.039457848
73.359375	0.104834059	0.10483732	3.26089E-06	0.0062	0.19550541
66.69433594	0.113173238	0.113175581	2.34264E-06	0.0049	0.154487645
60.37109375	0.121309327	0.121313305	3.97743E-06	0.0092	0.289768419
54.38964844	0.129218805	0.129223395	4.59051E-06	0.0118	0.371212586
48.75	0.136894246	0.136897566	3.31961E-06	0.0095	0.299495275
43.45214844	0.144333023	0.144338847	5.82378E-06	0.0188	0.589483721
38.49609375	0.151528056	0.151532228	4.17229E-06	0.0152	0.476689688
33.88183594	0.158478945	0.158481878	2.93257E-06	0.0121	0.380678832
29.609375	0.165164744	0.165169839	5.09519E-06	0.0241	0.756849056
25.67871094	0.171590441	0.171595397	4.95618E-06	0.0270	0.848890112
22.08984375	0.177766246	0.177770616	4.3704E-06	0.0277	0.870173962
18.84277344	0.18368194	0.183684883	2.94292E-06	0.0219	0.686929596
15.9375	0.189360262	0.189362522	2.25966E-06	0.0198	0.623592899
13.37402344	0.194809779	0.194811274	1.49508E-06	0.0157	0.491676318
11.15234375	0.200058619	0.200062277	3.65848E-06	0.0459	1.442820642
9.272460938	0.205152491	0.205159331	6.8398E-06	0.1033	3.244338414
7.734375	0.210083109	0.210087106	3.99622E-06	0.0723	2.272489104

**Table 3.21 (continued) :** Elongation, stress and axial force in hangers for case II

6.538085938	0.214830944	0.214837934	6.98993E-06	0.1497	4.702191142
5.68359375	0.219337008	0.219347435	1.0427E-05	0.2568	8.068878237
5.170898438	0.223543148	0.223555394	1.22463E-05	0.3316	10.41638311
5	0.227389824	0.227410411	2.05872E-05	0.5764	18.1094799
5.170898438	0.230778169	0.230802	2.38309E-05	0.6452	20.26992741
5.68359375	0.233647053	0.233687608	4.05553E-05	0.9990	31.38357917
6.538085938	0.235819007	0.235885347	6.634E-05	1.4205	44.62753864
7.734375	0.236992896	0.237092072	9.91764E-05	1.7952	56.39763376
9.272460938	0.236550354	0.236723821	0.000173467	2.6191	82.28094159
11.15234375	0.233406338	0.23360593	0.000199592	2.5056	78.71461474
13.37402344	0.227296894	0.227424787	0.000127894	1.3388	42.05958121
15.9375	0.219244291	0.219313839	6.95482E-05	0.6109	19.19303146
18.84277344	0.210156136	0.210199581	4.34455E-05	0.3228	10.14092667
22.08984375	0.200469633	0.200490401	2.07679E-05	0.1316	4.135027983
25.67871094	0.190527181	0.190541544	1.43631E-05	0.0783	2.460103632
29.609375	0.180505169	0.180511063	5.89428E-06	0.0279	0.875547458
33.88183594	0.170536417	0.170538418	2.00057E-06	0.0083	0.259695468
38.49609375	0.160719369	0.160723688	4.31863E-06	0.0157	0.493409323
43.45214844	0.151080015	0.151077814	-2.20096E-06	-0.0071	-0.222781435
48.75	0.141625134	0.141621621	-3.51333E-06	-0.0101	-0.316972926
54.38964844	0.132315894	0.132313496	-2.39884E-06	-0.0062	-0.193982799
60.37109375	0.123162595	0.123160858	-1.73762E-06	-0.0040	-0.126591448
66.69433594	0.114204793	0.114204912	1.18706E-07	0.0002	0.007828182
73.359375	0.105444021	0.105442733	-1.28749E-06	-0.0025	-0.077191162
80.36621094	0.096852475	0.096853573	1.09801E-06	0.0019	0.060091335
87.71484375	0.088350157	0.088351872	1.71585E-06	0.0027	0.086036837
95.40527344	0.079859616	0.079860621	1.00576E-06	0.0015	0.04636625
103.4375	0.07131441	0.071319836	5.42594E-06	0.0073	0.230714676
111.8115234	0.062674211	0.062681351	7.14013E-06	0.0089	0.280864967
120.5273438	0.053936312	0.053942519	6.20703E-06	0.0072	0.22650418

**Table 3.21 (continued) : Elongation, stress and axial force in hangers for case II**

129.5849609	0.045085323	0.045088996	3.67321E-06	0.0040	0.124672085
138.984375	0.036140319	0.036142658	2.33888E-06	0.0024	0.074014889
148.7255859	0.027137399	0.027141714	4.31482E-06	0.0041	0.127601178
158.8085938	0.018102849	0.018105008	2.15924E-06	0.0019	0.059800558
169.2333984	0.009060327	0.009059171	-1.15646E-06	-0.0010	-0.030055512

**Table 3.22 : Elongation, stress and axial force in hangers for case III**

Cable length	Deflection of the cable t = 48s (m)	Deflection of the Deck t = 48s (m)	Elongation (m)	Stress (MPa)	Axial Force (kN)
169.2333984	0.010737294	0.010738239	9.45E-07	0.0008	0.024559735
158.8085938	0.021468308	0.021470934	2.6257E-06	0.0023	0.072719305
148.7255859	0.032188564	0.032193513	4.94915E-06	0.0047	0.146360114
138.984375	0.042837844	0.04284306	5.2162E-06	0.0053	0.16506937
129.5849609	0.053382558	0.053392141	9.58312E-06	0.0104	0.325259519
120.5273438	0.063783483	0.063795069	1.15868E-05	0.0135	0.422818789
111.8115234	0.07396772	0.073976053	8.3337E-06	0.0104	0.327815394
103.4375	0.083877692	0.083887694	1.00024E-05	0.0135	0.425306483
95.40527344	0.093483013	0.093494123	1.11103E-05	0.0163	0.512191364
87.71484375	0.102845866	0.102856307	1.04403E-05	0.0167	0.523500786
80.36621094	0.112056435	0.112064669	8.23435E-06	0.0143	0.450644062
73.359375	0.121186951	0.121191265	4.31343E-06	0.0082	0.258609614
66.69433594	0.130311461	0.130315801	4.33981E-06	0.0091	0.286193728
60.37109375	0.139474586	0.139478947	4.36111E-06	0.0101	0.317720996
54.38964844	0.148735177	0.148741397	6.21928E-06	0.0160	0.502923187
48.75	0.158098712	0.158101883	3.17102E-06	0.0091	0.286089418
43.45214844	0.167519387	0.167516417	-2.96985E-06	-0.0096	-0.300608298
38.49609375	0.176991641	0.176996666	5.02573E-06	0.0183	0.574196555
33.88183594	0.186519649	0.186527767	8.11799E-06	0.0335	1.053803027
29.609375	0.196143179	0.196147255	4.07633E-06	0.0193	0.605505757
25.67871094	0.205841378	0.205849894	8.5166E-06	0.0464	1.458716145
22.08984375	0.215550579	0.215568344	1.77648E-05	0.1126	3.537088397

**Table 3.22 (continued) :** Elongation, stress and axial force in hangers for case III

18.84277344	0.225192194	0.225231769	3.95754E-05	0.2940	9.23758291
15.9375	0.234453688	0.234517206	6.35181E-05	0.5580	17.52893513
13.37402344	0.242866886	0.242978964	0.000112078	1.1732	36.85831006
11.15234375	0.249534879	0.249725862	0.000190982	2.3975	75.31912398
9.272460938	0.253258444	0.253449246	0.000190802	2.8808	90.50354556
7.734375	0.253991454	0.254106378	0.000114924	2.0802	65.35266033
6.538085938	0.252790641	0.252862173	7.15324E-05	1.5317	48.12047726
5.68359375	0.250410545	0.250458774	4.82288E-05	1.1880	37.32171459
5.170898438	0.247223612	0.247248747	2.51355E-05	0.6805	21.37961641
5	0.243487511	0.24350533	1.78195E-05	0.4989	15.67487453
5.170898438	0.239330319	0.239342366	1.20471E-05	0.3262	10.24693656
5.68359375	0.234896411	0.234905688	9.27789E-06	0.2285	7.17966457
6.538085938	0.230272896	0.230279961	7.06466E-06	0.1513	4.752460065
7.734375	0.225485644	0.225489991	4.34661E-06	0.0787	2.471742243
9.272460938	0.220545198	0.220549128	3.92957E-06	0.0593	1.863921022
11.15234375	0.215410395	0.215408807	-1.58859E-06	-0.0199	-0.626505509
13.37402344	0.210070825	0.210071316	4.91106E-07	0.0051	0.16150681
15.9375	0.204551492	0.204556366	4.87371E-06	0.0428	1.344985864
18.84277344	0.198867664	0.198868912	1.24776E-06	0.0093	0.29124964
22.08984375	0.193007872	0.193011467	3.59455E-06	0.0228	0.715698227
25.67871094	0.186931042	0.186936223	5.18083E-06	0.0282	0.887368326
29.609375	0.18058589	0.180589691	3.80103E-06	0.0180	0.564611314
33.88183594	0.17391362	0.173920179	6.55946E-06	0.0271	0.851489685
38.49609375	0.166889341	0.16689521	5.86901E-06	0.0213	0.670541909
43.45214844	0.159515292	0.159521055	5.7631E-06	0.0186	0.583341467
48.75	0.151812955	0.151819857	6.90211E-06	0.0198	0.622708882
54.38964844	0.143839834	0.143844194	4.35965E-06	0.0112	0.352543669
60.37109375	0.135628478	0.135633259	4.78085E-06	0.0111	0.348300276
66.69433594	0.127191516	0.127198476	6.9597E-06	0.0146	0.45896505
73.359375	0.118527694	0.118534051	6.35703E-06	0.0121	0.381133212

**Table 3.22 (continued) :** Elongation, stress and axial force in hangers for case III

80.36621094	0.109598019	0.109603176	5.15725E-06	0.0090	0.282242591
87.71484375	0.100382063	0.100386916	4.85341E-06	0.0077	0.24336156
95.40527344	0.090893005	0.090897268	4.26352E-06	0.0063	0.196550245
103.4375	0.081167945	0.081170468	2.52306E-06	0.0034	0.107282203
111.8115234	0.071264714	0.071267119	2.40469E-06	0.0030	0.094591004
120.5273438	0.061247874	0.061250793	2.91855E-06	0.0034	0.106502411
129.5849609	0.051172443	0.051174576	2.13307E-06	0.0023	0.072398394
138.984375	0.041052461	0.041054674	2.21272E-06	0.0022	0.070022601
148.7255859	0.03088494	0.030885662	7.21831E-07	0.0007	0.021346566
158.8085938	0.020656482	0.020654658	-1.82367E-06	-0.0016	-0.050506923
169.2333984	0.01035131	0.010350038	-1.27197E-06	-0.0011	-0.033057466

These tables shows us that in none of hangers yielding occurs and all of the hangers are in elastic region during vibration. Maximum stress occurred in Case I,II and III respectively are 3.713 MPa, 2.6191 MPa and 2.8808 MPa and maximum axial force appears in hangers for case I,II and III respectively are 116.647 kN, 82.2809 kN and 90.5305 kN.

### 3.2.3 Result for inextensible hangers

In previous section extensibility of the hangers were considered and it means during vibration amount of deflection that occurs in the deck and the cable were different. In this section obtained result for extensible hangers are compared with the result that obtained when hangers are inextensible. For this purpose equation 2.56 is used in which differential equation is only dependent on deflection of the deck.

#### 3.2.3.1 Case I result

In **Figure 3.32** maximum deflection in middle point of the deck plotted. Results indicate that maximum deflection occurs at 49.549 second when load close to middle of the deck.

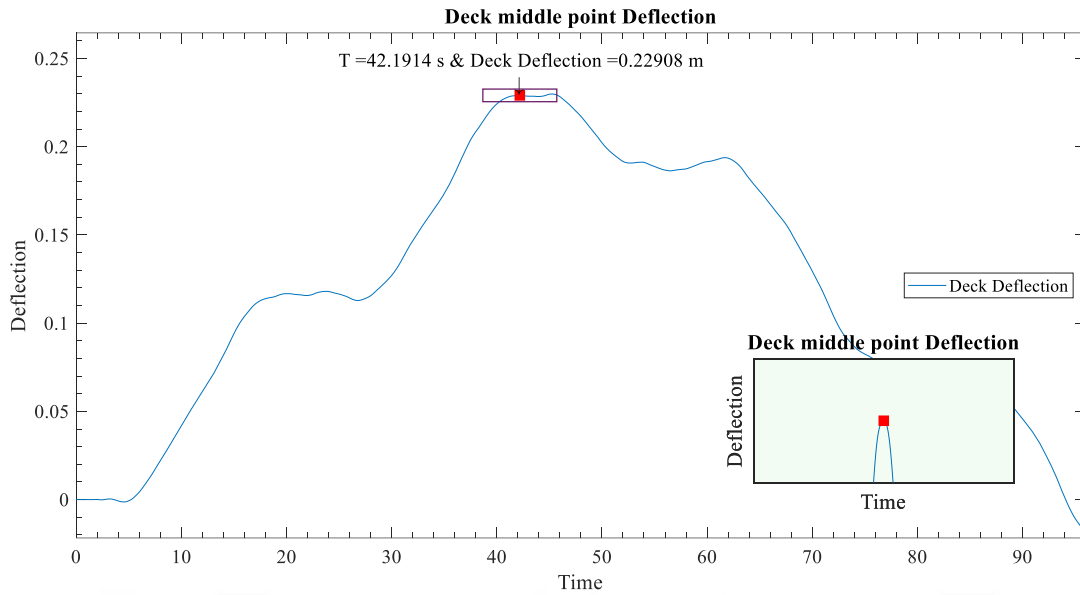


**Figure 3.32 :** Deck middle point deflection in case hangers are inextensible for Case I (In meters)  
 In **Figure 3.33** 3D plot of deck deflection has been depicted. In this figure x-axis represent time and y-axis represents location of the bridge, while z-axis positive direction shows deflection of the deck.

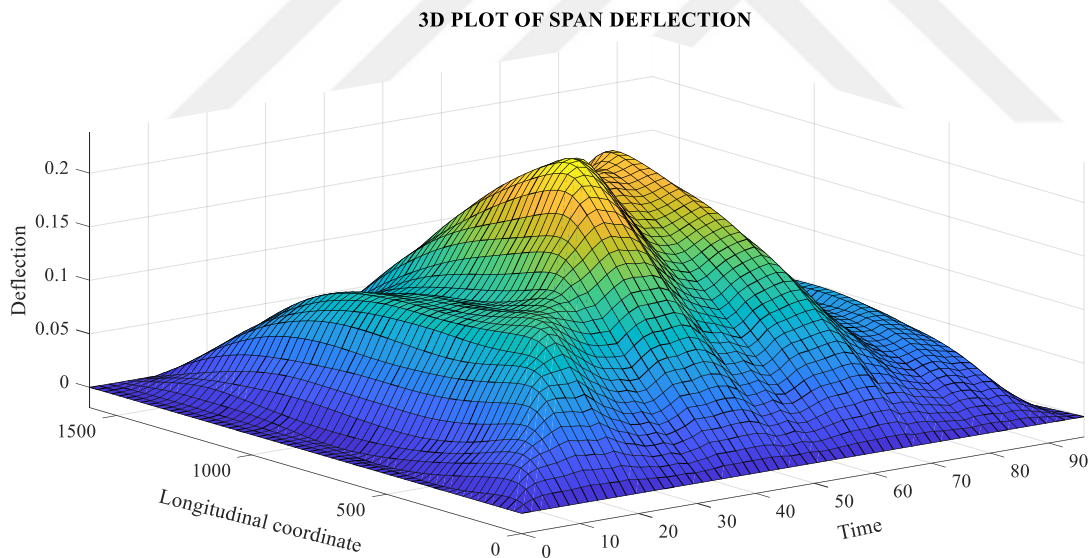


**Figure 3.33 :** 3D Plot of span deflection in case hangers are inextensible for Case I (In meters)

Max deflection of the deck when moving load reaches middle of the deck has been illustrated in **Figure 3.34**.

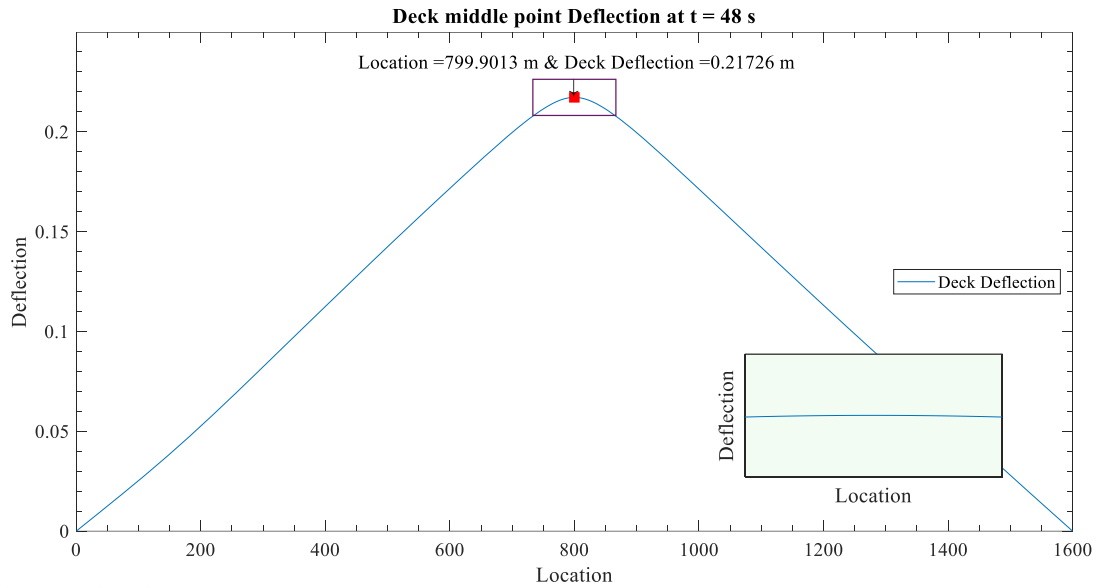


**Figure 3.34 :** The Case I middle point deflection of the deck at the time the moving load reach the span center (In meters)

### 3.2.3.2 Case II result

In **Figure 3.35** maximum deflection in middle point of the deck plotted. Results indicate that maximum deflection occurs at 31.6016 second when load close to middle of the deck.

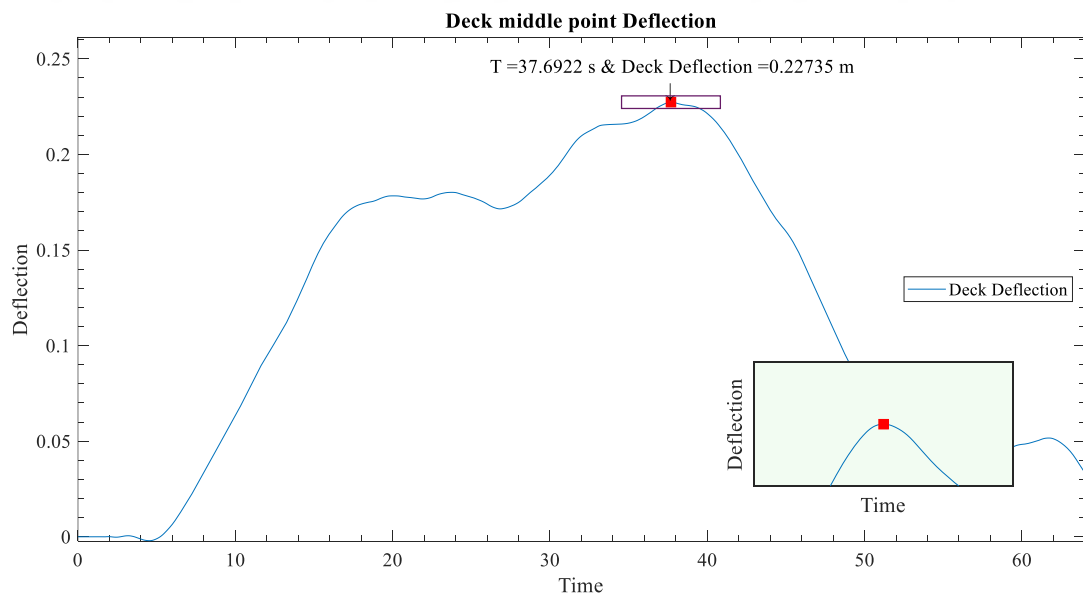


**Figure 3.35 :** Deck middle point deflection in case hangers are inextensible for Case II (In meters)

In **Figure 3.36** 3D plot of deck deflection has been depicted. In this figure x-axis represent time and y-axis represents location of the bridge, while z-axis positive direction shows deflection of the deck.

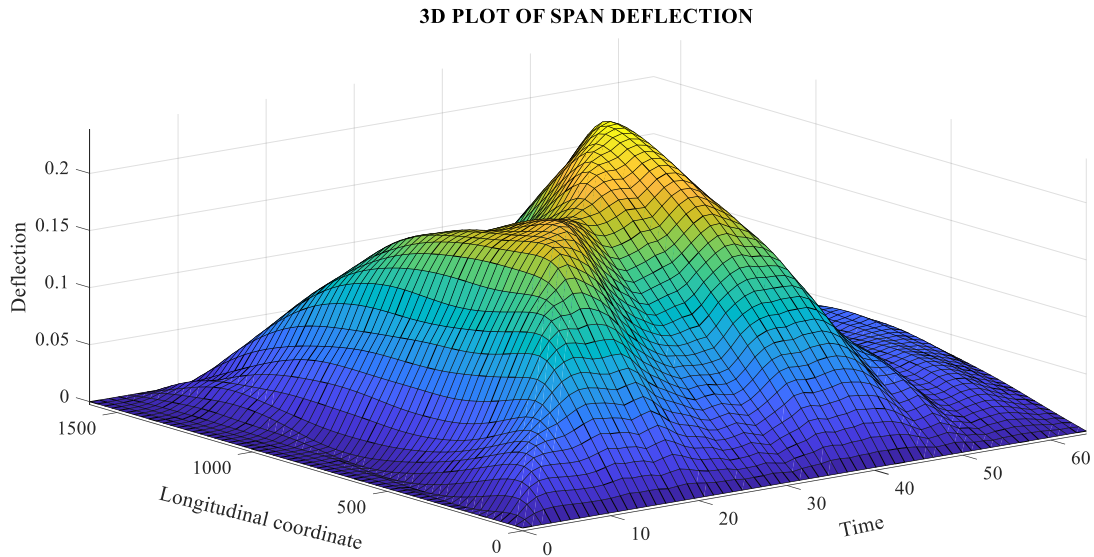


**Figure 3.36 :** 3D Plot of span deflection in case hangers are inextensible for Case II (In meters)  
 Max deflection of the deck when moving load reaches middle of the deck has been illustrated in **Figure 3.37**.

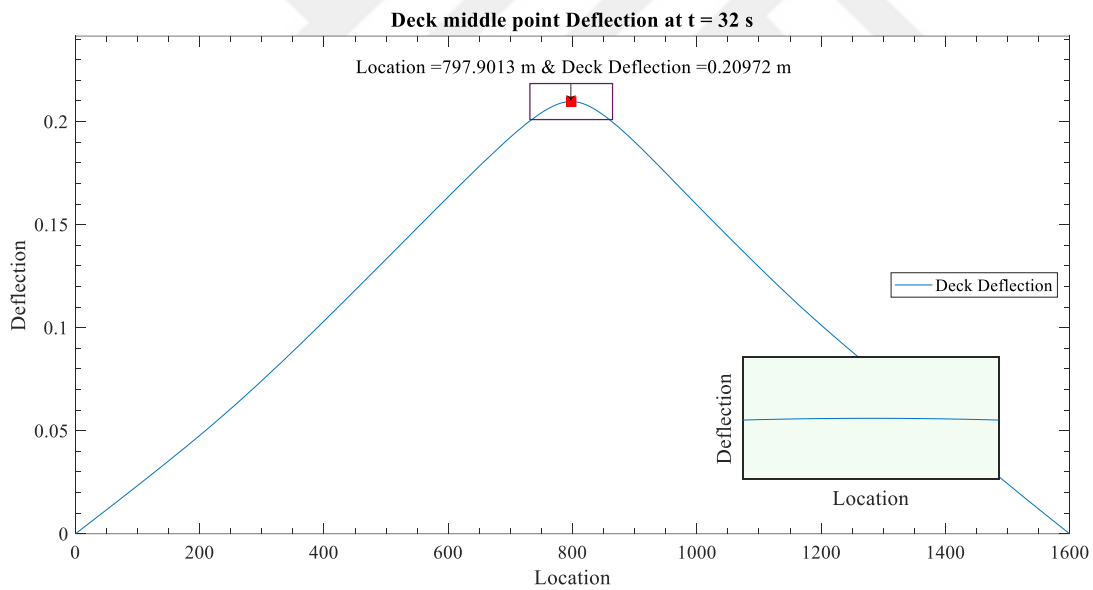


**Figure 3.37 :** The Case II middle point deflection of the deck at the time the moving load reach the span center (In meters)

### 3.2.3.3 Case III result

In **Figure 3.38** maximum deflection in middle point of the deck plotted. Results indicate that maximum deflection occurs at 23.6946 second when load close to middle of the deck.



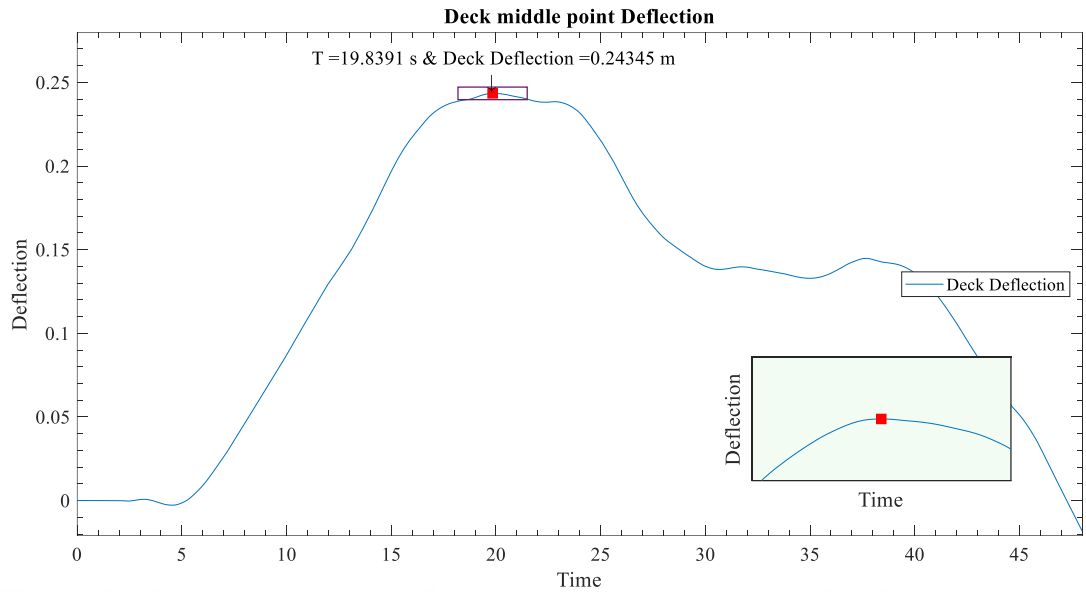


**Figure 3.38** : Deck middle point deflection in case hangers are inextensible for Case III (In meters)  
 In **Figure 3.39** 3D plot of deck deflection has been depicted. In this figure x-axis represent time and y-axis represents location of the bridge, while z-axis positive direction shows deflection of the deck.

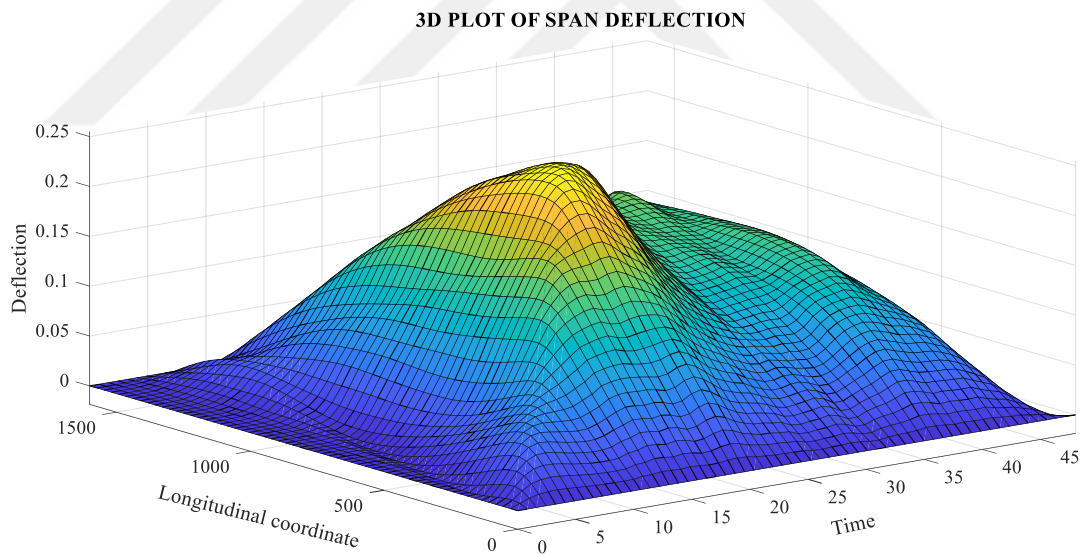


**Figure 3.39** : 3D Plot of span deflection in case hangers are inextensible for Case III (In meters)  
 Max deflection of the deck when moving load reaches middle of the deck has been illustrated in **Figure 3.40**.

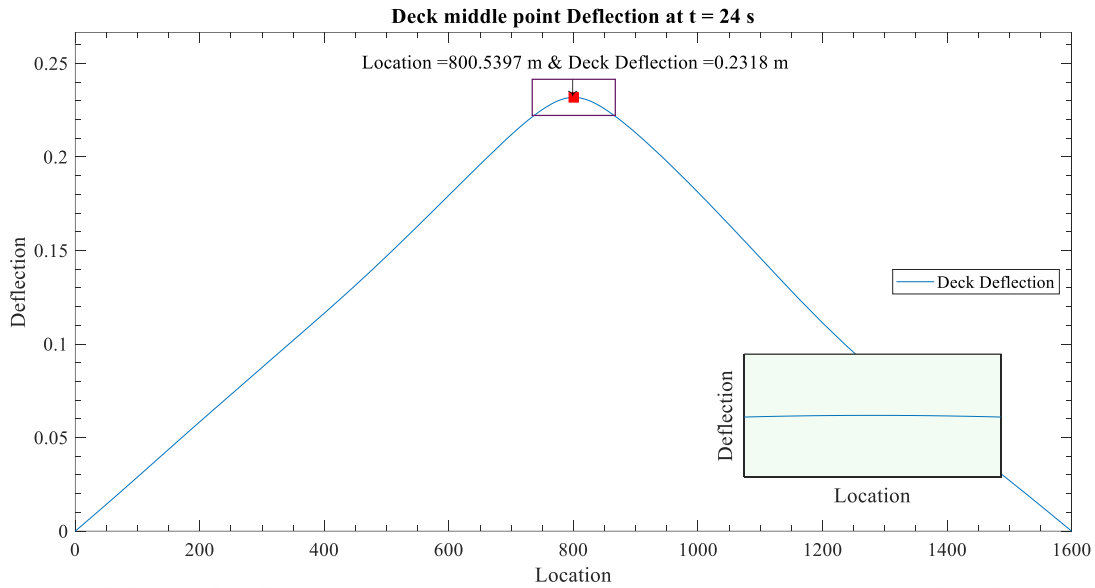


**Figure 3.40 :** The Case III middle point deflection of the deck at the time the moving load reach the span center (In meters)

### 3.2.4 Result comparison

Computed deflection of suspension bridge when a moving load reaches the middle of the span for both extensible and inextensible hangers are compared in **Table 3.23**. Comparison of these result are very important since for solving coupled differential equation a lot of time need to spent. On the other hand it is worth to note that, even though solving coupled differential equation needs a lot of time, solving this equation helps to determine axial loads in hangers and it is advantage of case in which hangers are considered extensible.

**Table 3.23 :** Comparison of Middle Point Deflection at the time moving load reaches middle of the span

Middle Point Deflection at the time load reaches middle of the span			
Case No.	Hangers type Extensible Hangers (m)	Inextensible Hangers (m)	Difference (%)
Case I	0.21738	0.21726	0.06%
Case II	0.20986	0.20972	0.07%
Case III	0.23195	0.2318	0.06%

Likewise Max deflection of the suspension bridge span from the time that moving load enters the span until it quits span for both extensible and inextensible hangers are compared in **Table 3.24**.

**Table 3.24** : Comparison of Middle Point Max Deflection

Middle Point Max Deflection			
Hangers type	Extensible Hangers (m)	Inextensible Hangers (m)	Difference (%)
Case I	0.22916	0.22908	0.03%
Case II	0.22741	0.22735	0.03%
Case III	0.24351	0.24345	0.02%

According to **Table 3.23** and **Table 3.24**, the difference in deflection of the cable and the deck does not exceed 0.1 percent for both extensible and inextensible hangers assumption. Another fact that tables shows are that extensibility of the hangers are not affecting final result and consideration of extensible hangers is acceptable and reliable.

### 3.2.5 Total deflection of the suspension bridge

In **Figures 3.41-3.43** total deflection of the bridge for Cases I, II and III has been illustrated respectively. In mentioned figures total deflection of the bridge computed by summing up static deflection and dynamical deflection due to the moving load.

3D PLOT OF SPAN DEFLECTION

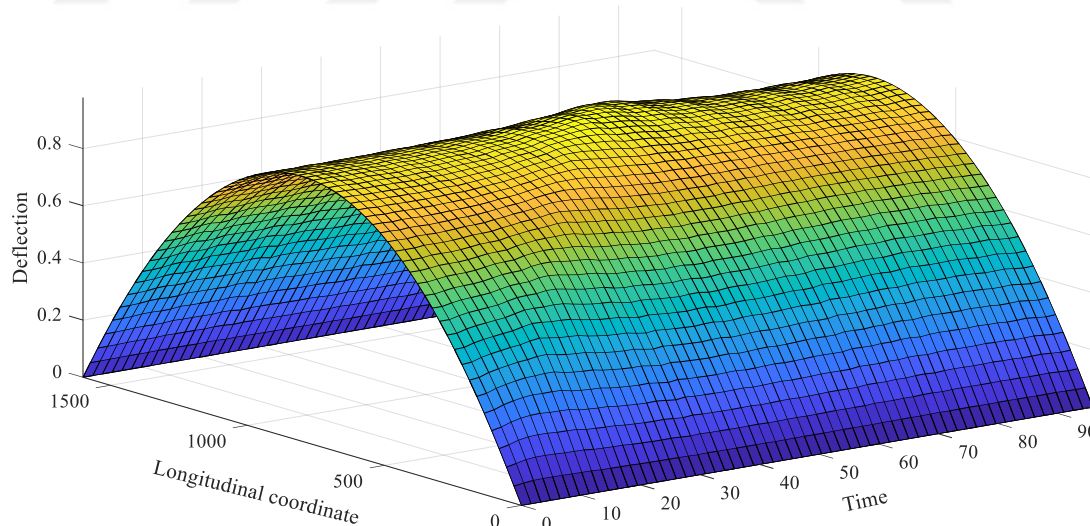


**Figure 3.41** : 3D Plot of Total Deflection of The Suspension bridge for Case I (In meters)

### 3D PLOT OF SPAN DEFLECTION

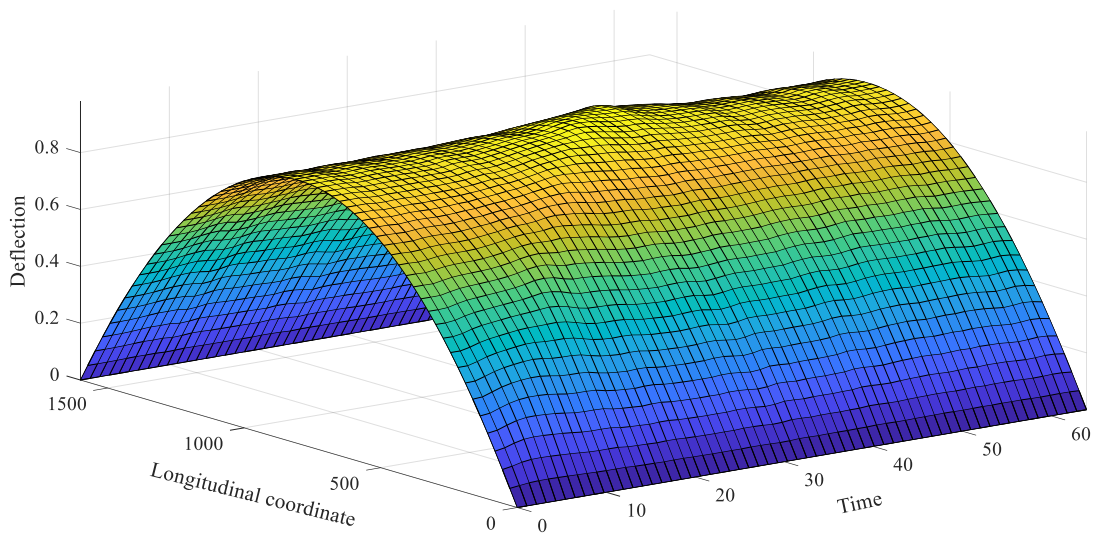


Figure 3.42 : 3D Plot of Total Deflection of The Suspension bridge for Case II (In meters)

### 3D PLOT OF SPAN DEFLECTION

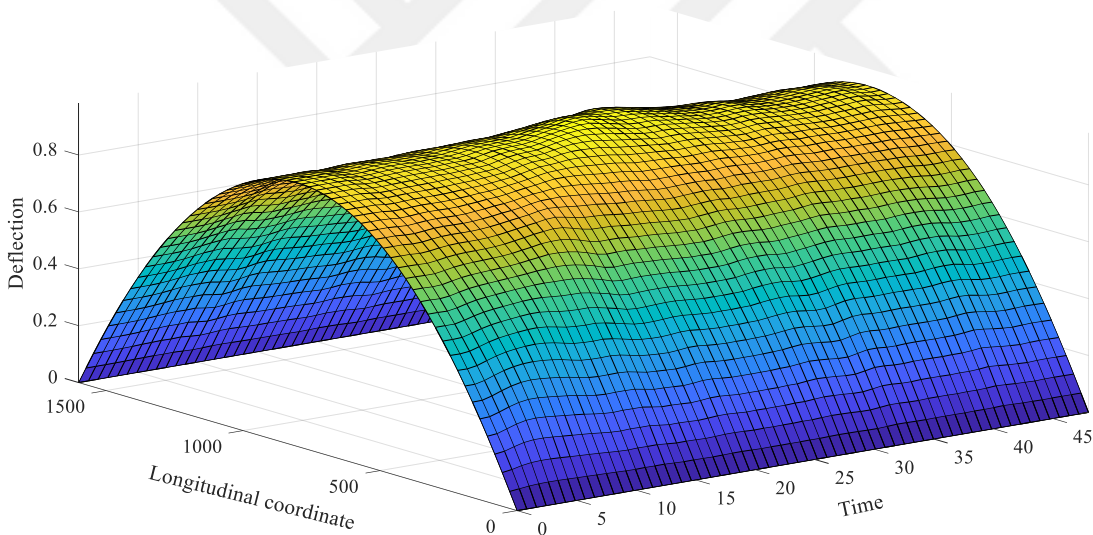


Figure 3.43 : 3D Plot of Total Deflection of The Suspension bridge for Case III (In meters)

### 3.2.6 Natural frequencies

In order to determine natural frequencies as it is explained in section 2.8, at first stiffness of the system is calculated and then after dividing it by mass the square of angular speed of the suspension bridge is achieved.

For determining angular speed equation 2.59 used and after computing angular speed equation 2.60 used for determining natural frequencies of the suspension bridge. Natural frequencies and angular speeds of the suspension bridge for 24 modes are computed and indicated in **Table 3.25**.

**Table 3.25** : Natural frequencies

Symmetric modes	Frequency (Hz)	Anti-symmetric modes	Frequency (Hz)
1	0.0430839	2	0.15360018
3	0.13347878	4	0.19338369
5	0.23592457	6	0.29670703
7	0.35669856	8	0.42660249
9	0.50030616	10	0.58220819
11	0.66975366	12	0.76509215
13	0.866972	14	0.97656482
15	1.0931863	16	1.21752571
17	1.34917721	18	1.48857042
19	1.63544911	20	1.79009362
21	1.952334	22	2.12236022
23	2.30005497	24	2.48555115

As it is mentioned earlier in chapter 1, it can be seen that second symmetric mode occurs before first anti-symmetric mode which is also observed by Abdel Ghaffar [3]. in other words first two modes are symmetric and after that anti-symmetric modes occur. First 24 Angular speeds of the suspension bridge is indicated in **Table 3.26**.

**Table 3.26** : Angular speed

Symmetric modes	Angular speed ( $rad/s$ )	Anti-symmetric modes	Angular speed ( $rad/s$ )
1	0.27070414	2	0.96509839
3	0.83867189	4	1.21506559
5	1.48235778	6	1.86426525
7	2.24120317	8	2.68042249
9	3.14351634	10	3.65812193
11	4.20818634	12	4.80721573
13	5.44734573	14	6.13593774
15	6.86869211	16	7.64993964
17	8.47713043	18	9.35296379

**Table3.26 (continued) : Angular speed**

19	10.2758298	20	11.2474899
21	12.2668763	22	13.3351826
23	14.4516716	24	15.6171785

In **Figures 3.44-3.49** first six mode shapes of the suspension obtained by ABAQUS software is illustrated respectively.

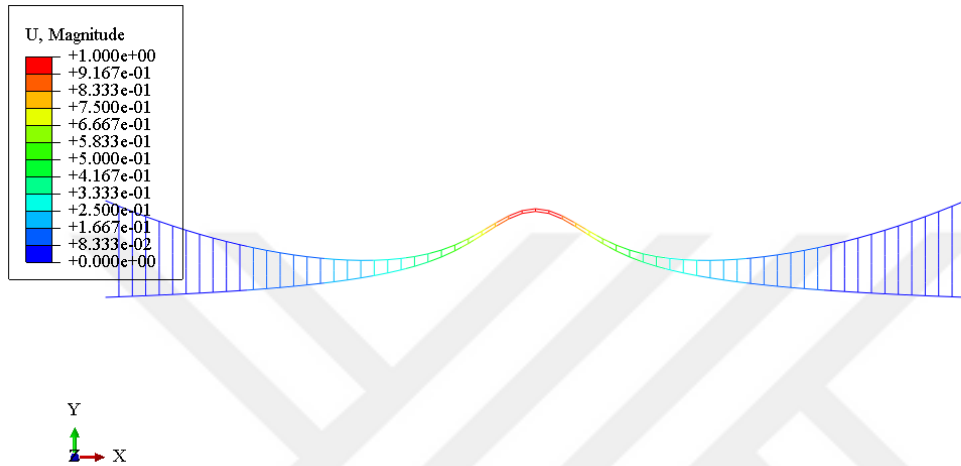


**Figure 3.44 : 1<sup>st</sup> Mode Shape**

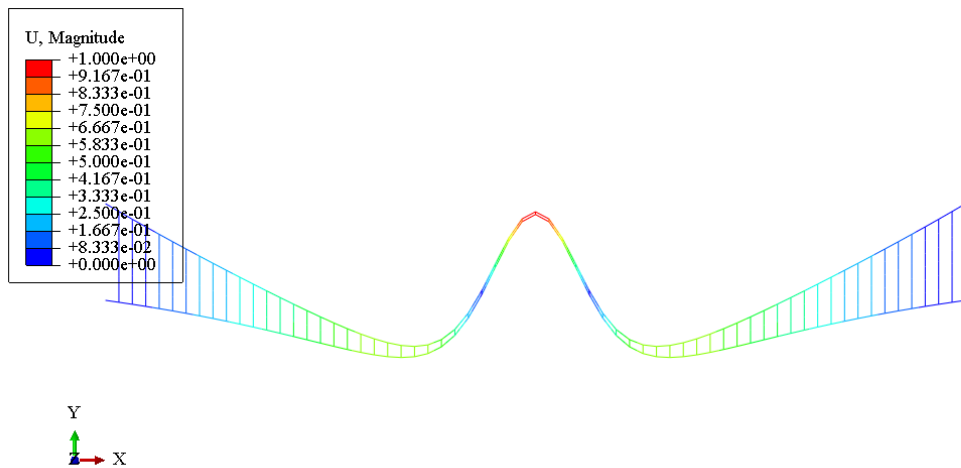


**Figure 3.45 : 2<sup>nd</sup> Mode Shape**

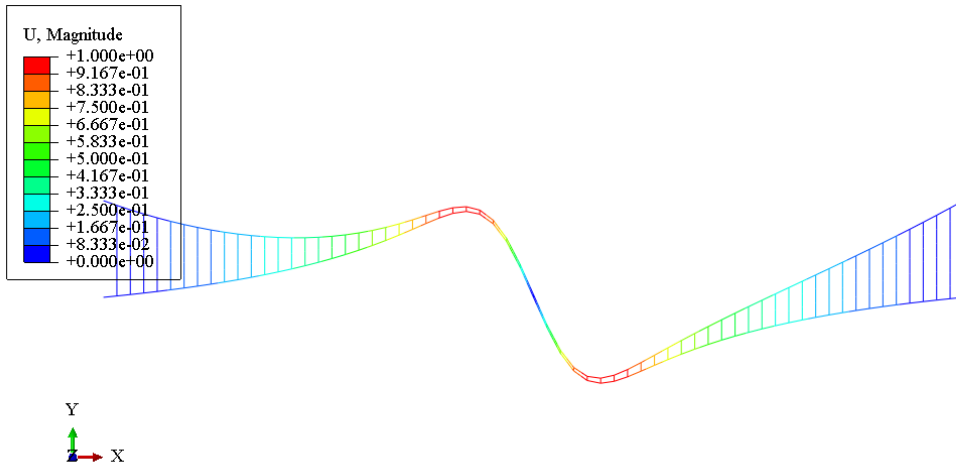


Figure 3.46 : 3<sup>rd</sup> Mode Shape

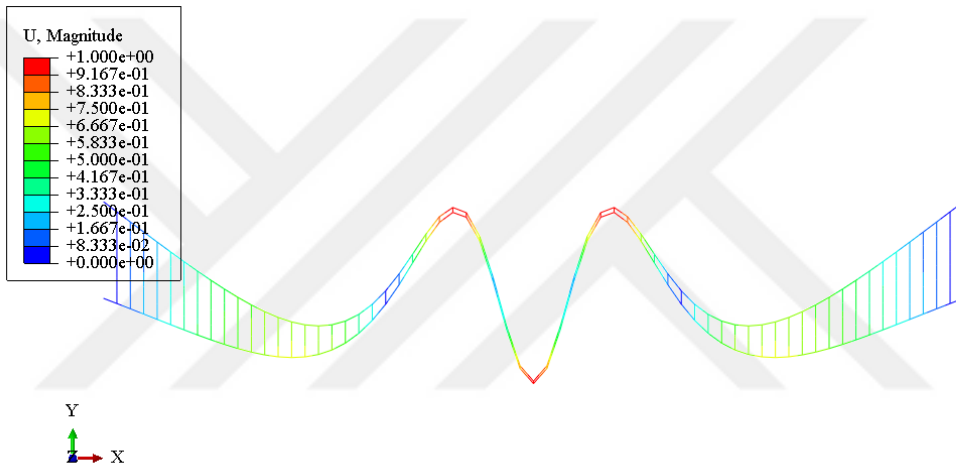


Figure 3.47 : 4<sup>th</sup> Mode Shape

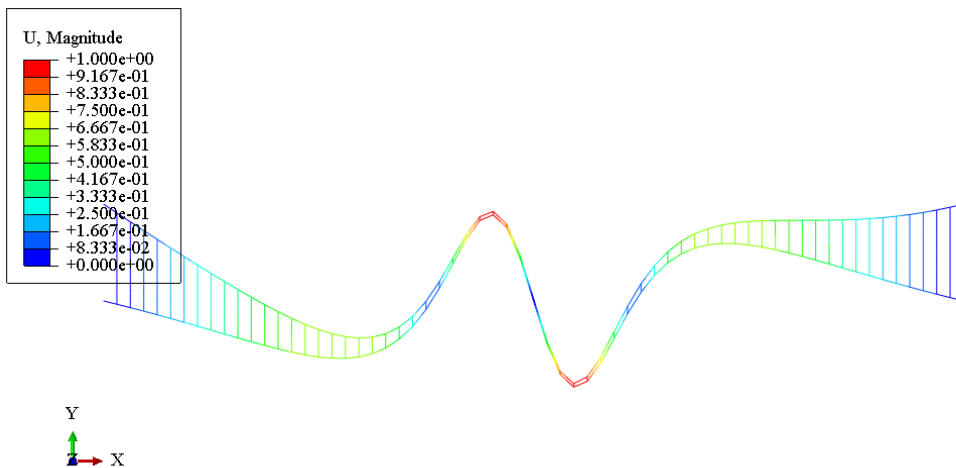
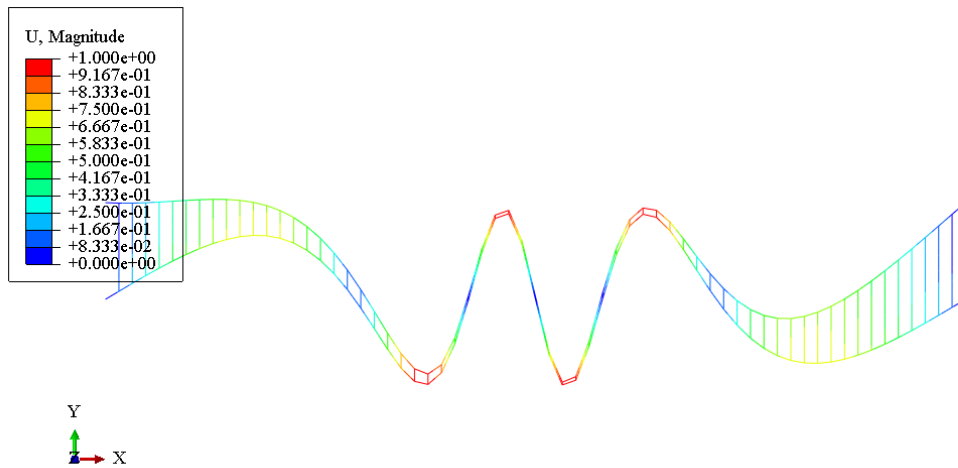


Figure 3.48 : 5<sup>th</sup> Mode Shape



**Figure 3.49 : 6<sup>th</sup> Mode Shape**

### 3.2.7 Maximum acceleration response

To investigate maximum of acceleration that occurs in bridge, differential equations solved for the total time that moving load cross the bridge. In **Figure 3.50** maximum value of suspension bridge acceleration response is displayed. Maximum acceleration of the suspension bridge at each point of the span is for whole time of the vibration. Figure 3.50 reveals that for higher speeds acceleration of the bridge increases significantly which emphasis on importance of the velocity of the moving load on acceleration response of the suspension bridge.

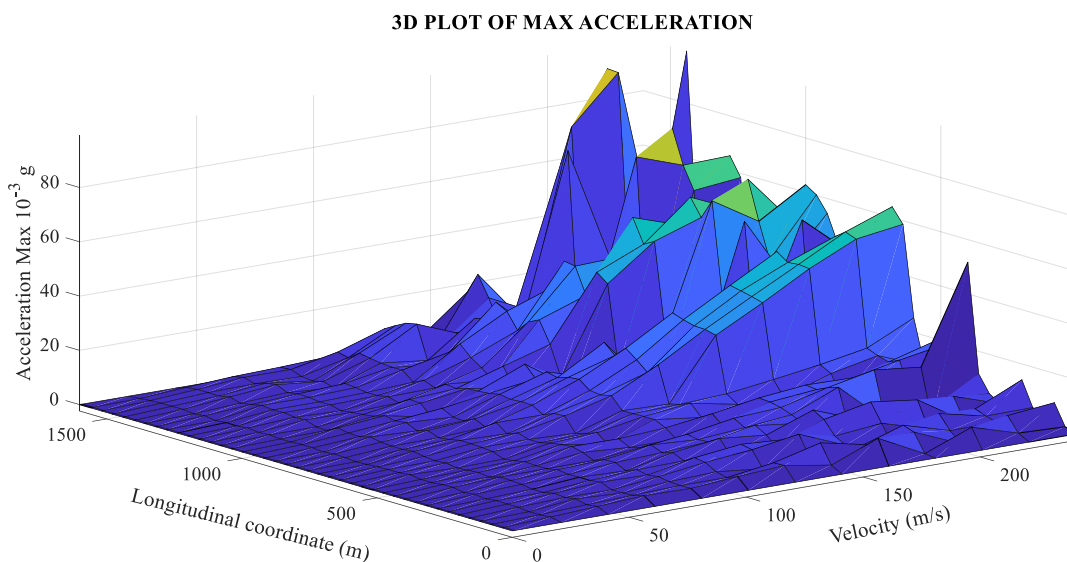


**Figure 3.50 : Max acceleration response of the suspension bridge**



### 3.3 FEM Result

Behavior of the suspension bridge simulated in ABAQUS software. ABAQUS use FEM method for analysis and computation. To simulate behavior of the suspension bridge in ABAQUS, same as mathematical approach, behavior of the suspension bridge evaluated in two steps. First step was static analysis when it is subjected to distributed live load and second step was dynamic analysis of the suspension bridge when it is subjected to the moving load with constant velocity.

In **Figure 3.51** model of the suspension bridge in ABAQUS software which has been provided for static analysis is shown.

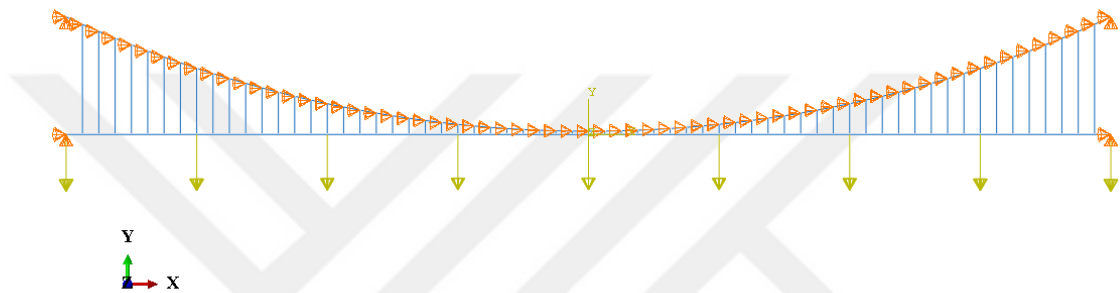


**Figure 3.51 :** ABAQUS model for static analysis

**Figure 3.52** and **Figure 3.53** displays 2D and 3D deformed shape of the suspension bridge when it is subjected to static live load.

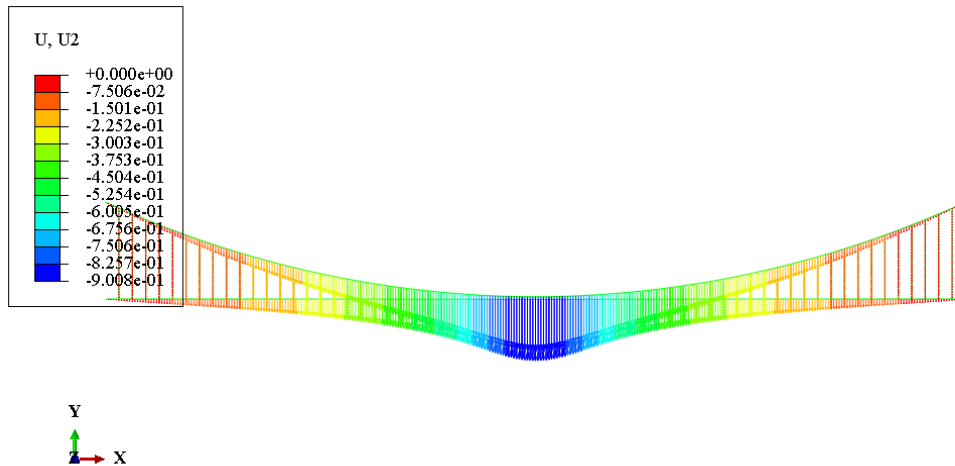


**Figure 3.52 :** Plot of static deformation (In meters)

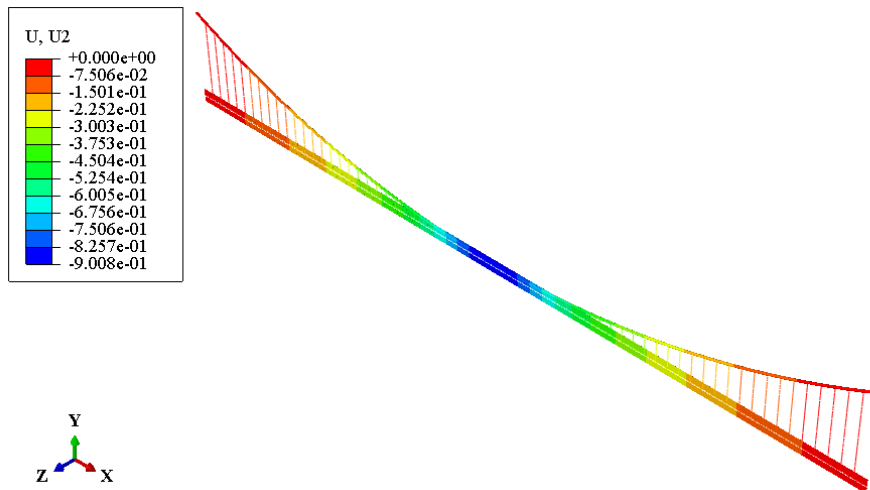


**Figure 3.53** : 3D plot of static deformation (In meters)

Comparison of computed results by MATLAB and ABAQUS for static analysis is manifested in **Table 3.27**.

**Table 3.27** : Comparison of Mid Point Deflection Computed by MATLAB and ABAQUS

		Deflection		
Element	Software	MATLAB (m)	ABAQUS (m)	Difference (%)
CABLE		0.926038715	0.900736000	2.732360%
DECK		0.927164841	0.900751000	2.848883%

Model of the suspension bridge for dynamic analysis is illustrated in **Figure 3.54**. For restricting bridge out-of plane deflection, 2D analysis has been performed and for avoiding displacement in horizontal direction supports has been provided for all of the points to restrain bridge movement in horizontal direction.

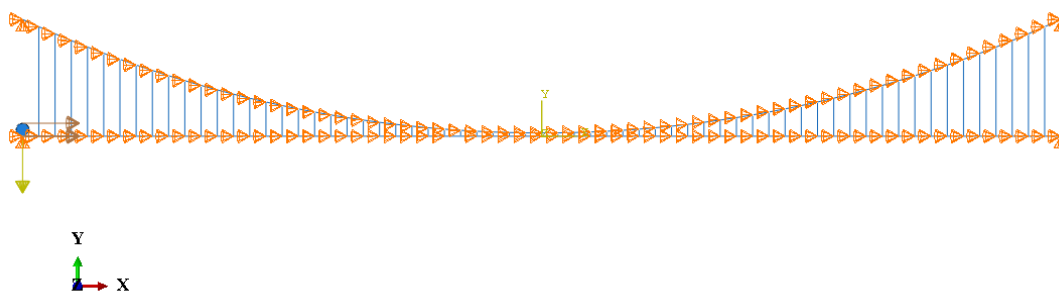


**Figure 3.54** : ABAQUS model for dynamic analysis

Middle point deflection in case I, II and III for the cable and the deck through the time has been plotted and displayed in **Figures 3.55-3.57**.

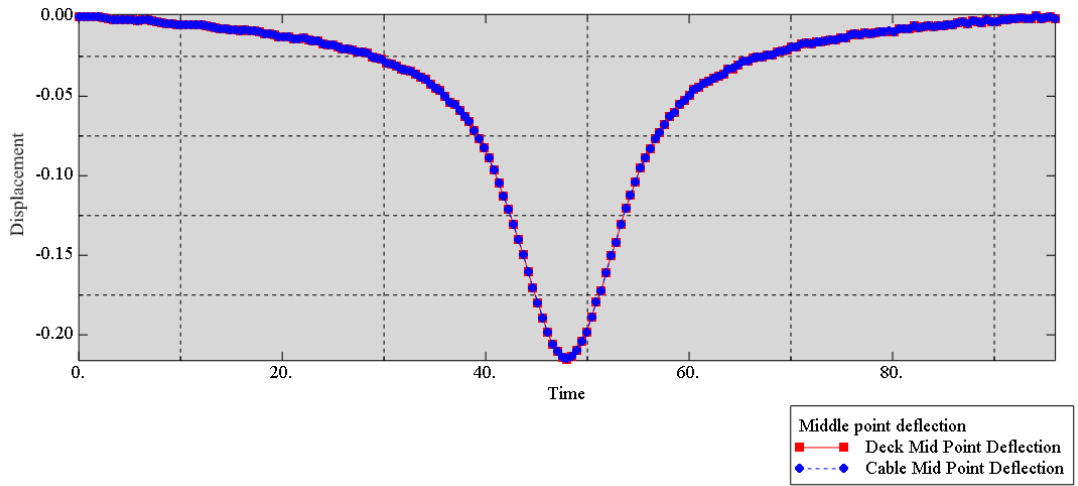


**Figure 3.55 : Middle Point Deflection For Case I (In meters)**

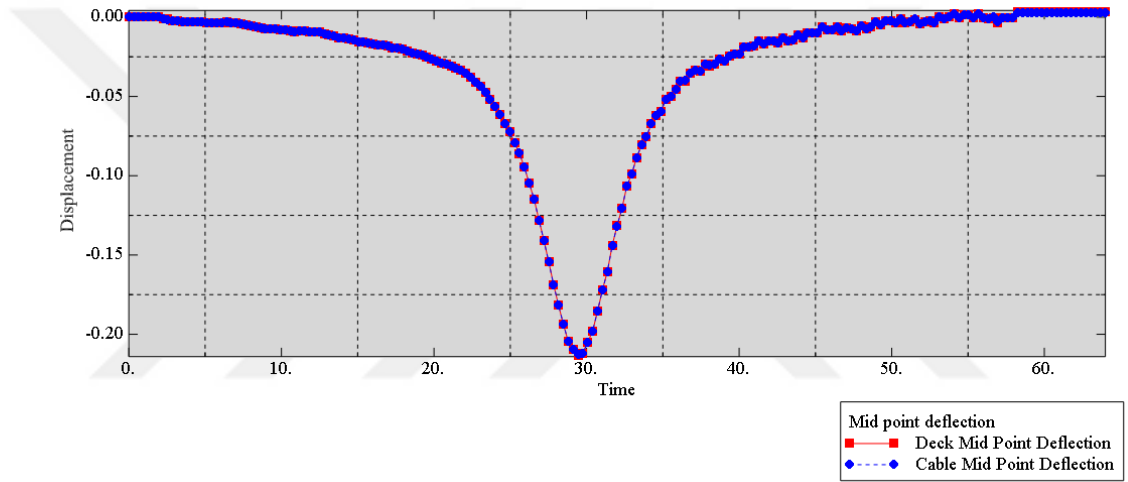


**Figure 3.56 : Middle Point Deflection For Case II (In meters)**

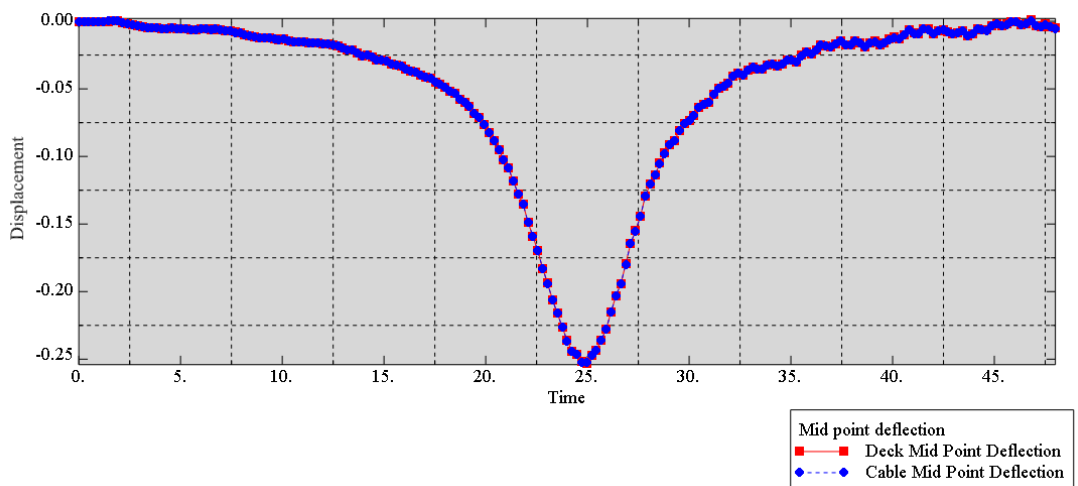


**Figure 3.57 : Middle Point Deflection For Case III (In meters)**

In **Figures 3.58-3.60** vector of U2 which represent displacement in y-direction are illustrated.

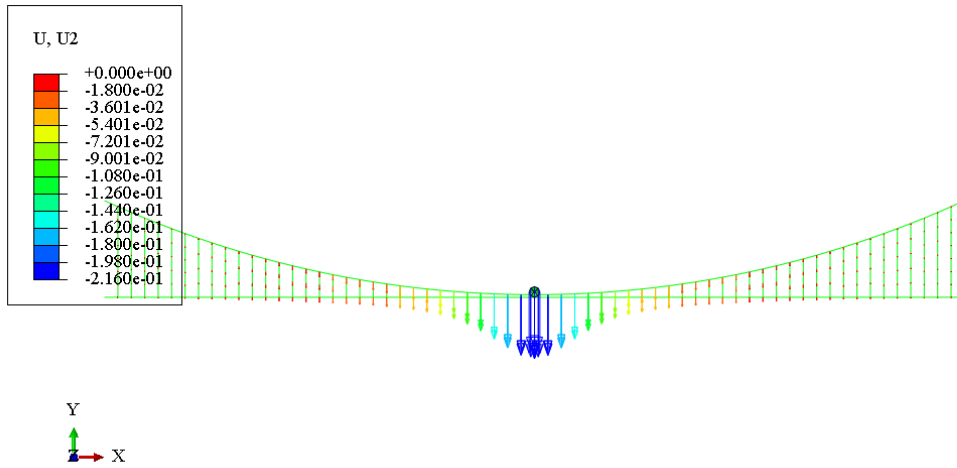


**Figure 3.58 : U2 Vector Deflection for Case I (In meters)**

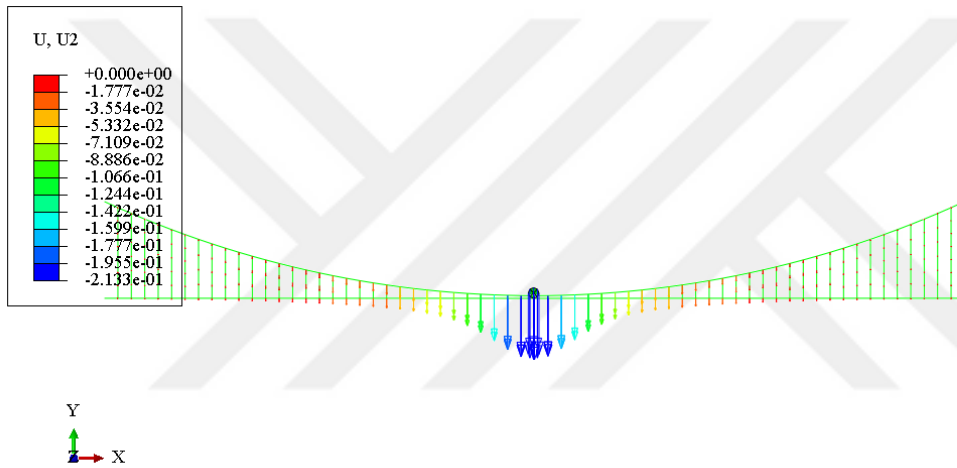


**Figure 3.59 : U2 Vector Deflection for Case II (In meters)**

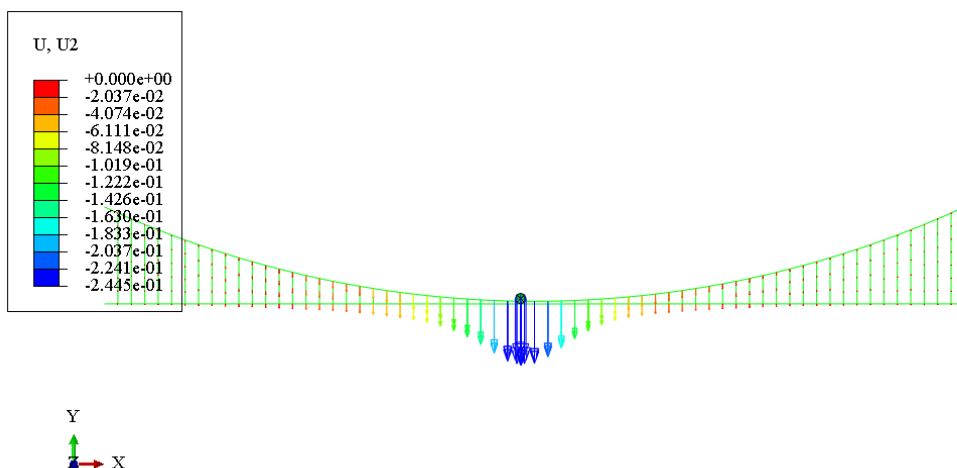


**Figure 3.60 : U2 Vector Deflection for Case III (In meters)**

In **Figures 3.61-3.63** 3D plot of deflected suspension bridge for cases I, II and III are respectively depicted.

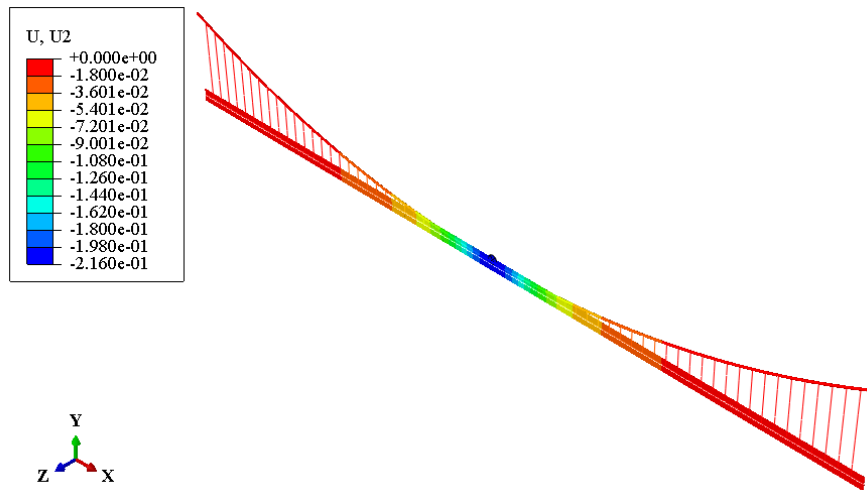


**Figure 3.61 :** 3D Plot of Suspension Bridge Deflection for Case I (In meters)

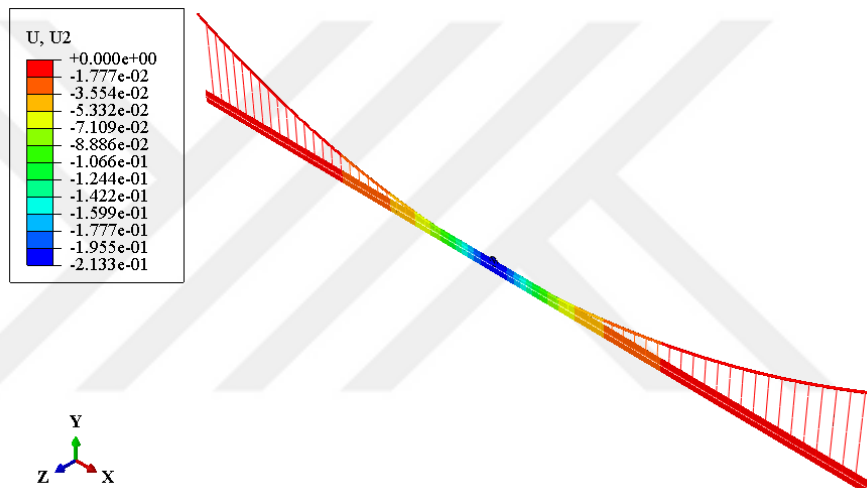


**Figure 3.62 :** 3D Plot of Suspension Bridge Deflection for Case II (In meters)

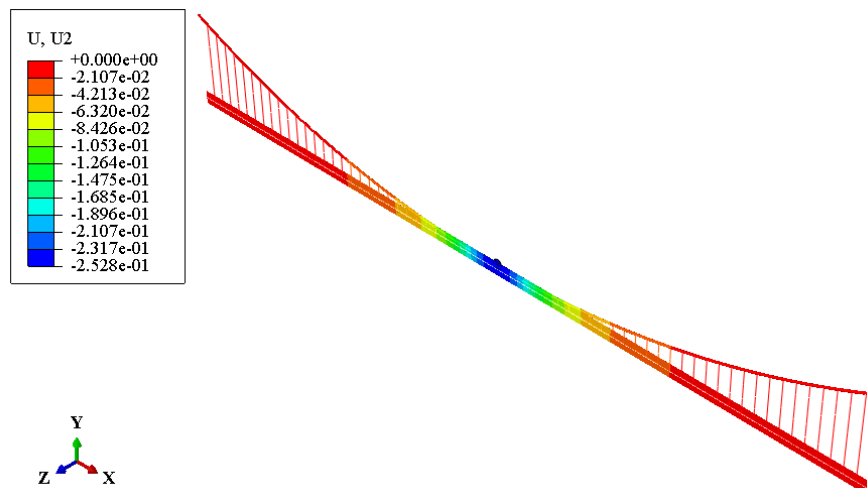


**Figure 3.63 :** 3D Plot of Suspension Bridge Deflection for Case III (In meters)

Result of analysis indicates that maximum deflection of the cable and the deck are close to results that obtained by MATLAB software. Middle point deflection of the

cable and the deck computed by MATLAB and ABAQUS are compared in **Table 3.28** and **Table 3.29**.

**Table 3.28 :** Comparison result of MATLAB and ABAQUS for cable mid point deflection

Cable middle point deflection			
Case	MATLAB (m)	ABAQUS (m)	Difference (%)
I	0.21717	0.215036	0.9826%
II	0.20966	0.212921	1.5554%
III	0.23174	0.25266	9.0274%

**Table 3.29 :** Comparison result of MATLAB and ABAQUS for deck mid point deflection

Deck middle point deflection			
Case	MATLAB (m)	ABAQUS (m)	Difference (%)
I	0.21738	0.215151	1.0254%
II	0.20986	0.21303	1.5105%
III	0.23195	0.252785	8.9825%

### 3.4 Ground Motion

In this section deflection response of the suspension bridge for three different ground motions investigated. In this section, effect of ground motion on response of suspension bridge investigated. To investigate response of suspension bridge, three different earthquake records likewise to effect of the ground motion considered for analyzing. The earthquake records considered for this analysis were the Coyote-Lake ground motion record, Kobe ground motion record and El-Mayor ground motion record. In analyzing, vertical acceleration due to ground motions considered to determine suspension bridge response, and for displacements at the top of tower which appears in equation 2.56, displacements of earthquake records were used. Horizontal displacements of the tower neglected and considered to be equal to zero. First fifty modes of the suspension were taken into account in order to compute response of the suspension bridge.

### 3.4.1 Coyote Lake

**Figure 3.64** displays vertical ground acceleration record for Coyote Lake ground motion.

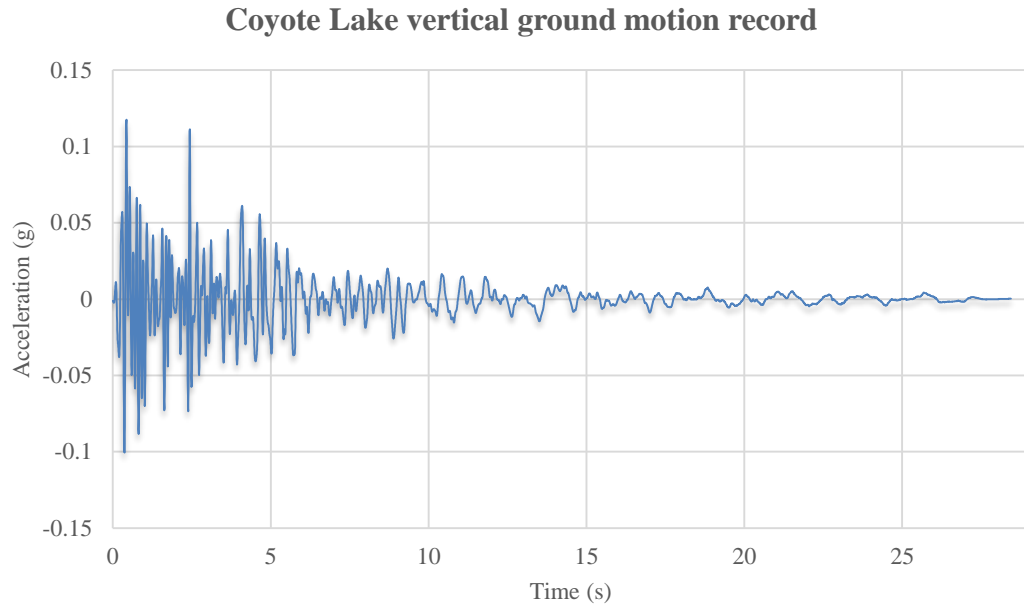


**Figure 3.64 :** Vertical Ground Acceleration Record for Coyote Lake Ground Motion

In **Figures 3.65-3.67** deflection response of the suspension bridge for case I, II and III when it is subjected to Coyote Lake earthquake motion has been illustrated.

**3D PLOT OF SPAN DEFLECTION DURING COYOTE LAKE GROUND EXCITATION**

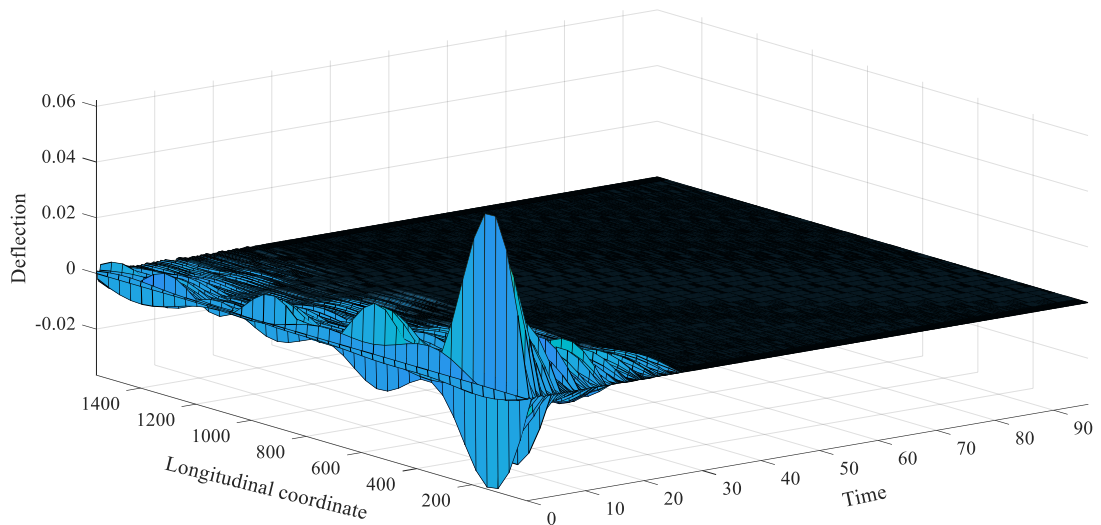


**Figure 3.65 :** 3D Plot of Span Deflection Due to the Coyote Lake Earthquake Motion for Case I (In Meters)

**3D PLOT OF SPAN DEFLECTION DURING COYOTE LAKE GROUND EXCITATION**

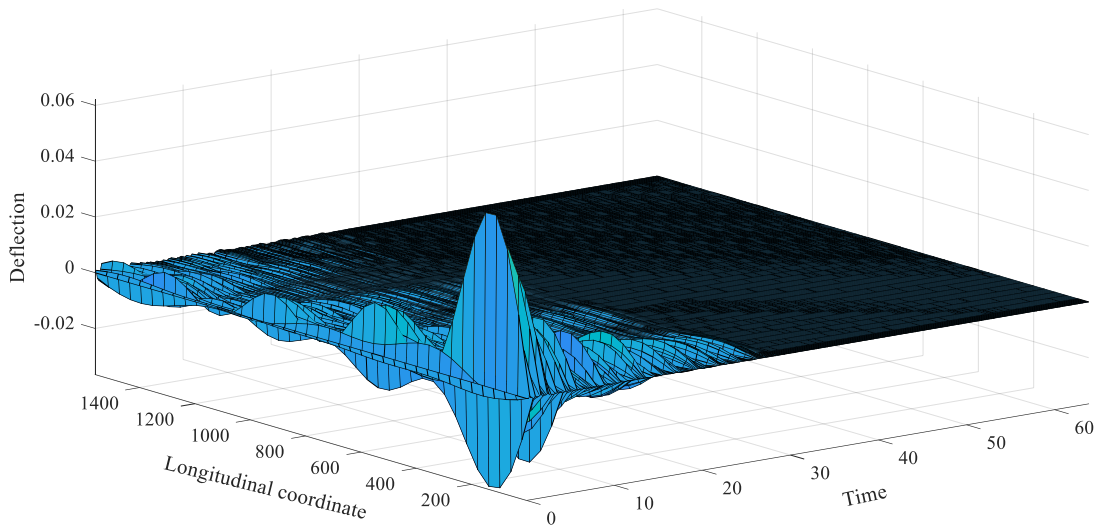


**Figure 3.66 :** 3D Plot of Span Deflection Due to the Coyote Lake Earthquake Motion for Case II (In Meters)

**3D PLOT OF SPAN DEFLECTION DURING COYOTE LAKE GROUND EXCITATION**

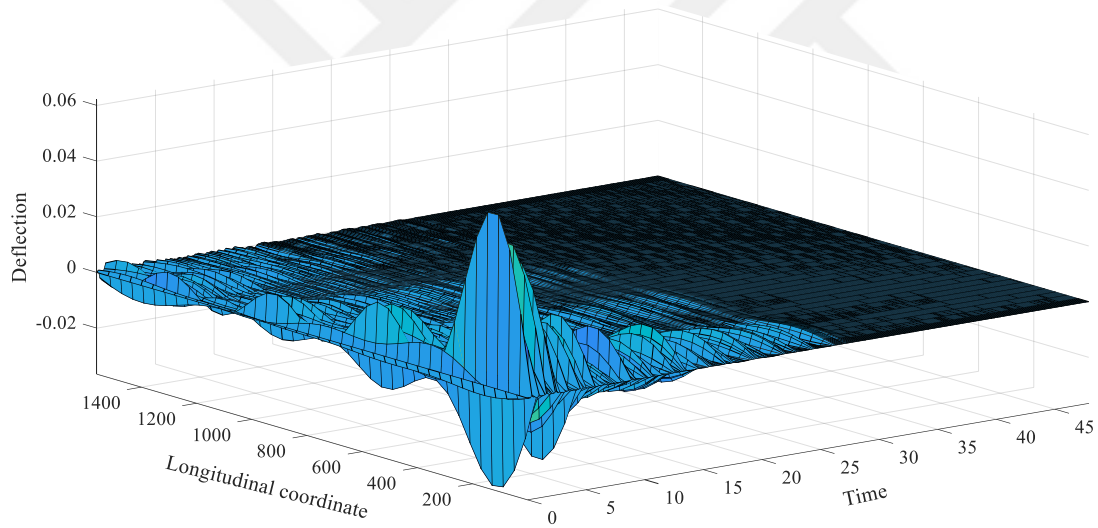


**Figure 3.67 :** 3D Plot of Span Deflection Due to the Coyote Lake Earthquake Motion for Case III (In Meters)

In **Figures 3.68-3.70** deflection response of the middle point of the suspension bridge for case I, II and III when it is subjected to Kobe earthquake motion has been depicted.



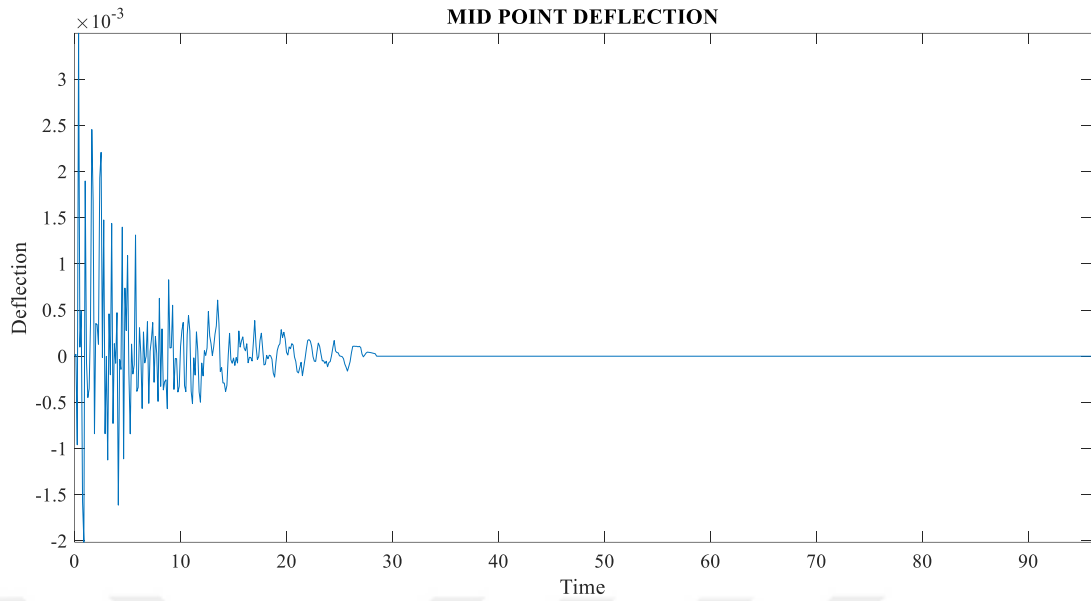


**Figure 3.68 :** Suspension Bridge Middle Point Deflection Due to the Coyote Lake Earthquake for Case I (In Meters)

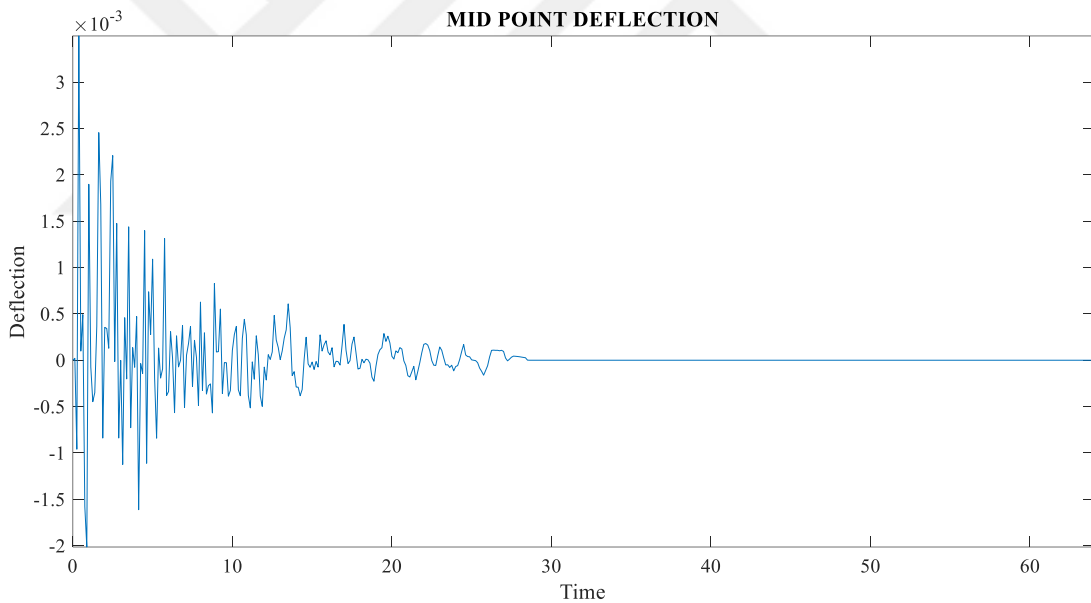


**Figure 3.69 :** Suspension Bridge Middle Point Deflection Due to the Coyote Lake Earthquake for Case II (In Meters)

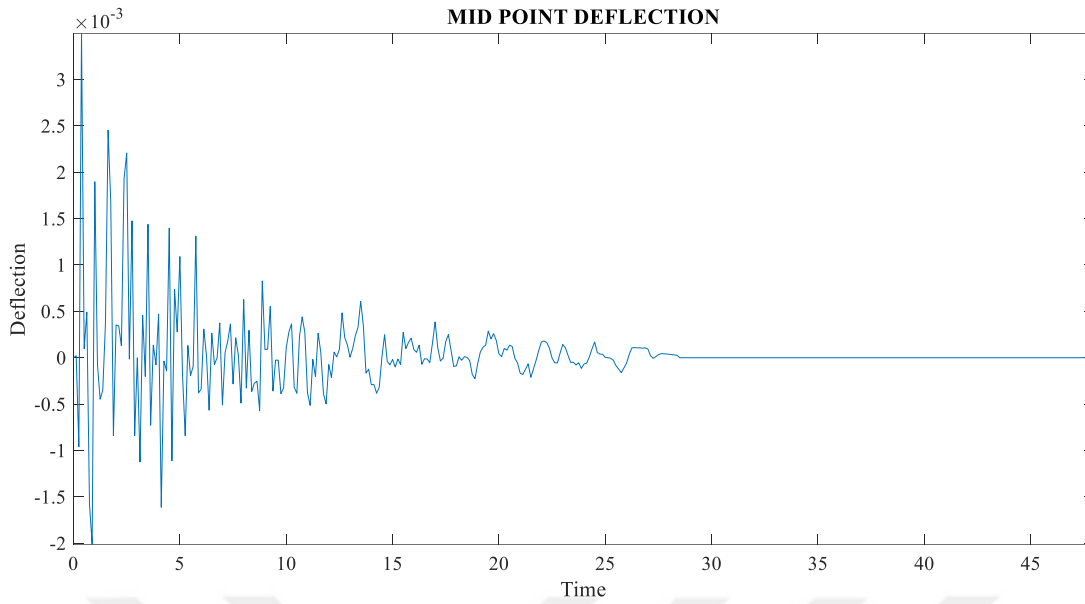


**Figure 3.70 :** Suspension Bridge Middle Point Deflection Due to the Coyote Lake Earthquake for Case III (In Meters)

### 3.4.2 Kobe

In **Figure 3.71** vertical ground acceleration record for Kobe ground motion has been illustrated.

**Kobe vertical ground motion record**

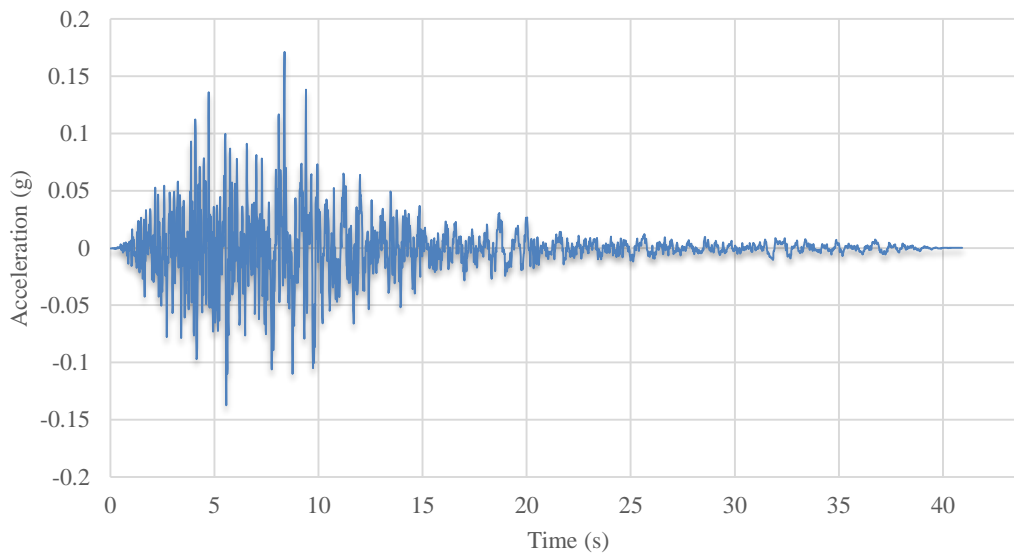


**Figure 3.71 :** Vertical Ground Acceleration Record for Kobe Ground Motion

In **Figures 3.72-3.74** deflection response of the suspension bridge for case I, II and III when it is subjected to Kobe earthquake motion has been illustrated.

3D PLOT OF SPAN DEFLECTION DURING KOBE GROUND EXCITATION

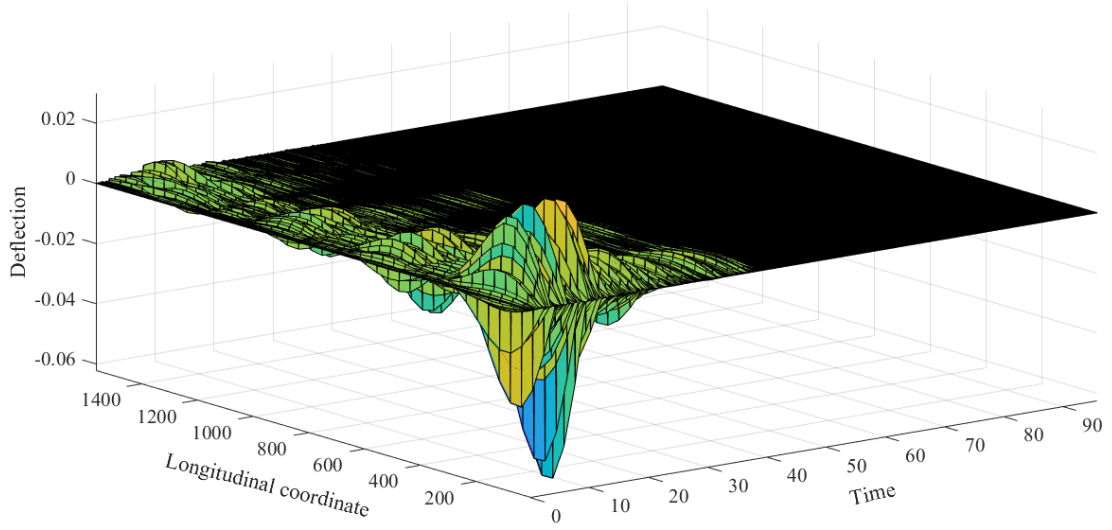


Figure 3.72 : 3D Plot of Span Deflection Due to the Kobe Earthquake Motion for Case I (In Meters)

3D PLOT OF SPAN DEFLECTION DURING KOBE GROUND EXCITATION

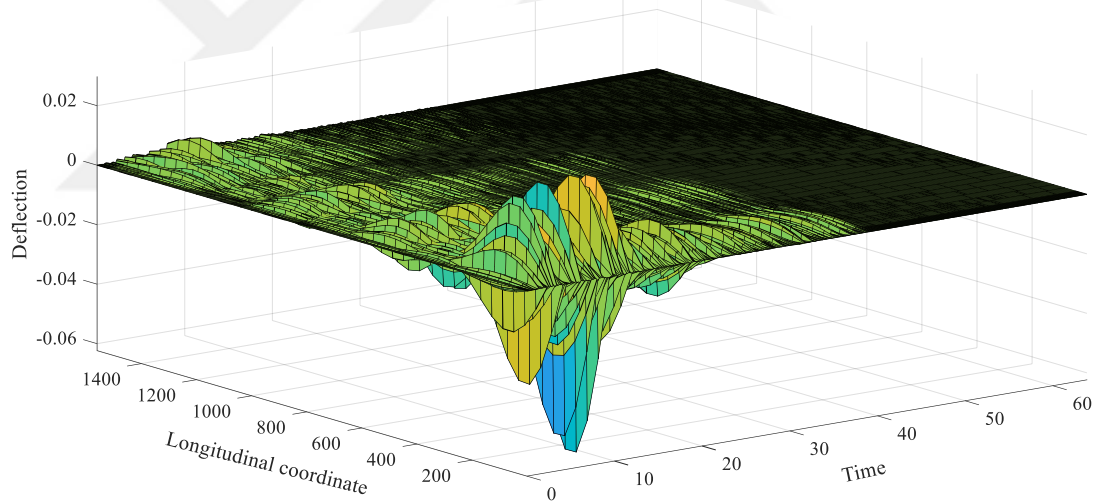
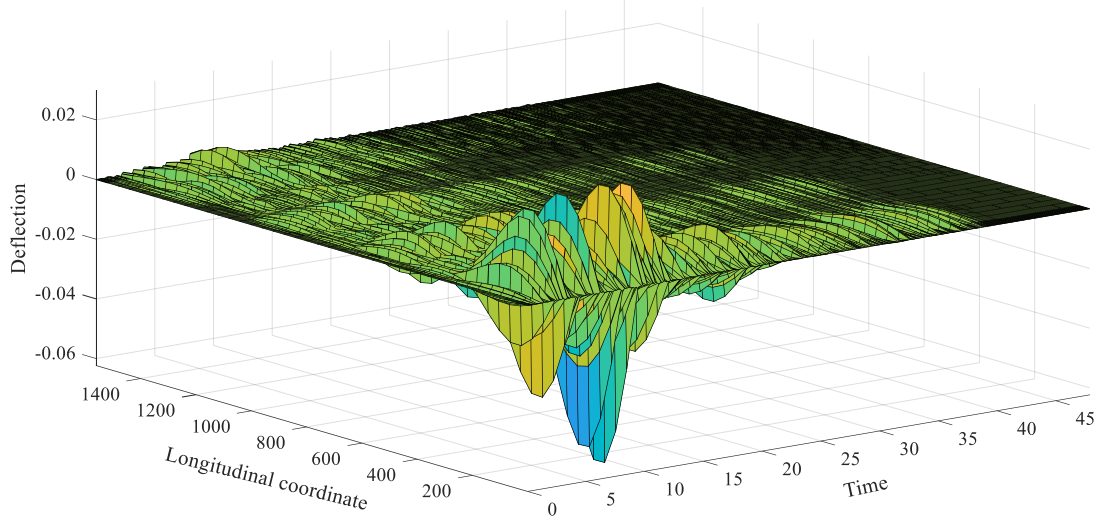
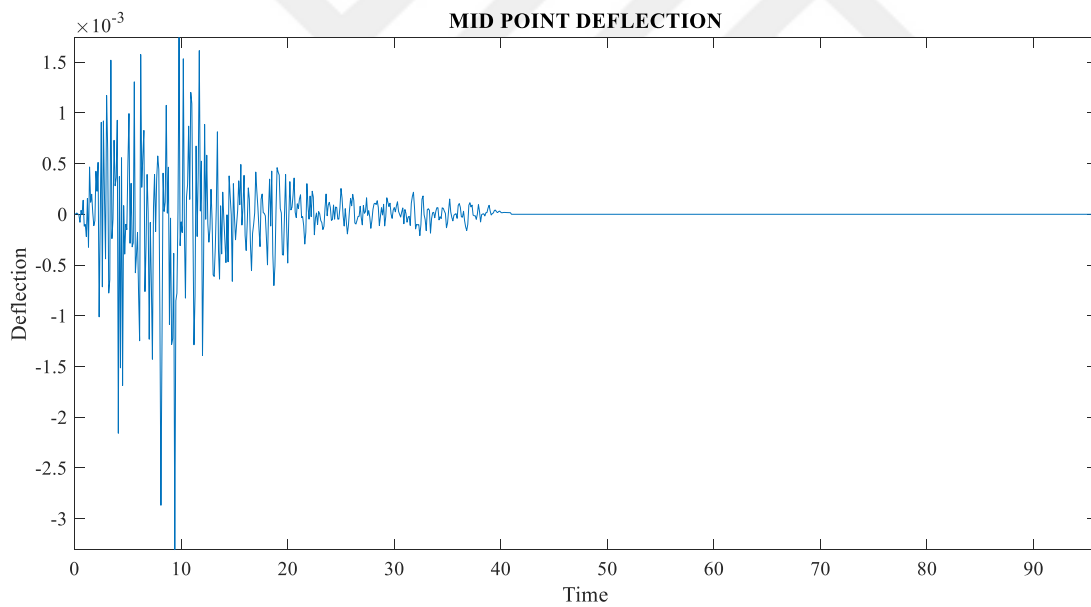


Figure 3.73 : 3D Plot of Span Deflection Due to the Kobe Earthquake Motion for Case II (In Meters)

**3D PLOT OF SPAN DEFLECTION DURING KOBE GROUND EXCITATION**



**Figure 3.74 :** 3D Plot of Span Deflection Due to the Kobe Earthquake Motion for Case III (In Meters)  
In **Figures 3.75-3.77** deflection response of the middle point of the suspension bridge for case I, II and III when it is subjected to Kobe earthquake motion has been depicted.



**Figure 3.75 :** Suspension Bridge Middle Point Deflection Due to the Kobe Earthquake for Case I (In Meters)

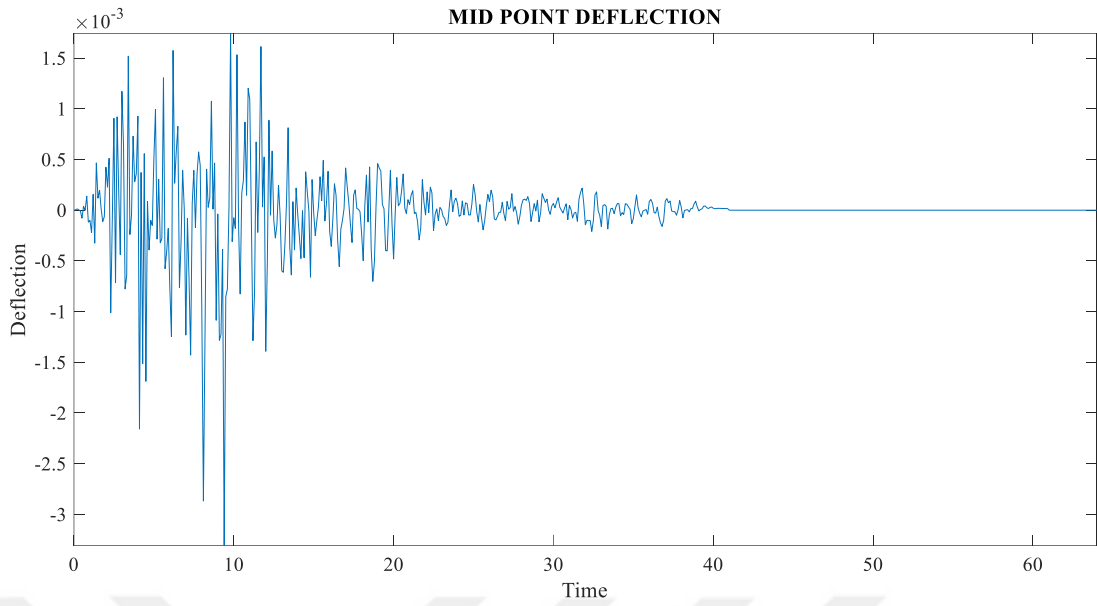


**Figure 3.76 :** Suspension Bridge Middle Point Deflection Due to the Kobe Earthquake for Case II (In Meters)

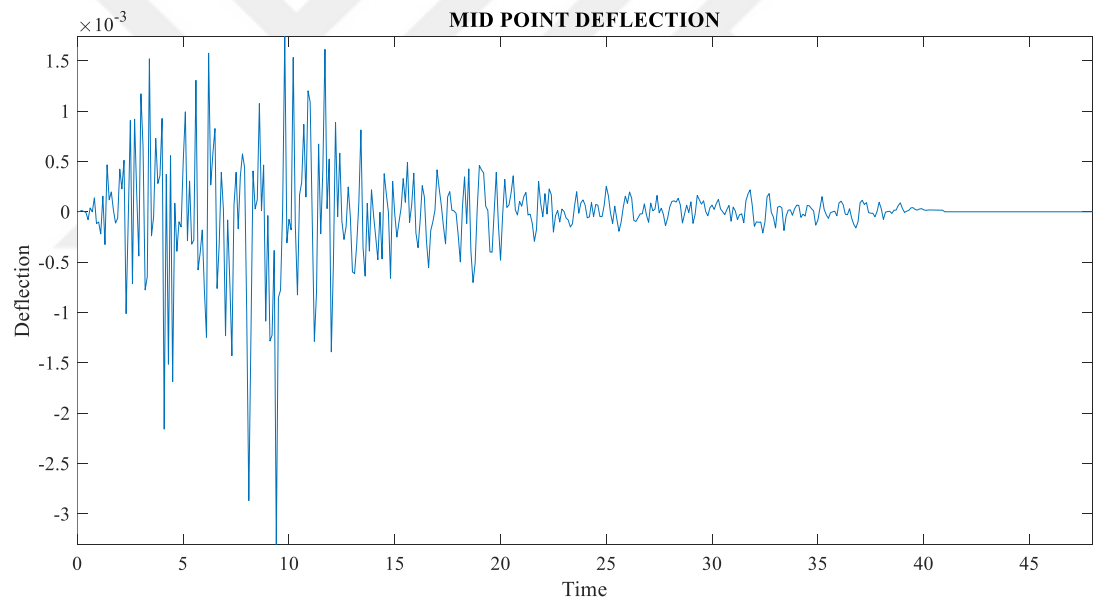


**Figure 3.77 :** Suspension Bridge Middle Point Deflection Due to the Kobe Earthquake for Case III (In Meters)

### 3.4.3 El Mayor

In **Figure 3.78** vertical ground acceleration record for El Mayor ground motion has been depicted.

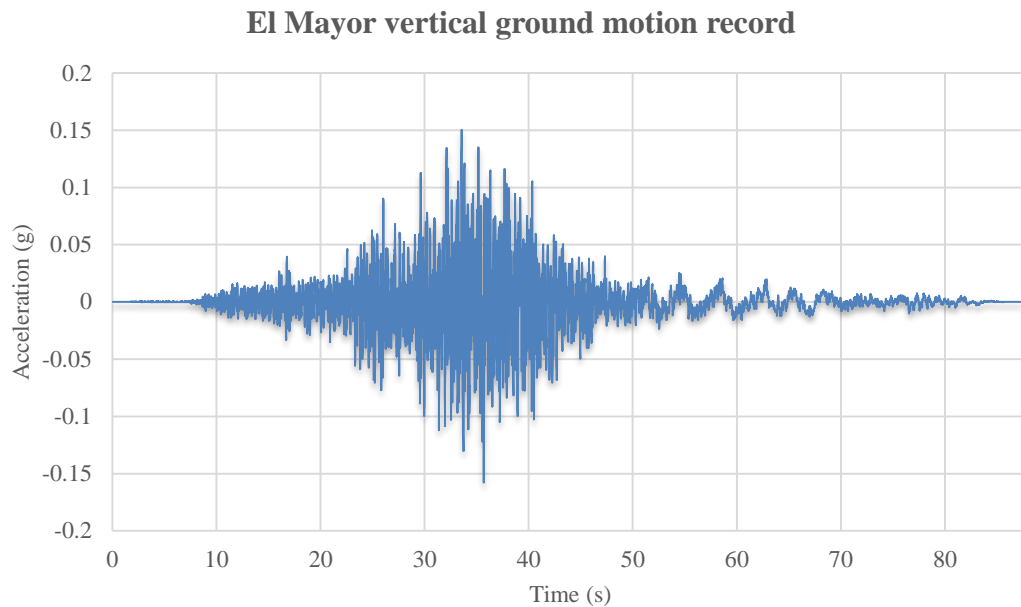


**Figure 3.78 :** Vertical Ground Acceleration Record for El Mayor Ground Motion  
In **Figures 3.79-3.81** deflection response of the suspension bridge for case I, II and III when it is subjected to El Mayor earthquake motion has been illustrated.

**3D PLOT OF SPAN DEFLECTION DURING EL MAYOR GROUND EXCITATION**

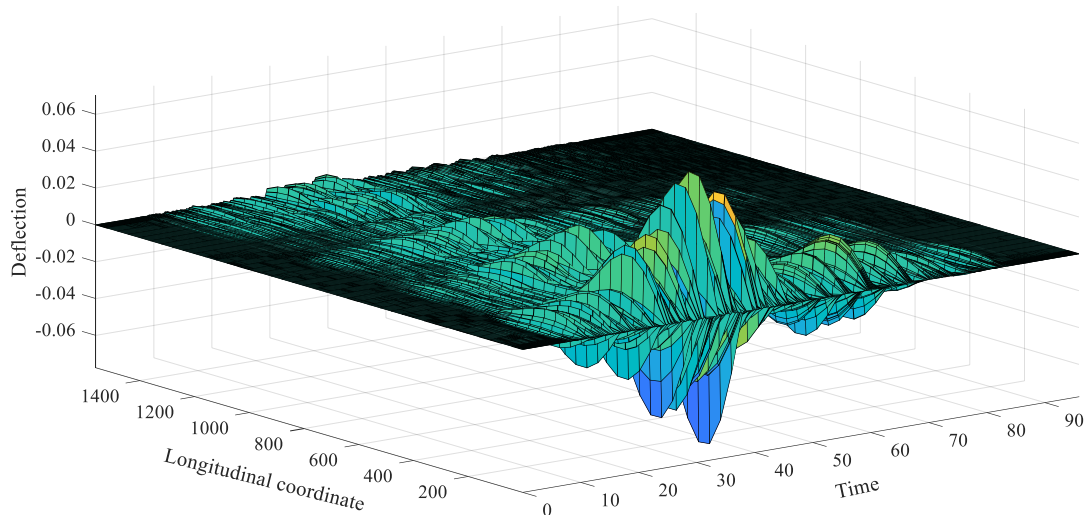


**Figure 3.79 :** 3D Plot of Span Deflection Due to the El Mayor Earthquake Motion for Case I (In Meters)

**3D PLOT OF SPAN DEFLECTION DURING EL MAYOR GROUND EXCITATION**

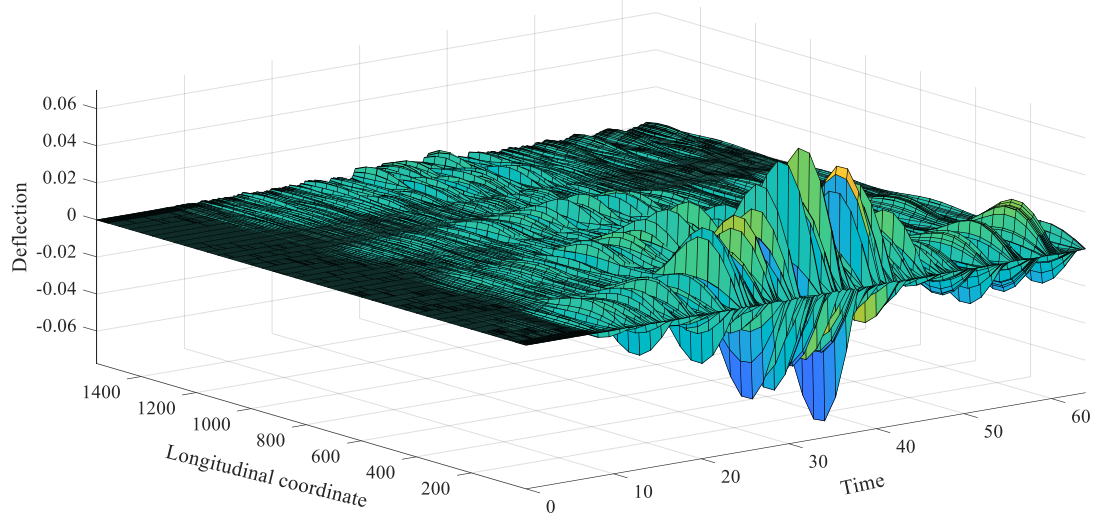


**Figure 3.80 :** 3D Plot of Span Deflection Due to the El Mayor Earthquake Motion for Case II (In Meters)

**3D PLOT OF SPAN DEFLECTION DURING EL MAYOR GROUND EXCITATION**

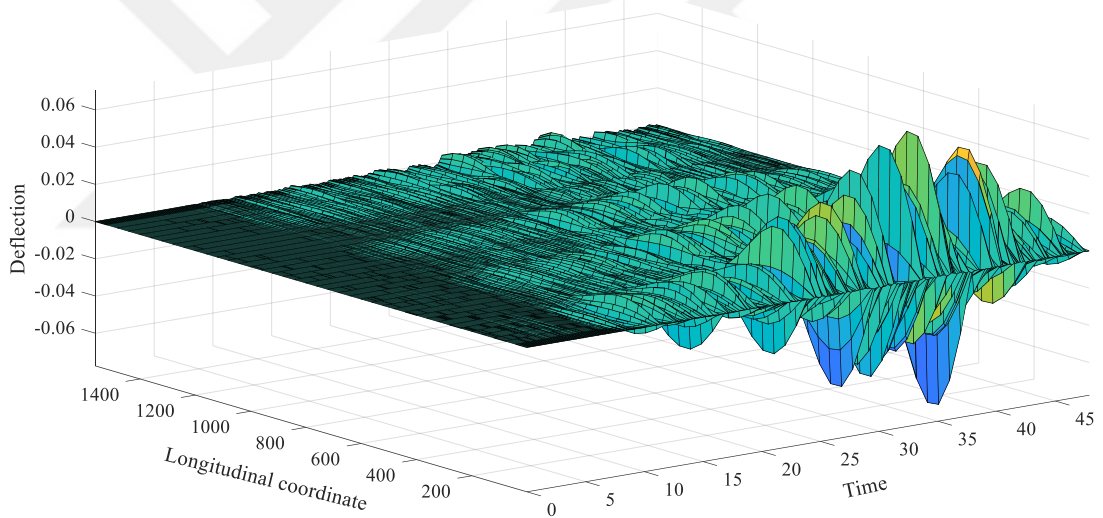


**Figure 3.81 :** 3D Plot of Span Deflection Due to the El Mayor Earthquake Motion for Case III (In Meters)

In **Figures 3.82-3.84** deflection response of the middle point of the suspension bridge for case I, II and III when it is subjected to El Mayor earthquake motion has been depicted.

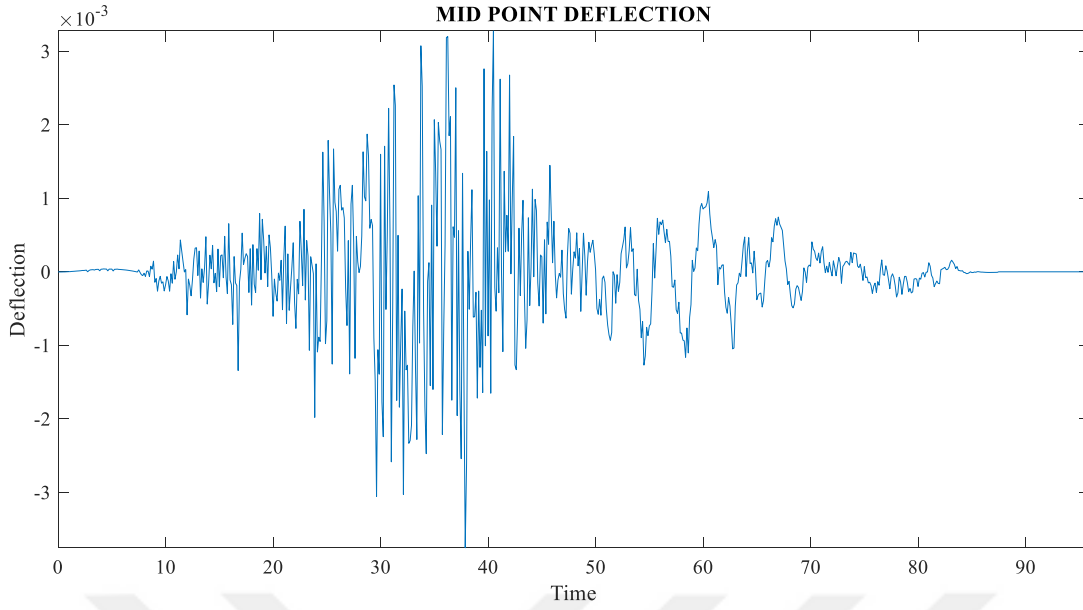


**Figure 3.82 :** Suspension Bridge Middle Point Deflection Due to the El Mayor Earthquake for Case I (In Meters)

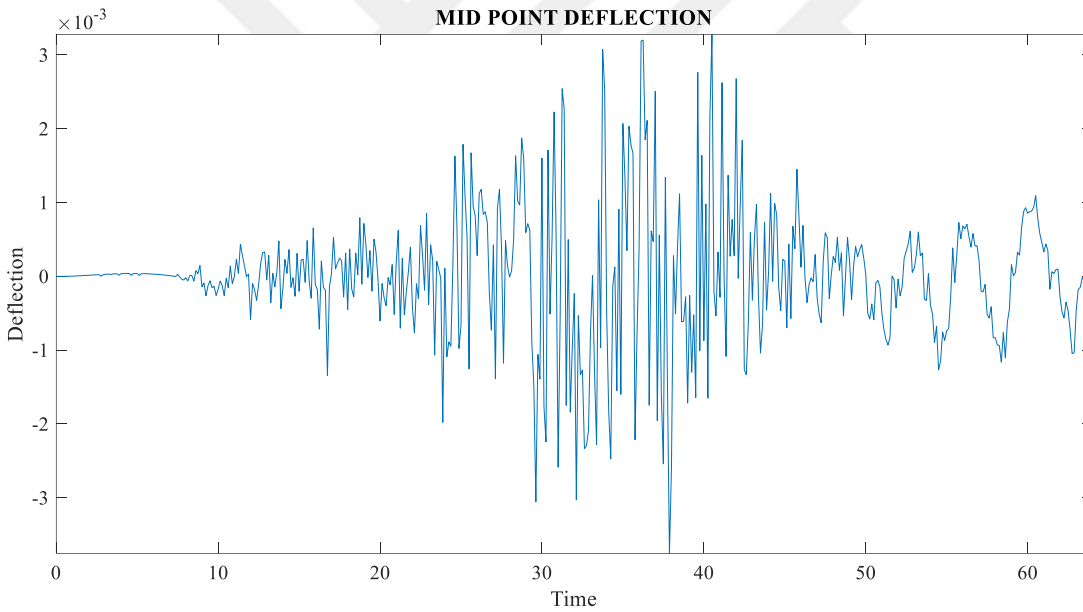


**Figure 3.83 :** Suspension Bridge Middle Point Deflection Due to the El Mayor Earthquake for Case II (In Meters)



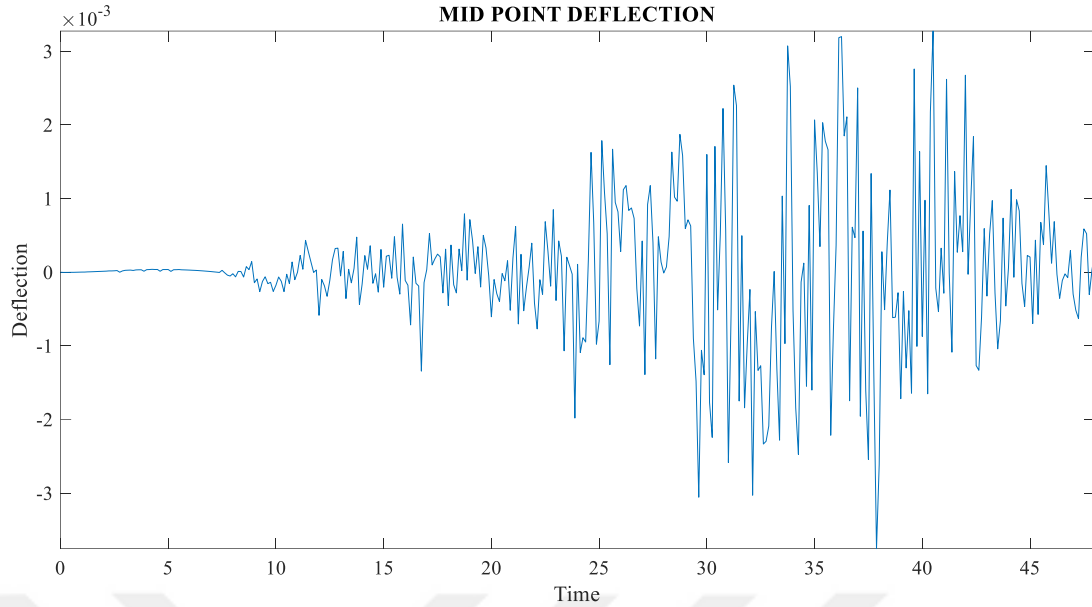


**Figure 3.84** : Suspension Bridge Middle Point Deflection Due to the El Mayor Earthquake for Case III (In Meters)

### 3.5 Ground Motion and Moving Load Simultaneously

In this section, effect of ground motion on response of suspension bridge investigated. To investigate response of suspension bridge, three different earthquake records likewise to effect of the ground motion considered for analyzing. The earthquake records considered for this analysis were the Coyote-Lake ground motion record, Kobe ground motion record and El-Mayor ground motion record. In analyzing, vertical acceleration due to ground motions considered to determine suspension bridge response, and for displacements at the top of tower which appears in equation 2.56, displacements of earthquake records were used. Horizontal displacements of the tower neglected and considered to be equal to zero. It must be noted that intervals for Coyote lake, Kobe and El Mayor ground motion acceleration was 0.005, 0.01 and 0.005 seconds. For determining the response these intervals increased by twenty times in order to decrease the amount of the time needed for computing the response. First eight modes of the suspension was taken into account in order to compute response of the suspension bridge.

### 3.5.1 Coyote Lake

In Figures 3.85-3.87 response of suspension bridge when it is subjected to Coyote Lake earthquake motion and moving load has been illustrated.

3D PLOT OF SPAN DEFLECTION DURING COYOTE LAKE GROUND EXCITATION

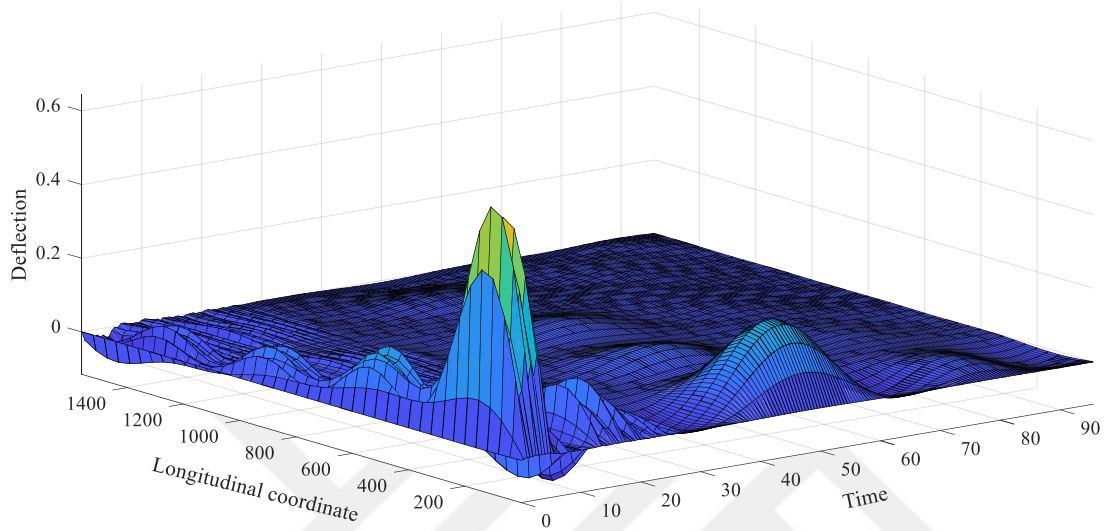


Figure 3.85 : 3D Plot of Span Deflection Due to the Coyote Lake Earthquake Motion and Moving Load for Case I

3D PLOT OF SPAN DEFLECTION DURING COYOTE LAKE GROUND EXCITATION

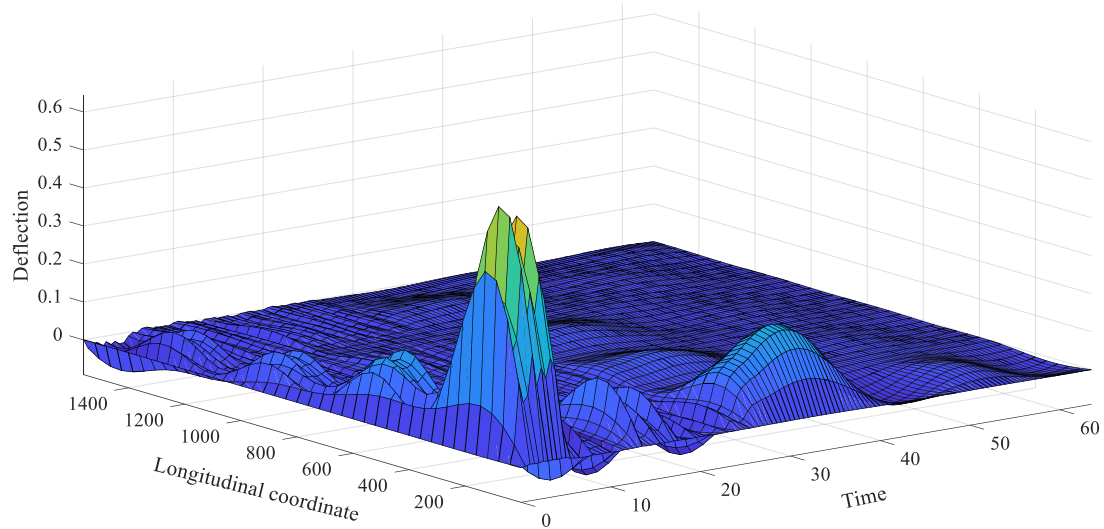
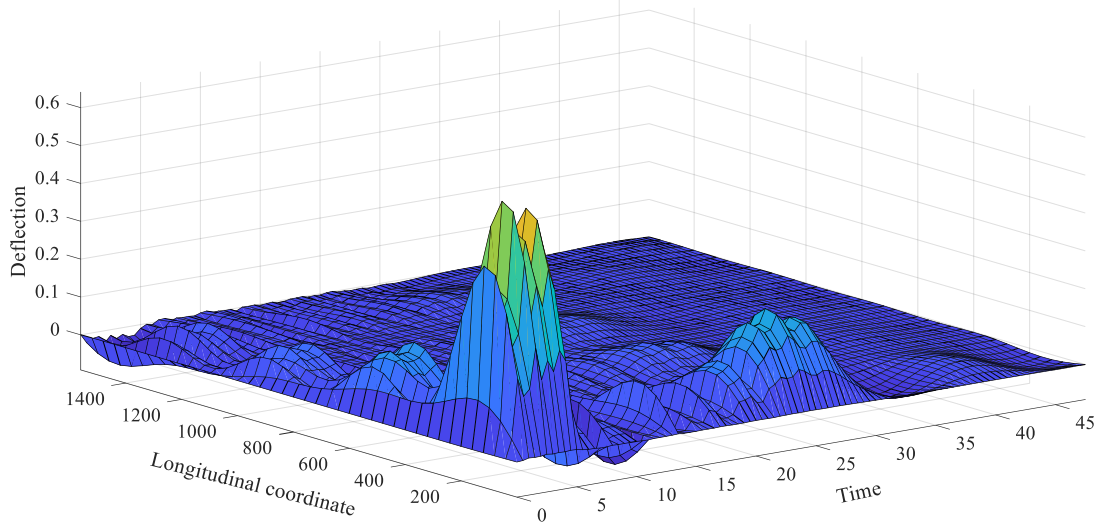


Figure 3.86 : 3D Plot of Span Deflection Due to the Coyote Lake Earthquake Motion and Moving Load for Case II

**3D PLOT OF SPAN DEFLECTION DURING COYOTE LAKE GROUND EXCITATION**



**Figure 3.87 :** 3D Plot of Span Deflection Due to the Coyote Lake Earthquake Motion and Moving Load for Case III

In **Figures 3.88-3.90** deflection for middle point of suspension bridge due to the Coyote Lake earthquake motion and moving load has been depicted.

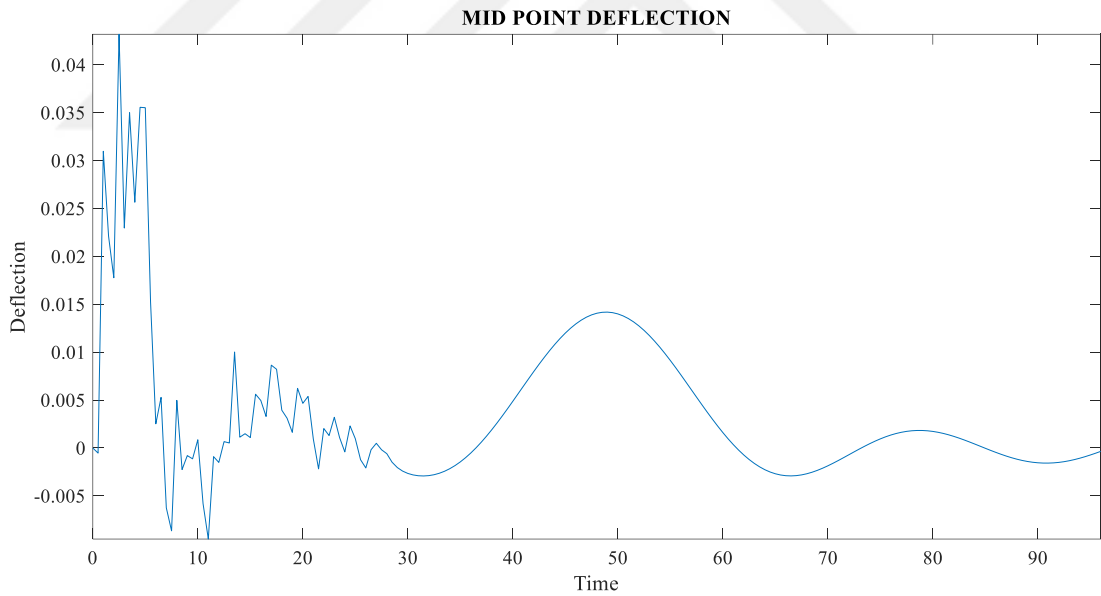


**Figure 3.88 :** Suspension Bridge Middle Point Deflection Due to the Coyote Lake Earthquake Motion and Moving Load for Case I

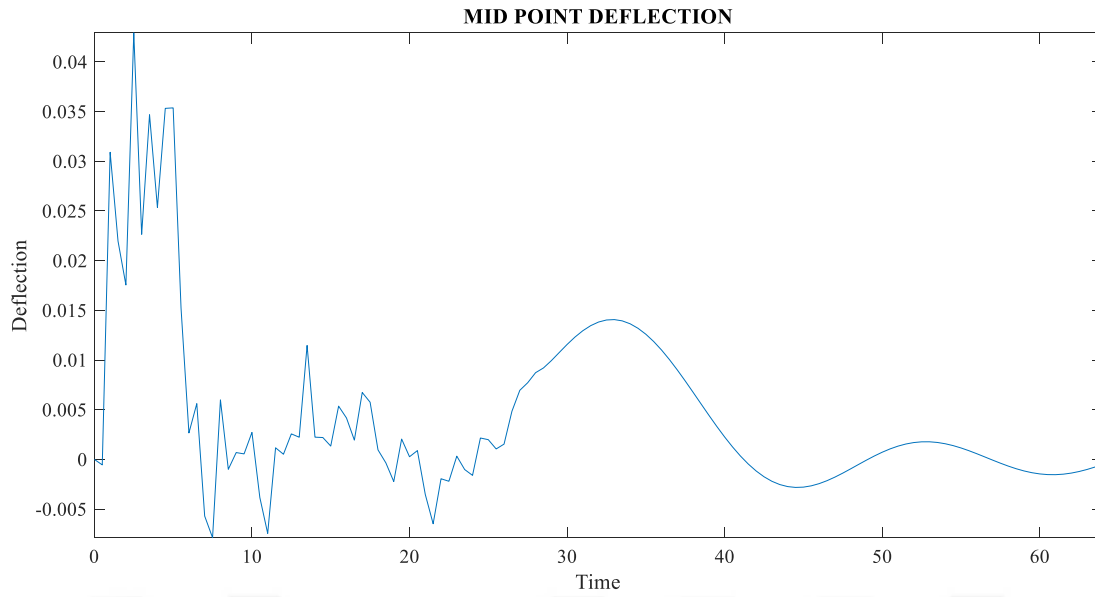


**Figure 3.89 :** Suspension Bridge Middle Point Deflection Due to the Coyote Lake Earthquake Motion and Moving Load for Case II

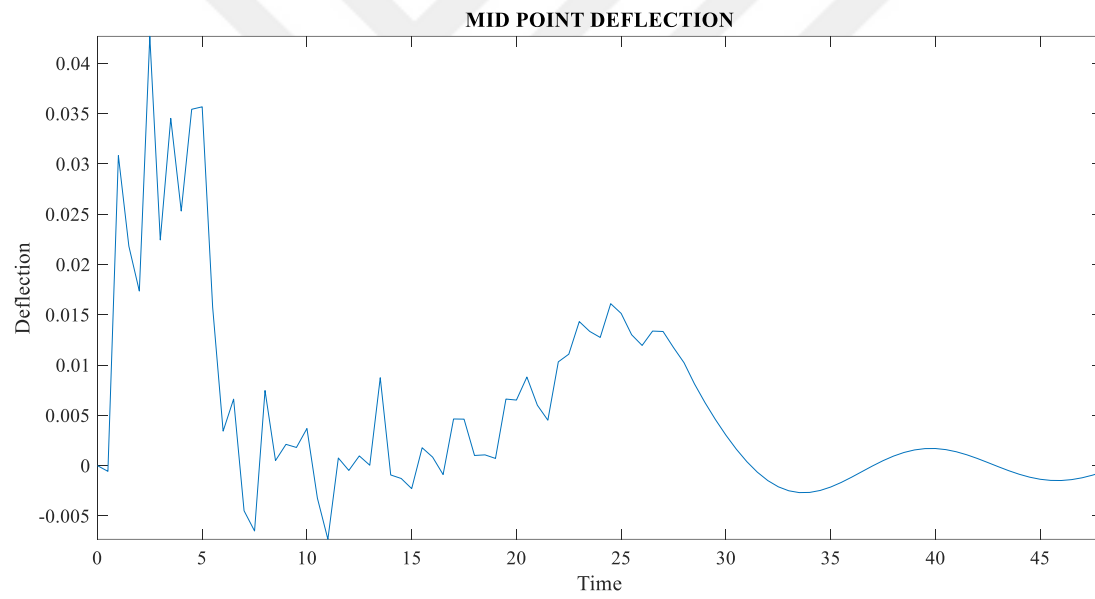


**Figure 3.90 :** Suspension Bridge Middle Point Deflection Due to the Coyote Lake Earthquake Motion and Moving Load for Case III

### 3.5.2 Kobe

In Figures 3.91-3.93 response of suspension bridge when it is subjected to Kobe earthquake motion and moving load has been shown.

3D PLOT OF SPAN DEFLECTION DURING KOBE GROUND EXCITATION

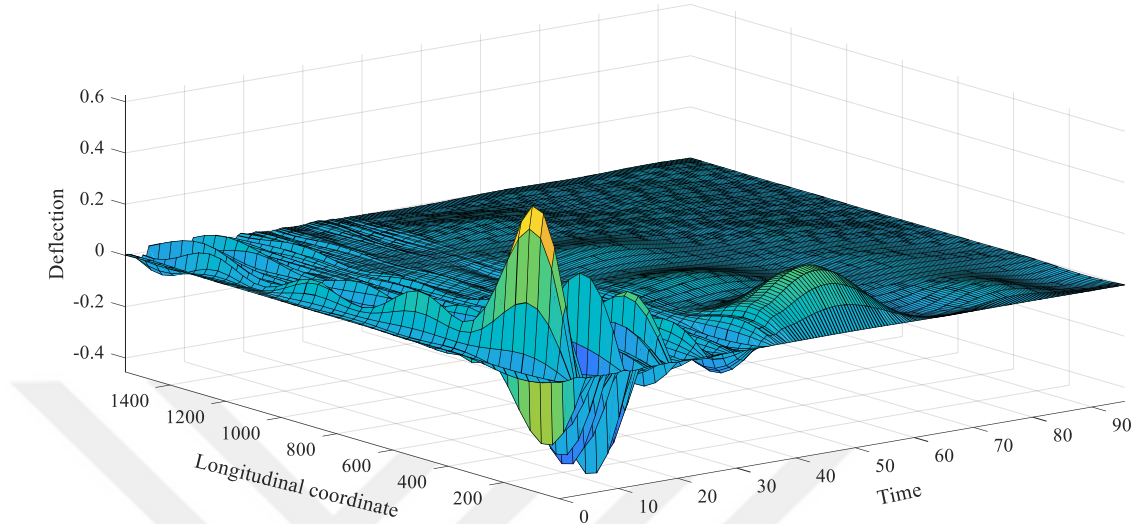


Figure 3.91 : 3D Plot of Span Deflection Due to the Kobe Earthquake Motion and Moving Load for Case I

3D PLOT OF SPAN DEFLECTION DURING KOBE GROUND EXCITATION

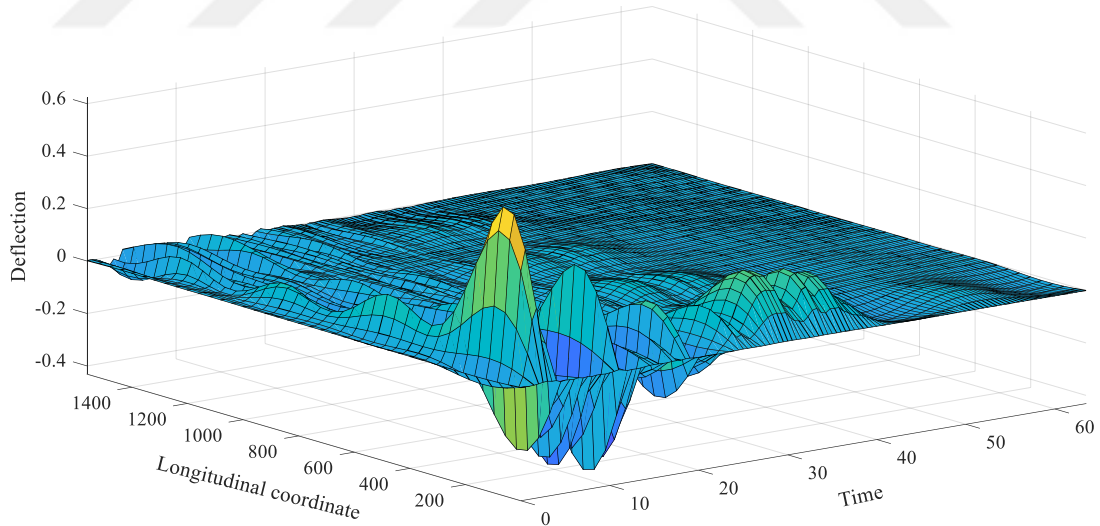
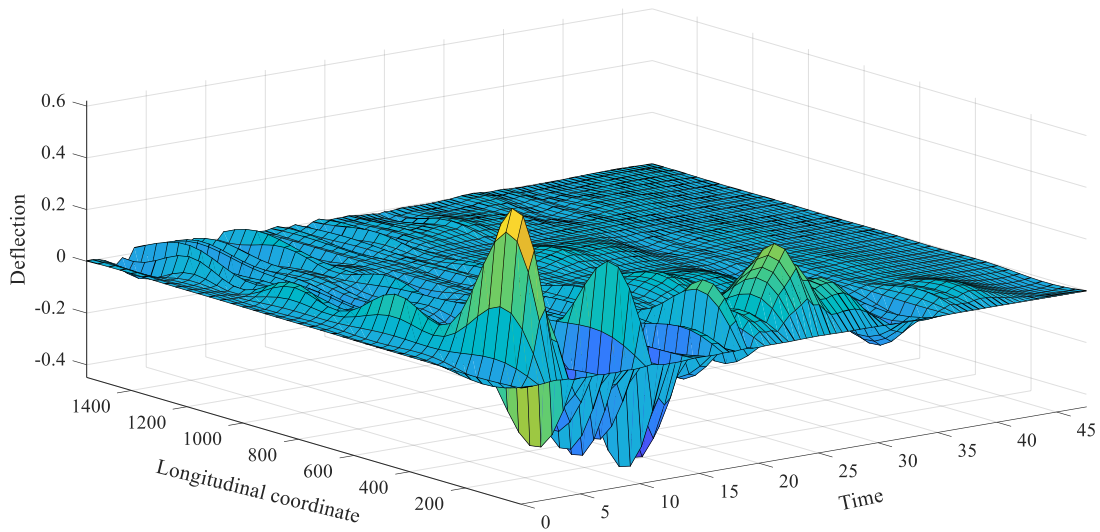


Figure 3.92 : 3D Plot of Span Deflection Due to the Kobe Earthquake Motion and Moving Load for Case II

**3D PLOT OF SPAN DEFLECTION DURING KOBE GROUND EXCITATION**



**Figure 3.93 :** 3D Plot of Span Deflection Due to the Kobe Earthquake Motion and Moving Load for Case III

In **Figures 3.94-3.96** deflection for middle point of suspension bridge due to the Kobe earthquake motion and moving load has been depicted.

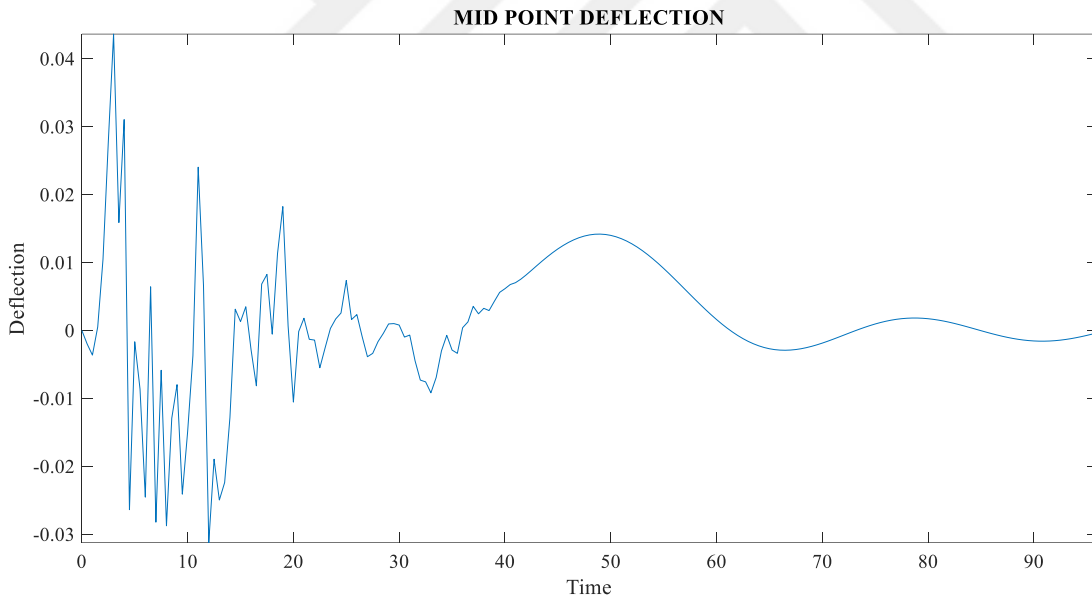


**Figure 3.94 :** Suspension Bridge Middle Point Deflection Due to the Kobe Earthquake Motion and Moving Load for Case I

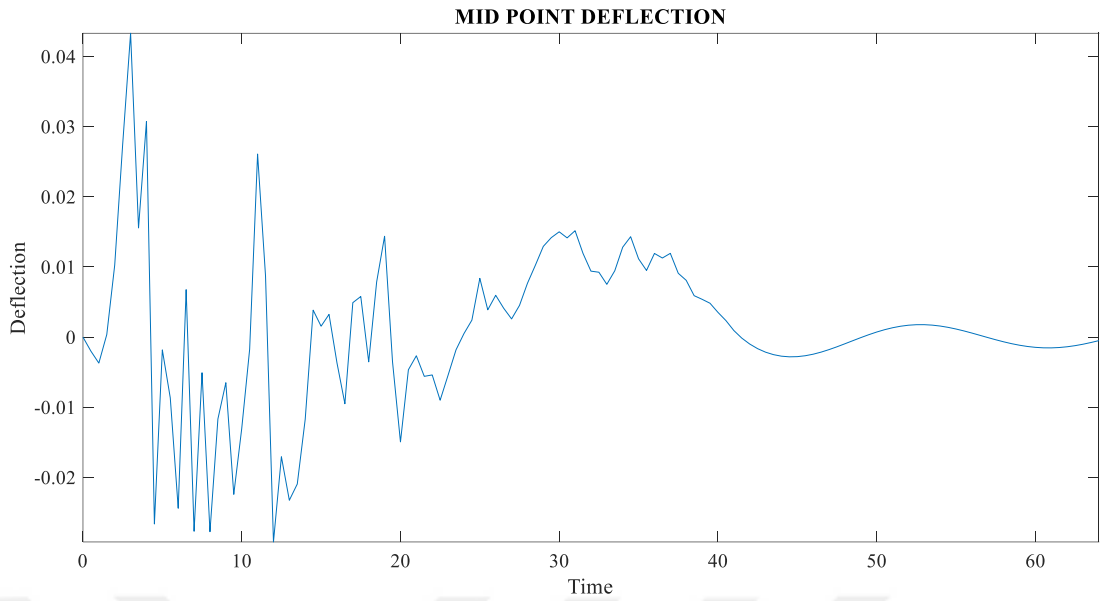


**Figure 3.95 :** Suspension Bridge Middle Point Deflection Due to the Kobe Earthquake Motion and Moving Load for Case II

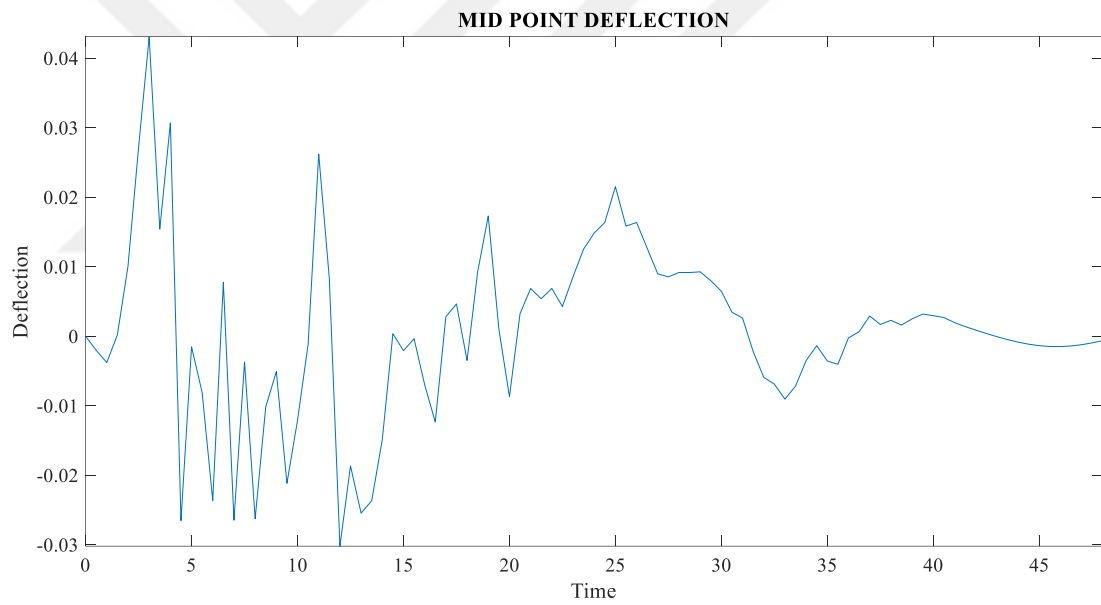


**Figure 3.96 :** Suspension Bridge Middle Point Deflection Due to the Kobe Earthquake Motion and Moving Load for Case III

### 3.5.3 El Mayor

In **Figures 3.97-3.99** response of suspension bridge when it is subjected to El Mayor earthquake motion and moving load has been shown.

**3D PLOT OF SPAN DEFLECTION DURING EL MAYOR GROUND EXCITATION**

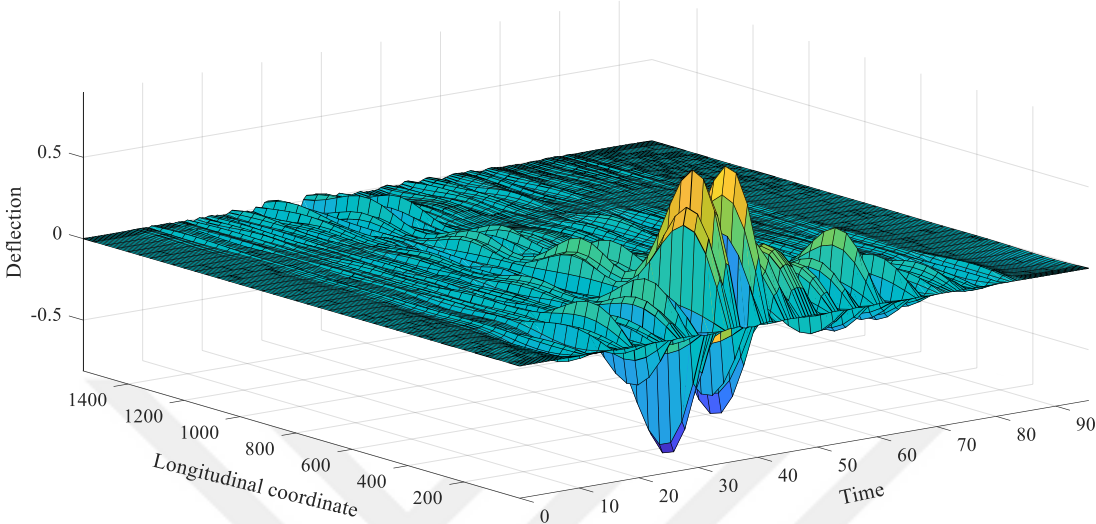


**Figure 3.97 :** 3D Plot of Span Deflection Due to the El Mayor Earthquake Motion and Moving Load for Case I

**3D PLOT OF SPAN DEFLECTION DURING EL MAYOR GROUND EXCITATION**

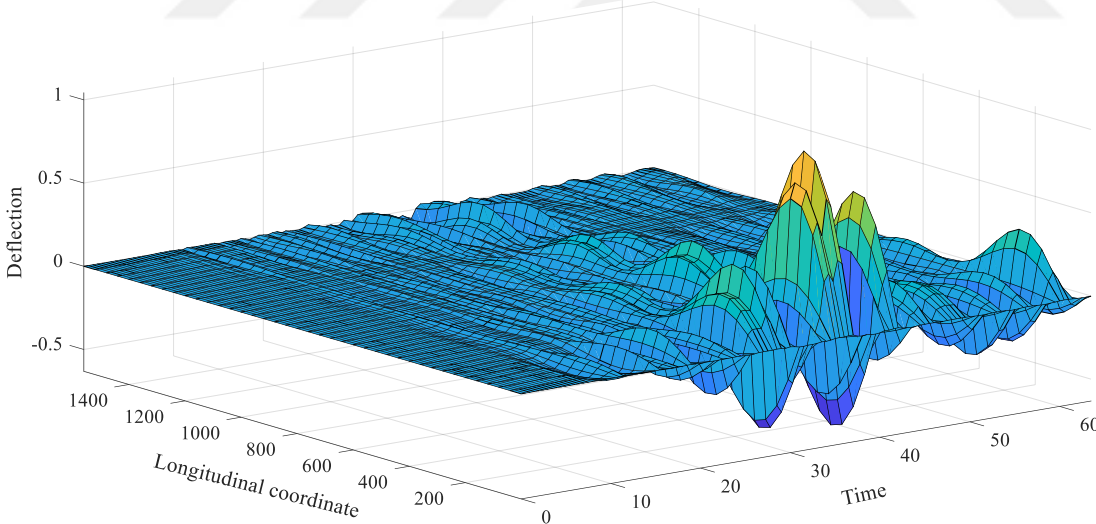


**Figure 3.98 :** 3D Plot of Span Deflection Due to the El Mayor Earthquake Motion and Moving Load for Case II



**3D PLOT OF SPAN DEFLECTION DURING EL MAYOR GROUND EXCITATION**

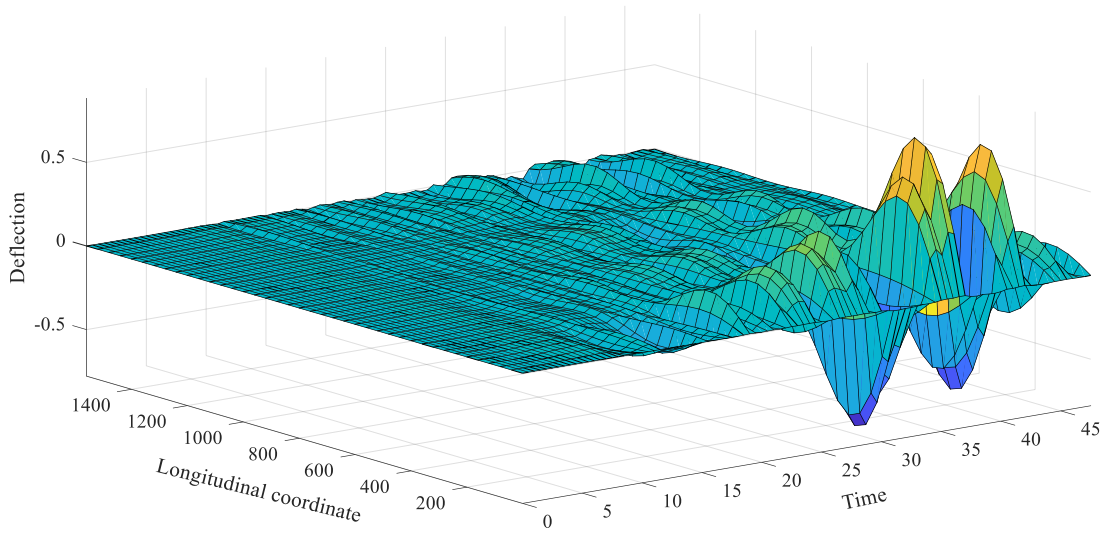


**Figure 3.99 : 3D Plot of Span Deflection Due to the El Mayor Earthquake Motion and Moving Load for Case III**

In **Figures 3.100-3.102** deflection for middle point of suspension bridge due to the El Mayor earthquake motion and moving load has been displayed.

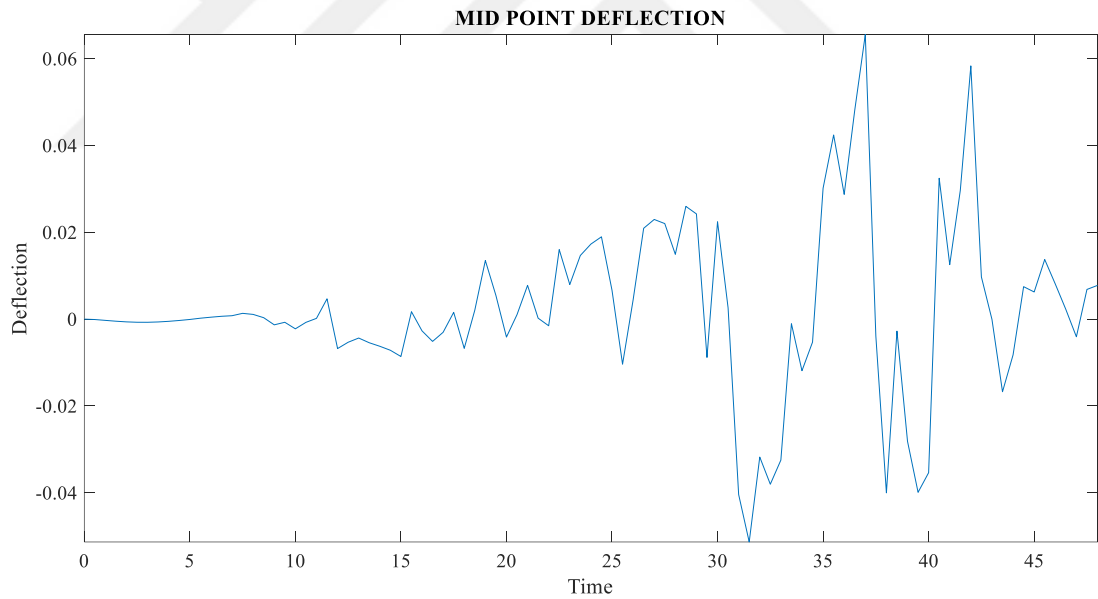


**Figure 3.100 : Suspension Bridge Middle Point Deflection Due to the El Mayor Earthquake Motion and Moving Load for Case I**

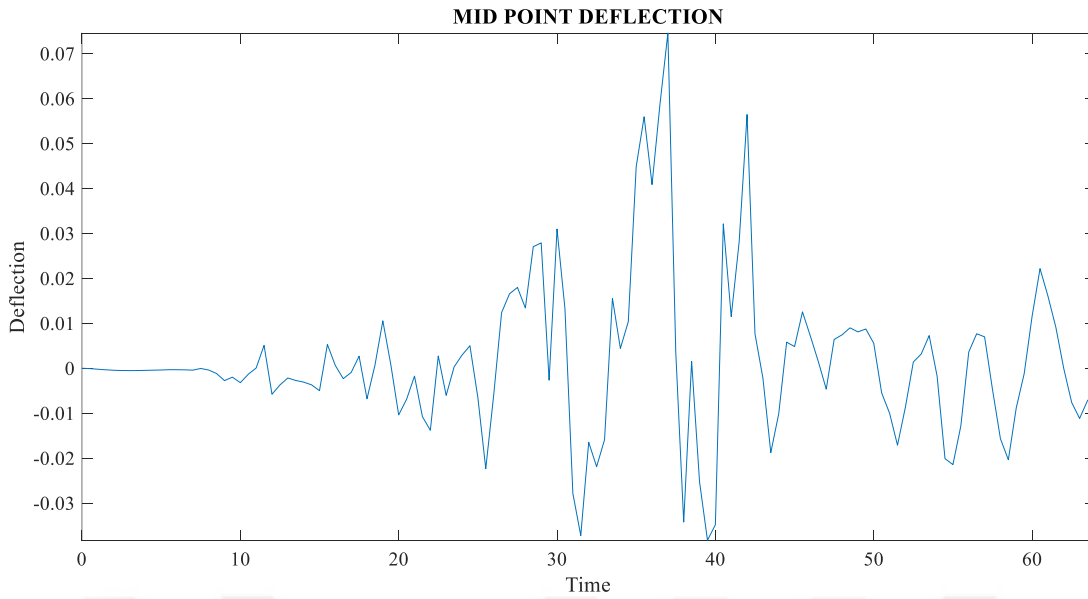


**Figure 3.101 :** Suspension Bridge Middle Point Deflection Due to the El Mayor Earthquake Motion and Moving Load for Case II

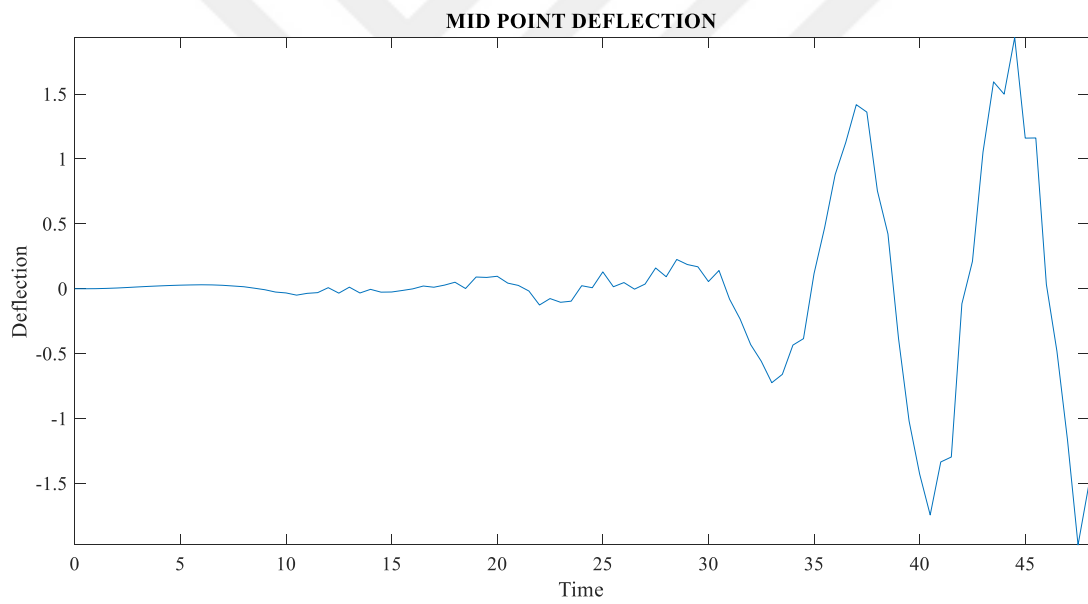


**Figure 3.102 :** Suspension Bridge Middle Point Deflection Due to the El Mayor Earthquake Motion and Moving Load for Case III

#### 4. CONCLUSION

In this study at first equation of motion for the suspension bridge for both extensible and inextensible hangers derived. Three different cases defined and equation of motions for mentioned cases solved in order to compute deflection, velocity and acceleration of the cable and the deck due to the moving load and ground excitation simultaneously. In **Table 4.1** and **Table 4.2** briefly results for extensible and inextensible hangers presented.

**Table 4.1 :** Comparison of Middle Point Deflection at the time moving load reaches middle of the span

Middle Point Deflection at the time load reaches middle of the span			
Case No.	Hangers type Extensible Hangers (m)	Inextensible Hangers (m)	Difference (%)
Case I	0.21738	0.21726	0.06%
Case II	0.20986	0.20972	0.07%
Case III	0.23195	0.2318	0.06%

**Table 4.2 :** Comparison of Middle Point Max Deflection

Middle Point Max Deflection			
Case No.	Hangers type Extensible Hangers (m)	Inextensible Hangers (m)	Difference (%)
Case I	0.22916	0.22908	0.03%
Case II	0.22741	0.22735	0.03%
Case III	0.24351	0.24345	0.02%

Obtained result shows that computed deflection of the suspension bridge from differential equation in which extensibility of the hangers considered are not much different from result that extensibility of the hangers are ignored. It is worth to note that, considering extensibility of the hangers, helps researchers to compute stress and axial force that appears in hangers during vibration.

Vibration modes of the bridge and natural frequency of the suspension bridge is depicted in **Table 4.3**. First two modes of the vibration are symmetric which also observed by Abdel Ghaffar [3].

**Table 4.3 :** Natural frequencies

Symmetric modes	Frequency (Hz)	Anti-symmetric modes	Frequency (Hz)
1	0.0430839	2	0.15360018
3	0.13347878	4	0.19338369

Results of this study compared with the result of ABAQUS software. In **Table 4.4** and **Table 4.5** obtained result from MATLAB and ABAQUS compared. Unlike mathematical assumption and written code in MATLAB, hangers in ABAQUS modeled as separate elements.

**Table 4.4 :** Comparison result of MATLAB and ABAQUS for cable mid point deflection

Cable mid point deflection			
Case	MATLAB (m)	ABAQUS (m)	Difference (%)
I	0.21717	0.215036	0.9826%
II	0.20966	0.212921	1.5554%
III	0.23174	0.25266	9.0274%

**Table 4.5 :** Comparison result of MATLAB and ABAQUS for deck mid point deflection

Deck mid point deflection			
Case	MATLAB (m)	ABAQUS (m)	Difference (%)
I	0.21738	0.215151	1.0254%
II	0.20986	0.21303	1.5105%
III	0.23195	0.252785	8.9825%

- Stress of hangers do not exceed yielding stress during vibration and none of the hangers elongate beyond the yielding strain.
- Computed deck deflection from deflection theory and improved deflection theory are very close and results from deflection theory method is also reliable.
- Convergence for deflection of the span occurs at lower modes while for velocity and acceleration computing higher modes effects are necessary which is why in this study effect of 50 modes computed.

- First two modes of the suspension bridge and the first antisymmetric mode appears after these two symmetric modes.
- Obtained result from MATLAB code was in good agreement with result computed by ABAQUS software. This fact shows reliability of the written code in MATLAB.

It is suggested for future researches and studies below parameters taken into account

- Inertial effect of the moving oscillators in which mass of the moving oscillators makes a coupled differential equation with differential equation of the deck and cable.
- Acceleration of the moving oscillators where moving oscillator do not have constant speed and the speed of the moving oscillators varies depending on the time.
- Series of moving loads, such as train crossing the suspension bridge.
- Moving loads that crosses suspension bridge in opposite direction of each other.
- Effect of the various damping values on the dynamic response of the suspension bridge.
- Effect of the track irregularity on the dynamic response of the suspension Bridge.
- Effect of the deck supports on the dynamic behavior of the suspension bridge.
- Effect of the cable support at the top of the tower on the dynamic behavior of the suspension bridge.
- Effect of the various damping's on the dynamic behavior of the suspension bridge.
- Non-uniform ground excitation (Near field and far field) at supports of the bridge, since suspension bridges are very large structures ground excitation could be different at each support.
- Suspension cable sag amount on dynamic response of the bridge.



## REFERENCES

- [1] **Okukawa, A., Suzuki, S., & Harazaki, I.** (2014). Suspension Bridges. In W.F. Chen, L. Duan (Eds.), *Bridge Engineering Handbook, Second Edition: Superstructure Design* (2nd ed., pp.363-398) . CRC Press, Boca Raton, London, New York
- [2] **Steinmen, D.B.** (1959). Modes and natural frequencies of suspension bridge oscillations, *Journal of the Franklin Institute.*, Vol. 268, pp.148-174. doi : 10.1016/s0016-0032(59)90395-3
- [3] **Xu, Y. L., Ko, J. M., and Zhang, W. S.** (1997). Vibration Studies of Tsing Ma Suspension Bridge, *Journal of Bridge Engineering.*, Vol. 2, No. 4, pp.149-156. doi : 10.1061/(asce)1084-0702(1997)2:4(149)
- [4] **Abdel-Ghaffar, Ahmed M., Scanlan, Robert H.** (1985). Ambient Vibration Studies of Golden Gate Bridge: I. Suspended Structure, *Journal of Engineering Mechanics.*, Vol. 111, No. 4, pp.463-482. doi : 10.1061/(asce)0733-9399(1985)111:4(463)
- [5] **Wollmann, G. P.** (2001). Preliminary Analysis of Suspension Bridges, *Journal of Bridge Engineering.*, Vol. 6, No. 4, pp.227–233. doi:10.1061/(asce)1084-0702(2001)6:4(227)
- [6] **Cobo del Arco, D., and Aparicio, Á.C.** (2001). Preliminary static analysis of suspension bridges. *Engineering Structures.*, Vol. 23, No. 9, pp.1096–1103. doi:10.1016/s0141-0296(01)00009-8
- [7] **Yau, J. D.** (2009). Dynamic response analysis of suspended beams subjected to moving vehicles and multiple support excitations. *Journal of Sound and Vibration.*, Nol. 325, No. 4–5, pp. 907–922. doi:10.1016/j.jsv.2009.04.013
- [8] **Liu, M.-F., Chang, T.-P., and Zeng, D.-Y.** (2011). The interactive vibration behavior in a suspension bridge system under moving vehicle loads and vertical seismic excitations. *Applied Mathematical Modelling.*, Vol. 35, No. 1, pp. 398–411. doi:10.1016/j.apm.2010.07.005
- [9] **Choi, D.-H., Gwon, S.-G., Yoo, H., and Na, H.-S.** (2013). Nonlinear static analysis of continuous multi-span suspension bridges. *International Journal of Steel Structures.*, Vol. 13, No. 1, pp. 103–115. doi:10.1007/s13296-013-1010-0

- [10] **Choi, D.-H., and Gwon, S.-G.** (2015). Effects of Hanger Extensibility on Responses of Suspension Bridges, *IABSE Symposium Report.*, Vol. 104, No. 32, pp. 1–6. doi:10.2749/222137815815773981
- [11] **Gwon, S.-G., and Choi, D.-H.** (2017). Improved Continuum Model for Free Vibration Analysis of Suspension Bridges, *Journal of Engineering Mechanics.*, Vol. 143, No. 7, p. 04017038. doi:10.1061/(asce)em.1943-7889.0001244
- [12] **Gwon, S.-G., and Choi, D.-H.** (2018). Static and dynamic analyses of a suspension bridge with three-dimensionally curved main cables using a continuum model, *Engineering Structures.*, Vol. 161, pp. 250–264. doi:10.1016/j.engstruct.2018.01.062
- [13] **Hayashikawa, Toshiro., and Watanabe, Noboru.** (1982). Dynamic Behavior of Suspension Bridges under Moving Loads. *Department of civil engineering.*, Hokkaido university, pp.1-12.
- [14] **Materazzi, A., and Ubertini, Filippo.** (2015). Vertical vibration of suspension bridges with damage.
- [16] **Jewel Sarker, J. S.** (2013). Optimum Dimensions of Suspension Bridges Considering Natural Period. *IOSR Journal of Mechanical and Civil Engineering*, Vol. 6, No.4, pp. 67–76. doi:10.9790/1684-646776
- [17] **Enrique Luco, J., and Turmo, J.** (2010). Linear vertical vibrations of suspension bridges: A review of continuum models and some new results. *Soil Dynamics and Earthquake Engineering*, Vol. 30, No.9, pp. 769–781. doi:10.1016/j.soildyn.2009.10.009
- [18] **Chatterjee, P. K., Datta, T. K., and Surana, C. S.** (1994). Vibration of Suspension Bridges under Vehicular Movement. *Journal of Structural Engineering*, Vol. 120, No.3, pp. 681–703. doi:10.1061/(asce)0733-9445(1994)120:3(681)
- [19] **Goremikins, V., Rocens, K., Serdjuks, D., and Sliseris, J.** (2013). Simplified Method of Determination of Natural-Vibration Frequencies of Prestressed Suspension Bridge. *Procedia Engineering*, 57, 343–352. doi:10.1016/j.proeng.2013.04.046
- [20] **Turmo, J., and Luco, J. E.** (2010). Effect of Hanger Flexibility on Dynamic Response of Suspension Bridges. *Journal of Engineering Mechanics*, Vol. 136, No. 12, pp. 1444–1459. doi:10.1061/(asce)em.1943-7889.0000185
- [21] **Frýba, L., and Yau, J.-D.** (2009). Suspended bridges subjected to moving loads and support motions due to earthquake. *Journal of Sound and Vibration*, Vol. 319, No. 1-2, pp. 218–227. doi:10.1016/j.jsv.2008.05.012
- [22] **Irvine, H.M.** (1981). *Cable Structures*. The MIT Press, Cambridge.



- [23] **Tao, T., Wang, H., Yao, C., and He, X.** (2017). Parametric Sensitivity Analysis on the Buffeting Control of a Long-Span Triple-Tower Suspension Bridge with MTMD. *Applied Sciences*, Vol. 7, No. 4, p. 395. doi:10.3390/app7040395





## APPENDICES

### APPENDIX A: Finite Difference Method

In finite difference method approximate values of derivatives would be computed. This method is a numerical method which is an easy way for differential equations that could not solve with conventional methods.

With using central difference rule first derivative according to FDM method provided in equation (A.1).

$$y'_{(i)} = \frac{y_{(i+1)} - y_{(i-1)}}{\Delta x} \quad (\text{A.1})$$

Implementing same method for second derivative would result in equation (A.2).

$$y''_{(i)} = \frac{y_{(i+1)} - 2y_{(i)} + y_{(i-1)}}{\Delta x^2} \quad (\text{A.2})$$

Third derivative equation manifested in equation (A.3).

$$y'''_{(i)} = \frac{\frac{-1}{2}y_{(i+2)} + y_{(i+1)} - y_{(i-1)} + \frac{1}{2}y_{(i-2)}}{\Delta x^3} \quad (\text{A.3})$$

And at last fourth derivative equation explained in equation (A.4).

$$y^{iv}_{(i)} = \frac{y_{(i+2)} - 4y_{(i+1)} + 6y_{(i)} - 4y_{(i-1)} + y_{(i-2)}}{\Delta x^4} \quad (\text{A.4})$$

To get trivial solution for system of equations which is produced by FDM method, extra equations will be need to solve this problem equations for boundary points will be used.

## APPENDIX B: Mathematics

Production of two sine terms is equal to difference of two cosine terms which is given in equation (B.1).

$$\sin A \sin B = \frac{1}{2} [\cos(A - B) - \cos(A + B)] \quad (\text{B.1})$$

Integration of two sine terms with different phases are presented in equation (B.2).

$$\begin{aligned} \int \sin\left(\frac{n\pi x}{L}\right) \sin\left(\frac{j\pi x}{L}\right) dx &= \frac{1}{2} \int \left\{ \cos\left(\frac{[n-j]\pi x}{L}\right) - \cos\left(\frac{[n+j]\pi x}{L}\right) \right\} dx \\ &= \frac{1}{2} \left\{ \left(\frac{L}{[n-j]\pi}\right) \sin\left(\frac{[n-j]\pi x}{L}\right) - \left(\frac{L}{[n+j]\pi}\right) \sin\left(\frac{[n+j]\pi x}{L}\right) \right\} \end{aligned} \quad (\text{B.2})$$

If  $n$  and  $j$  are separate integers any linear sum of them with integer coefficient would be integer which is given as mathematical expression in equation (B.3).

$$\forall n, j \in \mathbb{Z} \wedge n \neq j \Rightarrow \alpha n \pm \beta j \in \mathbb{Z} \wedge \alpha n \pm \beta j \neq 0 \quad (\text{B.3})$$

Equation B.2 will be equal to 0, because of given conditions in (B.4).

$$\sin\left(\frac{[n \pm j]\pi x}{L}\right) = 0 \quad (\text{B.4})$$

If  $n$  is equal to  $j$  equation B.2 would result in equation (B.5).

$$\begin{aligned} \int_{x=0}^{x=L} \sin^2\left(\frac{n\pi x}{L}\right) dx &= \int_{x=0}^{x=L} \left[ 1 - \cos\left(\frac{2n\pi x}{L}\right) \right] dx \\ &= \left[ \frac{x}{2} - \sin\left(\frac{2i\pi x}{L}\right) \right]_{x=0}^{x=L} = \frac{L}{2} \end{aligned} \quad (\text{B.5})$$

From above equations multiplications of two shape functions can be found and explained in equation (B.6).

$$\int_{x=0}^{x=L} \phi_{n(x)} \phi_{j(x)} \cdot dx = \begin{cases} 0, & n \neq j \\ \frac{L}{2}, & n = j \end{cases} \quad (\text{B.6})$$

## APPENDIX C: Cable Parabolic Equation

The Cable Shape Considered in current study is parabolic. Therefore, the coefficients of second-degree polynomial and the origin of the cable axis in horizontal direction is started from left tower, while the origin of the cable axis in vertical direction starts from top of the left tower and the positive direction is considered downward. In this order, the polynomial equation of the cable is provided in equation (C.1).

$$y = ax^2 + bx + c \quad (\text{C.1})$$

Three points coordinates are known which are brought in equation (C.2).

$$\begin{cases} y_0, y_L = 0 \\ y_{\frac{L}{2}} = \frac{L}{8} \end{cases} \quad (\text{C.2})$$

Coefficients computed by solving system of equations. Coefficients are brought in equation (C.3).

$$ax^2 + bx + c \Rightarrow \begin{cases} c = 0 \\ b = \frac{1}{2} \\ a = -\frac{1}{2L} \end{cases} \quad (\text{C.3})$$

## APPENDIX D: Deriving Equilibrium Equation

Horizontal equilibrium for infinitesimal element of the cable is manifested in equation (D.1).

$$\frac{d}{ds} \left( T \frac{dx}{ds} \right) \Delta s = 0 \quad (\text{D.1})$$

Vertical equilibrium of the cable is brought in equation (D.2).

$$\frac{d}{ds} \left( T \frac{dz}{ds} \right) \Delta s + mg \Delta s = 0 \quad (\text{D.2})$$

By rearranging equation D.2 and simplifying it, relation between tension and weight of the cable extracted. This relation provided in equation (D.3).

$$\frac{d}{ds} \left( T \frac{dz}{ds} \right) = -mg \quad (\text{D.3})$$

Chain differential equation is given in equation (D.4) for reminding.

$$\frac{dz}{ds} = \frac{dx}{ds} \cdot \frac{dz}{dx} \quad (\text{D.4})$$

Equation (D.5) provides relation between horizontal component of the cable tension and cable tension

$$T \frac{dx}{ds} = H \quad (\text{D.5})$$

Inserting equation D.4 into equation D.5 would lead to equation (D.6).

$$\frac{d}{ds} \left( T \frac{dx}{ds} \cdot \frac{dz}{dx} \right) = \frac{d}{ds} \left( H \cdot \frac{dz}{dx} \right) = -mg \quad (\text{D.6})$$

Multiplying both sides of equation D.6 with  $\frac{ds}{dx}$  would result into equation (D.7).

$$H \frac{d^2z}{dx^2} = -mg \frac{ds}{dx} \quad (\text{D.7})$$

## APPENDIX E: Deriving Equation For Increment In Horizontal Component Of Cable Tension

Equation (E.1) explains finite length of elongated cable.

$$ds' = \sqrt{(dx + du)^2 + (dy + dw)^2} \quad (\text{E.1})$$

Relation for force resulted from length increment is brought in equation (E.2).

$$\frac{P}{AE} = \frac{\Delta}{l} \quad (\text{E.2})$$

Thus, relation for axial force that cause by elongation in the cable is manifested in equation (E.3).

$$\frac{\tau}{EA} = \frac{ds' - ds}{ds} \quad (\text{E.3})$$

Multiplying both sides of the equation E.3 with  $\frac{ds'+ds}{ds'+ds}$  would result into equation E.4.

$$\frac{ds' - ds}{ds} \frac{ds' + ds}{ds' + ds} = \frac{ds'^2 - ds^2}{ds(ds' + ds)} \quad (\text{E.4})$$

Simplifying equation E.4 would result into equation (E.5).

$$\begin{aligned} & \frac{\overbrace{du^2}^{\cong 0} + 2dxdu + dw^2 + 2dwdz}{\sqrt{\underbrace{dx^2 + du^2}_{\cong 0} + \underbrace{2dxdu}_{\cong 0} + \underbrace{dz^2 + dw^2}_{\cong 0} + \underbrace{2dwdz}_{\cong 0}} + \sqrt{dx^2 + dz^2}} \\ &= \frac{du^2 + 2dxdu + dw^2 + 2dwdz}{2ds^2} \\ &= \frac{du}{ds} \frac{dx}{ds} + \frac{dz}{ds} \frac{dw}{ds} + \frac{1}{2} \left( \frac{dw}{ds} \right)^2 \end{aligned} \quad (\text{E.5})$$

## APPENDIX F: Integrating First Term In Equation 2.17

Integrating by parts  $\int_0^L \frac{dz}{dx} \cdot dw$  would result into equation (F.1).

$$\int_{x=0}^{x=L} \left( \frac{dz}{dx} \right) \cdot dw = w \frac{dz}{dx} - \int_{x=0}^{x=L} \left( \frac{d^2z}{dx^2} \right) w \cdot dx \quad (\text{F.1})$$

Knowing that  $\left( \frac{d^2z}{dx^2} \right) = -\frac{mg}{H} \frac{ds}{dx}$  and considering that  $\frac{ds}{dx}$  is equal to 1, equation (F.2)

expresses integration of  $\int_0^L \frac{dz}{dx} \cdot dw$ .

$$\begin{aligned} \int_{x=0}^{x=L} \left( \frac{dz}{dx} \right) \cdot dw &= \frac{dz}{dx} w \Big|_0^L + \frac{mg}{H} \int_{x=0}^{x=L} w \cdot dx \\ &= \left( \frac{1}{2} - \frac{x}{L} \right) w \Big|_0^L + \frac{mg}{H} \int_{x=0}^{x=L} w \cdot dx \\ &= \left( -\frac{1}{2} w_L - \frac{1}{2} w_0 \right) + \frac{mg}{H} \int_{x=0}^{x=L} w \cdot dx \\ &= -\left( \frac{1}{2} w_L + \frac{1}{2} w_0 \right) + \frac{mg}{H} \int_{x=0}^{x=L} w \cdot dx \end{aligned} \quad (\text{F.2})$$



## APPENDIX G: MATLAB Scripts

### G.1 Length Of The Cable

```
1 %%%%%%%%%%%%%%%%%%%%%%%%%%%%%%%%%%%%%%%%%%%%%%%%%%%%%%%%%%%%%%%%%%%%%%%%%%
2 %%%%%%%%%%%%%%%%%%%%%%%%%%%%%%%%%%%%%%%%%%%%%%%%%%%%%%%%%%%%%%%%%%%%%%%%%% COMPUTING LENGTH OF THE CABLE %%%%%%%%%%%%%%%%%%%%%%%%%%%%%%%%%%%%%%%%%%%%%%%%%%%%%%%%%%%%%%%%%%%%%%%%%%
3 %%%%%%%%%%%%%%%%%%%%%%%%%%%%%%%%%%%%%%%%%%%%%%%%%%%%%%%%%%%%%%%%%%%%%%%%%%
4 clc
5 clear all
6 syms x L
7 L = 1600;           % LENGTH OF THE SUSPENSION BRIDGE (m)
8 y0 = 175;          % SAG AMOUNT (m)
9 y = 4*y0*(x/L-(x/L)^2); % SHAPE FUNCTION OF THE CABLE (diminsionless)
10 yP = (1+(diff(y,x)^2));
11 yP = yP^(1.5);
12 Lc = int(yP,0,1600); % INTEGRATING FUNCTION OF THE CABLE
13 vpa(Lc)           % LENGTH OF THE CABLE
```

### G.2 Computing Cable Tension & Deflection Of The Bridge

```
1 %%%%%%%%%%%%%%%%%%%%%%%%%%%%%%%%%%%%%%%%%%%%%%%%%%%%%%%%%%%%%%%%%%%%%%%%%%
2 %%%%%%%%%%%%%%%%%%%%%%%%%%%%%%%%%%%%%%%%%%%%%%%%%%%%%%%%%%%%%%%%%%%%%%%%%% COMPUTING CABLE TENSION & DEFLECTION OF THE BRIDGE %%%%%%%%%%%%%%%%%%%%%%%%%%%%%%%%%%%%%%%%%%%%%%%%%%%%%%%%%%%%%%%%%%%%%%%%%%
3 %%%%%%%%%%%%%%%%%%%%%%%%%%%%%%%%%%%%%%%%%%%%%%%%%%%%%%%%%%%%%%%%%%%%%%%%%%
4 clc
5 clear all
6 tic
7 syms x z w L w_g w_c E_g E_c I_g H_w H_p p K z_s w_s
8
9
10 %% SUSPENSION BRIDGE IMPORT DETAILS (FORCE = kN, LENGTH = m)
11
```

```

12 E_g = 2.1e8;           % DECK YOUNG'S MODULUS (kN/m2)
13 E_c = 2e8;            % CABLE YOUNG'S MODULUS (kN/m2)
14 E_h = 1.4e8;         % HANGER YOUNG'S MODULUS (kN/m2)
15 A_g = 1.5;           % DECK AREA (m2)
16 A_c = 0.78539;       % SUSPENSION CABLE AREA (m2)
17 A_h = 0.0314159;    % HANGER AREA (m2)
18 I_g = 3.5;           % DECK MOMENT OF INERTIA (m4)
19 K = 8.88e3;          % HANGERS DISTRIBUTED STIFFNESS OVER THE SPAN (kN/m2)
20 E_t = 3e7;           % TOWER YOUNG'S MODULUS (kN/m2)
21 L_t = 180 + 50;     % TOWER HEIGHT (m)
22 I_t = 600;           % TOWER MOMENT OF INERTIA (m4)
23 K_t = 3*E_t*I_t/((L_t)^3); % TOWER LATERAL STIFFNESS (kN/m)
24 R1 = 0;              % NEWTON RAPHSON METHOD
25 R2 = 0;              % NEWTON RAPHSON METHOD
26 R1S = 0;            % NEWTON RAPHSON METHOD
27 R2S = 0;            % NEWTON RAPHSON METHOD
28
29 %% FORCES
30
31 w_c = 60.457;        % CABLE WEIGHT PER LENGTH (kN/m)
32 w_g = 115.465;      % DECK WEIGHT PER LENGTH (kN/m)
33 w_T = w_g + w_c;    % TOTAL WEIGHT
34 p = 10;              % MAIN SPAN LIVE LOAD
35 pS = 0;              % SIDE SPAN LIVE LOAD
36
37 %% MAIN SPAN DETAILS
38
39 L = 1600;            % SPAN LENGTH (m)
40 L_0 = 1757.42637;   % CABLE LENGTH (m)
41 y0 = 175;           % SAG
42 y = 4*y0*(x/L-(x/L)^2); % PARABOLIC SHAPE OF THE CABLE
43 Dy = diff(y,x);     % CABLE SLOPE FUNCTION
44 D2y = diff(y,x,2);  % CABLE SECOND DERIVATIVE W.R. TO X
45 H_w = -w_T/D2y;     % TENSION IN CABLE DUE TO THE DEAD LOAD
46 Dy_at_0 = subs(Dy,x,0);
47

```

```

48 %% SIDE SPAN DETAILS
49
50 L_S = 400; % LEFT SPAN LENGTH (m)
51 L_OS = 530.525876; % CABLE LENGTH (m)
52 y_S = -y; % PARABOLIC SHAPE OF THE CABLE
53 DyS = diff(y_S,x);
54 D2yS = diff(y_S,x,2);
55 H_ws = w_T/D2yS; % TENSION IN CABLE DUE TO THE DEAD LOAD
56 DyS_at_LS = subs(-DyS,x,12760/7);
57
58 %% ANGLES
59
60 ThetaR = atand(double(Dy_at_0)); % THETA AT TOWER'S LEFT
61 ThetaL = atand(double(DyS_at_LS)); % THETA AT TOWER'S RIGHT
62
63 %% ITERATION WHILE MINIMUM ERROR SATISFIED
64
65 Counter = 1; % NUMBER OF ITERATIONS
66 Err(Counter) = 1; % ERROR FOR MAIN SPAN
67 ErrS(Counter) = 1; % ERROR FOR SIDE SPAN
68 H_p_Iteration(Counter) = 1.6484e5; % TENSION DUE TO LIVE LOAD ASSUMPTION AT MAIN SPAN
69 H_pS_Iteration(Counter) = 1.5703e5; % TENSION DUE TO LIVE LOAD ASSUMPTION AT SIDE SPAN
70 while or(abs(Err(Counter)) > 5e-1,abs(ErrS(Counter)) > 5e-1)
71
72 %% MAIN SPAN FINITE DIFFERENCE
73
74 H_p = H_p_Iteration(Counter);
75 Tension = H_p_Iteration(Counter)/cosd(ThetaR);
76 H_pS_Iteration(Counter) = Tension * cosd(ThetaL);
77 H_pS = H_pS_Iteration(Counter);
78 Span = L ;
79 NO_Of_Divisions = 16 ;
80 Dx = Span/NO_Of_Divisions ;
81
82 %% MAIN SPAN
83

```

```

84 Z = sym('z', [1 i]);
85 eval(SymsVar(z,i));
86 W = sym('w', [1 i]);
87 eval(SymsVar(w,i));
88
89 %% LOOP FOR CREATING SYSTEM OF EQUATIONS
90
91 for j=3:i-2
92 SZ = PFiniteDy(Z,j,Dx);
93 PZ = PFiniteD2y(Z,j,Dx);
94 QZ = PFiniteD3y(Z,j,Dx);
95 RZ = PFiniteD4y(Z,j,Dx);
96 SW = PFiniteDy(W,j,Dx);
97 PW = PFiniteD2y(W,j,Dx);
98 QW = PFiniteD3y(W,j,Dx);
99 RW = PFiniteD4y(W,j,Dx);
100 eqns(j-2) = E_g*I_g*RZ(j-2) + K*(Z(j) - W(j)) == p;
101 eqns(j-2+i-2) = (H_w+H_p)*PW(j-2) + K*(Z(j) - W(j)) == H_p*w_T/H_w;
102 end
103
104 %% BOUNDARY CONDITIONS FOR DECK
105
106 eqns(j-2+i-2+1) = Z(3) == 0;
107 eqns(j-2+i-2+2) = Z(i-2) == 0;
108 BC_D2Z_0 = PFiniteD2y(Z,3,Dx);
109 eqns(j-2+i-2+3) = BC_D2Z_0 == 0;
110 BC_D2Z_L = PFiniteD2y(Z,i-2,Dx);
111 eqns(j-2+i-2+4) = BC_D2Z_L(end) == 0;
112
113 %% BOUNDARY CONDITIONS FOR CABLE
114
115 eqns(j-2+i-2+5) = W(3) == 0;
116 eqns(j-2+i-2+6) = W(i-2) == 0;
117
118 %% SOLUTION
119

```

```

120 Temp = Z;
121 Temp(i+1:2*i) = W;
122 sol = solve(eqns, Temp);
123 vpa(RR(end-2-NO_Of_Divisions-2-3),12);
124 vpa(RR(end-2),12);
125 Zsol = subs(Z,Z(1:i),RR(1:i)');
126 Wsol = subs(W,W(1:i),RR(i+1:2*i)');
127
128 %% ERROR PROCESS AND NUMERIC INTEGRATIONS FOR MAIN SPAN
129
130 Sum = 0;
131 for q = 1:NO_Of_Divisions
132 Sum = Sum + 0.5*(W_Numeric(q)+W_Numeric(q+1))*(L/NO_Of_Divisions);
133 end
134 Sum = -(w_T/H_w)*Sum;
135 Tension = H_p_Iteration(Counter)/cosd(ThetaR);
136 H_pS_Iteration(Counter) = Tension * cosd(ThetaL);
137 H_pS = H_pS_Iteration(Counter);
138 D_L = (H_w + H_p_Iteration(Counter) - H_ws - H_pS_Iteration(Counter))/K_t;
139 Err(Counter+1) = L_0*(H_p_Iteration(Counter)/(E_c*A_c)) + Sum + 2*D_L
140
141 %% ERROR FOR MAIN SPAN
142
143 if Err(Counter+1) > 0
144 H_p_Iteration(Counter+1) = 0.75*H_p;
145 P1 = H_p;
146 R1 = Err(Counter+1);
147 else
148 H_p_Iteration(Counter+1) = 1.25*H_p;
149 P2 = H_p;
150 R2 = Err(Counter+1);
151 end
152 if R1*R2 < 0;
153 H_p_Iteration(Counter+1) = (P1+P2)/2;
154 end
155

```

```

156 %% SIDE SPAN FINITE DIFFERENCE
157
158 H_pS = H_pS_Iteration(Counter);
159 SpanS = L_S ;
160 NO_Of_DivisionsS = 4 ;
161 DxS = SpanS/NO_Of_DivisionsS ;
162
163 %% SIDE SPAN
164
165 ZS = sym('zs', [1 iS]);
166 eval(SymsVar(zs,iS));
167 WS = sym('ws', [1 iS]);
168 eval(SymsVar(ws,iS));
169
170 %% LOOP FOR CREATING SYSTEM OF EQUATIONS SIDE SPAN
171
172 for j=3:iS-2
173 SZS = PFiniteDy(ZS,j,Dx);
174 PZS = PFiniteD2y(ZS,j,Dx);
175 QZS = PFiniteD3y(ZS,j,Dx);
176 RZS = PFiniteD4y(ZS,j,Dx);
177 SWS = PFiniteDy(WS,j,Dx);
178 PWS = PFiniteD2y(WS,j,Dx);
179 QWS = PFiniteD3y(WS,j,Dx);
180 RWS = PFiniteD4y(WS,j,Dx);
181 eqnsS(j-2) = E_g*I_g*RZS(j-2) + K*(ZS(j) - WS(j)) == pS;
182 eqnsS(j-2+iS-2) = (H_wS+H_pS)*PWS(j-2) + K*(ZS(j) - WS(j)) == H_pS*w_T/H_wS;
183 end
184
185 %% BOUNDARY CONDITIONS FOR DECK
186
187 eqnsS(j-2+iS-2+1) = ZS(3) == 0;
188 eqnsS(j-2+iS-2+2) = ZS(iS-2) == 0;
189 BC_D2Z_0_S = PFiniteD2y(ZS,3,Dx);
190 eqnsS(j-2+iS-2+3) = BC_D2Z_0_S == 0;
191 BC_D2Z_L_S = PFiniteD2y(ZS,iS-2,Dx);

```

```

192 eqnsS(j-2+iS-2+4) = BC_D2Z_L_S(end) == 0;
193
194 %% BOUNDARY CONDITIONS FOR CABLE
195
196 eqnsS(j-2+iS-2+5) = WS(3) == 0;
197 eqnsS(j-2+iS-2+6) = WS(iS-2) == 0;
198
199 %% SOLUTION
200
201 TempS = ZS;
202 TempS(iS+1:2*iS) = WS;
203 solS = solve(eqnsS, TempS);
204 SolzS = struct2cell(solS);
205 RRS = vpa(SolzS);
206 vpa(RRS(end-2-NO_Of_DivisionsS-2-3),12);
207 vpa(RRS(end-2),12);
208 ZsolS = subs(ZS,ZS(1:iS),RRS(1:iS)');
209 WsolS = subs(WS,WS(1:iS),RRS(iS+1:2*iS)');
210
211 %% ERROR PROCESS AND NUMERIC INTEGRATIONS FOR SIDE SPAN
212
213 Numeric_ResultS = vpa(RRS,5);
214 SumS = 0;
215 for q = 1:NO_Of_DivisionsS
216 SumS = SumS + 0.5*(W_NumericS(q)+W_NumericS(q+1))*(L_S/NO_Of_DivisionsS);
217 end
218 SumS = -(w_T/H_wS)*SumS;
219 D_LS = (H_wS + H_pS_Iteration(Counter) - H_w - H_p_Iteration(Counter))/K_t;
220 ErrS(Counter+1) = L_0S*(H_pS_Iteration(Counter)/(E_c*A_c)) + SumS + D_LS
221 if ErrS(Counter+1) > 0
222 H_pS_Iteration(Counter+1) = 0.75*H_pS;
223 P1S = H_pS;
224 R1S = ErrS(Counter+1);
225 else
226 H_pS_Iteration(Counter+1) = 1.25*H_pS;
227 P2S = H_pS;

```

```

228 R2S = ErrS(Counter+1);
229 end
230 if R1S*R2S < 0;
231 H_pS_Iteration(Counter+1) = (P1S+P2S)/2;
232 end
233 Counter = Counter + 1;
234 end
235
236 %% RESULT
237
238 Xlin = 0*Dx : Dx : NO_Of_Divisions*Dx;
239 Xlin = subs(Xlin,L,1600);
240 XlinLS = 0*Dx : Dx : NO_Of_DivisionsS*Dx;
241 XlinLS = subs(XlinLS,L_S,400);
242 XlinRS = 0*Dx : Dx : NO_Of_DivisionsS*Dx;
243 XlinRS = subs(XlinRS,L_S,400);
244 plot(Xlin + L_S,-W_Numeric)
245 hold on
246 plot(Xlin + L_S,-Z_Numeric)
247 hold on
248 plot(XlinLS,-W_NumericS)
249 hold on
250 plot(XlinLS,-Z_NumericS)
251 hold on
252 plot(XlinRS + L + L_S,-W_NumericS)
253 hold on
254 plot(XlinRS + L + L_S,-Z_NumericS)
255 title('Pseudo-Static Analysis Of The Suspension Bridge')
256 set(gca,'XMinorTick','on','YMinorTick','on')
257 set(gca,'FontName','Times New Roman','FontSize',16)
258 xlabel('Span Ordinate (m)')
259 ylabel('Span Defelection (m)')
260 legend('Cable Deflection In Main Span','Deck Deflection In Main Span','Cable Deflection In Left Side Span','Deck
Deflection In Left Side Span','Cable Deflection In Right Side Span','Deck Deflection In Right Side Span')
261 toc

```



### G.3 Fitting Equation For static Displacement

```
1 %%%%%%%%%%%%%%%%%%%%%%%%%%%%%%%%%%%%%%%%%%%%%%%%%%%%%%%%%%%%%%%%%%%%%%%%%%
2 %%%%%%%%%% FITTING EQUATION FOR STATIC DISPLACEMENT %%%%%%%%%%
3 %%%%%%%%%%%%%%%%%%%%%%%%%%%%%%%%%%%%%%%%%%%%%%%%%%%%%%%%%%%%%%%%%%%%%%%%%%
4 clc
5 clear all
6 syms x
7 W_Pseudo_Static = xlsread('STATIC.xlsx', 'Span', 'C3:C67');
8 Z_Pseudo_Static = xlsread('STATIC.xlsx', 'Span', 'D3:D67');
9 t = 0:25:1600;
10 XV = 0:25:1600;
11 Wp = polyfit(t',W_Pseudo_Static,20);
12 Zp = polyfit(t',Z_Pseudo_Static,20);
13 WEquation = poly2sym(Wp);
14 ZEequation = poly2sym(Zp);
15 WEquation = simplify(vpa(WEquation));
16 ZEequation = simplify(vpa(ZEequation));
17 for i = 1:65
18 Wspan(i) = subs(WEquation,x,XV(i));
19 Zspan(i) = subs(ZEequation,x,XV(i));
20 end
21 Wspan = double(Wspan');
22 Zspan = double(Zspan');
```

### G.4 Extensible Hangers

```
1 %%%%%%%%%%%%%%%%%%%%%%%%%%%%%%%%%%%%%%%%%%%%%%%%%%%%%%%%%%%%%%%%%%%%%%%%%%
2 %%%%%%%%%% EXTENSIBLE HANGERS %%%%%%%%%%
3 %%%%%%%%%%%%%%%%%%%%%%%%%%%%%%%%%%%%%%%%%%%%%%%%%%%%%%%%%%%%%%%%%%%%%%%%%%
4
5 clc
6 clear all
7 syms W(t) Z(t) wx wv zx zv t x n
8 tic
```

```

9
10 format long
11
12 %% UNKOWNS VALUES
13
14 E_g = 2.1e8; % DECK MOODULUS OF ELASITICITY (kN/m^2)
15 E_c = 2e8; % SUSPENSION CABLE MOODULUS OF ELASITICITY (kN/m^2)
16 E_h = 1.4e8; % HANGER MOODULUS OF ELASITICITY (kN/m^2)
17 I_g = 3.5; % DECK MOMENT OF INERTIA (m^4)
18 I_c = 0.05; % CABLE MOMENT OF INERTIA (m^4)
19 A_g = 1.5; % DECK AREA (m^2)
20 A_c = 0.78539; % SUSPENSION CABLE AREA (m^2)
21 A_h = 0.0314159; % HANGER AREA (m^2)
22 d_h = 25; % SPACE BETWEEN HANGER (m)
23 K = 8.88e3; % DISTRIBUTED HANGER STIFFNESS (kN/m^2)
24 M = 20.3956; % VEHICLE MASS (ton)
25 V = 120/3.6; % VELOCITY OF MOVING MASS (m/s)
26 m_g = 11.775; % DECK PER LENGTH MASS (ton/m)
27 m_c = 6.1653; % CABLE PER LENGTH MASS (ton/m)
28 H = 321685.942; % CABLE HORZONTAL TENSION (kN)
29 DH = 16484.597; % INCREMENT IN CABLE HORZONTAL TENSION (kN)
30 L = 1600; % SPAN LENGTH (m)
31 T = H+DH; % DEFINING H & DH (kN)
32 L_0 = 1757.42637; % CABLE LENGTH (m)
33 Alfa = -(E_c*A_c)/(L_0)/(L^2); % ALFA COEFFICENT
34 g = 9.806; % GRAVITY ACCELERATION (m/s^2)
35 u_0 = 0; % TOWER HORZONTAL DISPLACEMENT @ x = 0
36 u_L = 0; % TOWER HORZONTAL DISPLACEMENT @ x = L
37 w_0 = 0; % TOWER VERTICAL DISPLACEMENT @ x = 0
38 w_L = 0; % TOWER VERTICAL DISPLACEMENT @ x = L
39 N = 50; % NUMBER OF INVOLVED MODES
40 tMax = L/V;
41
42 %% DEFINING T & K_c & K_g
43 for n=1:N
44 K_c(n) = (K + T*((n*pi()/L)^2)-((2*Alfa*L)/((n*pi())^2))*((( -1)^n+1)^2)); % K VALUE IN EQUATION OF MOTION OF

```

```

THE CABLE
45 K_g(n) = (K + E_g*I_g*((n*pi()/L)^4)); % K VALUE IN EQUATION OF MOTION OF
THE DECK
46 Erq(n) = ((u_L-u_0) - (1/2)*(w_L+w_0))*((-1)^n+1);
47 end
48
49 %% DIFFERENTIAL EQUATIONS
50
51 for n=1:N
52 ODE1(n) = diff(W,t,2) + (K_c(n)*W - K*Z)/m_c - (Erq(n)*2*Alfa*L)/(n*pi()*m_c) == 0;
53 ODE2(n) = diff(Z,t,2) + (K_g(n)*Z - K*W)/m_g == (2*M*g/(m_g*L))*sin(n*pi()*V*t/L);
54 end
55 COND1 = W(0) == 0;
56 COND2 = dW(0) == 0;
57 COND3 = Z(0) == 0;
58 COND4 = dZ(0) == 0;
59 CONDS = [COND1, COND2, COND3, COND4];
60
61 %% SOLUTION
62
63 WsolN = 0;
64 WsolxN = 0;
65 ZsolN = 0;
66 ZsolxN = 0;
67 for n=1:N
68 ODES = [ODE1(n), ODE2(n)];
69 [Wsol(n), Zsol(n)] = dsolve(ODES, CONDS);
70 Wsolx(n) = Wsol(n) * sin(n*pi()*x/L);
71 WsolxN = WsolxN + Wsolx(n);
72 Zsolx(n) = Zsol(n) * sin(n*pi()*x/L);
73 ZsolxN = ZsolxN + Zsolx(n);
74 end
75
76 %% PLOTTING SPECIFIC POINT AT TOTAL TIME
77
78 format longG

```

```

79 figure(1)
80 fplot(WsolN,[0,tMax])
81 yLimits = get(gca,'YLim');
82 ylim([1.15*yLimits(1), 1.15*yLimits(2)])
83 hold on
84 fplot(ZsolN,[0,tMax])
85 ylim([1.15*yLimits(1), 1.15*yLimits(2)])
86 hold on
87 plot(WXminN,-WYminN,'s','MarkerSize',10,'MarkerEdgeColor','yellow','MarkerFaceColor',[1 1 0])
88 hold on
89 plot(ZXminN,-ZYminN,'s','MarkerSize',10,'MarkerEdgeColor','red','MarkerFaceColor',[1 0 0])
90 hold on
91 COORW = strcat('\uparrow');
92 StrW = strcat(' T = ', num2str(WXminN), ' s & ', ' Cable Deflection = ', num2str(double(-WYminN)), ' m');
93 COORW = {COORW, StrW};
94 PW = text(WXminN,-WYminN,COORW);
95 PW.FontSize = 16;
96 PW.FontName = 'Times New Roman';
97 PW.FontWeight = 'normal';
98 PW.HorizontalAlignment = 'center';
99 PW.VerticalAlignment = 'top';
100 COORZ = '\downarrow';
101 StrZ = strcat(' T = ', num2str(ZXminN), ' s & ', ' Deck Deflection = ', num2str(double(-ZYminN)), ' m');
102 COORZ = {StrZ, COORZ};
103 PZ = text(ZXminN,-ZYminN,COORZ);
104 PZ.FontSize = 16;
105 PZ.FontName = 'Times New Roman';
106 PZ.FontWeight = 'normal';
107 PZ.HorizontalAlignment = 'center';
108 PZ.VerticalAlignment = 'bottom';
109 legend({'Cable Deflection','Deck Deflection'},'Location','east')
110 title('Cable and Deck middle point Deflection')
111 xlabel('Time')
112 ylabel('Deflection')
113 set(gca,'FontName','Times New Roman','FontSize',16)
114 set(gca,'XMinorTick','on','YMinorTick','on')

```

```

115 X_Coor = double((WXminN + ZXminN)*(1/2));
116 Y_Coor = double((-WYminN - ZYminN)*(1/2));
117 Width_Rec1 = X_Coor/6;
118 yLimits = get(gca, 'YLim');
119 yLimits = abs(yLimits(2) - yLimits(1));
120 Height_Rec1 = yLimits/40;
121 rectangle('Position', [X_Coor - Width_Rec1/2, Y_Coor - Height_Rec1/2, Width_Rec1, Height_Rec1], 'EdgeColor',
[0.4,
0.1, 0.4], 'LineWidth', 1);
122 x_a = 0.65;
123 y_a = 0.2;
124 w_a = 0.2;
125 h_a = 0.2;
126 ax = axes('Units', 'Normalized', 'Position', [x_a, y_a, w_a, h_a], 'XTick', [], 'YTick', [], 'Box',
'on', 'LineWidth',
1, 'Color', [0.95, 0.99, 0.95]);
127 hold on
128 fplot(WsolN, [0, tMax]);
129 hold on;
130 fplot(ZsolN, [0, tMax]);
131 hold on
132 plot(WXminN, -WYminN, 's', 'MarkerSize', 10, 'MarkerEdgeColor', 'yellow', 'MarkerFaceColor', [1 1 0])
133 hold on
134 plot(ZXminN, -ZYminN, 's', 'MarkerSize', 10, 'MarkerEdgeColor', 'red', 'MarkerFaceColor', [1 0 0])
135 hold on
136 axis([X_Coor-Width_Rec1/5, X_Coor+Width_Rec1/5, Y_Coor-Height_Rec1/5, Y_Coor+Height_Rec1/5]);
137 title('')
138 xlabel('Time')
139 ylabel('Deflection')
140 set(gca, 'FontName', 'Times New Roman', 'FontSize', 16)
141
142 %% 3D PLOT OF SPAN DEFLECTION
143
144 figure(2)
145 ezsurf(WsolxN, [0, tMax, 0, L])
146 hold on

```

```

147 ezsurf(ZsolxN,[0,tMax, 0,L])
148 % legend('Cable Deflection','Deck Deflection')
149 title('3D PLOT OF SPAN DEFLECTION')
150 xlabel('Time')
151 ylabel('Longitudinal coordinate')
152 zlabel('Deflection')
153 set(gca,'FontName','Times New Roman','FontSize',16)
154 axis tight
155 xh = get(gca,'XLabel'); % Handle of the x label
156 set(xh, 'Units', 'Normalized')
157 set(xh, 'Position',[0.75,0.025,0], 'Rotation',12)
158 yh = get(gca,'YLabel'); % Handle of the y label
159 set(yh, 'Units', 'Normalized')
160 set(yh, 'Position',[0.175,0.05,0], 'Rotation',-14)
161
162 %% FUNCTIONS
163
164 WsoltNFun = matlabFunction(-WsoltN);
165 WXmintN = fminbnd(WsoltNFun,0,L);
166 WYmintN = subs(WsoltNFun,x,WXmintN);
167 WsoltNFun = matlabFunction(WsoltN);
168 WXmaxtN = fminbnd(WsoltNFun,0,L);
169 WYmaxtN = subs(WsoltNFun,x,WXmaxtN);
170 ZsoltNFun = matlabFunction(-ZsoltN);
171 ZXmintN = fminbnd(ZsoltNFun,0,L);
172 ZYmintN = subs(ZsoltNFun,x,ZXmintN);
173 ZsoltNFun = matlabFunction(ZsoltN);
174 ZXmaxtN = fminbnd(ZsoltNFun,0,L);
175 ZYmaxtN = subs(ZsoltNFun,x,ZXmaxtN);
176
177 %% PLOTTING SPAN DISPLACEMENT AT SPECIFIC TIME
178
179 format longG
180 figure(3)
181 fplot(WsoltN,[0,L])
182 yLimits = get(gca,'YLim');

```

```

183 ylim([1.15*yLimits(1), 1.15*yLimits(2)])
184 hold on
185 fplot(ZsoltN,[0,L])
186 yLimits = get(gca,'YLim');
187 ylim([1.15*yLimits(1), 1.15*yLimits(2)])
188 hold on
189 COORW = strcat('\uparrow');
190 StrW = strcat(' Location = ', num2str(WXmintN), ' m & ', ' Cable Deflection = ', num2str(double(-WYmintN)), '
m');
191 COORW = {COORW, StrW};
192 PW = text(WXmintN,-WYmintN,COORW);
193 PW.FontSize = 16;
194 PW.FontName = 'Times New Roman';
195 PW.FontWeight = 'normal';
196 PW.HorizontalAlignment = 'center';
197 PW.VerticalAlignment = 'top';
198 COORZ = '\downarrow';
199 StrZ = strcat(' Location = ', num2str(ZXmintN), ' m & ', ' Deck Deflection = ', num2str(double(-ZYmintN)), '
m');
200 COORZ = {StrZ, COORZ};
201 PZ = text(ZXmintN,-ZYmintN,COORZ);
202 PZ.FontSize = 16;
203 PZ.FontName = 'Times New Roman';
204 PZ.FontWeight = 'normal';
205 PZ.HorizontalAlignment = 'center';
206 PZ.VerticalAlignment = 'bottom';
207 legend({'Cable Deflection','Deck Deflection'},'Location','east')
208 TitleString = strcat({'Cable and Deck middle point Deflection at t = '}, num2str(tMax/2), ' s');
209 title(TitleString)
210 xlabel('Location')
211 ylabel('Deflection')
212 set(gca,'FontName','Times New Roman','FontSize',16)
213 set(gca,'XMinorTick','on','YMinorTick','on')
214 X_Coor = double((WXmintN + ZXmintN)*(1/2));
215 Y_Coor = double((-WYmintN - ZYmintN)*(1/2));
216 Width_Recl = X_Coor/6;

```

```

217 Height_Recl = Y_Coor/12;
218 rectangle('Position', [X_Coor - Width_Recl/2, Y_Coor - Height_Recl/2, Width_Recl, Height_Recl], 'EdgeColor',
[0.4,
0.1, 0.4], 'LineWidth', 1);
219 x_a = 0.65;
220 y_a = 0.2;
221 w_a = 0.2;
222 h_a = 0.2;
223 ax = axes('Units', 'Normalized', 'Position', [x_a, y_a, w_a, h_a], 'XTick', [], 'YTick', [], 'Box',
'on', 'LineWidth',
1, 'Color', [0.95, 0.99, 0.95]);
224 hold on
225 fplot(WsoltN, [0, L]);
226 hold on;
227 fplot(ZsoltN, [0, L]);
228 hold on
229 axis([X_Coor-Width_Recl/100, X_Coor+Width_Recl/100, Y_Coor-Height_Recl/100, Y_Coor+Height_Recl/100]);
230 title('')
231 xlabel('Time')
232 ylabel('Deflection')
233 set(gca, 'FontName', 'Times New Roman', 'FontSize', 16)
234
235 %% HANGERS ELONGATION
236
237 T_Max_Elongation = WXminN;
238 T_Middle_Elongation = WXmintN;
239 WsolElongation = subs(WsolxN, t, T_Max_Elongation);
240 ZsolElongation = subs(ZsolxN, t, T_Max_Elongation);
241 WsolMaxElongation = subs(WsolxN, t, T_Middle_Elongation);
242 ZsolMaxElongation = subs(ZsolxN, t, T_Middle_Elongation);
243 for i = 1 : 63
244 W_Elongation(i) = subs(WsolElongation, x, i*d_h);
245 Z_Elongation(i) = subs(ZsolElongation, x, i*d_h);
246 W_Middle_Elongation(i) = subs(WsolMaxElongation, x, i*d_h);
247 Z_Middle_Elongation(i) = subs(ZsolMaxElongation, x, i*d_h);
248 end

```



```

249
250 xlswrite('E:\ABAQUSTEZ\Software Modeling\MATLAB\Numeric Assumption\ElongationCaseIII.xlsx' , double(W_Elongation
(:)), 'Elongation' , 'C3:C66')
251 xlswrite('E:\ABAQUSTEZ\Software Modeling\MATLAB\Numeric Assumption\ElongationCaseIII.xlsx' , double(Z_Elongation
(:)), 'Elongation' , 'D3:D66')
252 xlswrite('E:\ABAQUSTEZ\Software Modeling\MATLAB\Numeric Assumption\ElongationCaseIII.xlsx' , double
(W_Middle_Elongation(:)), 'Elongation' , 'F3:F66')
253 xlswrite('E:\ABAQUSTEZ\Software Modeling\MATLAB\Numeric Assumption\ElongationCaseIII.xlsx' , double
(Z_Middle_Elongation(:)), 'Elongation' , 'G3:G66')
254
255 toc

```

## G.5 Inextensible Hangers

```

1 %%%%%%%%%%%%%%%%%%%%%%%%%%%%%%%%%%%%%%%%%%%%%%%%%%%%%%%%%%%%%%%%%%%%%%%%%
2 %%%%%%%%%%%%%%%%%%%%%%%%%%%%%%%%%%%%%%%%%%%%%%%%%%%%%%%%%%%%%%%%%%%%%%%%% INEXTENSIBLE HANGERS %%%%%%%%%%%%%%%%%%%%%%%%%%%%%%%%%%%%%%%%%%%%%%%%%%%%%%%%%%%%%%%%%%%%%%%%%
3 %%%%%%%%%%%%%%%%%%%%%%%%%%%%%%%%%%%%%%%%%%%%%%%%%%%%%%%%%%%%%%%%%%%%%%%%%
4 clc
5 clear all
6 syms Z(t) wx wv zx zv t x n
7 tic
8
9 format long
10
11 %% UNKOWNS VALUES
12
13 E_g = 2.1e8;           % DECK MOODULUS OF ELASITICITY (kN/m^2)
14 E_c = 2e8;           % SUSPENSION CABLE MOODULUS OF ELASITICITY (kN/m^2)
15 E_h = 1.4e8;         % HANGER MOODULUS OF ELASITICITY (kN/m^2)
16 I_g = 3.5;          % DECK MOMENT OF INERTIA (m^4)
17 I_c = 0.05;         % CABLE MOMENT OF INERTIA (m^4)
18 A_g = 1.5;          % DECK AREA (m^2)
19 A_c = 0.78539;      % SUSPENSION CABLE AREA (m^2)
20 A_h = 0.0314159;   % HANGER AREA (m^2)
21 d_h = 25;          % SPACE BETWEEN HANGER (m)

```

```

22 K = 8.88e3; % DISTRIBUTED HANGER STIFFNESS (kN/m^2)
23 M = 20.3956; % VEHICLE MASS (ton)
24 V = 120/3.6; % VELOCITY OF MOVING MASS (m/s)
25 m_g = 11.775; % DECK PER LENGTH MASS (ton/m)
26 m_c = 6.1653; % CABLE PER LENGTH MASS (ton/m)
27 H = 321685.942; % CABLE HORIZONTAL TENSION (kN)
28 DH = 16484.597; % INCREMENT IN CABLE HORIZONTAL TENSION (kN)
29 L = 1600; % SPAN LENGTH (m)
30 T = H+DH; % DEFINING H & DH (kN)
31 L_0 = 1757.42637; % CABLE LENGTH (m)
32 Alfa = -(E_c*A_c)/(L_0)/(L^2); % ALFA COEFFICIENT
33 g = 9.806; % GRAVITY ACCELERATION (m/s^2)
34 u_0 = 0; % TOWER HORIZONTAL DISPLACEMENT @ x = 0
35 u_L = 0; % TOWER HORIZONTAL DISPLACEMENT @ x = L
36 w_0 = 0; % TOWER VERTICAL DISPLACEMENT @ x = 0
37 w_L = 0; % TOWER VERTICAL DISPLACEMENT @ x = L
38 N = 50; % NUMBER OF INVOLVED MODES
39 tMax = L/V;
40
41 %% DEFINING T & K_c & K_g
42
43 for n=1:N
44 K_g(n) = ( E_g*I_g*((n*pi()/L)^4) + T*((n*pi()/L)^2) - ((2*Alfa*L)/((n*pi())^2))*(((-1)^n+1)^2)); % K VALUE IN
EQUATION OF MOTION OF THE CABLE
45 Erq(n) = ((u_L-u_0) - (1/2)*(w_L+w_0))*((-1)^n+1);
46 end
47
48 %% DIFFERENTIAL EQUATIONS
49
50 for n=1:N
51 ODE1(n) = diff(Z,t,2) + (K_g(n)*Z)/(m_g + m_c) == (2*M*g/((m_g + m_c)*L))*sin(n*pi()*V*t/L) + (Erq(n)
*2*Alfa*L)/(n*pi()*m_g + m_c));
52 end
53 COND1 = Z(0) == 0;
54 COND2 = dZ(0) == 0;
55 CONDS = [COND1, COND2];

```

```

56
57 %% SOLUTION
58
59 ZsolN = 0;
60 ZsolxN = 0;
61 for n=1:N
62 Zsol(n) = dsolve(ODE1(n), CONDS);
63 Zsolx(n) = Zsol(n) * sin(n*pi()*x/L);
64 ZsolxN = ZsolxN + Zsolx(n);
65 end
66
67 %% PLOTTING SPECIFIC POINT AT TOTAL TIME
68
69 format longG
70 figure(1)
71 fplot(ZsolN,[0,tMax])
72 yLimits = get(gca,'YLim');
73 ylim([1.15*yLimits(1), 1.15*yLimits(2)])
74 hold on
75 plot(ZXminN,-ZYminN,'s','MarkerSize',10,'MarkerEdgeColor','red','MarkerFaceColor',[1 0 0])
76 hold on
77 COORZ = '\downarrow';
78 StrZ = strcat(' T = ', num2str(ZXminN), ' s & ', ' Deck Deflection = ', num2str(double(-ZYminN)), ' m');
79 COORZ = {StrZ, COORZ};
80 PZ = text(ZXminN,-ZYminN,COORZ);
81 PZ.FontSize = 16;
82 PZ.FontName = 'Times New Roman';
83 PZ.FontWeight = 'normal';
84 PZ.HorizontalAlignment = 'center';
85 PZ.VerticalAlignment = 'bottom';
86 legend({'Deck Deflection'},'Location','east')
87 title('Deck middle point Deflection')
88 xlabel('Time')
89 ylabel('Deflection')
90 set(gca,'FontName','Times New Roman','FontSize',16)
91 set(gca,'XMinorTick','on','YMinorTick','on')

```

```

92 X_Coor = double(ZXminN);
93 Y_Coor = double(- ZYminN);
94 Width_Recl = X_Coor/6;
95 yLimits = get(gca,'YLim');
96 yLimits = abs(yLimits(2) - yLimits(1));
97 Height_Recl = yLimits/40;
98 rectangle('Position', [X_Coor - Width_Recl/2, Y_Coor - Height_Recl/2, Width_Recl, Height_Recl], 'EdgeColor', [0.4,
0.1, 0.4], 'LineWidth', 1);
99 x_a = 0.65;
100 y_a = 0.2;
101 w_a = 0.2;
102 h_a = 0.2;
103 ax = axes('Units', 'Normalized','Position', [x_a, y_a, w_a, h_a], 'XTick', [], 'YTick', [], 'Box',
'on', 'LineWidth',
1, 'Color', [0.95, 0.99, 0.95]);
104 hold on
105 fplot(ZsolN,[0,tMax]);
106 hold on
107 plot(ZXminN,-ZYminN,'s','MarkerSize',10,'MarkerEdgeColor','red','MarkerFaceColor',[1 0 0])
108 hold on
109 axis([X_Coor-Width_Recl/5, X_Coor+Width_Recl/5, Y_Coor-Height_Recl/5, Y_Coor+Height_Recl/5]);
110 title('')
111 xlabel('Time')
112 ylabel('Deflection')
113 set(gca,'FontName','Times New Roman','FontSize',16)
114
115 %% 3D PLOT OF SPAN DEFLECTION
116
117 figure(2)
118 ezsurf(ZsolxN,[0,tMax, 0,L])
119 title('3D PLOT OF SPAN DEFLECTION')
120 xlabel('Time')
121 ylabel('Longitudinal coordinate')
122 zlabel('Deflection')
123 set(gca,'FontName','Times New Roman','FontSize',16)
124 axis tight

```

```

125 xh = get(gca, 'XLabel');
126 set(xh, 'Units', 'Normalized')
127 set(xh, 'Position', [0.75, 0.025, 0], 'Rotation', 12)
128 yh = get(gca, 'YLabel');
129 set(yh, 'Units', 'Normalized')
130 set(yh, 'Position', [0.175, 0.05, 0], 'Rotation', -14)
131
132 %% PLOTTING SPAN DISPLACEMENT AT SPECIFIC TIME
133
134 format longG
135 figure(3)
136 fplot(ZsoltN, [0, L])
137 yLimits = get(gca, 'YLim');
138 ylim([1.15*yLimits(1), 1.15*yLimits(2)])
139 hold on
140 plot(ZXmintN, -ZYmintN, 's', 'MarkerSize', 10, 'MarkerEdgeColor', 'red', 'MarkerFaceColor', [1 0 0])
141 hold on
142 COORZ = '\downarrow';
143 StrZ = strcat(' Location = ', num2str(ZXmintN), ' m & ', ' Deck Deflection = ', num2str(double(-ZYmintN)), '
m');
144 COORZ = {StrZ, COORZ};
145 PZ = text(ZXmintN, -ZYmintN, COORZ);
146 PZ.FontSize = 16;
147 PZ.FontName = 'Times New Roman';
148 PZ.FontWeight = 'normal';
149 PZ.HorizontalAlignment = 'center';
150 PZ.VerticalAlignment = 'bottom';
151 legend({'Deck Deflection'}, 'Location', 'east')
152 TitleString = strcat({'Deck middle point Deflection at t = '}, num2str(tMax/2), ' s');
153 title(TitleString)
154 xlabel('Location')
155 ylabel('Deflection')
156 set(gca, 'FontName', 'Times New Roman', 'FontSize', 16)
157 set(gca, 'XMinorTick', 'on', 'YMinorTick', 'on')
158 X_Coor = double(ZXmintN);
159 Y_Coor = double(- ZYmintN);

```

```

160 Width_Recl = X_Coor/6;
161 Height_Recl = Y_Coor/12;
162 rectangle('Position', [X_Coor - Width_Recl/2, Y_Coor - Height_Recl/2, Width_Recl, Height_Recl], 'EdgeColor',
[0.4,
0.1, 0.4], 'LineWidth', 1);
163 x_a = 0.65;
164 y_a = 0.2;
165 w_a = 0.2;
166 h_a = 0.2;
167 ax = axes('Units', 'Normalized', 'Position', [x_a, y_a, w_a, h_a], 'XTick', [], 'YTick', [], 'Box',
'on', 'LineWidth',
1, 'Color', [0.95, 0.99, 0.95]);
168 hold on
169 fplot(ZsoltN, [0,L]);
170 hold on
171 axis([X_Coor-Width_Recl/100, X_Coor+Width_Recl/100, Y_Coor-Height_Recl/100, Y_Coor+Height_Recl/100]);
172 title('')
173 xlabel('Location')
174 ylabel('Deflection')
175 set(gca, 'FontName', 'Times New Roman', 'FontSize', 16)
176
177 toc

```

## G.6 Maximum Acceleration

```

1 %%%%%%%%%%%%%%%%%%%%%%%%%%%%%%%%%%%%%%%%%%%%%%%%%%%%%%%%%%%%%%%%%%%%%%%%%
2 %%%%%%%%%%%%%%%%%%%%%%%%%%%%%%%%%%%%%%%%%%%%%%%%%%%%%%%%%%%%%%%%%%%%%%%%% MAX ACCELERATION %%%%%%%%%%%%%%%%%%%%%%%%%%%%%%%%%%%%%%%%%%%%%%%%%%%%%%%%%%%%%%%%%%%%%%%%%
3 %%%%%%%%%%%%%%%%%%%%%%%%%%%%%%%%%%%%%%%%%%%%%%%%%%%%%%%%%%%%%%%%%%%%%%%%%
4
5 clc
6 clear all
7 syms W(t) Z(t) wx wv zx zv t x n V
8 tic
9
10 format long

```

```

11
12 %% UNKOWNS VALUES
13
14 E_g = 2.1e8;           % DECK MOODULUS OF ELASITICITY (kN/m^2)
15 E_c = 2e8;            % SUSPENSION CABLE MOODULUS OF ELASITICITY (kN/m^2)
16 E_h = 1.4e8;         % HANGER MOODULUS OF ELASITICITY (kN/m^2)
17 I_g = 3.5;           % DECK MOMENT OF INERTIA (m^4)
18 I_c = 0.05;          % CABLE MOMENT OF INERTIA (m^4)
19 A_g = 1.5;           % DECK AREA (m^2)
20 A_c = 0.78539;        % SUSPENSION CABLE AREA (m^2)
21 A_h = 0.0314159;     % HANGER AREA (m^2)
22 d_h = 25;           % SPACE BETWEEN HANGER (m)
23 K = 8.88e3;          % DISTRIBUTED HANGER STIFFNESS (kN/m^2)
24 M = 20.3956;         % VEHICLE MASS (ton)
25 m_g = 11.775;        % DECK PER LENGTH MASS (ton/m)
26 m_c = 6.1653;        % CABLE PER LENGTH MASS (ton/m)
27 H = 321685.942;     % CABLE HORZONTAL TENSION (kN)
28 DH = 16484.597;     % INCREMENT IN CABLE HORZONTAL TENSION (kN)
29 L = 1600;            % SPAN LENGTH (m)
30 T = H+DH;            % DEFINING H & DH (kN)
31 L_0 = 1757.42637;    % CABLE LENGTH (m)
32 Alfa = -((E_c*A_c)/(L_0))/(L^2); % ALFA COEFFICENT
33 g = 9.806;           % GRAVITY ACCELERATION (m/s^2)
34 u_0 = 0;             % TOWER HORZONTAL DISPLACEMENT @ x = 0
35 u_L = 0;             % TOWER HORZONTAL DISPLACEMENT @ x = L
36 w_0 = 0;            % TOWER VERTICAL DISPLACEMENT @ x = 0
37 w_L = 0;            % TOWER VERTICAL DISPLACEMENT @ x = L
38 N = 50;             % NUMBER OF INVOLVED MODES
39
40 %% DEFINING T & K_c & K_g
41
42 for n=1:N
43 K_g(n) = ( E_g*I_g*((n*pi()/L)^4) + T*((n*pi()/L)^2)-((2*Alfa*L)/((n*pi())^2))*(((-1)^n+1)^2)); % K VALUE IN
EQUATION OF MOTION OF THE CABLE
44 Erq(n) = ((u_L-u_0) - (1/2)*(w_L+w_0))*((-1)^n+1);
45 end

```

```

46
47 %% DIFFERENTIAL EQUATIONS
48
49 dZ = diff(Z,t);
50 for n=1:N
51 ODE1(n) = diff(Z,t,2) + (K_g(n)*Z)/(m_g + m_c) == (2*M*g/((m_g + m_c)*L))*sin(n*pi()*V*t/L) + (Erq(n)
*2*Alfa*L)/(n*pi()*m_g + m_c));
52 end
53 COND1 = Z(0) == 0;
54 COND2 = dZ(0) == 0;
55 CONDS = [COND1, COND2];
56
57 %% SOLUTION
58
59 ZsolN = 0;
60 ZsolxN = 0;
61 for n=1:N
62 Zsol(n) = dsolve(ODE1(n), CONDS);
63 Zsolx(n) = Zsol(n) * sin(n*pi()*x/L);
64 ZsolxN = ZsolxN + Zsolx(n);
65 end
66
67 %% FUNCTIONS
68
69 [MeshR, MeshC] = size(xV);
70 ZsolVN = diff(ZsolxN,t,1);
71 ZsolAN = diff(ZsolxN,t,2);
72 Step = 20;
73 VMAX = Step * 12;
74 VMAX = VMAX + 1;
75 for Vstep = 1 : Step : VMAX % VELOCITY OF MOVING LOAD (m/s)
76 tMax = L/Vstep;
77 for i = 1 : MeshC
78 ZsolANV = subs(ZsolAN,[x,V],[xV(i),Vstep]);
79 AV_Min_Location(Iteration,i) = fminbnd(matlabFunction(ZsolANV),0,tMax);
80 AV_Max_Location(Iteration,i) = fminbnd(matlabFunction(-ZsolANV),0,tMax);

```



```

81 en
82 end
83
84 for Vstep = 1 : Step : VMAX % VELOCITY OF MOVING LOAD (m/s)
85 for i = 1 : MeshC
86 ZsolANV = subs(ZsolAN,x,xV(i));
87 AV_Max(Iteration,i) = subs(ZsolANV,[t,V],[AV_Location(Iteration,i),Vstep]);
88 end
89 end
90
91 format longG
92
93 xV = [0,xV,L];
94 Intial = zeros([1,MeshC + 2]);
95 AV_Max = double([0,AV_Max,0]);
96 AV_Max = double([Intial;AV_Max]);
97 AV_Max = AV_Max * 1e3/9.81;
98 Vstep = 1 : Step : VMAX;
99 Vstep = [0,Vstep];
100 figure (1)
101 surf(Vstep',xV',AV_Max')
102 hold on
103 title('3D PLOT OF MAX ACCELERATION ')
104 xlabel('Velocity (m/s)')
105 ylabel('Longitudinal coordinate (m)')
106 zlabel('Acceleration Max 10^-^3 g')
107 set(gca,'FontName','Times New Roman','FontSize',16)
108 axis tight
109 xh = get(gca,'XLabel'); % Handle of the x label
110 set(xh, 'Units', 'Normalized')
111 set(xh, 'Position',[0.75,0.025,0],'Rotation',12)
112 yh = get(gca,'YLabel'); % Handle of the y label
113 set(yh, 'Units', 'Normalized')
114 set(yh, 'Position',[0.175,0.05,0],'Rotation',-14)
115
116 toc

```



## CURRICULUM VITAE



**Name Surname** : Ali AHANI  
**Place and Date of Birth** : Tabriz, 15.12.1991  
**E-Mail** : [AliAHANI91@gmail.com](mailto:AliAHANI91@gmail.com), [AHANI16@itu.edu.tr](mailto:AHANI16@itu.edu.tr)

### EDUCATION

:

- **B.Sc.** : 2014, University of Tabriz, Civil Engineering
- **High school** : 2010, NODET High schools (*National Organization for Development of Exceptional Talents*)

### LANGUAGE SKILLS

:

Language	Reading			Listening			Writing			Speaking		
	native	good	fair	basic	native	good	fair	basic	native	good	fair	basic
Azerbaijani	●				●				●			●
Persian	●				●				●			●
English	●				●				●			●
Turkish	●				●				●			●
Arabic		●					●			●		●

## **PUBLICATIONS :**

### **Journal Papers:**

- **Ahani, A., Ahani, E., Abbaszadeh, H.** (2018). *The Effects of Outrigger type and distribution on seismic behavior of super-tall building*. Journal of Computational Engineering and Physical Modeling.
- **Abbaszadeh, H., Ahani, A., Emami Azadi, M.** (2018). *Debonding and Fracture Behavior of Concrete Specimens Retrofitted by FRP Composite*. Journal of Computational Engineering and Physical Modeling, 1(2), 27-40. doi: 10.22115/cepm.2018.125309.1015

### **Conference Papers:**

- ***Seismic Behavior of Super-tall Building with different Outrigger type and distribution (location)***, 4<sup>th</sup> International Conference on Structural Engineering, May 2018, Tehran – Iran
- ***An experimental and analytical study on fracture behavior of concrete specimens retrofitted by FRP composite***, 4<sup>th</sup> International Conference on Structural Engineering, May 2018, Tehran – Iran.

## **COMPUTER SKILLS :**

Programming languages:

- MATLAB (Advanced)
- FORTRAN (Advanced)
- C++ (Advanced)
- Visual Basic (Intermediate)
- Python (Intermediate)

Software Skills:

- ABAQUS (Advanced)
- SAP2000 (Advanced)
- ETABS (Advanced)
- CSI Bridge (Advanced)
- AutoCAD (Advanced)
- ANSYS (Intermediate)
- OpenSees (Basic)

Common Software Skills:

- Microsoft Office (Excel, Word, Power Point)

Non-relating Software Skills:

- Adobe Photoshop (Advanced)
- Adobe Illustrator (Advanced)
- Corel Draw (Basic)

## Web Developing Skills:

- PHP (Basic)
- HTML (Basic)

